Palmitate induces insulin resistance and a pro-atherogenic phenotype in monocytes

DAN GAO

Doctor of Philosophy

ASTON UNIVERSITY

December 2008

Aston University

Palmitate induces insulin resistance and a pro-atherogenic phenotype in monocytes

Dan Gao

Doctor of Philosophy

December 2008

SUMMARY

Insulin resistance is strongly associated with increased risk of cardiovascular disease (CVD). Elevated plasma free fatty acids (FFA) have been shown to contribute to insulin resistance in peripheral tissues (skeletal muscle and adipose tissue). However, little is known about the role of FFA in atherosclerosis, the leading cause of CVD. The present study investigated the effect of the two most abundant FFA in plasma – palmitate and oleate – on insulin sensitivity and vascular function (monocyte phenotype and adhesion to endothelium) using in vitro cell culture models and Wistar rats. Palmitate at 300μM for 6h induced insulin resistance in THP-1 monocytes and L6 myotubes. The ceramide synthesis pathway partly accounted for the palmitate-induced insulin resistance in THP-1 monocytes but not for L6 myotubes. Oleate treatment did not induce insulin resistance in either cell type and co-incubation with oleate protected cells from palmitate-induced insulin resistance. Palmitate at 300μM for 24h significantly increased cell surface CD11b and CD36 expression in U937 monocytes. The increase in CD11b and CD36 expression was effectively inhibited by Fumonisin B1, an inhibitor of ceramide synthesis. Oleate treatment did not show any effect on CD11b and CD36 expression and co-incubation with oleate antagonised the effect of palmitate on CD11b and CD36 expression in U937 monocytes. The increase in CD11b expression did not affect U937 monocyte adhesion to ICAM-1. Treating Wistar rats with palmitate for 6h caused a transient delay in glucose disposal and an increase in adhesion of U937 monocytes to the aortic endothelium, particularly at bifurcations. In conclusion, the present study demonstrates that the saturated free fatty acid palmitate induces insulin resistance and a pro-atherogenic phenotype for monocytes, whereas the unsaturated free fatty acid oleate does not. In vivo studies also confirmed that palmitate induces insulin resistance and an increase in monocyte adhesion to aorta.

Key words: palmitate, oleate, integrin CD11b, scavenger receptor CD36, monocyte-endothelial interaction, ceramide.

To my nan and my parents

Acknowledgements

I would like to take this opportunity to thank my supervisor Professor Helen R Griffiths and Professor Cliff J Bailey for offering me this PhD position and giving me tremendous help, support, and encouragement throughout the project.

I would also like to thank Dr Andrew Devitt for providing me with the ICAM-1-Fc cDNA, Elizabeth Torr for teaching and helping me with the production of the ICAM-1-Fc protein, Professor Peter Lambert for his help with immunofluorescence microscopy. Thank you also to Brian Burford and Mel Gamble in the biomedical facility for their technical support and help with the animal studies in the project. Thanks also to Sue Turner for her technical support with 2-deoxy-D-[^{3}H] glucose uptake experiments.

Special thanks to all the volunteers for joining in the project and their generosity of donating their blood for the project: Alan Richardson, Eric Hill, Peter Lambert, James Barwell, Chris Dunston, Paul Fundak, Morteza Alhomoda, Ragit Kolamunne, Richard Darby, and Cliff Bailey.

Thanks also to Kam, Khujesta, Lili, Chris, Iru, Ragit, and Rachel for all the good times in the lab and all those outside the lab especially Dr Steve Russell, Dr Xiaolin Li, and Zhuo Wang.

A big thank to the International Student Scholarship provided by the School of Life and Health Sciences at Aston University and the Overseas Research Student Awards Scheme for financial support throughout my PhD study.

Finally, I would like to thank my parents and family members for making my dream come true to study in the UK and their great support and love over the years.

Abbreviations

Ac-DEVD-AMC	Acetyl Aspartic acid-Glutamic acid-Valine-Aspartic acid 7-amido-4-methylcoumarin
ANOVA	Analysis of variance
APS	Ammonium persulphate
ATP	Adenosine-5'-triphosphate
BCA	Bicinchoninic acid
BCECF-AM	2', 7'-Bis (2-carboxyethyl)-5(6)-carboxyfluorescein tetrakis (acetoxymethyl) ester
BMI	Body mass index
BSA	Bovine serum albumin
CHD	Coronary heart disease
CHO	Chinese hamster ovary
Chx	Cycloheximide
CoA	Coenzyme A
CVD	Cardiovascular disease
DAG	Diacylglycerol
DCFH-DA	2', 7',-dihydrodicholorofluorescein diacetate
2-DG	2-Deoxy-D-[^{3}H] glucose
DHR	Dihydrorhodamine123
DMEM	Dulbecco's modified Eagle's medium
DMF	Dimethylformamide
DMSO	Dimethyl sulphoxide
DNA	Deoxyribonucleic acid
ECL	Emission chemoiluminescence
EDTA	Ethylenediaminetetraacetic acid
FB1	Fumonisin B1
FBS	Foetal bovine serum
FFA	Free fatty acids
FITC	Fluorescein isothiocyanate
FS	Forward light scatter
GLUT	Glucose transporters

HBS	HEPES buffered saline
HBSS	Hank's buffered salt solution
HDL	High density lipoprotein
HEPES	4-(2-hydroxyethyl)-1-piperazineethanesulfonic acid
HRP	Horseradish peroxidase
HSL	Hormone sensitive lipase
HUVEC	Human umbilical vein endothelial cells
LB	Luria broth
ICAD	caspase-activated deoxyribonuclease
ICAM-1	Intercellular adhesion molecule-1
LDL	Low density lipoprotein
LDLR	LDL receptor
IGT	Impaired glucose tolerance
IKKβ	Inhibitor κB kinase β
IL-6	Interleukin-6
IMCL	Intramyocellular lipid
IRC	Insulin-responsive compartment
IRS	Insulin receptor substrate
LOX-1	Lectin-like ox-LDL receptor-1
LPS	Lipopolysaccharide
MAPP	1S,2R-D-erythro-2-(N-myristoylamino)-1-phenyl-1-propanol
MAPK	Mitogen-activated protein kinase
MCP-1	Monocyte chemoattractant protein-1
M-CSF	Monocyte-colony simulating factor
MdX	Median fluorescence intensity
MIDAS	Metal ion dependent adhesion site
MNC	Mononuclear cells
MRS	Magnetic resonance spectroscopy
MTT	3-(4,5-Dimethylthiazol-2-yl)-2,5-diphenyltetrazolium bromide
NAD^+	Nicotinamide adenine dinucleotide reduced form
NADH	Nicotinamide adenine dinucleotide
NEFA	Non-esterified fatty acids

NF-κB	Nuclear factor-κB
NMR	Nuclear Magnetic Resonance
NO	Nitric oxide
Oa	Oleate
OGTT	Oral glucose tolerance test
Ox-LDL	Oxidised LDL
Pa	Palmitate
PAGE	Polyacryamide gel electrophoresis
PBS	Phosphate buffered saline
PDK	3-phosphoinositide-dependent kinase
PE	Phycoerythrin
PECAM-1	Platelet/endothelial cell adhesion molecule-1
PF4	Platelet factor 4
PI	Propidium iodide
PI3-kinase	Phosphoinositide 3-kinase
PKB	Protein kinase B
PKC	Protein kinase C
PMA	Phorbol-12-myristate-13-acetate
PMN	Polymorphonuclear cells
PSGL-1	P-selectin glycoprotein-1 ligand
PVDF	Polyvinylidene fluoride
PPAR-γ.	Peroxisome proliferator-activated receptor-γ
PPA2	Phosphatase A2
RasGRP	Ras guanyl nucleotide-releasing protein
ROS	Reactive Oxygen Species
SD	Standard deviation
SDS	Sodium dodecyl sulphate
SEM	The standard error of the mean
SMase	Sphingomyelinase
SOC	Super optimal catabolite repression
S-1-P	Sphingosine-1-phosphate
SPT	Serine palmitoyltransferase

SRAI/II	Scavenger receptor A type I and II
SR-PSOX	Scavenger receptor-phosphatidylserine and oxidized lipoprotein
TAE	Tris-acetate-EDTA
TAG	Triacylglyceride
TEMED	1, 2-Bis (dimethylamino) ethane
TNF-α	Tumor necrosis factor α
TNFR	TNF-α receptor
UV	Ultraviolet rays
VAD-FMK	Benzyloxycarbonyl-Valine-Alanine-Asppartic acid (OMe)-fluoromethylketone
VCAM-1	Vascular cell adhesion molecule-1
VLA-4	Very late antigen-4
VLDL	Very low density lipoprotein

CONTENTS PAGE

Title Page		**1**
Thesis Summary		**2**
Dedication		**3**
Acknowledgements		**4**
Abbreviations		**5**
Chapter 1	**Introduction**	**17**
1.1	**Free fatty acids**	**18**
1.2	Insulin resistance	**21**
1.2.1	Insulin structure, synthesis and secretion	**21**
1.2.2	Insulin signal transduction pathways	**22**
1.2.3	Metabolic effects of insulin	**24**
1.2.4	Glucose transporters	**25**
1.2.5	Insulin resistance	**26**
1.2.6	Obesity-associated insulin resistance	**30**
1.2.6.1	Free fatty acids and insulin resistance	**30**
1.2.6.2	Inflammatory cytokines and insulin resistance	**32**
1.2.7	Molecular mechanisms of insulin resistance	**35**
1.2.8	Mechanisms of FFA-induced insulin resistance	**37**
1.3	**Cardiovascular disease**	**43**
1.3.1	Classification of atherosclerosis	**44**
1.3.2	Risk factors for atherosclerosis	**46**
1.3.3	Pathogenesis of atherosclerosis	**47**
1.3.3.1	The response-to-injury hypothesis	**48**
1.3.3.2	The oxidative modification hypothesis	**50**
1.3.4	Role of monocytes in atherosclerosis	**50**
1.3.4.1	Monocyte adhesion to endothelium	**51**
1.3.4.2	Formation of foam cells	**59**
1.3.4.3	Monocyte/macrophage-induced inflammatory response	**63**
1.4	**Hypothesis**	**63**
1.5	**Aims**	**64**
Chapter 2	**Materials and Methods**	**65**
2.1	**Preface**	**66**
2.2	**Cell Culture**	**66**
2.3	**Conjugation of fatty acids to BSA**	**69**
2.4	**Flow Cytometric analysis of cell surface antigens**	**72**
2.5	**2-Deoxy-D-[^{3}H] glucose (2-DG) uptake**	**75**
2.6	**Uptake and accumulation of palmitate in U937 and THP-1 monocytes**	**77**
2.7	**Production of recombinant human**	**78**

	ICAM-1-Fc protein	
2.8	**SDS-PAGE and Western blot**	**86**
2.9	**Immobilisation of ICAM-1-Fc protein to 96-well plate**	**91**
2.10	**Intracellular reactive oxygen species (ROS) measurement**	**94**
2.11	**Monocyte adhesion assay**	**95**
2.12	**Bicinchoninic acid (BCA) protein assay**	**99**
2.13	**Caspase-3 activity assay**	**100**
2.14	**Cell viability assay**	**102**
2.15	**Statistical analysis**	**106**
Chapter 3	**Palmitate-induced insulin resistance in monocytes**	**107**
3.1	**Preface**	**108**
3.2	**Introduction**	**108**
3.3	**Materials and Methods**	**112**
3.4	**Results**	**115**
3.4.1	Characterisation of monocytes in response to insulin	**115**
3.4.1.1	Insulin increases glucose uptake in THP-1 but not U937 monocytes and this effect does not require serum starvation	**115**
3.4.1.2	Insulin increases glucose uptake by THP-1 monocytes in a concentration and time dependent manner	**118**
3.4.1.3	Basal and insulin-stimulated glucose uptake is mediated by glucose transporters	**121**
3.4.2	Palmitate induces insulin resistance in THP-1 monocytes in a time and concentration dependent manner	**125**
3.4.3	Palmitate-induced insulin resistance in THP-1 monocytes is not reversible	**131**
3.4.4	Effect of palmitate on intracellular reactive oxygen species (ROS) generation in THP-1 monocytes	**134**
3.4.5	Fumonisin B1 prevents palmitate-induced insulin resistance in THP-1monocytes	**134**
3.4.6	Oleate does not induce insulin resistance but protects against palmitate-induced insulin resistance in THP-1 monocytes	**138**
3.5	**Discussion**	**141**
Chapter 4	**Oleate protects against palmitate-induced insulin resistance in L6 myotubes**	**150**

4.1	**Preface**	**151**
4.2	**Introduction**	**151**
4.3	**Materials and Methods**	**153**
4.4	**Results**	**155**
4.4.1	Effect of palmitate and oleate alone on glucose uptake	**155**
4.4.2	Oleate protects L6 cells from palmitate-induced insulin resistance	**157**
4.4.3	Oleate prevents the palmitate-induced alteration in L6 cell Morphology	**168**
4.4.4	Effect of free fatty acids on L6 cell viability	**160**
4.4.5	PI3-kinase activity is involved in oleate protection against palmitate-induced insulin resistance	**163**
4.4.6	Fumonisin B1 (FB1) dose not prevent palmitate-induced insulin resistance in L6 myotubes	**167**
4.4.7	FB1 does not prevent palmitate-induced alterations in L6 cell morphology	**178**
4.5	**Discussion**	**169**
Chapter 5	**Effect of insulin resistance risk factors on monocyte phenotype and adhesion**	**176**
5.1	**Preface**	**177**
5.2	**Introduction**	**177**
5.3	**Materials and Methods**	**181**
5.4	**Results**	**185**
5.4.1	Effect of glucose and free fatty acids on monocyte phenotype	**185**
5.4.1.1	Effect of glucose on CD11b expression in U937 monocytes	**185**
5.4.1.2	Effect of palmitate (30min) on CD11b expression in primary monocytes	**188**
5.4.1.3	Effect of free fatty acids (24h) on CD11b expression in primary viable monocytes	**189**
5.4.1.4	Effect of free fatty acids (24h) on CD11b expression in viable U937 monocytes	**192**
5.4.1.5	Fatty acid modulates CD36 expression in viable U937 monocytes	**194**
5.4.1.6	Effect of FB1 on palmitate-induced CD11b and CD36 expression in viable U937 monocyts	**198**
5.4.1.7	Palmitate-induced increase in CD11b and CD36 is associated with cell surface mannose receptor (CD206) expression	**201**
5.4.1.8	Effect of palmitate on reactive oxygen	**202**

	species (ROS) generation in U937 monocytes	
5.4.2	Effect of free fatty acids on monocyte adhesion to endothelium	**203**
5.4.2.1	Effect of palmitate on U937 monocyte adhesion to EAhy926 endothelial cells	**204**
5.4.2.2	Effect of free fatty acids on monocytes adhesion to ICAM-1	**205**
5.4.3	Effect of free fatty acids on U937 monocytes viability	**209**
5.4.3.1	Effect of free fatty acids on mononuclear cell viability	**210**
5.4.3.2	Effect of glucose and free fatty acids on U937 monocytes viability	**212**
5.5	**Discussion**	**218**
Chapter 6	***In vivo* study of palmitate effects on insulin sensitivity and vascular adhesion in Wistar rats**	**231**
6.1	**Preface**	**232**
6.2	**Introduction**	**232**
6.3	**Materials and Methods**	**234**
6.4	**Results**	**240**
6.4.1	Oral glucose tolerance test in untreated rats	**240**
6.4.2	Effect of palmitate on insulin sensitivity	**241**
6.4.3	Effect of palmitate on plasma free fatty acid (FFA) and triacylglyceride (TAG) concentrations	**244**
6.4.4	Effect of oleate on palmitate-induced insulin resistance	**245**
6.4.5	Effect of palmitate on monocytes adhesion to rat aorta	**248**
6.5	**Discussion**	**252**
Chapter 7	**Discussion and Future Work**	**260**
7.1	**Discussion**	**261**
7.2	**Future Work**	**268**
Chapter 8	**References**	**270**
Appendix I	**Animal study licence**	**303**
Appendix II	**Publications**	**309**

LIST OF TABLES

Table 1.1	Summary of risk factors of atherosclerosis	47
Table 1.2	Adhesion molecules and ligands known to play a role in atherosclerosis	53
Table 1.3	Macrophage scavenger receptors that bind lipoproteins	60
Table 2.1	Resolving and Stacking gel	88
Table 5.1	Demographic characteristics of the volunteers	190
Table 5.2	Effect of lipopolysaccharides (LPS) on expression of adhesion molecules in EAhy926 endothelial cells	207
Table 7.1	Results summary of the thesis	267

LIST OF FIGURES

Figure 1.1	Dietary fat and generation of free fatty acids (FFA).	21
Figure 1.2	Insulin signal transduction pathway	23
Figure 1.3	Molecular metabolism of free fatty acids (FFA) -induced insulin resistance	39
Figure 1.4	Ceramide synthesis pathways	40
Figure 1.5	Cellular components of the normal artery	46
Figure 1.6	Leukocytes adhesion cascade	52
Figure 1.7	Hypothesis of the project	64
Figure 2.1	FFA and plasma albumin equilibrium	71
Figure 2.2	Flow cytometric measurement of CD11b expression on mononuclear cells (MNC)	74
Figure 2.3	Time course of palmitic acid uptake by U937 and THP-1 monocytes	78
Figure 2.4	1% agarose gel plasmid DNA samples analysis	83
Figure 2.5	Absorbance of each elution fraction at 595nm by Bradford assay	86
Figure 2.6	Coomassie Blue staining of ICAM-1-Fc SDS-PAGE gel	89
Figure 2.7	Western blot of ICAM-1-Fc SDS-PAGE gel	91
Figure 2.8	Optimisation of human recombinant ICAM-1-Fc coating to 96-well plate	94
Figure 2.9	Resting U937 monocyte adhesion to 96-well plates directly coated with ICAM-1-Fc	98
Figure 2.10	Resting and PMA-activated U937 monocyte adhesion to 96-well plates indirectly coated with ICAM-1-Fc	99
Figure 2.11	Cell viability assay by flow cytometry	106
Figure 3.1	Insulin-stimulated 2-deoxy-D-glucose uptake into U937 and THP-1 monocytes	117
Figure 3.2	Effect of foetal bovine serum (FBS) on insulin-stimulated glucose uptake by THP-1 monocytes	117
Figure 3.3	Effect of insulin on glucose uptake by THP-1 monocytes	120
Figure 3.4	Cytochalasin B inhibits basal and insulin-stimulated	123

	glucose uptake (A) and does not affect total protein levels (B) in THP-1 monocytes	
Figure 3.5	Effect of cycloheximide (ChX) on glucose uptake by THP-1 monocytes (A) and cell viability (B)	124
Figure 3.6	Western blot analysis for glucose transporters in THP-1 monocytes	124
Figure 3.7	Time course of palmitate uptake by THP-1 monocytes	128
Figure 3.8	Effect of time and concentration of palmitate on THP-1 cell viability	128
Figure 3.9	Effect of palmitate on THP-1 cell viability	129
Figure 3.10	Effect of palmitate (Pa) concentration (A) and incubation time (B) on glucose uptake by THP-1 monocytes	130
Figure 3.11	Schematic graph of insulin resistance reversibility experimental design	132
Figure 3.12	Reversibility of palmitate-induced insulin resistance in THP-1 monocytes	133
Figure 3.13	Effect of palmitate on reactive oxygen species (ROS) generation	134
Figure 3.14	Effect of fumonisin B1 (FB1) on basal and insulin stimulated glucose uptake	137
Figure 3.15	Effect of fumonisin B1 (FB1) on palmitate-induced insulin resistance	138
Figure 3.16	Effect of oleate on glucose uptake by THP-1 monocytes	140
Figure 3.17	Fumonisin B1 inhibits *de novo* ceramide synthesis	147
Figure 4.1	Effect of palmitate (A) and oleate (B) alone on basal and insulin-stimulated 2-deoxy-D-glucose uptake by L6 myotubes	156
Figure 4.2	Effect of combinations of 300μM palmitate (Pa) with various concentrations of oleate (Oa) on basal and insulin-stimulated 2-deoxy-D-glucose uptake by L6 myotubes	157
Figure 4.3	Effect of palmitate (Pa), oleate (Oa), combinations of palmitate with various concentrations of oleate or BSA on L6 myotube morphology	159
Figure 4.4	Effect of palmitate (Pa) and oleate (Oa) on membrane integrity measured by trypan blue exclusion	161
Figure 4.5	Effect of palmitate (Pa) and oleate (Oa) on mitochondrial reducing activity measured by MTT assay	162
Figure 4.6	Effect of palmitate (Pa) and oleate (Oa) on caspase-3 activity	162
Figure4.7A	Effect of wortmannin on basal and insulin-stimulated 2-deoxy-D-glucose uptake by L6 myotubes	164
Figure 4.7B	Effect of LY-294,002 (6h) on basal and insulin-stimulated 2-deoxy-D-glucose uptake by L6 myotubes	165
Figure 4.7C	Effect of LY-294,002 (1h) on basal and	165

	insulin-stimulated 2-deoxy-D-glucose uptake by L6 myotubes	
Figure 4.8A	Effect of wortmannin on basal and insulin-stimulated 2-deoxy-D-glucose uptake by L6 myotubes in the presence of palmitate (Pa) plus oleate (Oa)	**166**
Figure 4.8B	Effect of LY-294,002 on basal and insulin-stimulated 2-deoxy-D-glucose uptake by L6 myotubes in the presence of palmitate (Pa) plus oleate (Oa)	**166**
Figure 4.9	Effect of fumonisin B1 (FB1) on basal and insulin-stimulated 2-deoxy-D-glucose uptake by L6 myotubes	**168**
Figure 4.10	Effect of fumonisin B1 (FB1) on L6 cell morphology	**169**
Figure 5.1	Time course of ^{3}H-glucose uptake into U937 monocytes	**187**
Figure 5.2	Effect of glucose on CD11b expression in U937 monocytes	**187**
Figure 5.3	Effect of palmitate (30min) on CD11b expression in primary monocytes ($CD14^{+}$ cells)	**189**
Figure 5.4	Effect of free fatty acids on CD11b expression in viable $CD14^{+}$ mononuclear cells	**191**
Figure 5.5	Effect of free fatty acids on CD11b expression in viable U937 monocytes	**193**
Figure 5.6	Palmitate increased CD11b expression in viable U937 monocytes	**194**
Figure 5.7	Effect of oleate (Oa) on palmitate (Pa)-induced CD11b (A) and CD36 (B) expression in viable U937 monocytes	**196**
Figure 5.8	Effect of oleate on palmitate-induced CD11b and CD36 expression in viable U937 monocytes	**197**
Figure 5.9	Effect of FB1 on palmitate-induced CD11b (A and C) and CD36 (B and D) expression in viable U937 monocytes	**200**
Figure 5.10	Effect of palmitate on CD206 expression in U937 monocytes	**202**
Figure 5.11	Effect of palmitate on reactive oxygen species (ROS) generation	**203**
Figure 5.12	Expression of adhesion molecule in unstimulated EAhy926 endothelial cells	**207**
Figure 5.13	Effect of palmitate on U937 monocyte adhesion to unstimulated EAhy 926 endothelium (A) and PECAM-1 (CD31) expression (B)	**208**
Figure 5.14	Effect of palmitate and oleate on mononuclear cells (MNC) total CD11b expression and adhesion to ICAM-1	**208**
Figure 5.15	Effect of free fatty acids on U937 monocytes adhesion to ICAM-1	**209**
Figure 5.16	Effect of free fatty acids on viability of primary monocyte	**211**
Figure 5.17	Effect of glucose on U937 monocyte viability	**213**
Figure 5.18	Effect of palmitate and oleate on U937 monocyte	**214**

viability
Figure 5.19 Effect of fumonisin B1 (FB1) on palmitate-treated U937 monocyte viability 214
Figure 5.20 Flow cytometric analysis of U937 monocyte cell viability with propidium iodide (PI) staining 217
Figure 6.1 Overview of the experimental design 236
Figure 6.2 Resting and PMA-activated U937 cells adhesion to rat aorta 239
Figure 6.3 Glucose tolerance test on untreated rats 241
Figure 6.4 Insulin sensitivity test on rats treated with palmitate and water as controls 243
Figure 6.5 Effect of palmitate on plasma free fatty acid (FFA) (A) and triglyceride (TAG) levels (B) in Wistar rats 245
Figure 6.6 Glucose tolerance test on rats treated with palmitate alone, oleate alone, and palmitate plus oleate 247
Figure 6.7 U937 monocyte adhesion to rat aorta 249
Figure 6.8 Effect of palmitate on U937 monocyte adhesion to rat aorta 251

Chapter 1 Introduction

The purpose of this thesis is to investigate the underlying mechanisms of accelerated atherosclerosis in insulin resistant conditions. The rationale for this thesis is based on the evidence that insulin resistance is an independent risk factor for the development of atherosclerosis. Increased plasma free fatty acid levels, particularly the saturated fatty acid palmitate, have been shown to induce insulin resistance in peripheral tissues such as skeletal muscle and adipose tissue and are associated with the *de novo* synthesis of ceramide. Therefore, to investigate the molecular mechanisms of atherosclerotic disease associated with insulin resistance, the formulated hypothesis of the current study is: the saturated free fatty acid palmitate induces insulin resistance in monocytes, alterations in the monocyte phenotype and adhesion that is mediated via disordered ceramide metabolism. This will be tested by measurement of *in vitro* glucose uptake into monocytes; cell surface integrin CD11b and scavenger receptor CD36 expression; and monocyte adhesion to endothelial cells/receptor ICAM-1 using monocytic cell lines and primary monocytes after exposure to pathological concentrations of palmitate.

1.1 Free fatty acids (FFA)

Dietary fat is derived from a wide variety of animal and plant sources such as animal adipose tissue, milk and its products (cream, butter, cheese and yogurt), vegetable seeds, nuts, oils, and eggs. In most western countries, dietary fat provides between 30-40% of total dietary energy intake while in most Asian countries and the developing world, the proportion of energy derived from dietary fat is usually much lower (Bray et al., 2004). For example, it has been reported

that in rural Chinese communities the dietary fat provides less than 20% of the total energy intake (Chen, 2000). 95% of dietary fat is triglyceride, which is composed of a glycerol moiety linked with 3 fatty acid chains. Each fatty acid is composed of a long hydrocarbon chain ranging from 4 to 30 carbons and a carboxylic acid group. Based on the number of double bonds, fatty acids are classified as: saturated fatty acids without any double bonds (e.g. palmitic acid and stearic acid); monounsaturated fatty acids with one double bond (e.g. oleic acid), and polyunsaturated fatty acids with at least two double bonds (e.g. linoleic acid). Usually, most native vegetable oils and fats favour polyunsaturates or monounsaturates in the sn-2 position whilst saturates are distributed at the sn-1/3 positions of triglycerides.

The current official dietary guidelines for fat intake are 15%-30% given by World Health Organisation (2003) and 30% given by the UK Department of Health (1991). These values are the percentage of daily energy intake recommended to come from a fat source. Special provisions are also given to saturated fatty acids (<10%) and the consumption of poly-unsaturated fatty acids (6%-10%). In the UK, total dietary fat comprised around 33.45% of total energy intake, which including 14.29% from saturated fatty acids, 12.99% from monounsaturated fatty acids, and 5.95% from polyunsaturated fatty acids (Arnoult, 2006).

Dietary triglycerides are mainly absorbed in the small intestine, where fatty acids with short chain or medium long chain (less than 12 carbon atoms) enter the portal vein by direct diffusion into enterocytes, while longer than 12 carbon fatty acids

are re-synthesised to triglyceride, incorporated into the chylomicron. After entering into the circulation via lymphatic system, chylomicron delivers free fatty acids hydrolysed by lipoprotein lipase to various tissues such as liver, skeletal muscle and adipose tissue. The remnant of the chylomicron is cleared from the circulation by apolipoprotein B/E receptors present in the liver and then used for the synthesis of very-low density lipoproteins (VLDL). These lipoproteins are major transporters delivering dietary fat to adipose tissues where fatty acid is stored as triglycerides and to peripheral tissues (skeletal muscles and heart) where fatty acid is utilised for energy production and maintenance of normal cell functions. (Fig.1.1)

Most of the fatty acids are esterified in the form of triglycerides and stored in adipose tissues and only 5% of fatty acids remain non-esterifed in the circulation. The non-esterified fatty acids in the circulation are also referred to as free fatty acids (FFA) and this is mainly provided by adipose tissue lipolysis under the action of hormone sensitive lipase (HSL). Fatty acids especially saturated fatty acids have very low solubility in the blood, typically about 1μM. However, binding to serum albumin increases their effective solubility to around 1mM. In this way, albumin transports FFA to organs such as muscle and liver for oxidation to provide energy. Typical plasma free fatty acid composition are 13% stearic acid, 31% palmitic acid, 32% oleic acid, 20% linoleic acid, 2% arachidonic acid, 1% docosahexaenoic acid, and 1% eicosapentaenoic acid (Chung et al., 1998)

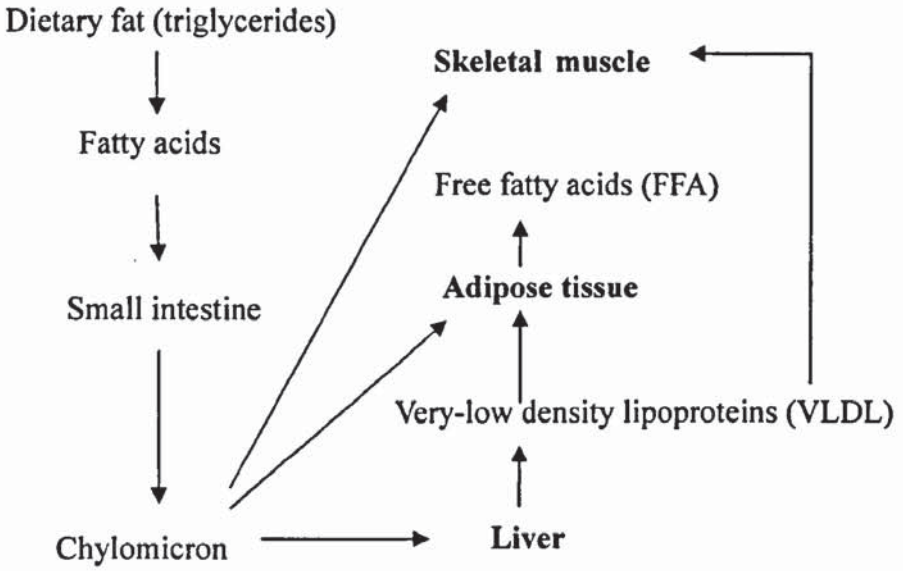

Figure 1.1 Dietary fat digestion and generation of fee fatty acids (FFA). Fatty acids (carbon chain longer than 12) released from dietary triglycerides are absorbed by small intestine and transported in the circulation by chylomicrons. Chylomicrons deliver fatty acids to liver, adipose tissue and skeletal muscle then are cleared by liver for the synthesis of very-low density lipoproteins (VLDL), a major transporter in the circulation and supply fatty acids to adipose tissue and skeletal muscle. The fatty acids stored in adipose tissue are hydrolysed by hormone sensitive lipase (HSL) and provide the major supply of plasma free fatty acids (FFA) in the circulation.

1.2 Insulin resistance

1.2.1 Insulin structure, synthesis and secretion

Insulin was first discovered in 1921 by Sir Frederick Grant Banting and Charles Herbert Best as a substance which when injected to diabetic dogs abolished the symptoms of diabetes. The primary structure of insulin was determined in 1953, by Frederick Sanger. It is a protein constructed of two peptide chains, referred to as A and B chains connected by two disulfide bonds between the cysteine amino acids. The molecular weight of insulin is 6kDa. Insulin is synthesised in and

secreted by the β cells within the islets of Langerhans in the pancreas in response to various nutritional stimuli such as increased circulating levels of glucose, amino acids, and free fatty acids.

1.2.2 Insulin signal transduction pathways

Insulin exerts its biological effects by binding to a receptor on its target cell surfaces. The insulin receptor is composed of two α-subunits and two β-subunits linked by a disulphide bound. The α-subunit contains 723 amino acids and has an approximate molecular weight of 130kDa as determined by SDS-PAGE. The α chains are entirely extracellular and contain the binding sites for insulin. The β-subunit contains 620 amino acids and has an approximate molecular weight of 95kDa. The β-subunit has three compartmental domains: extracellular, transmembrane, and cytosolic.

The signal transduction pathway induced by insulin binding to its receptor was informed by the observation that insulin receptor β-subunits function as a tyrosine kinase (Kasuga et al., 1982). The initial binding of insulin to the insulin receptor α-subunits results in autophosphorylation of the β-subunits on the tyrosine residue and causes a conformational change. The activated β-subunits then transfer phosphate groups from adenosine-5'-triphosphate (ATP) to tyrosine residues on intracellular target proteins, including the IRS (insulin receptor substrate) proteins, Shc (Src homology collagen) and APS [adaptor protein with a PH (pleckstrin homology) and SH2 (src homology 2) domain]. The phosphorylated proteins then dock downstream effector molecules which activate different signalling pathways.

For example, the MAPK (mitogen-activated protein kinase) pathway mediates the growth-promoting function of insulin; the PI 3-kinase (phosphatidylinositol 3-kinase) and the TC10 pathways are involved in the metabolic actions of insulin such as increasing glucose transport (Pessin and Saltiel, 2000). (Fig.1.2)

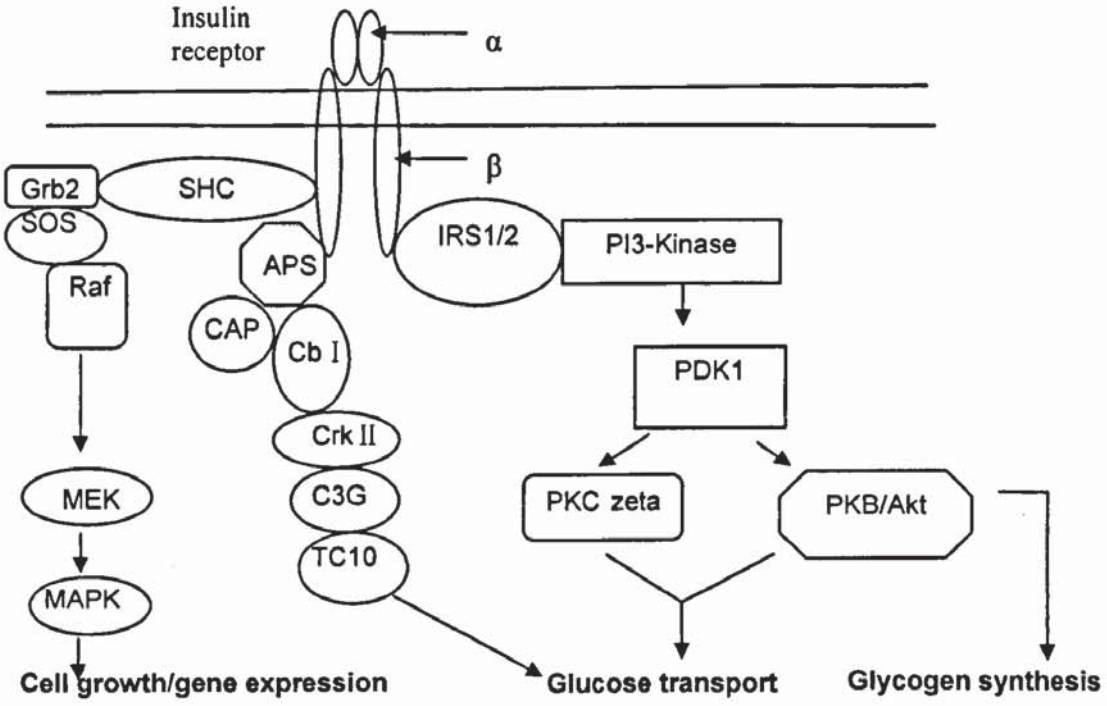

Figure 1.2 Insulin signal transduction pathway (adapted from Le Marchand-Brustel et al., 2003)

Insulin interacts with the α-subunits of its receptor, leading to an increase in the autophosphorylation and the tyrosine kinase activity of the β-subunits. This autophosphorylation of β-subunits enables a variety of scaffolding proteins including insulin receptor substrate 1/2 (IRS1/2), Src homology collage (SHC), the adaptor protein with a PH (pleckstrin homology) and SH2 (src homology 2) domain (APS) to bind to intracellular receptor sites and to become phosphorylated. These phosphorylated proteins then dock downstream effector molecules and activate different signalling pathways such as mitogen-activated protein kinase (MAPK) pathway, the phosphatidylinositol 3-kinase (PI 3-kinase) pathway. CAP, Cbl-associated protein; C3G, Crk SH_3 binding guanine-nucleotide releasing factor; MEK, MAPK/extracellular-signal-regulated kinase kinase; PDK1, 3-phosphoinositide-dependent protein kinase-1; PKB/Akt, protein kianse B; PKC, protein kinase C; SOS, son of sevenless.

1.2.3 Metabolic effects of insulin

Overview of effect on glucose metabolism

The overall effect of insulin on glucose metabolism is to maintain glucose homeostasis through promoting the uptake of glucose into muscle and adipose tissues and inhibiting endogenous glucose production from the liver. After digestion and absorption in the small intestine, glucose is released into the blood stream. This triggers the secretion of insulin from the pancreas into the blood, and insulin stimulates insulin-sensitive tissues such as skeletal muscles and adipose tissues to take up glucose. In the liver, glucose is mainly stored as glycogen and released back to the blood stream during an overnight fasting. In addition, insulin also facilitates the entry of glucose into adipocytes to synthesize glycerol.

Overview of effect on lipid metabolism

The overall effect of insulin on lipid metabolism is to promote the accumulation of fat in adipose tissues. Excessive fat is stored in adipose tissues in the form of triglycerides. Insulin affects the metabolism of fat in two ways. On the one hand, insulin inhibits the breakdown of fat in adipose tissue by inhibiting the intracellular hormone sensitive lipase that hydrolyzes triglycerides to release fatty acids. On the other hand, insulin promotes lipid synthesis in the liver and adipose tissue. When the liver is saturated with glycogen, any additional glucose taken up by hepatocytes is switched into pathways leading to the synthesis of fatty acids, which are exported from the liver as lipoproteins. The lipoproteins are degraded through enzyme catalysed reactions in the circulation, providing free fatty acids as energy for other tissues, including adipocytes, which use them to synthesize

triglyceride.

1.2.4 Glucose transporters

The effect of insulin on maintaining glucose homeostasis is mainly by regulating the trafficking of specific glucose transporters (GLUTs) in peripheral tissues such as skeletal muscle and adipose tissue. Glucose transporters are a class of integral membrane proteins containing 12 membrane-spanning helices with both the amino and carboxyl termini exposed on the cytoplasmic side of the plasma membrane. The molecular weight of glucose transporters is in the range 40-50kDa. To date, 13 members of the glucose transporter family have been identified. The most widely studied transporters are GLUT1, GLUT2, GLUT3, and GLUT4 (reviewed by Gould and Holman, 1993).

The effect of GLUTs on glucose metabolism includes basal glucose uptake and insulin-stimulated glucose uptake. In most tissues, GLUT1 is responsible for the glucose uptake during basal conditions. In adipose tissue and skeletal muscle, GLUT4 is the major transporter responsible for the insulin-stimulated glucose uptake (Douen et al., 1990; Zorzano et al., 1989). Under basal conditions, GLUT4 is stored in a poorly characterised intracellular vesicular compartment (also called insulin-responsive compartment (IRC)) and only 5% of GLUT4 cellular protein is expressed on the cell surface. During insulin stimulation, 50% of intracellular GLUT4 transporters are translocated to the cell surface in the presence of ATP and fuse with the cell membrane to increase the uptake of extracellular glucose into cells (Holman and Sandoval, 2001). GLUT4 is then retrieved from the cell surface

plasma membrane by endocytosis and trafficked through a complexed pathway which may include endosome compartments, the trans-Golgi network, and the IRC. It has been demonstrated by immunoelectron microscopy that 60% of the GLUT4 protein is present in tubulo-vesicular elements underneath the plasma membrane and the remaining protein is localised to the trans-Golgi network, clathrin-coated vesicles and endosome structures (Hou and Pessin, 2007). The signal transduction mechanism in this process includes the autophosphorylation of insulin receptor and its substrate (IRS-1), which results in the activation of phosphatidylinositol (PI) PI3-kinase and subsequent phosphorylation of protein kinaseB (PKB)/Akt which is translocated to the membrane vesicles and ultimately the translocation of vesicular GLUT4 to cell membrane. A recent study also identified a low-density microsome fraction that is critical for insulin-stimulated GLUT4 translocation by increasing IRS-1 phosphorylation and subsequent translocation of PI3-kinase from the cytosol to this fraction (Ogihara et al., 2004)

1.2.5 Insulin resistance

Insulin resistance is a condition in which insulin-sensitive tissues such as skeletal muscle, liver, and adipose tissue show an impaired response to physiological concentrations of insulin. It may be also manifested as an increase in plasma insulin concentrations due to the compensatory secretion of insulin from the pancreas. Insulin resistant conditions are often seen in obesity, glucose intolerance, pre-diabetes, and type 2 diabetes. The major features of insulin resistance are disordered macronutrient (e.g. glucose and lipid) metabolism, such as reduced glucose uptake and glycogen synthesis in skeletal muscles, an increased lipolysis

in adipose tissues, and an increased glucose output from the liver. Overall, the blood glucose level in insulin resistant conditions can be still maintained in a normal range up to several years because of a compensatory secretion of insulin by pancreatic β cells leading to hyperinsulinemia (Ramlo-Halsted and Edelman, 2000). However, after the long term requirement for high levels of insulin to maintain the normal glucose level, the pancreatic β cells gradually become dysfunctional and there is loss of β cell mass due to apoptosis (Rhodes, 2005). Fasting insulin levels are typically observed in humans in a range of 10^{-12}-10^{-9}M according to *in vivo* studies in humans (Ramlo-Halsted and Edelman, 2000) in healthy and insulin resistant conditions. The insulin levels in most type 2 diabetic patients are increased due to the compensatory secretion of insulin by pancreatic β cells whereas the primary defect in type 1 diabetes is the loss function of pancreatic β cells to secretion insulin (Kahn, 1998).

Fasting blood glucose concentrations can increase from a normal level of ≤5.5mM to glucose intolerance level of 5.5-7.0mM and type 2 diabetes level of ≥7.0mM. In contrast to plasma glucose, plasma free fatty acids levels are always increased in insulin resistant conditions due to the increased lipolysis of triglycerides in adipose tissue associated with obesity (Guo et al., 1999). Plasma FFA levels can be increased from a range of 200-400μM under healthy conditions (Belfort et al., 2005) to 400-1000μM in obesity or type 2 diabetes (Kashyap et al., 2004). The details of altered metabolism of glucose and lipids in insulin resistance are further discussed for each of the following three major insulin-targeting tissues.

Skeletal muscle

Skeletal muscle is the major site for glucose metabolism and accounts for about 70% of glucose disposal during postprandial states (DeFronzo, 1981). After digestion of carbohydrate in the small intestine, glucose is released into the blood stream which stimulates the secretion of insulin from the pancreas into the circulation. Glucose uptake is mainly mediated by the insulin-responsive glucose transporter, GLUT4 (Holman and Kasuga, 1997). GLUT1 is also expressed in skeletal muscle but is mainly considered to play a role in the uptake of glucose at a 'basal' rate. Similar to the effect in liver, insulin stimulates the enzyme glycogen synthase and inhibits glycogen phophorylase in skeletal muscle, therefore promoting glucose storage as glycogen. During the insulin resistant state, the insulin-stimulated glucose uptake by skeletal muscle is impaired and it has been estimated that the disposal of glucose in skeletal muscle is reduced by 40-60% (DeFronzo et al., 1981; Baron et al., 1991; Jackson et al., 2000).

Liver

The major metabolic functions of liver with respect to carbohydrate metabolism are to store glucose as glycogen in the absorptive state and to release glucose from the glycogen stores during the overnight fasting state. The entry of glucose into liver hepatocytes is simply dependent on the extracellular glucose level since the predominant glucose transporter in these cells is GLUT2 which is not responsive to insulin (Kemp et al., 1997). Glucose metabolism in the liver is regulated by the effect of insulin and glucose on glycogen synthesis and breakdown. This is achieved through activating glycogen synthase (the main regulatory enzyme of

glycogen synthesis) and inhibiting glycogen phosphorylase (the enzyme responsible for glycogen breakdown). During insulin resistance, the inhibitory effect of insulin on glycogen breakdown is impaired; therefore, the glucose production from the liver is increased and contributes to the increased glucose level in diabetic conditions.

Adipose tissue

The major metabolic role for adipose tissue is to store energy in the form of TAG and release it in the form of free fatty acids when it is needed by other tissues. The formation of the fat stores in adipose tissue is comprised of two major pathways: uptake of TAG from plasma and *de novo* lipogenesis of TAG from other sources particularly glucose. The uptake of TAG is mediated by lipoprotein lipase, an enzyme hydrolyses the TAG in TAG rich particles (chylomicrons and very low density lipoproteins) to release free fatty acids. Insulin promotes the synthesis of TAG in adipose tissue through stimulating TAG uptake by activating lipoprotein lipase (Farese et al., 1991) and prevents TAG release as fatty acids in the plasma (Jensen et al., 1989). Another important metabolic event in adipose tissue is fat mobilisation which involves the liberation of free fatty acids from the stored TAG to the bloodstream for energy supply to other tissues during fasting conditions. This process is called lipolysis and is facilitated under the actions of hormone-sensitive lipase (HSL) (Holm, 2003). Insulin inhibits lipolysis through inactivation of HSL by dephosphorylation, which further contributes to its roles in promoting fat stores in adipose tissue (Degerman et al., 1998). During insulin resistance, the major defect in adipose tissue metabolism is the lack of inhibitory

effect of insulin on fat store mobilization, which results in increased lipolysis of TAG and consequently increased plasma free fatty acid level (Sethi and Vidal-Puig, 2007).

1.2.6 Obesity-associated insulin resistance

1.2.6.1 Free fatty acids and insulin resistance

Insulin resistance has been shown to co-exist with a number of other diabetes and cardiovascular disease risk factors, among them obesity, in particular central obesity with which it has been shown to have the closest relationship. Obesity has become a major health problem in developed countries. In the UK, it is estimated that 1 in 5 adults are obese and two-thirds are overweight (Skidmore and Yarnell, 2004).

Abnormal accumulation of fat in non-adipose tissue such as muscle and liver plays an important role in the aetiology of insulin resistance. The development of the ^{1}H magnetic resonance spectroscopy (^{1}H MRS) technique has successfully established the negative relationship between intramyocellular lipid and whole-body insulin sensitivity (McGarry, 2002). In order to establish 'cause and effect' relationships between fat accumulation in muscle and insulin resistance, several research groups have demonstrated that in healthy, insulin-sensitive subjects, an increase in intramyocellular lipid (IMCL) caused a significant decrease in whole body insulin sensitivity (Boden et al., 1994; Brechtel et al, 2001). These studies also showed that there is a clear positive relationship

between circulating free fatty acid levels and the accumulation of IMCL in skeletal muscles. Interestingly, both of these studies found that after 5h infusion of lipid, the accumulation of TAG in muscle is coincident with the decreased insulin-stimulated glucose disposal. Roden et al. (1996) also reported that the rate of whole-body glucose uptake was not affected during the first 3.5h of lipid infusion, but it significantly decreased to 46% of control values after 6h. These studies demonstrated that an acute increase in the circulating FFA induces a significant suppression of insulin-mediated glucose uptake into muscle in healthy people, indicating an important role for FFA in the establishment of insulin resistance in skeletal muscles.

Furthermore, dietary intervention studies using animals fed with different types of fatty acids provides more convincing evidence for the role of individual fatty acids in insulin resistance in skeletal muscles. Storlien et al. (1991) reported that high saturated fat fed rats developed insulin resistance; whereas those fed with diets high in n-3, with a low n-6/n-3 ratio, maintained insulin action at normal levels, indicating a role of saturated fatty acids in insulin resistance. In vitro cell culture studies also supported the idea that saturated fatty acids are more potent to induce insulin resistance than unsaturated fatty acids. Chavez et al. (2003) reported that exposure of muscle cells particularly to saturated FFA such as palmitate and stearate, rather than a mono-unsaturated FFA such as oleate, caused a reduction in insulin-stimulated glucose uptake.

In addition, epidemiological studies in human subjects also support the association of saturated fat intake and insulin resistance. For example, Mayer-Davis et al. (1997) reported that high intake of saturated fatty acids is associated independently with higher fasting insulin concentrations (as an indicator of insulin resistance), and this relationship may be dependent on increased body adiposity. In contrast, several cross-sectional studies have found that intake of both saturated and trans FAs is associated with hyperinsulinemia and with risk of type 2 diabetes, independent of general obesity (Maron et al., 1991; Parker et al., 1993; Marshall et al., 1997). The causal relationship between saturated fat intake and insulin resistance has been implicated by several lines of evidence in dietary intervention studies. Reducing saturated fat intake starting in infants for up to 9 years has been shown to be associated with an improvement in insulin sensitivity (Kaitosaari et al., 2006). Furthermore, another intervention study giving healthy subjects high-saturated fat diet for 3 months reported a 10% reduction of insulin sensitivity (Vessby et al., 2001).

Taken together, data from *in vitro* and *in vivo* studies suggest a clear association between elevated circulating FFA, especially saturated FFA, and insulin resistance.

1.2.6.2 Inflammatory cytokines and insulin resistance

Adipose tissues especially the visceral adipose tissues are not only considered as a temporary site fatty acids storage, but more importantly function as metabolically active organs, secreting adipokines including inflammatory cytokines such as

tumour necrosis factor α (TNF-α) and interleukin-6 (IL-6), leptin, adiponectin, and resistin. Overall, these molecules have significant effects on the regulation of body metabolism, the inflammatory response, and also are implicated in the development of insulin resistance. The following section is mainly focused on the role of the adipose tissue-related inflammatory cytokines TNF-α and IL-6 in insulin sensitivity. However, there is also more and more evidence showing that the inflammatory response in adipose tissue might due to the infiltration of macrophages (Surmi and Hasty, 2008).

TNF-α

TNF-α is a pro-inflammatory cytokine that has been implicated in the pathogenesis of insulin resistance (Borst, 2001). It is produced as a 26kDa cell surface transmembrane protein that undergoes cleavage to produce a 17kDa soluble, biologically active form. TNF-α exerts its biological effect by binding to TNF-α receptors (TNFR1 and TNFR2) on cell membranes (reviewed by Locksley et al., 2001).

There were controversial data on the role of TNF-α in contributing to insulin resistance. The production of TNF-α is observed to be increased in adipose tissues from virtually all obese and insulin resistant rodent models as well as human subjects (Kern et al., 1995; Hotamisligil et al., 1995; Saghizadeh et al., 1996). *In vitro* incubation of adipocytes with TNF-α caused a reduction in insulin-stimulated glucose uptake (Hotamisligil et al., 1994a) while in vivo treatment with TNF-α also caused a similar effect (Hotamisligil et al., 1994b). In

addition, animal studies using either genetically engineered TNF-α knockout mouse or experimentally neutralising TNF-α found an amelioration of insulin resistance, which further provided a direct link between TNF-α and insulin resistance (Uysal et al., 1997; Hotamisligil et al., 1993). However, inhibition of tumor necrosis factor (TNF)-α action using a recombinant-engineered human TNF-α-neutralising antibody failed to improve insulin sensitivity in obese type 2 diabetes human subjects (Ofei et al., 1996). Taken together, the existing data seem to support a more important role of TNF-α in rodent obesity-linked insulin resistance than in humans.

IL-6

IL-6 is another pro-inflammatory cytokine that has been associated with insulin resistance. It is secreted by several cell types, including immune cells, fibroblasts, endothelial cells, skeletal muscle, and adipose tissue. IL-6 circulates as a variably glycosylated protein with molecular weight 22-27kDa. IL-6 initiates its signal transduction cascade through binding to a transmembrane receptor which induces homodimerisation with another transmembrane receptor, gp130.

The association between IL-6 and insulin resistance is supported by epidemiological studies which show that plasma IL-6 levels are positively correlated with human obesity and insulin resistance (Vozarova et al., 2001; Kern et al., 2001). This association is further supported by the observation that weight loss causes a significant reduction of IL-6 levels in both adipose tissue and serum (Bastard et al., 2000). Compared to the epidemiological studies, the direct effects

of IL-6 on insulin sensitivity are less consistent. There is some evidence supporting a direct of role of IL-6 in inducing insulin resistance. For example, one in vitro study culturing hepatocytes with IL-6 reported an inhibition of insulin receptor signal transduction (Senn et al., 2002). However, the acute administration of IL-6 did not impair glucose homeostasis in healthy volunteers (Steensberg et al., 2003) and IL-6-deficient mice were not protected from development of obesity and glucose intolerance (Wallenius et al., 2002). More studies are required to clarify its role in insulin resistance.

1.2.7 Molecular mechanisms of insulin resistance

It is now widely acknowledged that the development of insulin resistance is a consequence of more than one molecular defect resulting from altered attenuated functional changes in both insulin signalling and effector molecules that mediate the various metabolic pathways activated by insulin. The effect of insulin on glucose transport and metabolism is one of the most important metabolic pathways associated with insulin resistance in skeletal muscle and adipose tissue.

Insulin receptor

The major defect of the insulin receptors in insulin resistance is the reduced insulin receptor tyrosine kinase activity rather than the number of receptors expressed on the cell membrane. Insulin receptor numbers are reduced in isolated adipocytes (Sinha et al., 1987) but remain normal or only slightly decreased in skeletal muscles from obese type 2 diabetes patients (Arner et al., 1987; Caro et al., 1987). In contrast, insulin receptor tyrosine kinase activity has been reported

to be reduced in both muscle and adipose tissue from obese rodents (Le Marchand-Brustel et al., 1985) and insulin-resistant individuals (Grasso et al., 1995).

IRS proteins

Insulin receptor substrate proteins (IRS-1 and IRS-2) play critical roles in mediating insulin signal transduction from the insulin receptor and PI3-kinase. There is much evidence indicating that the elevated ser/thr phosphorylation of IRS-1 (and possibly IRS-2) in muscle and adipose tissue is an important molecular defect contributing to insulin resistance in obesity and diabetes (reviewed by Le Marchand-Brustel et al., 2003). For example, the insulin resistance induced by TNF-α is associated with a marked increase in IRS-1 ser/thr phosphorylation through inhibiting the insulin receptor tyrosine kinase activity (Hotamisligil et al., 1996). Furthermore, *in vitro*, increased ser/thr phosphorylation of IRS-1 and IRS-2 caused an inhibition of IRS protein binding to the juxtamembrane region of the insulin receptor. This impaired the activity of the IRS protein as substrates for insulin-stimulated tyrosine phosphorylation (Paz et al., 1997).

PI3-kinase/PKB-signalling

The role of PI3-kinase and associated PKB signalling on insulin-stimulated glucose metabolism has been firmly established during the last two decades. Reduced PI3-kinase and PKB activity in skeletal muscles has been well documented in both obese and type 2 diabetic patients (Goodyear et al., 1995;

Krook et al., 1998; Baynes et al., 2000; Cozzone et al., 2008).

Glucose transporters

Glucose uptake in skeletal muscle and adipose tissue is mainly mediated by cell surface glucose transporters: GLUT1, responsible for non-insulin-stimulated glucose uptake and GLUT4, responsible for insulin-stimulated glucose uptake. The possible defects in glucose transporters are considered mainly as glucose transporter expression and translocation.

Total GLUT4 expression was reported to be reduced in adipose tissue of animals with obesity and type 2 diabetes (Tsakiridis et al., 1994) and also in isolated adipocytes from patients with type 2 diabetes (Sinha et al., 1991). However, there was no significant change in total GLUT4 proteins in skeletal muscle in type 2 diabetes patients (Handberg et al., 1990; Eriksson et al., 1992; Pedersen et al., 1990). The existing evidence suggests that the impaired GLUT4 translocation is the primary defect in insulin resistance.

1.2.8 Mechanisms of FFA-induced insulin resistance

The classical mechanism of FFA-induced insulin resistance proposed by Randle et al. (1965) was that fatty acids compete with glucose for substrate oxidation. The increased availability of fatty acids to skeletal muscle cells causes an increase in the intramitochondrial acetyl Coenzyme A (CoA)/CoA and Nicotinamide adenine dinucleotide/Nicotinamide adenine dinucleotide reduced form ($NADH/NAD^{+}$) ratios, which inactivates pyruvate dehydrogenase. This in turn would increase

intracellular citrate concentration leading to inhibition of phosphofructokinase, a key enzyme in controlling glycolysis. Consequent accumulation of glucose-6-phosphate would inhibit hexokinase 2 activity and result in an increase in intracellular glucose concentration and decreased glucose uptake. However, using ^{13}C and ^{31}P Nuclear Magnetic Resonance (NMR) spectroscopy technique, this hypothesis has been challenged and several studies reported that glucose-6-phosphate concentration is reduced during lipid-infusion–induced insulin resistance, indicating that glucose uptake and phosphorylation is the rate-limiting step in FFA-induced muscle insulin resistance (Roden et al., 1996; Dresner et al., 1999). Overall, these studies suggest that lipid oversupply to skeletal muscle contributes to the development of insulin resistance at the level of glucose uptake perhaps by promoting the accumulation of lipid metabolites that are capable of inhibiting signal transduction. Two major intracellular fatty acid metabolites that have been implicated in the development of insulin resistance are ceramide and diacylglycerol (DAG) (Fig.1.3).

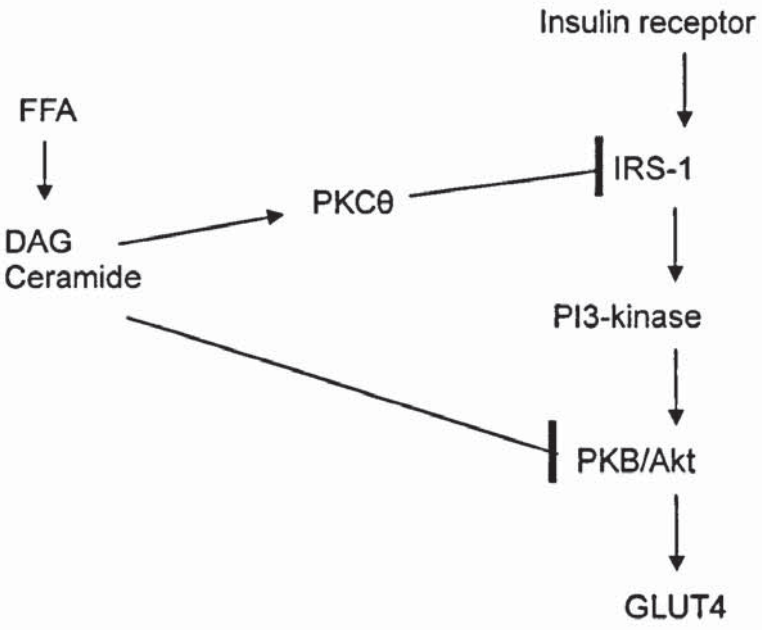

Figure 1.3 Molecular mechanisms of free fatty acid (FFA)-induced insulin resistance. The sites at which dacylglyceride (DAG) and ceramide inhibits insulin signal are also indicated. PKCθ, protein kinase Cθ; IRS-1, insulin receptor substrate-1; PI3-kinase, phosphatidylinositol 3-kinase; PKB/Akt, protein kinase B; GLUT4, glucose transporter 4.

Ceramide

Ceramide is a sphingolipid metabolite and acts as a second messenger in cellular signal transduction pathways where it may be responsible for cell proliferation, differentiation, apoptosis, cell adhesion, or migration. There are two major pathways to generate ceramide in cells (Fig.1.4). The first pathway, called the metabolic pathway, was described by Okazaki et al. (1989) and involves reversible ceramide formation from sphingomyelin catalyzed by sphingomyelinase (SMase). Two SMase enzymes have been reported to be involved in the hydrolysis of sphingomyelin to ceramide: the neutral SMase and the acid SMase (Augé et al., 2000). These pathways can be activated by adipokines such as TNF-α through increasing the activity of neutral SMase

(Sawada et al., 2004). Secondly, ceramide can be biosynthesized *de novo* from exogenous palmitate (the synthetic pathway) (Augé et al., 2000). This occurs in the endoplasmic reticulum (ER), starting from the condensation of serine with palmitoyl-CoA to give 3-ketosphinganine reduction which subsequently generates sphinganine (Merrill and Jones, 1990). Then following the activation of ceramide synthase, the N-acylation of sphinganine produces dihydroceramide with further desaturation resulting in ceramide (Michel et al., 1997).

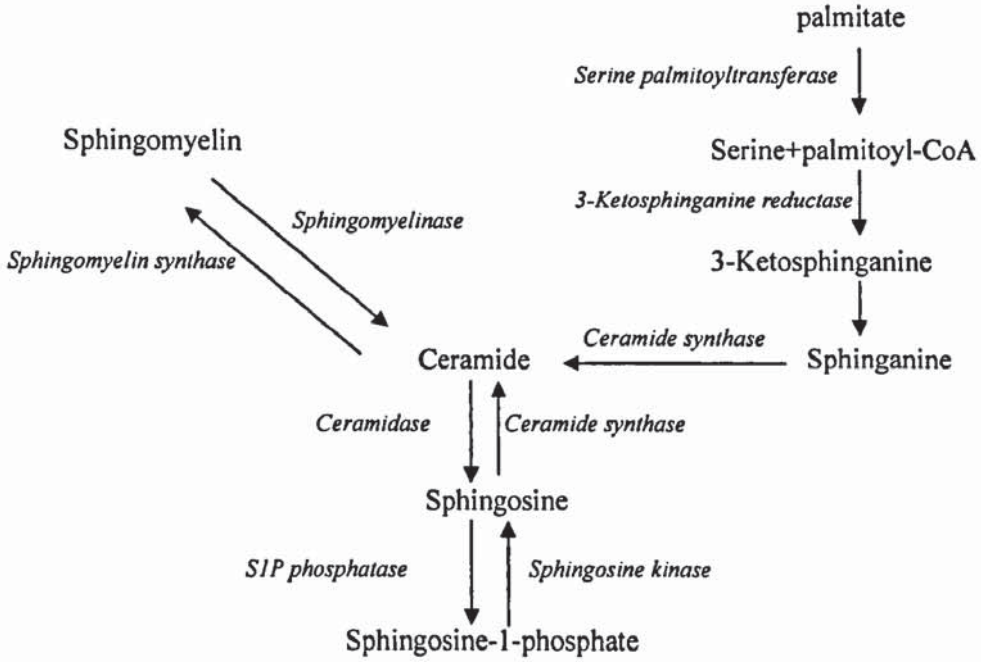

Figure 1.4 Ceramide synthesis pathways. Ceramide can be generated either through the hydrolysis of sphingomyelin or by *de novo* synthesis from palmitate.

Studies using muscle cells exposed to saturated FFAs such as palmitate or stearate strongly support a role for ceramide in saturated FFA-induced insulin resistance through its effect on different insulin signalling transduction pathways (Fig 1.4). Schmitz-Peiffer et al. (1999) first reported an increase in the intracellular pool of ceramide after treating C2C12 myotubes with physiological concentrations of saturated FFA palmitate, and this is associated with inhibition of PKB/Akt

activation. Similarly, Chavez et al. (2003) reported that the saturated FFA palmitate concomitantly increases the accumulation of ceramide and DAG, and inhibits PKB/ Akt activation. Importantly, the Chavez study demonstrated that only manipulation of ceramide metabolism rather than DAG led to the change in PKB/Akt activity, indicating a role of ceramide in mediating saturated FFA-induced insulin resistance. However, there are controversial data on the role of ceramide in mediating insulin resistance *in vivo*. Two epidemiological studies reported an increase in ceramide content in skeletal muscles in obese insulin resistant humans (Adams et al., 2004) and men at risk of developing type 2 diabetes (Straczkowaski et al., 2007). However, a recent study comparing total muscle ceramide content in individuals with normal insulin sensitivity, impaired glucose tolerance, and type 2 diabetes did not find a significant difference, indicating that ceramide content is not a major factor for muscle insulin resistance (Skovbro et al., 2008). In order to investigate the causal role of FFA in inducing insulin resistance, several lipid infusion studies were carried out. One study using lipid infusion further confirmed that palmitate-derived ceramide is the major component of ceramides in skeletal muscles in subjects who show insulin resistance after lipid infusion (Straczkoski et al., 2004). However, Yu et al. (2002) reported that there was no significant change in skeletal ceramide level in subjects after a 5h lipid infusion, indicating that ceramide is not associated with increased plasma free fatty acid-induced insulin resistance. The discrepancies between these studies might be due to the fatty acid amount and composition in the lipid infusion and duration of the challenge. More studies are required to clarify this issue.

The mechanism of ceramide-induced insulin resistance has been extensively studied using *in vitro* cultured muscle cells and adipocytes. Collectively, these studies indicate that a ceramide-induced defect in insulin signal transduction can occur through the activation of protein kinase Cζ (PKCζ) (Powell et al., 2004), down-regulation of GLUT4 gene transcription (Long et al., 1996) and GLUT4 translocation (Summers et al., 1998), decreasing tyrosine phosphorylation of the insulin receptor (IRS-1/IRS2) through activating phosphatase A2 (PPA2), increasing serine/threonine phosphorylation (Storz et al., 1999). Additionally, ceramide has been shown to play an important role in the lipid raft formation and stability (Xu et al., 2001). Therefore, it is possible that ceramide may affect the insulin signal transduction by altering the composition of lipid rafts since the insulin receptor and its down stream has been reported to be present in caveolae, a morphological correlate of rafts (Bickel, 2002).

DAG

DAG is another lipid intermediate metabolite that has been shown to be associated with lipid-induced insulin resistance (Yu et al., 2002; Montell et al., 2001). DAG can be either generated by the breakdown of phospholipids or through *de novo* synthesis via the esterification of long chain acyl CoA to glycerol-3-phosphate. The generation of DAG is specifically associated with saturated fatty acids rather than the unsaturated fatty acids (Montell et al., 2001; Coll et al., 2008). In biological systems, DAG functions as a potent activator of PKC and thereby mediates downstream phosphorylation (Marquez and Blumberg, 2003). However, recent studies also suggest that DAG is an important lipid intermediate strongly

associated with insulin resistance in skeletal muscle through interfering with insulin signalling transduction. First of all, the skeletal muscle DAG content has been shown to be increased in high-fat fed insulin resistant rats (Turinsky et al., 1990) and lipid-infusion-induced insulin resistant rats (Yu et al., 2002). Furthermore, in vitro incubation of skeletal muscle with saturated fatty acids caused an accumulation of DAG and desensitised insulin-stimulated glucose uptake (Montell et al., 2001). The possible mechanism of DAG mediated FFA-induced insulin resistance is related to its ability to activate PKCθ, the predominant PKC isoform in skeletal muscle. As a serine kinase, the activation of PKCθ has been shown to contribute to increased IRS-1 serine phosphorylation and associated reduced activity of PI3-kinase and reduced insulin-stimulated glucose uptake (De Fea and Roth, 1997).

1.3 Cardiovascular disease

Cardiovascular disease (CVD) refers to a class of diseases that affect the cardiovascular system including the heart and / or blood vessels (artery and vein). The main forms of CVD are coronary heart disease (CHD) and stroke.

CVD is the leading cause of global morbidity and mortality. According to the World Health Organisation report (2003), CVD is responsible for 30% of deaths in the general population. In type 2 diabetes, CVD is the principal complication and responsible for 60-65% of total death.

The underlying cause of CVD is atherosclerosis often associated with thrombosis. Atherosclerosis is a progressive condition characterised by the thickening of the

arterial wall mainly due to the accumulation of lipids and fibrous tissue in the inner wall of blood vessels, resulting in the narrowing of the artery lumen and reduced supply of oxygen to the heart.

1.3.1 Classification of atherosclerosis

Atherosclerosis is an intimal disease characterised by the formation of atheromatous plaques containing cholesterol and lipids in the inner layer of the vascular intima of large and medium-sized arteries including the aorta, the carotid arteries, the coronary arteries and the femoral arteries. The principal sites of atherosclerotic plaques are mainly in the artery vessel branching areas due to turbulent flow and shear forces. The development of atherosclerotic plaque is a chronic, progressive process. According to changes in the anatomical morphology of the lesions, atherosclerosis can be classified into three major stages: fatty streak, fibrolipid plaque, and complicated plaque with thrombus formation.

Normal artery

The normal artery consists of three distinct layers: the intima, the media, and the adventitia (Fig.1.5). The intima is composed of a thin layer of endothelial cells that forms a barrier in contact with the circulating blood within the lumen. The media is the middle, thickest layer of the vessel composed mainly of smooth muscle cells and a matrix of collagen, elastin, and proteoglycans. The adventitia is the outermost layer of the artery vessel containing fibroblasts, collagen, blood vessels, nerves, and lymphatics.

Fatty streak

The earliest lesion of atherosclerosis is called the fatty streak, which is even initiated in human infants and children (Napoli et al., 1997). It appears as either fatty spots less than 1mm in diameter or streaks 1 to 2 mm wide and up to 1cm long. The fatty spots or streaks are barely raised above the intimal surface. Each lesion is characterised by the focal accumulation of lipid-filled macrophages (foam cells) within the intima.

Fibrolipid plaque

The fibrolipid plaque is the most important pathologic lesion of atherosclerosis because it represents the clinical manifestation of the disease. It has a characteristic microanatomy with a core of extracellular lipid separated from the media by smooth muscle cells and usually covered by a thick cap of collagen-rich fibrous tissue composed of smooth muscle cells in a connective tissue matrix. Surrounding the lipid core are lipid-filled foam cells. Much of the lipid core is thought to be derived from the death of lipid-containing macrophage derived foam cells and the release of their intracytoplasmic content (Guyton and Klemp, 1996). The fibrolipid plaque may project into the arterial lumen and therefore reduce blood flow through the vessel.

Complicated plaque

The major complications of the fibrolipid plaque include calcification, thrombosis, plaque haemorrhage, and aneurysm, which subsequently contribute to the initiation of the clinical symptoms.

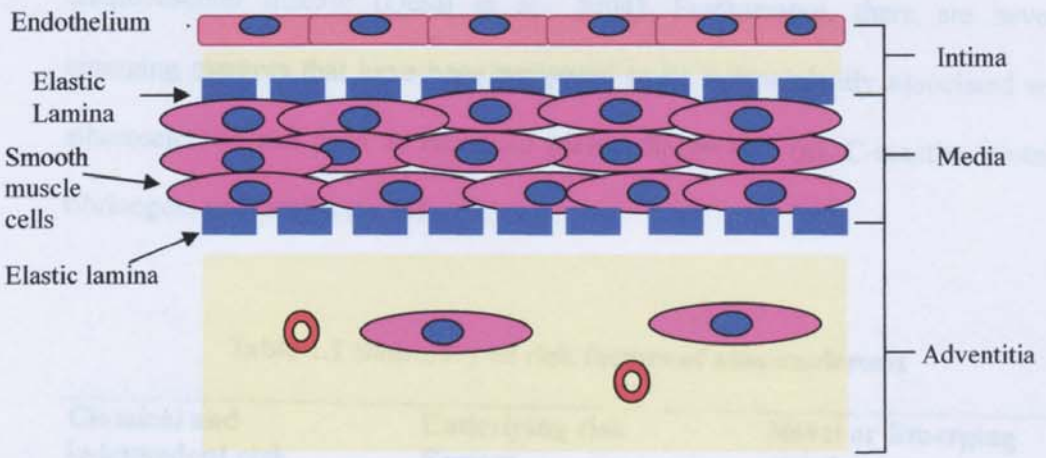

Figure 1.5 Cellular components of the normal artery (adapted from Ross and Glomset, 1976). The normal artery is composed by three distinct layers: the endothelium, the medium containing mainly sooth muscle cells and the adventitia.

1.3.2 Risk factors for atherosclerosis

The development of atherosclerosis involves multifactorial processes contributed to by genetic and environmental factors. The classification of risk factors contributing to this process is shown in Table 1.1.

Male sex, postmenopausal females, advancing age, family history of heart disease, tobacco smoking, higher plasma total and LDL cholesterol, lower plasma high density lipoprotein (HDL) cholesterol, hypertension, and diabetes are classical risk factors independently associated with increased risk of atherosclerotic heart disease (Solberg and Strong, 1983). Since there are large amount of mortality and morbidity related to cardiovascular disease can not be explained by the classical risks factors, other "conditional" and "underlying" risk factors such as physical inactivity (Berlin and Colditz, 1990; Leon and Connett, 1991) and obesity (Hubert et al., 1983; Manson et al., 1995) play an important role in the development of

cardiovascular disease (Desai et al., 2004). Furthermore, there are several emerging markers that have been suggested to be independently associated with atherosclerotic risk such as increased plasma lipoprotein (a), C-reactive protein, fibrinogen, and homocysteine.

Table 1.1 Summary of risk factors of atherosclerosis

Classical and independent risk factors (Solberg and Strong, 1983)	**Underlying risk Factors** (Desai et al., 2004)	**Novel or Emerging risk factors** (Anand et al., 2000)
Male sex	Diet and alcohol	Lipoprotein (a)
Age	Physical inactivity	C-reactive protein
Presence of atherosclerotic disease	Obesity and overweight	Fibrinogen
Family history of atherosclerotic disease	Psychosocial factors	Homocysteine
Smoking		Microalbuminuria and creatinine
Total cholesterol and LDL cholesterol		
HDL cholesterol		
Triglyceride		
High blood pressure		
Diabetes		
Genetic risk factors		

LDL: low density lipoprotein; HDL: high density lipoprotein.

1.3.3 Pathogenesis of atherosclerosis

The currently accepted mechanistic models for initiation of atherosclerosis include the response-to-injury theory and the oxidation theory (Steinberg and Witztum, 2002). According to both theories, endothelial dysfunction and LDL oxidation can cause increased circulating monocyte recruitment into sub-endothelial spaces, which is believed to be the earliest and the most critical event in atherogenesis. The

recruited monocytes then differentiate into macrophages, take up oxidised LDL and transform into lipid-laden foam cells forming fatty streaks, the earliest atherosclerotic lesion.

1.3.3.1 The response-to-injury hypothesis

The response-to-injury hypothesis, originally proposed as endothelial desquamation, is a key event in atherogenesis (Ross et al., 1977). However, due to a lack of definitive evidence *in vivo* that endothelial injury is either necessary or sufficient for lesion formation and the fact that the development of atherosclerotic lesion is covered by an intact endothelial layer throughout most stages of lesion progression (Taylor et al.,1989), a refined response-to-injury hypothesis is proposed and suggests that endothelial dysfunction is sufficient to initiate atherosclerosis through increased endothelial permeability to atherogenic lipoproteins (Ross, 1993). According to this theory, endothelial dysfunction increases endothelial permeability for entry of cells and plasma substances into the sub-endothelial space; enhances endothelial adhesiveness for leukocytes or platelets which cause endothelial cells to become pro-coagulant. Recruited leukocytes and platelets release vasoactive molecules such as platelet factor 4 (PF4), monocyte chemoattractant protein-1 (MCP-1), cytokines (e.g. IL-1, TNF-α), and growth factors (e.g. monocyte-colony simulating factor (M-CSF)) which promote an inflammatory response characterised by migration and proliferation of smooth muscle cells into the intima and the recruitment of macrophages into the arterial wall taking up deposited LDL to form lipid-laden foam cells (reviewed by Crowther, 2005). Accumulation of lipid and formation of

foam cells in turn promote the inflammatory response. Thus, the continued inflammation leads to the formation of advanced atherosclerosis.

Endothelium dysfunction

The normal, healthy endothelium regulates many important aspects of vascular homeostasis such as vascular tone, vascular smooth muscle cell proliferation, leukocyte adhesion and migration to and through the endothelium, thrombosis and thrombolysis (Kinlay et al., 2001). In response to various mechanical and chemical stimuli, endothelial cells produce and release a large number of vasoactive substances, growth modulators, and other factors that mediate these functions (Kinlay et al., 2001).

Endothelial dysfunction is characterised as a partial or complete imbalance between vasodilators and vasoconstrictors such as a reduced production of nitric oxide (NO) (Arnal et al., 1999) and an increased production of endothelin 1 (Luft, 2002). This leads to an impairment of endothelium-dependent vasodilatation which is considered as an early marker for atherosclerosis that may even precede the development of clinically detectable atherosclerotic plaques in the coronary arteries (Mano et al., 1996). The second characteristic of endothelial dysfunction is endothelial activation displayed as an increased expression of the pro-inflammatory factors (e.g. expression of endothelial adhesion molecules such as vascular cell adhesion molecule-1 (VCAM-1), intercellular adhesion molecule-1 (ICAM-1), E-selectin, and P-selectin), growth promoting and pro-coagulant factors. This dysfunction plays an important role in the initiation and progression of atherosclerosis by promoting the adhesion of leukocytes to the

artery and the proliferation and migration of smooth muscle cells into the subintimal spaces (Bonetti et al., 2003).

1.3.3.2 The oxidative modification hypothesis

This hypothesis is based on the observation that native LDL has no apparent atherogenic property but chemically modified LDL (e.g. oxidized LDL) is readily internalized by macrophages through a scavenger receptor pathway (Lougheed et al., 1996) by recognising the oxidised lipid and the modification of apoB-100 in LDL (Endemann et al., 1993; Andrews et al., 1995; Feng et al., 2000). LDL has been shown to be susceptible to oxidation in vitro (Hurtado et al., 1996). Also, the oxidised LDL could be taken up by the scavenger receptors expressed on macrophages and endothelial cells, which would transform into the foam cells (Endemann et al. 1993). Furthermore, oxidised LDL has been shown to stimulate the expression of MCP-1 in both smooth muscle and endothelial cells (Cushing et al., 1990; Navab et al., 1991), resulting in the recruitment of monocytes and lymphocytes into the intima; promote differentiation of monocytes into macrophages (Frostegård et al., 1990); and stimulating the proliferation of smooth muscle and endothelial cells (Rajavashisth et al., 1990). Taken together, these studies indicate that oxidised LDL plays a central role in the initiation and the progression of the atherosclerotic lesions.

1.3.4 Role of monocytes in atherosclerosis

Monocytes are a member of the leukocytes in the blood circulation and represent 3~8% of the total leukocyte population. They are usually identified in stained smears by their large bilobate nucleus. Monocytes are produced by the bone

marrow from haematopoietic stem cell precursors called monoblasts. After circulating in the bloodstream for about 1 to 3 days, monocytes migrate into various tissues throughout the body, where they undergo final differentiation into heterogeneous macrophages depending on the type of tissue.

Monocytes play a central role in the initiation and progression of atherosclerotic lesions. First of all, in response to inflammation, there is an increase in monocyte adhesion to the endothelium of the vessel wall, which triggers the initiation of the atherosclerotic lesion. Following subsequent transmigration into the subendothelial intima, these circulating monocytes differentiate into macrophages which take up the lipid such as Ox-LDL and in this way are transformed into foam cells forming fatty streak, the earliest clinical detectable lesion of atherosclerosis.

1.3.4.1 Monocyte adhesion to endothelium

Recruitment of monocytes from the peripheral blood into the intima of the vessel wall is a critical event in early atherogenesis. The current model for this emigration includes three distinct events which act together or in sequence (Fig 1. 6). The first step includes selectin-mediated transient adhesion events which allow circulating monocytes to tether and subsequently roll along the vessel wall. The second step involves a rapid activating signal which increases adhesion and arrests the cell by an integrin-dependent firm adhesion to the endothelium. The final step takes place by chemotaxis causing the transmigration of monocytes across the endothelial layer into the tissue. The adhesion molecules and its ligands mediating monocytes adhesion to endothelium are summarised in Table 1.2.

Several studies have suggested that the insulin resistant condition is associated with an increased ability of mononuclear cells to bind to the endothelium. For example, it has reported by Chen et al. (1999) that insulin resistance was significantly correlated with concentrations of soluble E-selectin, soluble ICAM-1, and soluble VCAM-1 in healthy subjects. Also, the CD11b expression has been reported to be significantly increased in monocytes and neutrophils in type 2 diabetic patients compared to healthy controls (Van Oostrom et al., 2004). Furthermore, another study showed an enhanced neutrophil CD11b expression after *ex vivo* stimulation in comparison with controls in patients with type 2 diabetes (Senior et al., 1999). Collectively, these studies suggest that insulin resistance may predispose individuals to coronary heart disease by activation of cellular adhesion molecules.

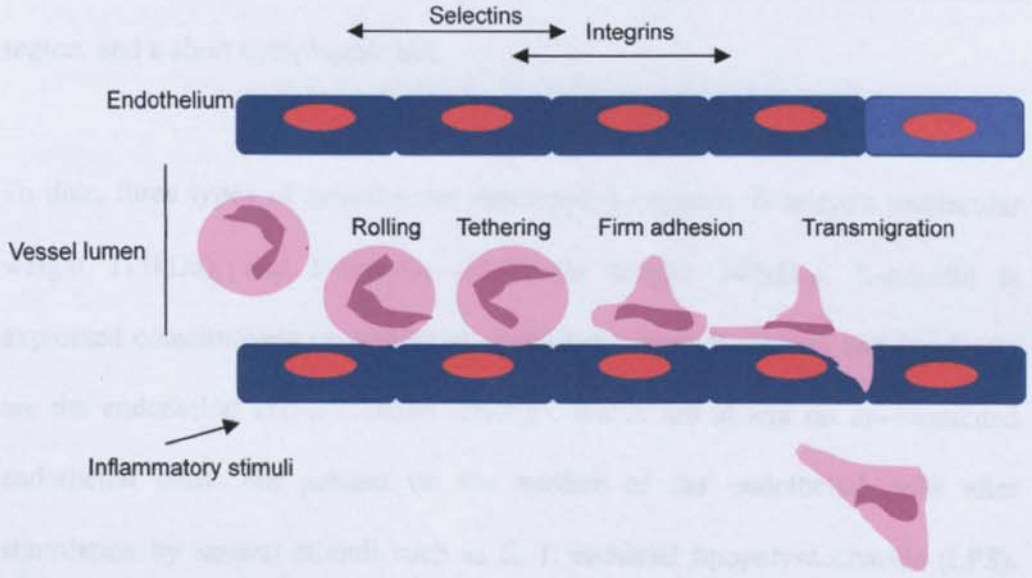

Figure 1.6 Leukocytes adhesion cascade (adapted from Quehenberger, 2005) The circulating leukocytes adhesion to endothelium includes selectin-mediated rolling and tethering and integrin-mediated firm adhesion.

Table 1.2 Adhesion molecules and ligands known to play a role in atherosclerosis (Galkina and Ley, 2007)

Adhesion Molecule	Ligand	Expressing Cells
P-selectin	PSGL-1	Endothelial cells
E-selectin	PSGL-1	Endothelial cells
L-selectin	CD34	Monocytes, PMN
ICAM-1	CD11a/CD18 CD11b/CD18	Monocytes, PMN. Lymphocytes
VCAM-1	CD49d(VLA-4)	Monocytes, PMN
PECAM-1	PECAM-1	Monocytes, PMN, EC, lymphocytes

EC: endothethial cells; ICAM-1: Intercellular adhesion molecule-1; PECAM-1: Platelet/endothelial cell adhesion molecule-1; PMN: polymorphonuclear leukocytes; PSGL-1: P-selectin glycoprotein-1 ligand; VCAM-1: Vascular cell adhesion molecule-1; VLA-4: Very late antigen-4.

Selectins

The selectins are a family of glycoproteins with specific structural moieties in common: an amino terminal lectin-like domain, followed by an epidermal growth factor-like domain, numerous cysteine-rich tandem motifs, a transmembrane region, and a short cytoplasmic tail.

To date, three types of selectins are described: L-selectin, E-selectin (molecular weight 115kDa), and P-selectin (molecular weight 140kDa). L-selectin is expressed constitutively on almost all leukocytes. Both P-selectin and E-selectin are the endothelial cell-associated selectins, which are absent on un-stimulated endothelial cells, but present on the surface of the endothelial cells after stimulation by several stimuli such as IL-1, bacterial lipopolysaccharide (LPS), thrombin, phorbol esters, and TNF-α (Krieglstein and Granger, 2001). The major ligands for all three selectins are highly fucosylated and sialylated carbohydrates (Varki, 1994; Ley and Kansas, 2004)

The major function of selectins as adhesion molecules is to target leukocytes to areas of inflammation or atherosclerosis-prone sites by causing a transient adherence of leukocytes to the activated endothelium termed as tethering and rolling. Among these three selectins, P-selectin has been implicated as a critical molecule in atherosclerosis especially the initiation of this process. The direct support for this hypothesis comes mostly from various studies using transgenic mice. For example, P-selectin-knockout mice (P-selectin -/-) subjected to a high-fat diet for 20 weeks were found to be significantly less prone to fatty streak formation than the wild type (Dong et al., 1998). The combination of the P-selectin and LDL receptor (LDLR) knockout mice (P-selectin -/- and LDLR -/-) under the high-fat diet for 8weeks developed significantly smaller fatty streaks than the wild type. Furthermore, it has been reported that in apoE-deficient mice (Apo E -/-) which spontaneously develop atherosclerotic lesions even fed with a standard Chow diet for 20 weeks, the size of fibrous plaque lesions was reduced to 25% in P-selectin -/- mice compared to that in mice with wild type P-selectin (Dong et al., 2000). There is one study using *ex vivo* monocyte adhesion to mouse aorta which has shown that the adherence and rolling of the U937 monocytes on the carotid artery isolated from ApoE -/- mice fed with a high-fat diet for 4-5 weeks was significantly reduced when P-selectin or its ligand P-selectin glycoprotein-1 ligand (PSGL-1) was blocked by specific antibodies (Ramos et al., 1999).

Although the role of selectins in atherosclerosis has been established by the fact that deletion of P and E selectin markedly reduces atherosclerotic lesions in

several transgenic mouse models such as LDLR -/- mice and ApoE -/- mice (Dong et al., 1998), only integrin-mediated firm adhesion of monocytes to the endothelium can cause the subsequent monocyte extravasations.

Integrins

The integrins are a broad family of receptors that mediate a large number of cellular interactions. In the vasculature, platelets, endothelial cells, smooth muscle cells, fibroblasts, and leukocytes express one or more integrin proteins and use these integrins to mediate cell-cell and cell-matrix interactions.

All integrins are composed of an α- and a β-subunit, which bind noncovalently to form a heterodimer. Each subunit consists of a relatively large NH_2-terminal extracellular domain, a single transmembrane domain, and a COOH-terminal cytoplasmic tail. 16 α subunit and 8 β subunit are reported at present.

Monocytes express both β_1 and β_2 integrins, which interact with adhesion molecules expressed on endothelium and mediate the adhesion of monocytes to the endothelium. The β_1 integrin family consists of at least six different heterodimer complexes (β_1 subunit complexed with one of the six α subunits (α_1-α_6) and act as receptors for fibronectin, collagen, and laminin. Among the β_1 integrins expressed on monocytes, Very Late Antigen-4 (VLA-4, $\alpha_4\beta_1$) has been reported to have an important role in regulating monocyte entry into early and advanced atherosclerotic lesions (Shih et al., 1999; Patel et al., 1998). It was also suggested by *in vitro* studies that the VLA-4 integrin mediates the adhesion of

monocytes to cytokine-stimulated endothelial cells (Elices et al., 1990) through interactions with its ligand VCAM-1. The β_2 integrins consist a common β_2 chain (CD18), but different α subunits (α_L or CD11a, α_M or CD11b or Mac-1, α_X or CD11c, α_D or CD11d). CD11b is the most abundant α-subunit of integrin expressed on monocytes. The ligands for β_2 integrins include extracellular matrix proteins such as fibronectin and adhesion molecule (ICAM-1) on endothelium to mediate the cell-matrix and cell-cell interactions.

The integrin-mediated firm adhesion of monocytes to endothelium requires the activation of integrin. Integrin activation can be referred to as an increase in the affinity of the receptor for ligand and/or an increase in avidity on the cell surface (Van Kooyk and Figdor, 2000; Hogg et al., 2002). Studies have shown that integrins have ligand binding sites on both α and β subunits (Takada et al., 2007). There are three major regions called the α subunit I-domain, the seven NH_2-teminal repeats of the α subunit, and a conserved region of the β subunits that appears to be a functional and structural homologue of the α subunit I-domain (Calderwood, 1997).

The first form of integrin activation is a conformational change of integrin I-domain which causes a greater receptor-ligand binding strength (higher affinity). For example, divalent cations such as Mg^{2+} and Mn^{2+} have been shown in vitro to induce integrin conformational change into high affinity states by binding to a region near to the N-terminus called metal ion dependent adhesion site (MIDAS) (Mould and Humphries, 2004).The second form of integrin activation is an

increase of integrin expression on the cell surface caused by enhanced mobilization of intracellular stored integrins to the cell surface to increase the overall binding strength. PMA is one of the typical reagents used in vitro to increase leukocytes' (e.g. neutrophil and monocyte) integrin (CD11b) expression in both short-term (10-30 min) (Siddiqi et al., 2001) and longer-term (24h-72h) (Miranda et al., 2003). The short-term effect of PMA on increasing integrin expression is through activating PKC and Ras guanyl nucleotide-releasing protein (RasGRP) (Tognon et al., 1998; Zheng et al., 2005) while the long-term effect is through inducing monocyte differentiation. In addition, inflammatory cytokines have been reported to be potent stimuli of integrin activation. C-reactive protein has been shown to increase the cell surface CD11b expression on human monocytes within 30min (Woollard et al., 2002).

VCAM-1

VCAM-1 is the receptor for the ligand for VLA-4 and belongs to a class of immunoglobulin superfamily protein (molecular weight of 100-119kDa). VCAM-1 is not normally expressed on resting endothelial cells, but is induced on the surface of endothelial cells after stimulation during incubation with specific cytokines such as IL-1 and TNF-α. *In vitro*, the level of endothelial cell surface VCAM-1 expression has been reported to peak at 6-10h and persist for 48-72h after IL-1 or TNF-α stimulation (Osborn et al., 1989; Carols et al., 1990). VCAM-1 has been suggested to play a unique role in the early stage of atherosclerosis. First of all, the expression of VCAM-1 has been shown to be rapidly induced from undetectable expression level under baseline conditions to a

high expression level in early lesions and lesion-prone regions by pro-atherosclerotic conditions in mice (Nakashima et al., 1998) and humans (O'Brien et al., 1993). Secondly, the partially VCAM-1 knockout mouse with an LDLR-/- genetic background and given a cholesterol-rich diet for 8 weeks showed a significant reduction in the areas of early atherosclerotic lesions compared to wild-type (Cybulsky et al., 2001). These studies provide direct evidence of the role of VCAM-1 in the development of atherosclerosis. In addition to the role of VCAM-1 and VLA-4 β_1 integrin mediated firm adhesion of monocytes to endothelium; VCAM-1 is also involved in the initial tethering and rolling step (Alon et al., 1995; Berlin et al., 1995). Finally, the firm adhesion is mediated by the interaction between VLA-4 and VCAM-1. Firm adhesion occurs without chemokine-mediated conformational change of VLA-4 (Gerszten et al., 1996), indicating that VCAM-1 can directly regulate the adhesion of monocytes to the endothelium.

ICAM-1

ICAM-1 is another member of the immunoglobulin superfamily of adhesion protein (molecular weight of 100kDa). Unlike the expression pattern of VCAM-1, ICAM-1 is expressed constitutively at low levels on the surface of endothelial cells and also can be induced by cytokine stimulation such as IL-1 and TNF-α within 4-6h and with maximal expression at 24h (Kevil et al., 2001). As an adhesion molecule, ICAM-1 is also implicated in the process of atherosclerosis. The expression of ICAM-1 is up-regulated at atherosclerosis-prone sites on the endothelium in the ApoE-deficient mice (Nakashima et al., 1998) and correlates

with increased infiltration of monocytes (Scalia et al., 1998). The direct evidence for its involvement in CVD comes from transgenic mice studies in which C57BL/6 mice depleted of ICAM-1 receiving a high-fat diet showed a significant reduction in aortic lesion size compared to wild-type (Nageh et al., 1997; Collins et al., 2000). ICAM-1 mediates monocyte adhesion to the endothelium via interacting with the β_2 integrins such as CD11b/CD18 and CD11a/CD18. Studies using antibody to block ICAM-1 and CD11b/CD18 in hypercholesterolaemic mice showed inhibition of mononuclear cell recruitment into the aortic intima (Nie et al., 1997). Furthermore, mice with a mutation in the gene of the common CD18 subunit of β_2 integrins showed a reduction in the aortic size when fed with a high-fat diet (Nageh et al., 1997).

1.3.4.2 Formation of foam cells

Following the transmigration of monocytes into the sub-endothelial layer of the intima, the major fate of monocytes is to differentiate into macrophages, generate oxidizing radical species, take up oxidised lipoproteins/lipids, and transform into lipid-laden foam cells. The formation of foam cells (also called the fatty streak) is the hallmark and the earliest clinically detectable atherosclerotic lesion. It is achieved by the accumulation of cholesteryl ester from oxidised LDL in macrophages via scavenger receptors (Table 1.3).

Table 1.3 Macrophage scavenger receptors that bind lipoproteins (van Berkel et al., 2005)

Receptors	Ligand	Expressing Cells
Scavenger receptor class A, type I and II (SR-A AI/II)	Ox-LDL, Ac-LDL, long chain fatty acids	Φ, SMC
CD36	Ox-LDL, long chain fatty acids	Φ, monocytes, platelets, SMC
CD68	Ox-LDL	Φ, neutrophils, mast cells
Scavenger receptor class B, type Ⅰ (SR-B Ⅰ)	HDL	Φ, epithelial cells
Lectin-like ox-LDL receptor-1 (LOX-1)	Ox-LDL	Φ, SMC
Scavenger receptor-phosphatidylserine and oxidized lipoprotein (SR-PSOX)	Ox-LDL	Φ

Ox-LDL: oxidised low-density lipoprotein; Φ: macrophages; SMC: smooth muscle cells.

Since the first macrophage scavenger receptor was cloned in 1990, 8 subclasses of receptors have been characterised with different structures that can bind and internalise a wide range of polyanionic ligands, including modified forms of LDL (Matsumoto et al., 1990; Freeman, 1997). Among all the scavenger receptors, scavenger receptor A type I and II (SRAI/II) and CD36 have been implicated to play important roles in the macrophage uptake of modified LDL and the development of atherosclerosis.

SR-A

SR-AI/II was the first macrophage scavenger receptor to be purified and cloned (Kodama et al., 1990; Rohrer et al., 1990). SR-AI/II are expressed not only on the cell surface of tissue macrophages, but also detected on macrophage foam cells

and on aortic endothelial cells within atherosclerotic plaque (Naito et al., 1992; Daugherty et al., 1997). Regarding the uptake of lipid, these receptors have been shown in vitro to mediate the majority (~80%) of macrophage uptake of acetylated LDL and ox-LDL through recognising the modified Apo B protein component (Kunjathoor et al., 2002; Zhang and Yang, 1993). However, data from in vivo transgenic animal studies on the role of SR-A in atherosclerosis are controversial. Studies using hyperlipidemic mouse models with depletion of SR-AI/II gene demonstrated a marked reduction (80% to 85%) in lesion area and arterial lipid accumulation (Sakaguchi et al., 1998; Babaev et al., 2000). However, mice overexpressing the SR-A in either LDLR -/- or ApoE -/- genetic backgrounds did not further exacerbation of the atherosclerosis lesions and in contrast showed a 74% reduction in atherosclerotic lesion sizes in the aortic arch (van Eck et al., 2000; Herijgers et al., 2000).

CD36

CD36 is an 88 kDa plasma membrane glycoprotein originally identified in the late 1980s as glycoprotein IV, a platelet receptor that bound thrombospondin and *Plasmodium falciparum* parasitized erthrocytes (Silverstein et al., 1989; Oquendo et al., 1989). CD36 is expressed on a wide range of cell types such as monocytes/macrophages, endothelial cells, platelets, and myotubes (Greenwalt et al., 1992). The role of CD36 in lipid uptake was suggested by Endemann et al. (1993) that CD36 was a macrophage receptor for taking up moderately ox-LDL. In the formation of atherosclerotic lesions, CD36 has been demonstrated in vitro to be the major receptor mediating the uptake of ox-LDL uptake by macrophages,

contributing 60% to 70% of cholesterol ester accumulation in macrophages exposed to either Cu^{2+}- or myeloperoxidase/peroxynitrite-oxidised LDL (ox-LDL; Huh et al., 1996; Kunjathoor et al., 2002; Podrez et al., 2000). The component in ox-LDL recognised by CD36 is a class of oxidised phosphatidylcholine molecules (Podrez et al., 2002). *In vivo*, studies using ApoE -/- mice with CD36 knock out fed with a high-fat diet for 12 weeks showed a significant decrease (76%) in atherosclerotic lesion area compared to ApoE -/- control mice (Febbraio et al., 2000). This further supports the role of CD36-mediated ox-LDL uptake in the formation of foam cells and atherosclerosis. A similar result is observed in less hyperlipidemic ApoE -/- mice fed a chow diet with a daily CD36 ligand injection for 4-12 weeks (Marleau et al., 2005). Furthermore, transplantation studies have demonstrated that ApoE -/- mice with CD36-/- bone marrow resulted in a large reduction in aortic lesions in hypercholesterolemic mice, indicating that macrophage CD36 may also contribute to atherosclerotic lesion progression (Febbraio et al., 2004).

Others

There are also other scavenger receptors such as lectin-like ox-LDL receptor-1 (LOX-1) and Scavenger receptor-phosphatidylserine and oxidized lipoprotein (SR-PSOX) that have been identified as receptors for oxidised LDL (ox-LDL) (Sawamura et al., 1997; Minami et al., 2001). Although there is some evidence showing that these receptors are expressed in macrophages in atherosclerotic lesions of humans and hyperlipidemic mice (Kataoka et al., 1999; Chen et al., 2000), more studies are needed to further clarify their direct role in

atherosclerosis.

1.3.4.3 Monocyte/macrophage-induced inflammatory response

It is now widely accepted that atherosclerosis is an inflammatory disease. This is supported by the observation that many inflammatory cells such as monocyte-derived macrophages and T lymphocytes are present in atherosclerotic lesions (Jonasson et al., 1986). Cytokines such as TNF-α, IL-1-β produced by these inflammatory cells are found in the atherogenic lesions. These cytokines, through different pathways, can accelerate the formation of foam cells and the progression of atherosclerotic lesions. One possible way is that both TNF-α and IL-1β are potent monocyte and endothelium activators, consequently causing more monocyte adhesion to the endothelium through the up-regulation of adhesion molecule expression on monocytes and the endothelium (Szmitko et al., 2003). Another pathway could be inducing the secretion of reactive oxygen species which further contribute to the oxidation of LDL (Shoelson et al., 2006).

1.4 Hypothesis

Obesity-induced insulin resistance is caused by FFA partly via altered ceramide metabolism in peripheral tissues. Both obesity and insulin resistance are important risk factors for atherosclerosis, and an elevated plasma FFA level is a common feature of individuals with obesity/insulin resistance. Therefore, it is possible to postulate that obesity/insulin resistance may contribute to the development of atherosclerosis by increased FFA via altered ceramide metabolism and functional disturbances in inflammatory cells (Fig1.7).

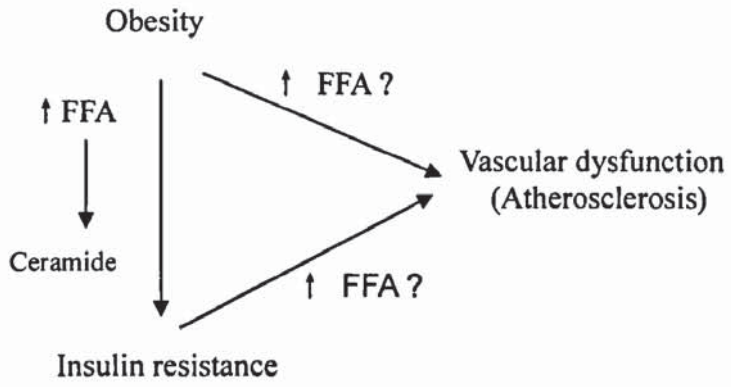

Figure 1.7 Hypothesis of the project. FFA: free fatty acids.

1.5 Aims

The aim of this project is to investigate whether saturated fatty acid-induced insulin resistance contributes to changes in monocyte function and any role for altered ceramide metabolism in these effects.

This will be achieved through the following objectives:

- To investigate the induction of insulin resistance in monocytes by culturing cells (monocytes and myotubes) with free fatty acids (palmitate and oleate).

- To investigate the effect of free fatty acids (palmitate and oleate) on CD11b and CD36 expression on monocytes and the adhesion of monocyte to endothelium/the endothelial receptor ICAM-1.

- To investigate whether inhibition of ceramide synthesis can prevent any change in insulin sensitivity and monocyte phenotype due to free fatty acids.

Chapter 2

Materials and Methods

2.1 Preface

This chapter describes the general methods used within this thesis, including cell culture, preparation of fatty acid-bovine serum albumin (BSA) solutions, flow cytometry, 2-deoxy-D-[^{3}H] glucose uptake, monocyte adhesion assay, intracellular reactive oxygen species (ROS) measurement, cell viability assays, sodium dodecyl sulphate polyacrylamide gel electrophoresis (SDS-PAGE) and western blot. This thesis developed the methods for cell surface receptor expression by flow cytometry, western blot for glucose transporters, and monocyte adhesion to ICAM-1-Fc and aorta. Fatty acids conjugation to BSA, ROS measurement, 2-deoxy-D-[^{3}H] glucose uptake, protein assays and cell viability assays were already in place.

2.2 Cell Culture

Materials

All gases were from BOC Ltd (Guildford, UK).

The human monocyte cell lines U937 and THP-1 and rat L6 skeletal muscle cell line were purchased from Health Protection Agency Culture Collections (Porton Down, Salisbury UK).

Foetal bovine serum (FBS), RPMI 1640 (UltraGlutaMax), Dulbecco's modified Eagle's medium (DMEM, high glucose), Trypsin-EDTA solution (0.05% trypsin, 0.53mM EDTA), Penicillin (100U/ml) and Streptomycin (100μg/ml) were obtained from Cambrex (Verviers, Belgium). Trypan Blue solution (0.4%) was purchased from Sigma (UK). Lymphoprep was from Axis-shield (Nycomed

Pharma AS, Oslo, Norway).

Methods

2.2.1 U937 and THP-1 Monocytes

Monocytes were routinely maintained in RPMI 1640 medium containing 11mM glucose, supplemented with 10% heat-inactivated foetal bovine serum (FBS), with 100U/ml penicillin and 100μg/ml streptomycin. Cells were grown at 37°C in a humidified 5% CO_2/95% air incubator. U937 cells were passaged every 3 or 4 days and THP-1 cells were passaged every 5 or 6 days. The number of viable cells was determined by trypan blue exclusion using a Neubauer haemocytometer. Cell densities were maintained between $1\sim10\times10^5$/ml and cells in exponential growth phase were used for experimentation.

2.2.2 EAhy926 endothelial cells

Eahy926 cells were a kind donation from Dr D Lamb (University of Surrey). EAhy926 endothelial cells were maintained in Dulbecco's modified Eagle's medium (DMEM) medium containing 25mM glucose supplemented with 10% heat-inactivated foetal bovine serum (FBS) with 100U/ml penicillin and 100μg/ml streptomycin and 100μM hypoxanthine, 0.4μM aminopterin, 16μM thymidine (HAT), which is referred as DMEM complete medium. Cells were grown in T75 flasks at 37°C in a humidified 5% CO2/95% air incubator.

EAhy926 cells were passaged at a ratio of 1:10 after removal from the flask with Trypsin–Ethylenediaminetetraacetic acid (EDTA) every 3 or 4 days. In brief, the

cell monolayer was gently washed twice with 10ml sterile PBS, then incubated with 2.5ml pre-warmed Trypsin–EDTA for 2min at 37°C to dislodge adherent cells from flasks. After incubation with DMEM (5ml) containing 10% FBS to neutralise trypsin activity, cells were transferred to 20ml universal tubes and centrifuged at 150g for 5min. The supernatant was then removed and the cell pellets were re-suspended into DMEM complete medium. Viable cells were determined by trypan blue exclusion using a Neubauer haemocytometer.

2.2.3 L6 skeletal muscle cells

Rat L6 myoblasts were maintained in DMEM containing 5% heat-inactivated foetal bovine serum (FBS) (v/v), 25mM D-glucose, 1mM sodium pyruvate, 1mM L-glutamine, 100U/ml penicillin and 100μg/ml streptomycin. Cells were grown at 37°C in a humidified 5% CO2/95% air incubator and were passaged at a ratio of 1:15 after removal from the flask with Trypsin–EDTA every 3 days as for EAhy926 cells. Experiments were undertaken in 24-well plates seeded from preconfluent flasks with 5×10^4 cells/ml. The cells were grown to reach ~70-80% confluence and the medium was changed to DMEM containing 0.5% FBS for 24h to induce differentiation and fusion of myoblasts into myotubes for subsequent experimentation.

2.2.4 Primary mononuclear cell (MNC) isolation and culture

2.2.4.1 Separation of MNC from whole blood

Peripheral blood mononuclear cells (MNC) were isolated by density gradient

centrifugation using Lymphoprep. 25ml venous blood was obtained from consenting healthy adults and mixed with sterile 4% sodium citrate at 9:1 ratio to prevent coagulation. Under sterile conditions, the whole blood was diluted with pre-warmed sterile PBS/0.1%BSA solution at 1:1 (v/v) ratio. The diluted blood (25ml) was carefully layered onto 15ml lymphoprep solution in 50ml conical tubes. Tubes were then centrifuged at 160×g (Sigma benchtop centrifuge Type 1-13, rotor # 12027, Osterode am Harz, Germany) for 15min at 20°C. Then the top plasma-platelet layer was removed by aspiration until 1.5ml remained above the buffy coat. Tubes were then centrifuged at 350×g for 20min at 20°C. MNC was collected from the interface between the plasma and lymphoprep by gentle suction using a Pasteur pipette and transferred to 15ml conical tubes. The cell suspensions were diluted 1:10 with phosphate buffered saline (PBS)/0.1%BSA and washed three times with PBS/0.1%BSA by centrifugation at 225×g for 10min at 4°C. The typical recovery of MNC is 90% and the purity of MNC fraction is 85%.

2.2.4.2 MNC cell culture

MNC at 10^6/ml were cultured in RPMI 1640 medium supplemented with 10% FBS, 100U/ml penicillin and 100μg/ml streptomycin at 37°C in a humidified 5% CO_2/95% air incubator.

2.3 Conjugation of fatty acids to BSA

Materials

Glucose-free RPMI 1640 was from Lonza (Verviers, Belgium). Sodium palmitate,

sodium oleate and fatty-acid-free BSA were from Sigma (Poole, Dorset, UK).

Principle

Free fatty acids (also called non-esterified fatty acids) circulate in the bloodstream mainly in the form of free fatty acid-albumin complexes so that they can be transported into target tissues to be metabolised or stored (Fig.2.1). Albumin acts as a carrier of free fatty acids through two different binding affinities and 6 binding sites. In this way, there is only low concentration of fatty acids which are unbound in plasma (Spector and Fletcher, 1978). The number of unbound fatty acids is dependent on the molar ratio of total fatty acids to plasma BSA. The higher the molar ratio, the more unbound fatty acid remains. The molar ratio for free fatty acids and albumin is between 1 and 3 under physiological conditions and can be increased in disease states. It has been reported that under pathophysiological conditions such as coronary heart disease there is an elevation in plasma free fatty acid level, however, the plasma albumin level is relatively stable or decreased (Kleinfeld et al., 1996; Hostmark, 2003). This consequently causes a higher fatty acid/albumin molar ratios and an increase in plasma unbound free fatty acid.

Figure 2.1 Free fatty acids (FFA) and plasma albumin equilibrium. (Richieri and Kleinfeld, 1995)

Methods

A stock solution of palmitate (200mM) and oleate (100mM) were prepared by dissolving sodium palmitate and sodium oleate into 70% ethanol in 0.1M NaOH at 60°C for palmitate and at room temperature for oleate for 4h as described previously (Zhang et al., 2006). Fatty acids were then complexed with 5% fatty acid-free BSA using a concentration of 5mM fatty acid at 37°C, stirring for 4h and adjusted to pH 7.4. After sterilising through a 0.2μm filter, solutions were stored at 4°C for no longer than 2 weeks. A control solution was made by mixing 70% ethanol in 0.1M NaOH with BSA in the absence of fatty acids. The final fatty acids to BSA ratio is 2:1 for experimental conditions using monocytes and 6:1 for experimental conditions using L6 skeletal muscle cells.

2.4 Flow Cytometric analysis of cell surface antigens

Materials

Mouse anti-human monoclonal CD11b-PE (IgG) antibody, mouse anti-human CD36-FITC (IgG), mouse anti-human CD206-PE (IgG) antibody and mouse anti-human CD14-PE-Cy5 (IgG) antibody and appropriate negative control antibodies were purchased from Serotec (Oxford, UK). 1% sodium hypochlorite and human IgG were from Sigma. Isoton diluent II was from Beckman-Coulter (High Wycombe, Buckinghamshire, UK).

Principles

Flow cytometry can be used to quantify the relative level of specific cell antigens which have been fluorescently labelled. Antibodies conjugated with fluorophores such as phycoerythrin (PE) or fluorescein isothiocyanate (FITC) can label specific cell surface antigens in non-permeabilised cells. Total cellular DNA can be labelled e.g. with propidium iodide after cells are fixed and permeabilised. When the cell suspensions are passed through the flow cytometer laser beam, the cell surface antigens can be determined according to the fluorescence intensities and cells can be further distinguished according to the cell size (forward scatter) and granularity (side scatter).

Methods

2.4.1 Measurement of the expression of cell surface CD11b, CD36 and monocyte differentiation marker CD206 in viable U937 monocytes

After various treatments, U937 monocytes were incubated in RPMI 1640 medium

containing 10% FBS and leave on ice for 15min to block Fc receptors. Cells were then incubated with a saturating concentration of monoclonal mouse anti-human antibodies CD11b-PE or CD36-FITC or CD206-PE for 30 min on ice in the dark. Negative controls were prepared by mixing cells randomly taken from four wells and incubating with isotype negative antibodies under the same conditions. After incubation, the monocytes phenotype was determined by measuring the expression of cell surface integrin CD11b, scavenger receptor CD36, and monocyte differentiation marker mannose receptor CD206 using flow cytometry. Data was acquired from 10,000 cells. Data were expressed as median fluorescence intensity (MdX).

2.4.2 Measurement of the expression cell surface CD11b in viable mononuclear cells (MNC)

The expression of cell surface integrin CD11b was determined in $CD14^+$ cell population which represents monocytes in mononuclear cells isolated from whole blood. After various treatments, MNC were collected into 1.5ml Eppendorf tubes and centrifuged at 2000×g for 5min. After removal of supernatant, cell pellets were resuspended into 100μl Fc receptor blocking buffer (PBS/0.1%BSA/10μg/ml human IgG) for 30min on ice. Cells were incubated with antibodies (anti-human CD14-PE-Cy5 and anti-human CD11b-PE) for a further 30min on ice in the dark. In order to measure the viable cell CD11b expression, cells were incubated with propidium iodide (PI) after staining with antibodies. PI is a fluorescent molecule with a molecular mass of 668.4 Da that can be used to stain DNA. It is excluded by viable cells but can penetrate cell membranes of dying or dead cells. Therefore,

it can be used to distinguish necrotic, apoptotic and normal cells when combined with forward scatter parameter by flow cytometry (Mangan and Wahl, 1991).

After antibody staining, cells were washed three times with washing buffer (PBS/0.1%BSA/1μg/ml human IgG) and resuspended in 1ml PI solution (25μg/ml PI in PBS/0.1BSA/1μg/ml human IgG) for 15min on ice in the dark. CD11b expression on primary monocytes was immediately determined by counting 5000 $CD14^+$ PI negative (viable) cells and expressed as MdX (Fig.2.2 A-G.).

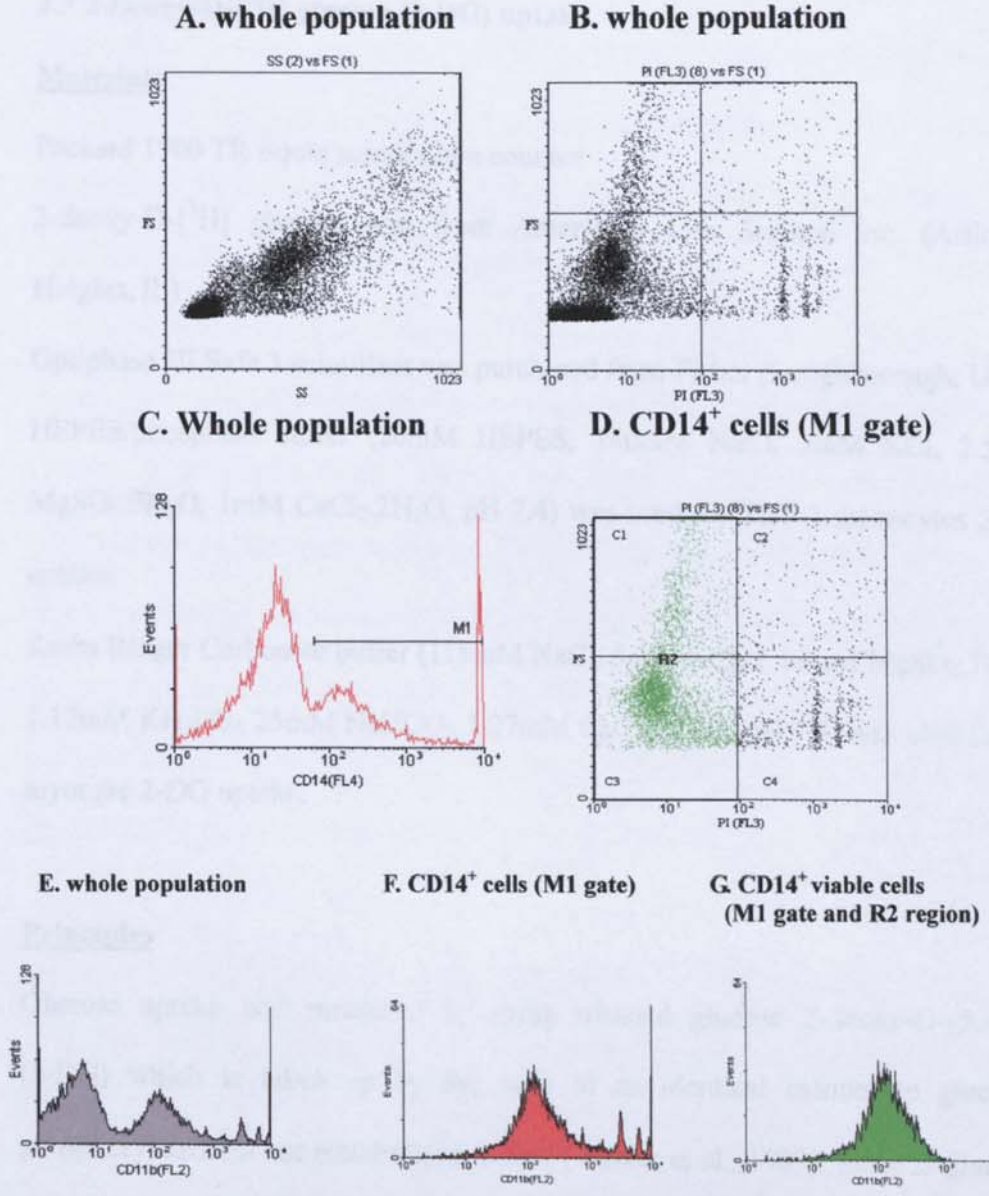

Figure 2.2 Flow cytometric measurement of CD11b expression on mononuclear cells (MNC). Human mononuclear cells (MNC) (10^6/ml) were isolated from whole

blood by density centrifugation and incubated with 10μg/ml monoclonal mouse anti-human CD11b-PE antibody for 30min on ice and in the dark and then co-stained with 25μg/ml propidium iodide (PI) for 15min. The cell surface expression of CD11b was determined by flow cytometry. A. A dot graph of the whole mononuclear cells (MNC) population according to cell size measured by the forward scatter (FS) and the granularity measured by the side scatter (SS). B. A PI versus FS graph of viable and dead cells by FS and propidium iodide (PI) exclusion in MNC whole population. C. A histogram of $CD14^-$ and $CD14^+$ cells in MNC whole population. Cells in M1 gate are $CD14^+$. D. A PI versus FS graph of viable and dead cells in $CD14^+$ cells. Cells in R2 region are viable cells (PI negative). E. A Histogram of the expression of CD11b on the whole MNC population. F. A histogram of the expression of CD11b expression on $CD14^+$ cells. G. A histogram of the expression of CD11b expression in the $CD14^+$ viable cells.

2.5 2-Deoxy-D-[^{3}H] glucose (2-DG) uptake

Materials

Packard 1900 TR liquid scintillation counter

2-deoxy-D-[^{3}H] glucose was from Amersham Life Science Inc. (Arlington Heights, IL)

Optiphase Hi-Safe 3 scintillant was purchased from Fisher (Loughborough, UK).

HEPES/phosphate buffer (20mM HEPES, 140mM NaCl, 5mM KCl, 2.5mM $MgSO_4.7H_2O$, 1mM $CaCl_2.2H_2O$, pH 7.4) was used for THP-1 monocytes 2-DG uptake.

Krebs Ringer Carbonate buffer (118mM NaCl, 5mM KCl, 1.18mM $MgSO_4.7H_2O$, 1.17mM KH_2PO_4, 25mM $NaHCO_3$, 1.27mM $CaCl_2.2H_2O$, pH 7.4) was used for L6 myotube 2-DG uptake.

Principles

Glucose uptake was measured by using tritiated glucose 2-deoxy-D-glucose (2-DG) which is taken up by the cells in an identical manner to glucose, phosphorylated but not metabolised further (Walker et al., 1989). Since D-glucose

and 2-DG uptake were mediated by the same glucose transporter system (Scharrer and Amann, 1980), the glucose uptake can be measured by incubating L6 skeletal muscle cells or monocytes with unlabeled 2-DG and a trace amount of radiolabeled 2-deoxy-D-[^{3}H] glucose.

Methods

2.5.1 2-DG uptake by U937 and THP-1 monocytes

After various treatments, U937 or THP-1 monocytes were collected into 1.5ml Eppendorf tubes and centrifuged at 150×g for 5min. Cells were washed once with glucose-free 4-(2-hydroxyethyl)-1-piperazineethanesulfonic acid (HEPES) /phosphate buffer (pH 7.4) at 22°C. Cells were then incubated with 0.5ml HEPES/phosphate buffer supplemented with 0.1mM unlabelled 2-deoxy-D-glucose and 2-deoxy-D-[^{3}H] glucose at 0.1μCi/ml for 10min at room temperature when the glucose uptake was in the linear range (Bailey and Turner, 2004). The uptake was stopped by adding 1ml ice-cold glucose-free HEPES/phosphate buffer and cells were centrifuged at 150×g for 5min. Cells were then washed twice with the above buffer. After centrifugation, cell pellets were lysed by addition of 0.5ml 1M NaOH. Cells were then transferred to scintillation vials, to which 5ml Hi-Safe 3 scintillant was added and the cell associated radioactivity was determined by liquid scintillation counting. Uptake of 2-deoxy-D-glucose by cells exposed to varying treatments was expressed as the percentage compared with control (100%), which is typically 5-8pmol/10^5 cells/min for basal uptake of 2-DG as reported previously (Bailey and Turner, 2004).

2.5.2 2-DG uptake by L6 myotubes

After various treatments, L6 myotubes were washed with glucose-free KRB buffer at room temperature. Cells were then incubated with 0.5ml of KRB buffer supplemented with 0.1mM 2-deoxy-D-glucose and 2-deoxy-D-[^{3}H] glucose at 0.1μCi/ml for 10min at room temperature when the glucose uptake was in a linear range. After washing cells three times with ice-cold KRB, cells were lysed with 0.5ml 1M NaOH and radioactivity was counted in 5ml Hi-Safe 3 scintillant using a Packard 1900 TR liquid scintillation counter. Uptake of 2-deoxy-D-glucose was expressed as the percentage compared with control (100%), which was typically 5-8pmol/10^5cells/min for basal uptake of 2-DG as reported previously (Bailey and Turner, 2004).

2.6 Uptake and accumulation of palmitate in U937 and THP-1 monocytes

Materials

[9, 10-^{3}H] palmitic acid was purchased from Amersham (UK).

Methods

To test whether palmitate was up taken by monocytes, U937 or THP-1 cells (3×10^5/ml) in 12-well plates were incubated with 100μM (non-toxic concentration of palmitate) unlabeled palmitate-conjugated to 5% fatty acid free-BSA and 0.1μCi/ml [9, 10-^{3}H] palmitic acid for 0-72h in RPMI1640 supplemented with 10% FBS and 100U/ml penicillin and 100μg/ml streptomycin. Cells were washed with PBS containing 0.1% fatty acid free BSA and cell pellets were lysed with 0.5ml 1M NaOH for at least 1h at room temperature. Radioactivity in cell lysate

was determined by scintillation counting.

Figure 2.3 shows that palmitic acid was taken up by U937 and THP-1 cells in a time dependent manner. In both type of cells, palmitic acid was rapidly taken up into cells up to 12h. Over 50% uptake was observed at 6h compared to 0h. The maximal uptake of palmitic acid was observed at 24h (91±1%). Further incubation (48h and 72h) did not increase the uptake above that seen at 24h.

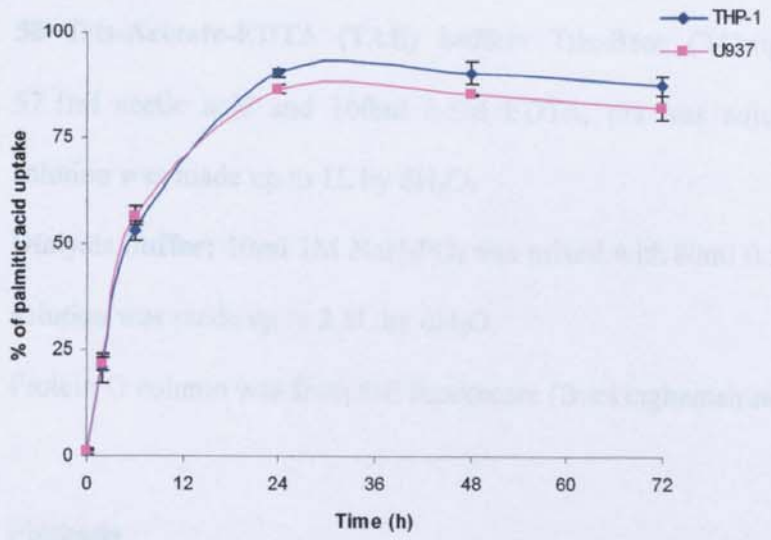

Figure 2.3 Time course of palmitic acid uptake by U937 and THP-1 monocytes. U937 and THP-1 monocytes (10^6/ml) incubated with 0.1μCi/ml of ^{3}H-palmitic acid and 100μM unlabeled palmitate in 12-well plates for 0-72h at 37°C. The uptake of palmitic acid was calculated as the percentage of cell associated radioactivity of total radioactivity (radioactivity in cell pellets and supernatants). Data are Mean±SEM from 3 independent experiments performed in triplicate.

2.7 Production of recombinant human ICAM-1-Fc protein

Materials

Luria Broth (LB), agar, tetracycline (5mg/ml), carbenicillin (100mg/ml), and ethidium bromide were obtained from Sigma.

MC1061/p3 competent bacteria cells and NoVaBlue cells were from Invitrogen (Paisley, UK). The MC1061/P3 cells were used for pIg vector and selection on Ampicillin and Tetracycline. The NovaBlue cells are routinely used for DNA cloning due to their high transformation efficiencies.

Buffer E 10× and *Hind* III enzyme were from Promega (Southampton, Hampshire, UK).

2×HEPES buffered saline (HBS) and 1M $CaCl_2$ were from Sigma (Poole, Dorset, UK)

50×Tris-Acetate-EDTA (TAE) buffer: Tris-Base (242mg) was mixed with 57.1ml acetic acid and 100ml 0.5M EDTA, pH was adjusted to 8.5 and the solution was made up to 1L by dH_2O.

Dialysis buffer: 10ml 1M NaH_2PO_4 was mixed with 80ml 0.5M Na_2HPO_4 and the solution was made up to 2.5L by dH_2O.

Protein G column was from GE Healthcare (Buckinghamshire, UK).

Methods

2.7.1 Preparation of LB broth and LB agar

LB broth solution (25g/L) was prepared by mixing 10g of LB with 400ml dH_2O. LB agar solution (15g/L) was prepared by mixing 4.5g agar and 7.5g LB with 300ml dH_2O. After autoclaving, LB agar solution was supplemented with 10μg/ml tetracycline and 100μg/ml carbenicillin. LB agar plates were prepared by pouring 25ml LB agar solution into Petri dishes and were allowed to set at room temperature for subsequent experimentations. LB broth solution was stored at 4-8°C.

2.7.2 Transformation of E. coli with ICAM-1-Fc and ICAM-1-transmembrame cDNA

The MC1061/P3 cells were used for ICAM-1-Fc cDNA transformation and the NovaBlue cells were used for ICAM-1-transmembrane cDNA transformation. In brief, 2μl of ICAM-1-Fc cDNA or ICAM-1-transmembrane cDNA was mixed with the MC1061/P3 cells or the Nova Blue cells on ice for 5min. Then the NovaBlue cells were heated at 42°C for 30 seconds while the MC1061/P3 cells were heated at 37°C water bath for 1min. Both cells were then incubated on ice for a further 2min. After addition of 250μl SOC (Super Optimal catabolite repression) bacterial growth medium, the NovaBlue cells were immediately plated on LB agar Petri dishes. MC1061/P3 cells were incubated at 37°C for 1h and then plated in LB agar Petri dishes. The Petri dishes were placed up-side down and incubated at 37°C overnight.

2.7.3 Miniprep of bacteria plasmid DNA

After overnight growth, a single bacterial colony was carefully selected from each Petri dish. The bacteria cells were then cultured in 5ml LB broth with antibiotic added overnight with shaking at 37°C. Bacterial cell suspensions (1-1.5ml) were then transferred to sterile 1.5ml Eppendorf tubes and centrifuged at 13,000×g for 5min to obtain the cell pellets. After removal of supernatant, bacterial cells were resuspended in 200μl GTE buffer (50mM Glucose, 25mM Tris, 10mM EDTA, pH 8.0), mixed with 400μl 1%SDS/0.2M NaOH and incubated on ice for 5min. The bacterial cell lysates were then mixed with 300μl of 3M K^+/5M Acetate and incubated on ice for another 5min to precipitate chromosomal deoxyribonucleic

acid (DNA) and proteins. After centrifugation at 13,000×g for 5min, the supernatants containing DNA were collected into new Eppendorf tubes and mixed with 600µl ice-cold isopropanol and incubated on ice for 10min. The tubes were then centrifuged at 13,000×g for 5min. After removal of the supernatants, the pellets of nucleic acid was dissolved in 500µl of 80% ethanol and centrifuged at 13,000×g for 5min. After removal of ethanol completely, the nucleic acid pellets were air dried and resuspended in 50µl TE buffer (10mM Tris-HCl, 1mM EDTA, pH 8.0) and stored at -20°C.

2.7.4 Maxiprep of bacteria plasmid DNA

Large scale plasmid DNA preparation was conducted according to the manufacturer's instructions using a Promega Maxiprep kit. In brief, after overnight growth of 50-100ml transformed *E.coli* bacterial cell cultures at 37°C, cells were centrifuged at 3000×g for 10min. The cell pellets were mixed with Cell Lysis Solution and incubated at room temperature for 3min. After mixing with Neutralisation Solution, the cells were left for 2-3min in an upright position to allow a white flocculent precipitate to form. The precipitates were then passed through a PureYield Column and lysate filtrate was collected into a 50ml conical tube and centrifuged at 1500×g for 5min. The filtered lysate was then placed onto the PureYield Binding Column and centrifuged at 1500×g for 3min. After that, the column was washed with 5ml Endotoxin Removal Wash solution (with isopropanol added) and followed by 20ml of Column Wash Solution (with ethanol) by centrifugation to remove excessive ethanol. The DNA was eluted by adding 600µl Nuclease-Free Water to DNA binding membrane in the PureYield Binding

Column and centrifuged at 2000×g for 5min. The filtrates were collected into 1.5ml Eppendorf tubes and stored at -20°C.

2.7.5 DNA 1% agarose gel

DNA (10-20µl) samples prepared from either Miniprep or Maxiprep were digested by incubating with HIII enzyme in reaction buffer for 4h at 37°C. Then the 24µl of digested DNA mixture was mixed with 6µl 6×DNA loading buffer (12% glycerol v/v, 60mM Na_2EDTA pH 8, 0.6% SDS w/v, 0.003% bromphenol blue w/v, 0.003% xylene cyanol w/v).

1% agarose gel was prepared by dissolving agarose (1.7g) in 170ml 1×TAE buffer and heated in a microwave for 3min until the agarose was completely dissolved. After cooling, 150ml of agarose solution was gently poured into a horizontal gel tank (15.5cm×10cm×3cm, length×width×height) and the comb was immediately inserted. After the gel was set, the comb was gently removed and DNA samples (20µl) and DNA HyperLadder I (Bioline, London, UK) were loaded into each well. The gel was run in 1×TAE buffer at 150V, 250mA for 80min. DNA bands were visualized under ultraviolet rays (UV) light.

Figure 2.4 shows that the ICAM-1-Fc cDNA fragments from maxiprep (Lane 7 and 8) were in same postion size as original cDNA (Lane 1 and 2). However, the ICAM-1-TM cDNA fragments from the miniprep were not the same as the original cDNA. Therefore, in the subsequent experiment, ICAM-1-Fc cDNA was used for transfection into 293T cells to generate human recombinant ICAM-1-Fc protein.

Figure 2.4 1% agarose gel plasmid DNA samples analysis.
Lane 1 and Lane 2: original ICAM-1-Fc cDNA
Lane 4 and Lane 5: original ICAM-1-TM cDNA
Lane 7 and Lane 8: ICAM-1-Fc cDNA from maxiprep
Lane 10: ICAM-1-TM cDNA from miniprep
Lane 12: DNA marker.

2.7.6 Transient transfection of ICAM-1-Fc DNA into 293T cells

293T cells are derivative of a human renal epithelial cell line called 293 and stably express the large SV40 T antigen, allowing episomal replication of plasmids containing the SV40 origin and early promoter region. Because of their high transfection efficiency, 293T cells are widely used for transfection and production of recombinant proteins.

ICAM-1-Fc DNA (32μl) was mixed with 1.6ml 0.25M of $CaCl_2$ solution. This mixture was added drop wise to 1.6ml 2×HBS solution for 10min until the formation of a visible precipitate. Then the precipitate was added to 239T cell suspensions (5×10^6/ml) and further diluted with DMEM supplemented with 10% FBS, 25mM D-glucose, 1mM L-glutamine, 100U/ml penicillin, and 100μg/ml streptomycin to a density of 2.5×10^5/ml. The cells were incubated at 37°C

overnight. Subsequently, the cell culture medium was removed and replaced by DMEM supplemented with 2%FBS, 25mM D-glucose, 1mM L-glutamine, 100U/ml penicillin, and 100μg/ml streptomycin. 239T cells were further incubated in the above medium for 72h until confluent.

2.7.7 Dialysis of cell culture medium protein

After 72h, the cell culture medium was collected into 50ml conical tubes and centrifuged at 2000×g for 5min. The supernatant was added with 0.02% sodium azide and transferred to dialysis membrane tubes (Medicell International Ltd, London, UK) with molecular weight cut-off 12000-14000 Daltons. The tubes were immersed in the dialysis buffer (4mM NaH_2PO_4, 16mM Na_2HPO_4) for two and half days with daily change of buffer at 4°C.

2.7.8 Purification of ICAM-1-Fc protein by protein G column

After dialysis, the ICAM-1-Fc protein was purified from the cell culture medium by protein G affinity chromatography. The protein G column was first equilibrated with PBS for 15min. Then the cell culture medium after dialysis was passed through the column. After that, the column was washed with PBS for 15min. The ICAM-1-Fc protein was eluted by 0.1M glycine solution (pH 2.7) and fractions were collected into at least 8 different 1.5ml Eppendorf tubes containing 200μl 1M Tris-HCl (pH 9.0). Finally, the column was washed with 15ml PBS and 3ml 70% ethanol and stored at 4-8°C for re-use.

2.7.9 Protein assay by Bradford method

The protein concentrations of each eluted fraction were determined by the Bradford protein assay (Bradford, 1976). The Bradford protein assay is based on the equilibrium between the three forms of Coomassie Blue G dye. The dye exists in three forms: cationic (red), neutral (green), and anionic (blue). Under acidic conditions, the dye is predominantly in the doubly protonated red cationic form (Maximum absorbance = 470 nm). However, when the dye binds to protein, it is converted to a stable unprotonated blue form (Maximum absorbance = 595nm). This blue protein-dye form can be detected at 595nm in the assay using a spectrophotometer or microplate reader.

10µl of each fraction eluted from the protein G column was mixed with 200µl dye and 790µl dH_2O and incubated at room temperature for 5min before reading absorbance at 595nm using a spectrometer. Figure 2.5 shows a typical protein concentration profile of each elution fraction. Protein concentration was estimated from a BSA calibration curve.

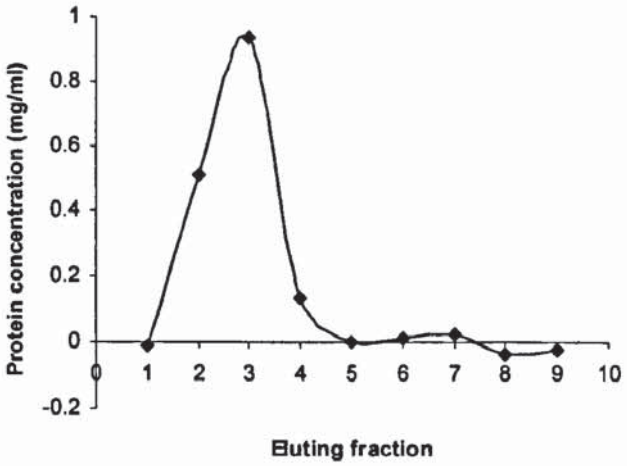

Figure 2.5 Absorbance of each elution fraction at 595nm by Bradford assay. ICAM-1-Fc protein was produced according to 2.7 and purified by protein G column according to 2.7.8. Nine different fractions were collected from the protein G column and protein concentration was determined by mixing 10µl of each fraction eluted from the protein G column with 990µl dH_2O and incubated at room temperature for 5min. The absorbance was read at 595nm using a spectrometer.

2.8 SDS-PAGE and Western Blot

Materials

ICAM-1 standard was from IDS (Tyne & Wear, UK).

ICAM-1-Fc protein was obtained according to section 2.7.

Goat anti-human ICAM-1 polyclonal primary antibody was from R&D (Minneapolis, MN, USA).

Polyclonal rabbit anti-goat IgG secondary antibody conjugated with HRP was from DAKO (Cambridgeshire, UK).

Resolving gel buffer: Tris-Base (18.15g) was dissolved in 50ml water. SDS (0.4g) was added and dissolved. pH was adjusted to 8.4 and the solution was made up to 100ml.

Stacking gel buffer: Tris-Base (6.05g) was dissolved in 50ml water. SDS (0.4g) was added and dissolved. pH was adjusted to 6.8 and the solution was made up to 100ml.

10% Ammonium persulphate (APS): 10% APS solution was aliquoted to 200µl and stored at -20°C.

TBS buffer (10×concentrations): Tris-Base (30g) and NaCl (60g) were dissolved in 900ml H_2O. pH was adjusted to 7.5 and the solution was made up to 1L.

Running buffer: Tris-Base (3.0g), Glycine (14.4g), and SDS (1.0g) was dissolved in 1L water.

Transfer buffer: Tris-Base (4.5g) and Glycine (21.6g) was dissolved in 1200ml water. Methanol (300ml) was added just before the transfer of gel to PVDF membrane.

Blocking buffer: 5% non-fat milk in 0.1% tween-20 in TBS.

Washing buffer: 0.1%Tween-20 in TBS

Acrylamide-bisacrylamide solution: Protogel containing acrylamide (30% w/v)-bisacrylamide (0.8% w/v) solution (37.5:1) is purchased from Geneflow (Staffordshire, UK).

TEMED (1, 2-Bis (dimethylamino) ethane): TEMED contains tertiary amine base to catalyse the formation of free radicals which will cause acrylamide to polymerise to form a gel matrix.

Methods

2.8.1 Sample preparation

The ICAM-1 standard protein was reconstituted in dH_2O at a concentration of

2mg/ml. Both ICAM-1 standard protein and purified ICAM-1-Fc protein which contains the entire extracelluar domain of the human ICAM-1 molecule and the Fc portion of human IgG1 was mixed with 2×sample buffer (20%glycerol, 4% SDS, and 10% 2-mercapto-ethanol, 0.02% bromophenol blue and freshly added 100mM dithiothreitol) and boiled for 10min on a heat block at 95°C. The samples were then resolved by 10% SDS-polyacryamide gel electrophoresis (SDDS-PAGE).

2.8.2 SDS-PAGE

The resolving gel was prepared according to Table 2.1 and set in plates using a BioRad Mini Protean II cell. After polymerisation of the resolving gel, stacking gel was prepared subsequently and poured on top of the resolving gel. A 10-well comb was inserted immediately. The comb was gently pulled out after the stacking gel was fully polymerised. Protein samples (20μg) and Kaleidoscope prestained markers (Bio-Rad, CA, USA) (5μl) were loaded into each well. The gel was submerged in running buffer and electrophoresed at 115V, 310mA for 1h 45min.

Table 2.1 Resolving and Stacking gel

Resolving Gel (12ml)	10%	Stacking Gel (7.5ml)	4%
H_2O	4.8 ml	H_2O	4.87 ml
Buffer 1	3 ml	Buffer 1	1.87 ml
Acrylamide solution	4 ml	Acrylamide solution	0.75 ml
10% APS (added freshly)	200 μl	10% APS	75 μl
TEMED	20 μl	TEMED	10 μl

2.8.3 Coomassie Blue Staining

After migration of the dye front to the end of the gel, the gel was stained with 20ml Coomassie blue staining solution (0.05% Coomassie Blue in 50% methanol and 10% acetic acid) for 2h at room temperature with gentle agitation. After that, the gel was gently washed once with tap water and washed with 20ml destain solution (5% methanol and 7% acetic acid in distilled water) for 15 minutes for 3 to 4 times until the protein bands were present. Figure 2.6 shows the ICAM-1 and ICAM-1-Fc protein band after 10% SDS-PAGE and stained with 0.05% Coomassie Blue.

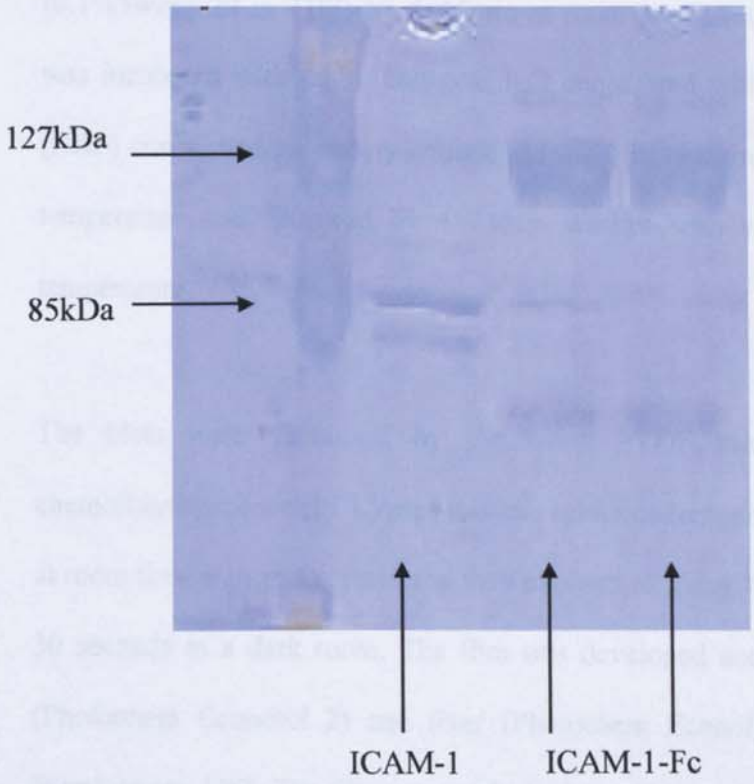

Figure 2.6 Coomassie Blue staining of ICAM-1-Fc and ICAM-1 SDS-PAGE gel. ICAM-1 and ICAM-1-Fc protein was resoled on 10% gel and stained with Coomassie Blue.

2.8.4 Western Blot

To confirm the recombinant ICAM-1-Fc protein identity, Western blot analysis was carried out. After resolution by 10% SDS-PAGE, the proteins were transferred to polyvinylidene fluoride (PVDF) membrane (GE Healthcare, Buckinghamshire, UK) in transfer buffer with an ice-pack at 115V, 240mA for1h 45min. The membrane was blocked at 4°C overnight in 5% non-fat milk and 0.1% tween-20 in TBS and then incubated with goat anti-human ICAM-1 primary antibody (1:1000 dilution in blocking buffer) for 2h at room temperature with gentle agitation. After that, the membrane was washed with 20ml washing buffer

(0.1%Tween-20 in TBS) by 4×15min at room temperature. Then the membrane was incubated with rabbit anti-goat IgG conjugated with horseradish peroxidise (HRP) conjugated secondary antibody (1:4000 in blocking buffer) for 1h at room temperature and followed by 4×15min washes with washing buffer at room temperature.

The blots were visualised by incubating PVDF membrane with emission chemoiluminescence (ECL) plus mixture solutions (reagent A: reagent B, 40:1 v/v) at room temperature for 1min and then exposed to X-ray film (GE Healthcare) for 30 seconds in a dark room. The film was developed and fixed using developer (Photochem Econotol 2) and fixer (Photochem Econofix 2) solution (Jessop, Birmingham, UK). The film was washed with cold water for 2min and air dried.

As shown in Figure 2.7, under reducing conditions, ICAM-1-Fc protein resolved

by 10% SDS-PAGE and detected with anti-ICAM-1 antibody showed a protein band at 127kDa while ICAM-1 protein showed a molecular weight around 85kDa.

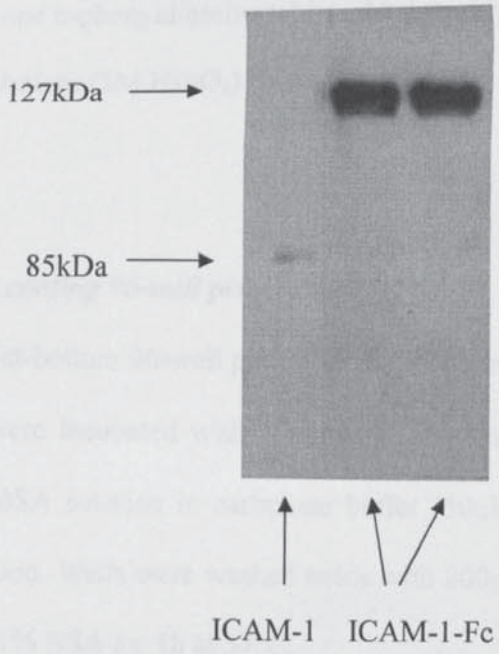

Figure 2.7 Western blot of ICAM-1-Fc SDS-PAGE gel. ICAM-1 and rICAM-1-Fc protein was resolved on 10% SDS-PAGE gel and blot with anti-ICAM-1 antibody. The protein band was visualised by an ECL plus kit.

2.9 Immobilisation of ICAM-1-Fc protein to 96-well plate

Materials

Capture monoclonal antibody (mAb): mouse anti-human IgG (Fc specific) (Sigma)

Goat anti-human ICAM-1 polyclonal primary antibody (R&D)

Polyclonal rabbit anti-goat IgG secondary antibody conjugated with HRP (DAKO)

Coating buffer: PBS + 20mM sodium carbonate, pH 9.2

Blocking buffer and antibody diluting buffer: 1% BSA in PBS

Substrate buffer: 10ml citrate phosphate solution (0.15M, pH 5.0) with 8µl H_2O_2 (8.8M) and one o-phenyldiamine tablet added freshly.

Stopping solution: (2M H_2SO_4)

Methods

2.9.1 Direct coating 96-well plate with ICAM-1-Fc

MaxiSorp flat-bottom 96-well plates (NUNC, Thermo Fisher Scientific, Roskilde, Denmark) were incubated with 10µg/ml ICAM-1 standard, ICAM-1-Fc, human IgG, or 1%BSA solution in carbonate buffer (50µl/well) overnight at 4°C with gentle agitation. Wells were washed twice with 200µl/well PBS and blocked with 200µl /well 1% BSA for 1h at 37°C.

2.9.2 Indirect coating 96-well plate with ICAM-1-Fc

ICAM-1-Fc protein was immobilized to 96-well plates through the following procedures. The MaxiSorp flat-bottom 96-well plates were first incubated with 50µl/well mouse anti-human IgG (Fc specific) $F(ab')_2$ antibody (20µg/ml in 20mM carbonate buffer, pH 9.2) overnight at 4°C with 30rpm rotation. The plates were then washed twice with 200µl/well PBS and blocked with 200µl/well PBS-1% BSA (blocking buffer) for 1h at 37°C. ICAM-1-Fc protein and human IgG were diluted in PBS-1% BSA at concentrations from 0-20µg/ml (50µl/well) were incubated for 2h at 37°C. To verify the orientation of ICAM-1-Fc protein, human IgG (300µg/ml) was co-incubated as a competitor for the binding of ICAM-1-Fc to anti-Fc mAb.

After that, the plates were washed twice with 200µl/well PBS and blocked with 200µl/well PBS-1% BSA for 1h at 37°C. Then the plates were incubated with 50µl/well goat anti-human ICAM-1 primary antibody (1:1000 dilution in blocking buffer) for 2h at 37°C. After washing twice with 200µl/well PBS, the plates were incubated with rabbit anti-goat IgG conjugated to HRP secondary antibody (1:2000 dilution in blocking buffer) for 1h at 37°C. After that, the plates were washed four times with 200µl/well 0.1% Tween-20 in PBS and twice with PBS. The plates were then incubated with 50µl substrate solution at room temperature for 20min and the reaction was stopped by the addition of 50µl 2M H_2SO_4 solution. The optical absorbance was read at 490nm by a spectrophotometer.

Figure 2.8 shows that the binding of ICAM-1-Fc to anti-Fc antibody was increased in a concentration dependent manner. ICAM-1-Fc at the concentration of 1µg/ml was sufficient for saturated binding to anti-Fc antibody and the binding was almost completely blocked by co-incubation with 300µg/ml human IgG. Therefore, 1µg/ml of ICAM-1-Fc was used for coating plates and for investigating monocyte adhesion.

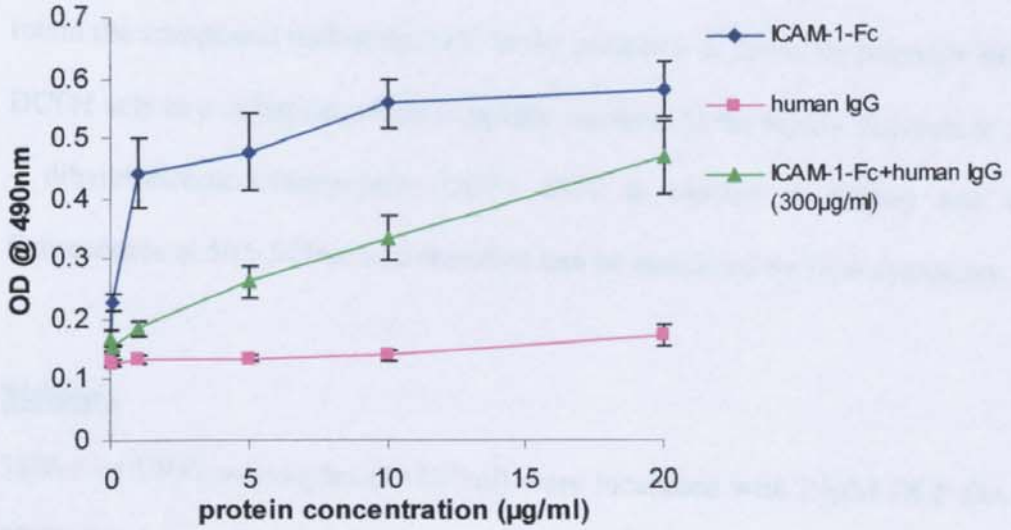

Figure 2.8 Optimisation of human recombinant ICAM-1-Fc coating to 96-well plate. Mouse anti-human Fc mAb at 1µg/well was added to 96-well plate overnight at 4°C with gentle rotation. After washing and blocking with 1%BSA for 1h at 37°C, the plate was incubated with various concentrations of ICAM-1-Fc, human IgG and both for 2h at 37°C. After washing and blocking, the binding was quantified by ELISA. Data are mean±SEM of 3 independent experiments performed in triplicate.

2.10 Intracellular reactive oxygen species (ROS) measurement

Materials

2', 7',-dihydrodicholorofluorescein diacetate (DCFH-DA) was purchased from Sigma.

Principles

Intracellular ROS levels were determined using the membrane permeable peroxide sensitive dye 2', 7',-dihydrodicholorofluorescein diacetate (DCFH-DA), which is a non-polar, non-fluorescent compound. Intracellular DCFH-DA is activated by intracellular esterases to hydrolyse the acetate groups forming the

non-fluorescent 2', 7', - dihydrodichlorofluorescein (DCFH), which effectively retain the compound within the cell. In the presence of cytosolic peroxide ROOH, DCFH acts as a substrate which is rapidly oxidised to the highly fluorescent 2', 7' – dihydrodicholorofluorescein (DCF). DCF is excited at 488nm and emits fluorescence at 505-545nm and therefore can be measured by flow cytometry.

Methods

THP-1 or U937 monocytes (1×10^6/ml) were incubated with 25μM DCF-DA dye 37°C for exactly 20min in the dark and the intracellular levels of ROS were determined as DCF fluorescent intensity by flow cytometry.

2.11 Monocyte adhesion assay

Materials

2', 7'-Bis (2-carboxyethyl)-5(6)-carboxyfluorescein tetrakis (acetoxymethyl) ester (BCECF-AM) was purchased from Sigma (UK).

Medium 199H (M199 medium with 10mM HEPES) was from Cambrex (Belgium).

Microplate Spectrofluorometer (Spectramax Gemini XS, Molecular Devices, Sunnyvale, USA).

BCECF-AM is an acetoxymethyl ester of BCECF. BCECF-AM is intrinsically nonfluorescent, it is converted to a green fluorescein derivative (BCECF) on hydrolysis by cytosolic esterases in mammalian cells at λ_{ex} 485nm; λ_{em} 535nm.

Stock BCECF-AM (10mg/ml) was prepared by dissolving BCECF-AM in 200μl Dimethyl sulphoxide (DMSO) and diluted to 1ml by PBS. The stock solution was stored at -20°C and protected from light.

Methods

2.11.1 Labelling monocytes with BCECF-AM

U937 monocytes, THP-1 monocytes or mononuclear cells (5 $\times 10^6$/ml) in RPMI 1640 (10% FBS) were incubated with 10μg/ml BCECF-AM for 30min at room temperature in the dark. The dye loading was quenched by adding 10-fold excess of M199H medium and centrifuged at 100×g for 5min. Cells were then washed twice with M199H medium and resuspended in M199H medium at a final density of 2.5×10^5/ml.

2.11.2 Monocyte adhesion assay

EAhy926 endothelial cells (1×10^5/ml) were seeded in 24-well plates and grown in DMEM medium supplemented with 10%FBS, 100U/ml penicillin and100μg/ml streptomycin, and 100μM hypoxanthine, 0.4μM aminopterin, 16μM thymidine (HAT) at 37°C for 48h to be confluent.

Labelled monocytes (2.5×10^5/ml) in M199H medium were incubated with confluent EAhy926 endothelial monolayer in 24-well plates (in Chapter 5) or ICAM-1-Fc coated 96-well plates (in Chapter 5) or segments of rat aorta (in Chapter 6) for 30min at 37°C. Non-adherent cells were removed by inverting the plate onto a paper tissue. The adherent cells were lysed with 1ml lysis buffer

(0.1% Triton X-100; 0.1M Tris-Base, pH 8.0) for 2h at room temperature in the dark. The fluorescence intensity was measured at an excitation of 485nm and emission of 535nm by a fluorometer using the cut off filter at 520nm. The adhesion was calculated from standard curves prepared with different cell densities.

The adhesion of U937 monocytes to ICAM-1 was investigated using direct and indirect immobilisation of ICAM-1-Fc to 96-well plates. Figure 2.9 shows the adhesion of U937 monocytes to 96-well plates directly immobilised with various proteins as indicated in the figure. Both IgG and ICAM-1-Fc at 10μg/ml increased cell adhesion by approximately 30% and 40% respectively compared to BSA (p<0.001). Pre-incubation of U937 monocytes with 10μg/ml IgG to block the Fc receptor on monocyte completely prevented the cell adhesion to ICAM-1-Fc. This suggests that the adhesion of U937 monocytes ICAM-1-Fc is mediated by Fc receptor expressed on monocytes and this direct immobilisation of ICAM-1-Fc method is not suitable for investigation of monocytes adhesion to ICAM-1.

Figure 2.10 shows the adhesion of U937 monocytes to 96-well plates by an indirect coating method which used mouse anti-human Fc mAb (Sigma) to capture the Fc fragment of ICAM-1-Fc. Incubation of U937 monocytes with 10^{-6}M PMA for 24h increased the cell adhesion to ICAM-1 by 2.5-fold compared resting cells (p<0.001). However, there was no significant difference in adhesion of resting and PMA-activated U937 monocytes to BSA or IgG coated plates under the same conditions. Therefore, this indirect coating method was used for *in vitro*

monocyte adhesion assay.

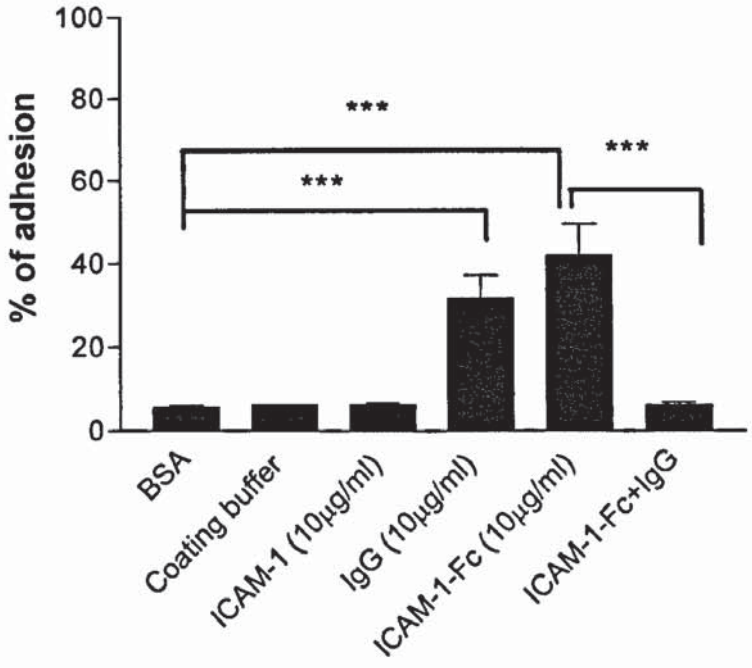

Figure 2.9 Resting U937 monocyte adhesion to 96-well plates directly coated with ICAM-1-Fc. 96-well plates were coated with 1%BSA, carbonate coating buffer, ICAM-1-Fc (10µg/ml), human IgG (10µg/ml), ICAM-1-Fc (10µg/ml) overnight at 4°C and blocked with 1% BSA for 1h at 37°C. Resting U937 monocytes (100µl, 5×10^5/ml) labelled with 10µg/ml BCECF-AM with and without blocking of Fc receptor with human IgG (10µg/ml) for 10min was added to each well and incubated for 30min at 37°C. The adhesion assay was carried out according to section 2.11.2. Data are mean±SEM of 3 independent experiments performed in triplicate. *** $p<0.001$.

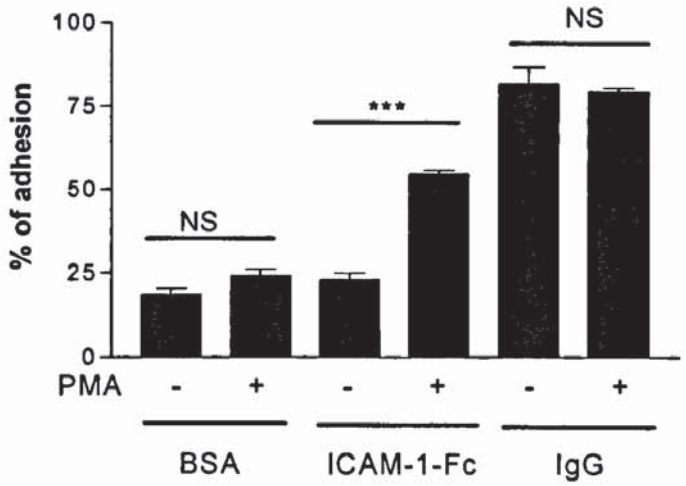

Figure 2.10 Resting and PMA-activated U937 monocyte adhesion to 96-well plates indirectly coated with ICAM-1-Fc. 96-well plates were coated with mouse anti-human IgG (Fc specific) monoclonal antibody (20μg/ml, 50μl/well) overnight at 4°C. After washing and blocking with 1% BSA for 1h at 37°C, the plates were incubated with 1% BSA, ICAM-1-Fc (1μg/ml), human IgG (1μg/ml) for 2h at 37°C and the plates were further blocked with 1% BSA for 1h at 37°C. Resting and PMA-activated U937 (10^{-6} M PMA, 24h) monocytes (100μl, 5 $\times 10^5$/ml) labelled with 10μg/ml BCECF-AM were added to each well and incubated for 30min at 37°C. The adhesion assay was carried out according to section 2.11.2. Data are mean±SEM of 3 independent experiments performed in triplicate. *** $p<0.001$. NS: non significant.

2.12 Bicinchoninic acid (BCA) protein assay

Materials

Protein BSA standard (1mg/ml), Bicinchoninic acid reagent solution, 4% Copper (II) sulphate solution were from Sigma (Poole, Dorset, UK).

Principles

The BCA assay is based on the formation of a Cu^{2+}-protein complex under alkaline conditions by BCA solution (a highly alkaline solution with a pH 11.25 and contains bicinchoninic acid, sodium carbonate, sodium bicarbonate, sodium

tartrate and cupric sulfate pentahydrate), followed by reduction of the Cu^{2+} to Cu^{1+}. The amount of reduction is proportional to the protein present. Then two molecules of bicinchoninic acid chelate with each Cu^{1+} ion, forming a purple-colored product that absorbs light at a wavelength of 562 nm.

Methods

Protein samples (10µl) or BSA standard (0, 2, 4, 6, 8 and10µl of BSA plus 10, 8, 6, 4, 2, 0µl of dH_2O) was added to each well in 96-well plates in triplicate. Each well was then incubated with 200µl cupper sulphate-bicinchoninic acid mix solutions (1:50 v/v) for 30min at 37°C. The absorbance was read at 570nm and protein concentrations were determined from a BSA standard curve.

2.13 Caspase-3 activity assay

Materials

Buffer A (lysis buffer): 10mM Tris-HCl pH 7.5, 130mM NaCl, 1% TritonX-100, 10mM NaH_2PO_4, 0.4mM PMSF, 0.2mM NaF, 0.2mM Na_3VO_4, 0.3mg/ml leupeptin.

Buffer B: 20mM HEPES pH 7.8, 10% glycerol, 2mM DTT

Caspase-3 substrate II: Ac-DEVD-AMC (Merk Calbiochem, Nottingham, UK)

Principles

Caspase-3 is an intracellular cysteine protease that exists as a proenzyme, becoming activated during the cascade of events associated with apoptosis. Caspase-3 cleaves

a variety of cellular molecules that contain the amino acid motif. Caspase-3 activity analysis is based on the hydrolysis of acetyl Aspartic acid-Glutamic acid-Valine-Aspartic acid 7-amido-4-methylcoumarin (Ac-DEVD-AMC) by caspase 3, resulting in the release of the fluorophore 7-amino-4-methylcoumarin (AMC). The maximum excitation and emission wavelengths of AMC are 360 nm and 460 nm respectively.

Methods

THP-1 or L6 cells were collected after various treatments by centrifugation in conical tubes at 250×g for 5min and washed once with ice-cold PBS. Cell pellets (10^6 cells) were incubated with 100µl lysis buffer with 10µl freshly added protease inhibitor cocktail (Sigma) on ice for 30min. After centrifugation at 14, 000xg for 30sec, supernatants (containing caspase-3) were collected and were used for BCA protein assay. The caspase-3 assay was performed in 96-well plates. After adding 175µl buffer B and 25µl of supernatant in each well, the caspase-3 assay was started by incubating with 50µl caspase-3 substrate Ac-DEVD-AMC (25µM) overnight at room temperature in the dark. The fluorescence intensity of the proteolytic cleavage product of the substrate was measured by a fluorescence microplate reader (SpectraMax; Molecular Devices, Corp., Sunnyvale, CA) using an excitation wavelength of 380 nm and an emission wavelength of 460 nm with the cut off filter at 455nm. Caspase-3 activity was calculated as fluorescence intensity/mg protein and data were expressed as fold change over control.

2.14 Cell viability assay

2.14.1 Trypan blue exclusion assay

Materials

0.4% trypan blue solution (Sigma); Haemocytometer (Weber Scientific International Ltd, UK)

Principles

The trypan blue exclusion method is the most basic, simple and quick method for differentiating live and dead cells in cell biology. Trypan blue is a dye which indicates cell membrane integrity. Dead cells lose cell membrane integrity so that the dye can be taken up and become blue. Live cells have intact cell membranes, therefore, the dye can not be taken up and cells show bright under light microscopy.

Methods

Cell suspension (15µl) was mixed with 0.4% trypan blue solutions (15µl) and 10µl of the mixture was inserted to each chamber of a haemocytometer. The dead cells show blue while live cells show bright. The live cells numbers and dead cells numbers were counted and the cell viability was expressed as percentage of total cells.

2.14.2 MTT assay

Materials

3-(4, 5 dimethylthiazol-2-yl)-2, 5-diphenyltetrazolium (MTT) was from Sigma. Dimethylformamide (DMF) and glacial acetic acid were from Fisher Scientific (Loughborough, Leicestershire, UK).

MTT solution (5mg/ml) was prepared in 0.15M PBS and filtered (0.2μm) before use.

Lysis buffer: 20% SDS in DMF (50%), dH_2O (50%), pH was adjusted to 4.7 with 2% glacial acetic acid.

Principles

The MTT assay is a standard colorimetric assay and measures mitochondrial reducing capacity. The MTT salt can only be taken up and reduced by mitochondrial succinate dehydrogenase which generates a purple colour formazan product (Mossman, 1983). This product can not pass through the cell plasma membrane. Therefore by lysing the cells, the formazan product can be solubilised and can be read and quantified by a colorimetric method. The ability of cells to reduce MTT represents mitochondrial reducing capacity which may be interpreted as a measure of viability and/or live cell numbers. Since there is a linear relationship between live cell numbers and the absorbance, the effect of treatment on cell viability can be determined by comparing with control cells.

Methods

2.14.2.1 MTT assay for U937 and THP-1 cells

Two hours prior to completion of each experiment, U937 or THP-1 cell suspensions (100µl) in 96-well plates were incubated with 25µl MTT solution (5mg/ml) for a further 2 hours at 37°C 5% CO_2. Lysis buffer (100µl) was then added to each well and the plates were incubated for a further 16h at 37°C in a humidified 5% CO_2 air incubator. The absorbance of each well was read at 570nm using an MRX Microplate reader. Blank wells contained RPMI 1640 medium without cells.

2.14.2.2 MTT assay for L6 myotubes

The medium from treated and control L6 myotubes in 24-well plates was removed and replaced with 0.5 ml fresh DMEM with 0.5% FBS. Cells were incubated with 100µl MTT solution (5mg/ml) for 4h at 37°C. Lysis buffer (100µl) was added to each well and the plates were incubated for a further 16h at 37°C in a humidified 5% CO_2 air incubator. The absorbance was read at 570 nm using an MRX Microplate reader. Blank wells contained DMEM without cells.

2.14.3 Flow cytometric analysis of cell viability of mononuclear cells.

Materials

Propidium iodide (PI) solution (25µg/ml in 0.1%BSA in PBS)

Principle

PI is a fluorescent dye which can be taken up by cells losing membrane integrity such as cells undergoing apoptosis or necrosis. The viable cells with intact membrane do not take up the dye. Therefore, cell viability can be measured by using flow cytometry. Cell size can also be determined simultaneously by forward light scatter (FS). It has been reported that cells undergoing apoptosis display a characteristic shrinking of the cells whereas cells undergoing necrosis show swelling of the cells (Papucci et al., 2004). Therefore, the dual parameter histogram of FS and Log FL3 (PI) can be used to distinguish the viable and dead cells. Apoptotic cells are displayed as low FS and high PI fluorescence and necrotic cells are displayed as high FS and high PI fluorescence.

Methods

U937, THP-1, or MNC (10^6/ml) was incubated with PI solution (25μg/ml in 0.1% BSA in PBS) for 15min on ice in the dark. After that, cells were immediately analysed by flow cytometry. As shown in Figure 2.11, viable cells exclude the uptake of PI and were shown in the PI negative regions (R1 and R3). Apoptotic cells are displayed as low FS and high PI fluorescence (R4) and necrotic cells are displayed as high FS and high PI fluorescence (R2).

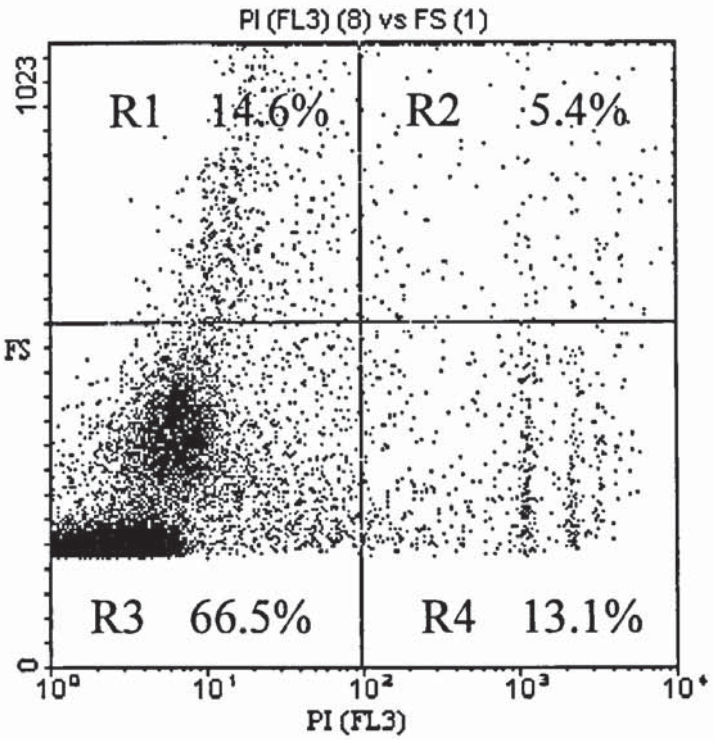

Figure 2.11 Cell viability assay by flow cytometry. MNC cells were stained with 25μg/ml PI for 15min on ice in the dark. Cell viability was determined according to forward scatter and PI staining. Cells in R1 and R3 regions are viable cells with intact cell membrane shown as low PI fluorescence; cells in R2 region are necrotic cells shown as high FS and high PI fluorescence; cells in R4 region are apoptotic cells shown as low FS and high PI fluorescence. The number of cells in each region was displayed as % of total cells and the cell viability was determined by % of total cells in R1 plus R3.

2.15 Statistical analysis

Data are expressed as mean ± SEM. Statistical analyses were performed by one-way ANOVA with Tukey-Kramer post hoc tests. The detailed statistical and data analysis are provide in each individual chapter. A p value less than 0.05 was considered significant.

Chapter 3

Palmitate-induced insulin resistance in monocytes

3.1 Preface

This chapter describes an investigation of palmitate effects on insulin sensitivity in monocytes. Initial experiments were carried out to characterise the effects of serum starvation, insulin concentration and incubation time on insulin stimulation of glucose uptake by monocytes (U937 and THP-1 monocytes). Subsequent experiments were conducted to investigate the concentration and the time course of the effect of palmitate on insulin sensitivity in THP-1 monocytes. Finally, potential mechanisms (e.g. via ceramide and/or ROS) of palmitate-induced insulin resistance and the effect of oleate on this action of palmitate were examined.

3.2 Introduction

Insulin resistance is a state of reduced responsiveness of tissues such as liver, skeletal muscle, and adipose tissue to the action of insulin. The major metabolic and systemic changes associated with insulin resistance are displayed by a group of disorders including type 2 diabetes, hypertension, hyperlipidemia, central obesity, atherosclerotic heart disease, and other abnormalities.

As insulin resistance plays a central role in the development of above metabolic abnormalities, lack of sensitivity to insulin has been assessed widely using in vitro and *in vivo* models. The most common *in vitro* method for evaluation of insulin sensitivity is comparing insulin-stimulated glucose uptake in insulin responsive tissues such as skeletal muscle and adipose tissue to basal glucose uptake (without insulin stimulation). In this way, the metabolic effect of insulin on glucose metabolism in these tissues can be assessed from a concentration-response curve

constructed from a series of physiological and supra-physiological concentrations of insulin (10^{-12}-10^{-6}M). The effect of insulin on glucose metabolism is mainly through its ability to regulate the trafficking of glucose transporters in insulin targeting tissues such as skeletal muscles and adipose tissue. Glucose transporter 1 (GLUT1) is mainly responsible for the glucose uptake during non-insulin stimulated conditions whereas glucose transporter 4 (GLUT4) mediated the insulin-stimulated glucose uptake. Insulin can increase the glucose uptake within a short time (a few minutes) by promoting the rapid translocation of intracellular GLUT4 storage vesicles to the cell membrane (Bell et al., 1990). In addition, insulin exerts its effect on glucose transport through a long-term regulation of glucose transporter protein synthesis and degradation. It has been reported that the continuous insulin stimulation of 3T3-L1 adipocytes induced an increased rate of synthesis of GLUT1 and GLUT4 (Sargeant and Paquet, 1993). The methods for the determination of insulin resistance in vivo are much more diverse and complicated. Some studies have described increased plasma insulin levels as a marker of insulin resistance and as an independent predictor of Type 2 diabetes (Samaras et al., 2006). However, the most two accurate and reproducible methods for measuring insulin resistance are the euglycaemic hyperinsulinaemic clamp and the intravenous glucose tolerance test with minimal model analysis (Bergman et al., 1979).

Although the precise mechanism of insulin resistance in still not clear, the role of increased plasma free fatty acids has been strongly implicated in the pathogenesis of insulin resistance. Several *in vivo* lipid-infusion studies in humans and animals

have consistently showed that increasing plasma free fatty acids levels for 3-5h causes both whole body and peripheral tissue insulin resistance (Boden, 1994; Jucker et al., 1997; Park et al., 1998; Dresner et al., 1999; Griffin et al., 1999). Further studies using cultured rat L6 skeletal muscle cells and 3T3-adipocytes and high-fat-diet fed rats have suggested that the saturated fatty acid palmitate was the main contributor to insulin resistance compared to unsaturated fatty acids (Sinha et al., 2004; Hunnicutt et al., 1994; Jong et al., 2006). Furthermore, a recent study using rats administered intraperitoneally with palmitic acid reported a delay in response to insulin of glucose metabolism and a defect in early insulin signal transduction in skeletal muscle, supporting the critical role of palmitate in inducing whole body and muscle insulin resistance in vivo (Reynoso, 2003).

As one of the intermediate metabolites generated from palmitate, the role of ceramide in lipid-induced insulin resistance is controversial. In vitro studies have supported a central role of ceramide mediating palmitate-induced insulin resistance in muscle cells through its ability to reduce the activation of PKB/Akt, a kinase that directly regulates the GLUT4 translocation to cell membrane and glucose uptake (Schmitz-Peiffer et al., 1999, Powell et al., 2004). However, results from rats infused with a lipid emulsion consisting most of 18:2 fatty acids for 5h showed a significant reduction in insulin-stimulated glucose transport activity but lack of changes in ceramide content in skeletal muscles (Yu et al., 2002). The discrepancies may due to the free fatty acids species used in vitro and *in vivo*.

Circulating monocytes have been reported to have comparable numbers of insulin receptors on their cell surface compared to classical insulin targeting cells such as skeletal muscle cells, adipocytes and hepatocytes (Montague, 1983). Previous studies have demonstrated monocytes rather than lymphocytes were the insulin binding cells in the circulation and the binding of monocytes to insulin was decreased in obese subjects (Schwartz et al., 1975; Olefsky, 1976). Other studies also showed that monocytes respond to short term stimulation of physiological concentrations of insulin (Daneman, 1992; Cutfield et al., 2000; Dimitriadis et al., 2004). Although skeletal muscle, adipose tissue, and liver are the major sites for regulating glucose metabolism and maintaining glucose haemostasis in the body, the difficulty to get access to these tissues for in vitro studies makes them inconvenient targets to study the mechanism of insulin resistance. Therefore, as a relatively easily accessible cell type in the human body, monocytes are a potential useful tool to evaluate insulin resistance and to investigate the underlying molecular mechanisms of insulin resistance. In addition, the monocyte is a critical cell in atherogenesis, the principal complication in obesity and Type 2 diabetes.

Therefore, the present study aims to investigate the effect of palmitate on insulin sensitivity in human monocyte cell lines as cell models and also to investigate the potential mechanism(s) for any palmitate-mediated changes in glucose metabolism.

3.3 Materials and Methods

3.3.1. Cell Culture

U937 and THP-1 monocytes cell culture was carried out according to the method described in Section 2.2.1.

3.3.2 Cell treatment

Insulin stock solution (10^{-4}M) was prepared by dissolving 5.6mg insulin in 10ml PBS and filtered through a 0.2μm filter. The insulin stock solution was aliquoted, stored at -20°C and used freshly for each experiment.

To characterise the effect of insulin on monocyte glucose uptake, U937 and THP-1 cells were incubated with insulin (0, 10^{-9}, 10^{-8}, 10^{-7}, and 10^{-6}M) for various time periods (6h, 12h, and 24h) in RPMI 1640 supplemented with 10% FBS and 100U/ml penicillin and 100μg/ml streptomycin at 37°C. Insulin concentrations used from 10^{-9}-10^{-8}M correspond to physiological levels whereas 10^{-7}-10^{-6}M has been used in *in vitro* investigations (Dimitriadis et al., 2005).

To investigate the effect of palmitate on inducing insulin resistance in monocytes, THP-1 cells were incubated with palmitate (0, 50, 150 and 300μM) for various time periods (0, 2h, 4h, and 6h). Control cells received BSA equivalent to the BSA present in the cells treated with the highest palmitate concentration (300μM). The concentration of palmitate chosen are based on the typical plasma free fatty acids composition in which palmitate or oleate has been reported to be around 30% in

human plasma. Since the plasma FFA level in insulin resistant conditions are increased up to ~1000μM from 200-400μM in healthy conditions, therefore, 300μM could represent plasma palmitate or oleate level in insulin resistant conditions whereas 50μM and 150μM are concentrations representing a healthy range of plasma palmitate or oleate levels.

3.3.3 2-Deoxy-D-glucose (2-DG) uptake

2-Deoxy-D-glucose uptake into THP-1 monocytes was carried out after various incubations according to the method described in Section 2.5.

3.3.4 Cell viability assay

MTT assay, PI staining by flow cytometry, and caspase-3 assay were carried out after various incubations according to section 2.14.2.1, 2.14.3, and 2.13 to test whether incubation conditions have any adverse effect on cell viability.

3.3.5 Cell membrane extraction

THP-1 cells (6×10^6) were collected into 15ml centrifuge tubes and washed twice with 5ml ice-cold PBS. After re-suspended into 250mM sucrose, 20mM HEPES, 1mM EDTA, 1mM PMSF buffer, cell suspensions were sonicated three times in an ice bath. The cell homogenate was then centrifuged at 900×g for 10min at 4°C, and the supernatant was centrifuged at 100,000×g for 1h at 4°C. The high speed pellets were then re-suspended in 0.2-0.3ml of 20mM Hepes, 1mM EDTA, and 1mM PMSF by gentle pipetting.

3.3.6 Western blot analysis for glucose transporters

SDS-PAGE and Western blot analysis were carried out according to methods described in Section 2.8 to characterise the glucose transporters in both the whole cell lysates and membrane extractions in THP-1 monocytes with and without 10^{-6}M insulin stimulation for 12h. In brief, the cell lysates and extracted membrane proteins (50μg/lane) were subjected to SDS-PAGE on 10% gel. Glucose transporter isoforms were detected by immunoblotting using polyclonal rabbit anti-GLUT1 (1:1000), anti-GLUT3 (1:1000), anti-GLUT4 (1:1000) (Merk Calbiochem, Nottingham, UK); secondary mouse anti-rabbit conjugated with HRP (1:4000) (Sigma, Dorset, UK); and the protein bands were visualised by ECL plus kit (GE Healthcare).

3.3.7 Intracellular reactive oxygen species (ROS) determination

THP-1 monocytes were incubated with 300μM palmitate for 0-6h at 37°C and then analysed by flow cytometry for intracellular ROS levels using the peroxide sensitive permeable dye dihydrodicholorofluorescein diacetate (DCF-DA) as described in Section 2.10.

3.3.8 Statistical analysis

Data are expressed as mean ± SEM of at least three independent experiments, and 2-deoxy-D-glucose uptake is expressed as percentage compared with control (100%). Statistical analyses were performed by one-way ANOVA with Tukey-Kramer post hoc tests. A p value less than 0.05 was considered significant.

3.4 Results

3.4.1 Characterisation of monocytes in response to insulin

Human U937 and THP-1 monocytic cell lines were chosen for studying insulin sensitivity in monocytes as they have been extensively characterised for their function as human monocytes (Auwerx, 1991). The effect of insulin on monocytes was determined by *in vitro* uptake of 2-deoxy-D-glucose and characterised by requirement for serum starvation, insulin conc2entration and stimulation time periods.

3.4.1.1 Insulin increases glucose uptake in THP-1 but not U937 monocytes and this effect does not require serum starvation.

After 12h incubation with 10^{-7}M insulin, THP-1 monocytes showed an approximate 30% increase in glucose uptake compared to control cells without insulin stimulation ($p<0.001$; DPM 1792 ± 57.69 versus 1362 ± 5.53). This increase remained at a similar level after increasing the insulin concentration to 10^{-6}M ($p<0.001$). However, there was no difference between insulin-stimulated glucose uptake and basal glucose uptake in U937 monocytes incubated with any of the insulin concentrations tested (Fig.3.1). Therefore, THP-1 monocytes were chosen for subsequent experiments to investigate the development of insulin resistance monocytes.

In vitro studies using skeletal muscle cells and adipocytes showed that serum starvation increased insulin-stimulated glucose uptake by deactivating basal

GLUT4 level on adipocytes membrane (Garvey et al., 1987) and increasing the binding of skeletal muscle cells to insulin (Brady et al., 1981). Therefore, the effect of serum starvation was also investigated in monocytes. THP-1 monocytes were incubated in RPMI 1640 medium supplemented with FBS concentrations from 1% to 10% for 4h at 37°C followed by a further incubation with 10^{-6}M insulin for 12h.

As shown in Figure 3.2, there was approximately a 30% increase in glucose uptake after insulin stimulation in THP-1 monocytes incubated in medium supplemented with 10% FBS. However, reducing FBS concentration from 10% to lower concentrations (5%, 2% and 1%) did not additionally increase insulin-stimulated glucose uptake (p>0.05). Therefore, in the subsequent experiments, 10% FBS was used in the cell incubation medium for evaluating the effects of insulin on glucose uptake in THP-1 monocytes.

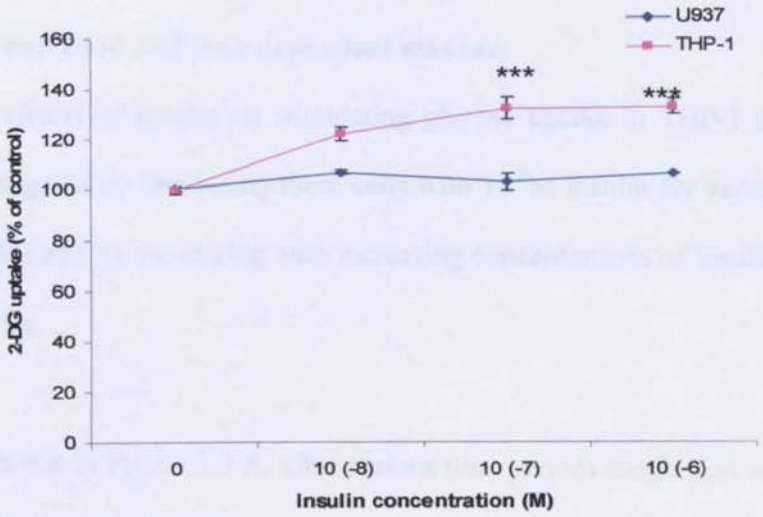

Figure 3.1 Insulin-stimulated 2-deoxy-D-glucose (2-DG) uptake into U937 and THP-1 monocytes. U937 and THP-1 monocytes were seeded at 10^6/ml in 24-well plates and incubated with insulin (10^{-8}-10^{-6}M) for 12h at 37°C. 2-DG uptake was determined after completion of incubation. Data are mean±SEM of 3 independent experiments performed in triplicate. *** $p<0.001$ compared to U937 monocytes.

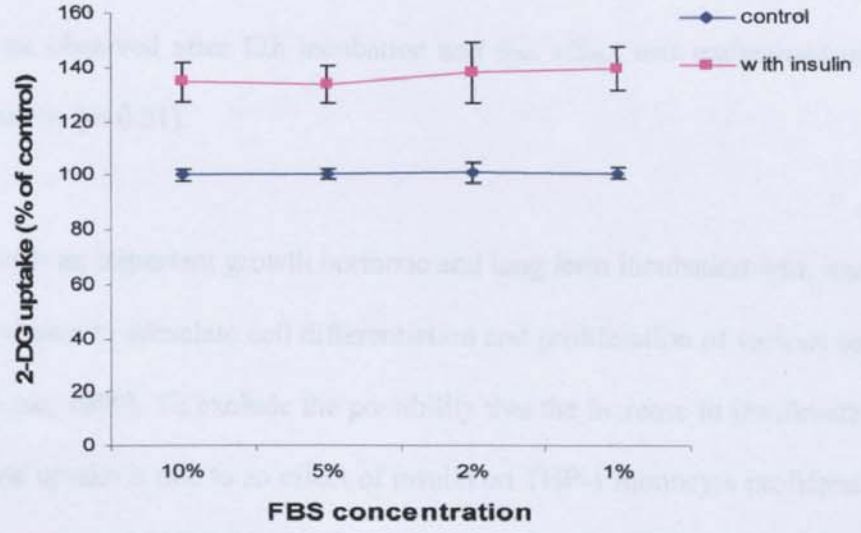

Figure 3.2 Effect of foetal bovine serum (FBS) on insulin-stimulated glucose uptake by THP-1 monocytes. THP-1 monocytes were incubated with different concentrations of FBS (1%, 2%, 5% and 10%) for 4h, and then stimulated with 10^{-6}M insulin for 12h. 2-deoxy-D-glucose uptake was measured after completion of incubation. Data are mean±SEM of 3 independent experiments performed in triplicate.

3.4.1.2 Insulin increases glucose uptake by THP-1 monocytes in a concentration and time dependent manner.

The effects of insulin on stimulating glucose uptake in THP-1 monocytes were investigated by incubating these cells with 10^{-6}M insulin for various time periods (0-36h) and by incubating with increasing concentrations of insulin (10^{-10}-10^{-5} M) for 12h.

As shown in Figure 3.3 A, after various time periods incubation without and with insulin, the basal and insulin-stimulated glucose uptake in THP-1 monocytes showed a similar pattern with a rapid increase in glucose uptake from 6h to12h, then a slight increase to 24h and a mild decline to 36h. Compared to basal glucose uptake, the insulin-stimulated glucose uptake in THP-1 monocytes was not evident at 6h incubation ($p>0.05$), but there was a significant approximate 30% increase observed after 12h incubation and this effect was maintained until 36h incubation ($p<0.01$).

Insulin is an important growth hormone and long term incubation with insulin has been shown to stimulate cell differentiation and proliferation of various cell types (Hainque, 1990). To exclude the possibility that the increase in insulin-stimulated glucose uptake is due to an effect of insulin on THP-1 monocyte proliferation, the MTT assay was carried out to evaluate the mitochondrial activity of cell as a measure of cell number with insulin incubation after various time periods. As shown in Figure 3.3 B, overall, there was a gradual increase in mitochondrial reductive activity in cells without insulin and with insulin from 6h to 36h

incubation. This effect was not significantly different in cells after 6h and 12h incubation compared to 0h ($p>0.05$). However, cells incubated with insulin showed a significant increase in mitochondrial reductive activity at 24h and 36h incubation compared with cells incubated without insulin ($p<0.01$). Therefore, 12h was chosen to investigate the concentration effect of insulin on glucose uptake in THP-1 monocytes in order to avoid any effect from increase in viable cell numbers after insulin stimulation.

Subsequently, the effect of insulin on glucose uptake in THP-1 monocytes was tested with a range of insulin concentrations from 10^{-10}M to 10^{-5}M. As shown in Figure 3.3 C, compared to basal glucose uptake, there was no significant increase in glucose uptake at insulin concentrations of 10^{-10}M and 10^{-9}M ($p>0.05$); the increase in insulin-stimulated glucose uptake was observed at 10^{-8}M with a maximal increase to approximate 30% at 10^{-6}M insulin; increasing insulin concentration further to 10^{-5}M did not show an additional increase but a significant reduction in glucose uptake ($p<0.01$).

Thus, insulin at 10^{-6}M for 12h incubation caused the maximal uptake of glucose and this condition was used for subsequent experiments to investigate palmitate-induced insulin resistance in THP-1 monocytes.

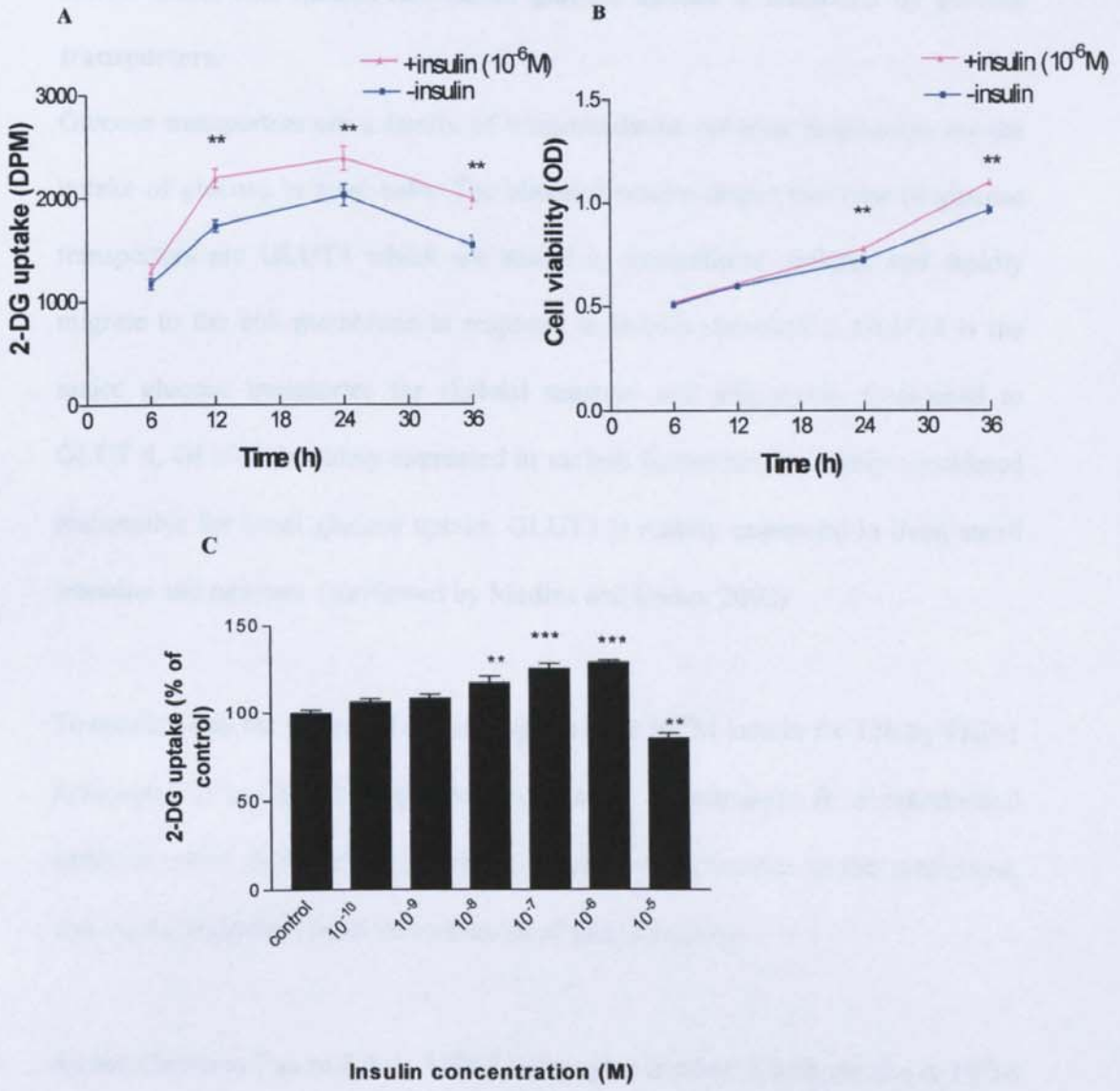

Figure 3.3 Effect of insulin on glucose uptake by THP-1 monocytes. THP-1 cells were seeded at 10^6/ml in 24-well plates and incubated with insulin (10^{-6}M) for 6-36h (A) or with insulin (10^{-10}-10^{-5}M) for 12h (C) at 37°C. 2-deoxy-D-glucose (2-DG) uptake was carried out after completion of incubation. MTT assay as a measurement of viable cell numbers was conducted after incubating THP-1 monocytes with 10^{-6}M insulin for 6-36h (B). Data are mean±SEM of 3 independent experiments performed in triplicate. Controls are cells incubated with PBS without insulin stimulation. ** p <0.01 compared with THP-1 cells without insulin stimulation (A and B). **p<0.01, *** p<0.001 compared with control (C).

3.4.1.3 Basal and insulin-stimulated glucose uptake is mediated by glucose transporters.

Glucose transporters are a family of transmembrane proteins responsible for the uptake of glucose in most cells. The classical insulin-responsive type of glucose transporters are GLUT4 which are stored in intracellular vesicles and rapidly migrate to the cell membrane in response to insulin stimulation. GLUT4 is the major glucose transporter for skeletal muscles and adipocytes. Compared to GLUT 4, GLUT1 is widely expressed in various tissues and generally considered responsible for basal glucose uptake. GLUT3 is mainly expressed in liver, small intestine and neurons. (Reviewed by Medina and Owen, 2002)

To confirm that the increased glucose uptake after 10^{-6}M insulin for 12h by THP-1 monocytes is attributed to glucose transporters, cytochalasin B, a cytoskeletal inhibitor which will prevent glucose transporter mobilisation to the membrane, was used during the 10min measurement of glucose uptake.

As has shown in Figure 3.4 A, THP-1 monocytes incubated with insulin at 10^{-6}M insulin for 12h caused a significant approximate 30% increase in glucose uptake compared to control ($p<0.001$). With the addition of 10μM cytochalasin B to the 2-deoxy-D-glucose uptake buffer, there was more than 80% reduction in glucose uptake in both control and insulin-stimulated cells, and the increase in insulin-stimulated glucose uptake was completely abolished. In order to exclude the possibility that the loss of cell protein content may contribute to the reduction in glucose uptake caused by cytochalasin B, the BCA protein assay was carried

out in the cell lysates after glucose uptake. As shown in Figure 3.4 B, there was no significant difference in total protein content between cell lysates without and with the addition of cytochalasin B ($p>0.05$), indicating the inhibition of basal and insulin-stimulated glucose uptake by cytochalasin B treatment was not related to cell viability loss. Together, these data indicate that the glucose transporters were responsible for basal and insulin-stimulated glucose uptake in THP-1 monocytes.

It has been reported in the literature that long term insulin stimulation promotes glucose transporter gene expression in adipocytes (Hajduch et al., 1995) and muscle (Holmäng et al., 1995). Therefore, cycloheximide, a non-specific protein synthesis inhibitor, was used to examine whether the increase in insulin-stimulated glucose uptake in THP-1 monocytes is due to the increase in protein synthesis by insulin. As shown in Figure 3.5 A, co-incubation of THP-1 monocytes with cycloheximide (0.1-10μM) for 12h in the presence of 10^{-6}M insulin significantly reduced more than 50% of both basal and insulin-stimulated glucose uptake and also abolished the increase in insulin-stimulated glucose uptake. The cell viability measured in parallel experiments showed that cycloheximide at concentrations of 0.1μM and 0.5μM did not exert any adverse effect on THP-1 monocytes cell viability, although there was a slight reduction in cell viability at 5μM and 10μM cycloheximide (Fig 3.5 B). These data suggest that protein synthesis is involved in the insulin-stimulated glucose uptake in THP-1 monocytes.

To further examine the role of glucose transporters in mediating the

insulin-stimulated glucose uptake in THP-1 monocytes, SDS-PAGE and Western blot was carried out in both whole cell lysates and membrane extractions after stimulation with 10^{-6}M insulin for 12h. As shown in Figure 3.6, THP-1 monocytes express GLUT1 and GLUT3 as detected in both the whole cell lysates and membrane extractions. The expression of GLUT4 is not detectable in THP-1 monocytes; expression of GLUT4 in L6 skeletal muscle cells is shown as a positive control. Therefore, these data may suggest that the increase in insulin-stimulated glucose uptake is associated with GLUT1 and/or GLUT3.

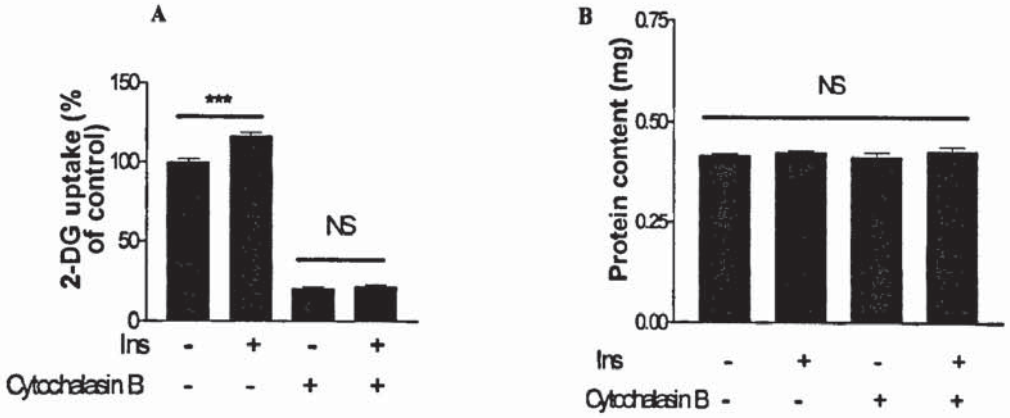

Figure 3.4 Cytochalasin B inhibits basal and insulin stimulated glucose uptake (A) and does not affect total protein levels (B) in THP-1 monocytes. THP-1 cells (2×10^6/ml) were incubated with insulin (Ins) (10^{-6}M) for 12h at 37°C. 2-deoxy-D-glucose (2-DG) in THP-1 cells was carried out for 10min at room temperature with and without 10μM cytochalasin B. After lysing cells with 1M NaOH, the total protein content in cell lysates was determine by BCA protein assay. Data are mean±SEM of 3 independent experiments performed in triplicate. ***$p<0.001$. NS: non significant.

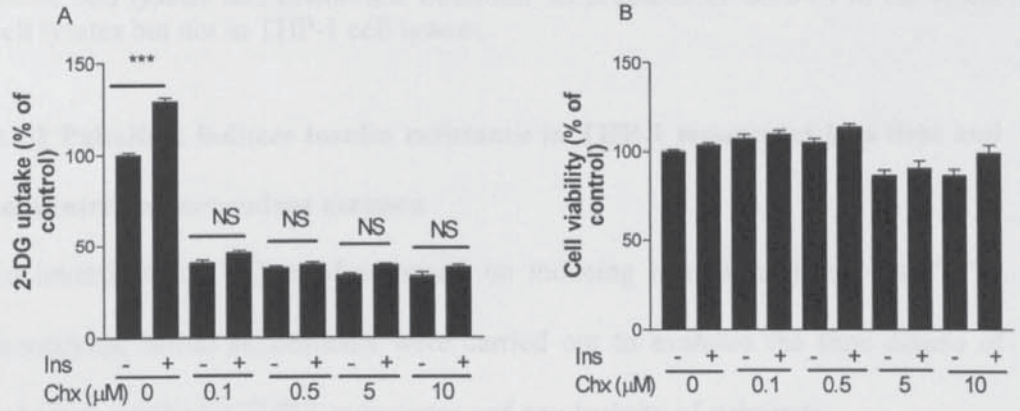

Figure 3.5 Effect of cycloheximide (ChX) on glucose uptake by THP-1 monocytes (A) and cell viability (B). THP-1 cells (10^6/ml) were incubated with various concentrations of cycloheximide (ChX) (0.1-10μM) with and without insulin (Ins) (10^{-6}M) for 12h at 37°C. 2-deoxy-D-glucose (2-DG) uptake and cell viability measured by MTT assay were carried out after completion of incubation. Data are mean±SEM of 3 independent experiments performed in triplicate. ***p<0.001. NS: non significant.

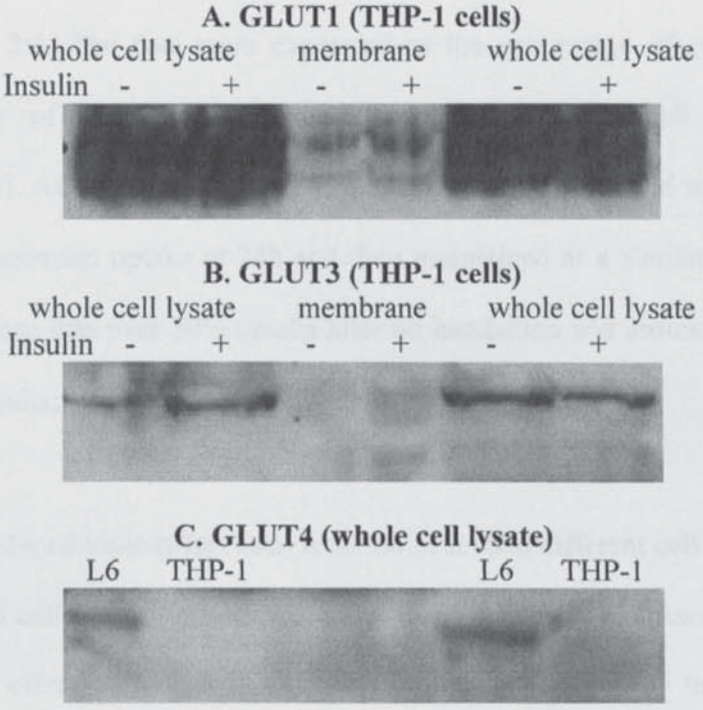

Figure 3.6 Western blot analysis for glucose transporters in THP-1 monocytes. THP-1 cells (10^6/ml) were incubated with 10^{-6}M insulin for 12h at 37°C. Whole cell lysates and extracted membrane proteins (50μg/lane) were prepared and separated by 10% SDS-PAGE and detected by anti-GLUT1, anti-GLUT3, and anti-GLUT4 as described in the Section 3.3.5. **A:** presence of GLUT1in THP-1 whole cell lysates and membrane fractions. **B:** presence of GLUT3 in THP-1

whole cell lysates and membrane fractions. **C:** presence of GLUT4 in L6 whole cell lysates but not in THP-1 cell lysates.

3.4.2 Palmitate induces insulin resistance in THP-1 monocytes in a time and concentration dependent manner.

To investigate the effect of palmitate on inducing insulin resistance in THP-1 monocytes, initial experiments were carried out to evaluate the time course of palmitate uptake by THP-1 monocytes and any toxicity of palmitate.

The uptake and accumulation of palmitate in THP-1 monocytes was determined by incubating cells with RPMI 1640 medium (10% FBS) supplemented 0.1μCi/ml [^{3}H]-palmitic acid in the presence 100μM palmitate bound to BSA with a final molar ratio 2:1. The data were expressed as the percentage of cell-associated radioactivity of the total radioactivity (radioactivity in cell lysates and supernatants). As shown in Figure 3.7, the uptake of palmitic acid was rapid over 12h with maximum uptake at 24h and then maintained at a similar level at 48h and 72h. There was over 50% uptake after 6h incubation and around 90% uptake after 24h incubation (p<0.001).

Palmitate-induced toxicity has been reported in several different cell types such as pancreatic β cells (Cnop et al., 2001) and cardiomyocytes (Hickson-Bick et al., 2002). The effect of palmitate on monocyte cell viability was investigated in THP-1 monocytes incubated with 50, 150 and 300μM palmitate for 24h using the MTT assay. Cells were treated with BSA alone as controls. The data were expressed as % of control cells. As shown in Figure 3.8, 50μM palmitate did not

have any significant effect on THP-1 cell viability whereas 150μM and 300μM palmitate caused a rapid and time dependent decrease in cell viability. There was a significant decrease in cell viability at 8h and with further decrease at 24h in both 150μM and 300μM palmitate treatments ($p<0.01$). Further analysis of cell viability by caspase 3 activity assay and propidium iodide staining consistently showed that 300μM palmitate for 6h treatment did not cause significant apoptosis to THP-1 monocytes (Fig. 3.9 A, B, and C).

Therefore, the effect of palmitate on glucose uptake was investigated within 6h in the subsequent experiments in order to prevent significant cell loss.

The effect of palmitate-induced insulin resistance in monocytes was carried out by incubating THP-1 cells with 10^{-6} M insulin for 12h during which 300μM palmitate was added for the last 2h, 4h and 6h or 50-300μM palmitate were added for the last 6h. Justifications of insulin and palmitate concentrations are presented in Section 3.3.2. As shown in Figure 3.10A, there was a time dependent decrease in insulin-stimulated glucose uptake in THP-1 monocytes after incubation with 300μM palmitate. There was no significant effect of 300μM palmitate on basal glucose uptake in THP-1 monocytes up to 6h incubation. However, the reduction in insulin-stimulated glucose uptake was evident at 2h ($p<0.05$) and insulin-stimulated glucose uptake was almost completely abolished at 6h ($p<0.001$).

Therefore, based on the above data, the effect of palmitate concentrations on basal

and insulin-stimulated glucose uptake in monocytes was studied using 6h incubation. As shown in Figure 3.10 B insulin-stimulated glucose uptake was not affected by 50μM palmitate ($p>0.05$). Increasing the palmitate concentration to 150μM caused a significant reduction in insulin-stimulated glucose uptake compared to cells without insulin stimulation ($p<0.001$). Palmitate (300μM) completely abolished the increase in insulin-stimulated glucose uptake. (101±4.9% versus 134.1±2.9%, $p<0.001$).

Taken together, the data show that co-incubation with 300μM palmitate for 6h causes insulin resistance in human THP-1 monocytes and this effect is not associated with palmitate toxicity.

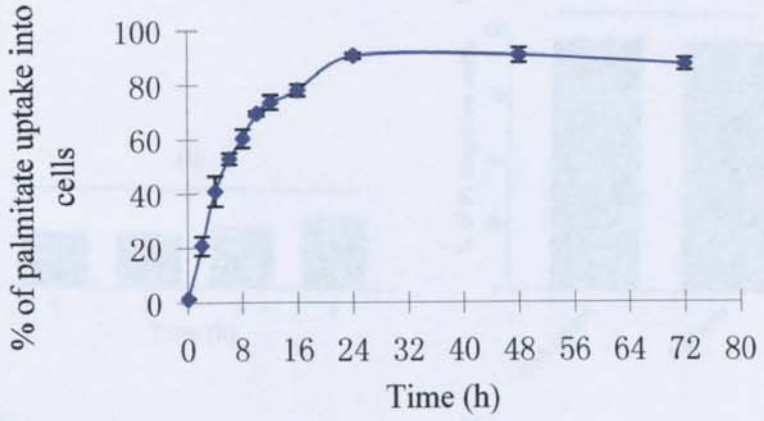

Figure 3.7 Time course of palmitate uptake by THP-1 monocytes. THP-1 cells (10^6/ml) were seeded into 12-well plates with 0.1μCi/ml of ^{3}H-palmitic acid and 100μM unlabeled palmitate conjugated to albumin for various time points (0-72h). The percentage of uptake of palmitate by cells was determined by cell specific radioactivity relative to radioactivity in supernatants. Data are from 3 independent experiments performed in triplicate and are expressed as mean±SEM.

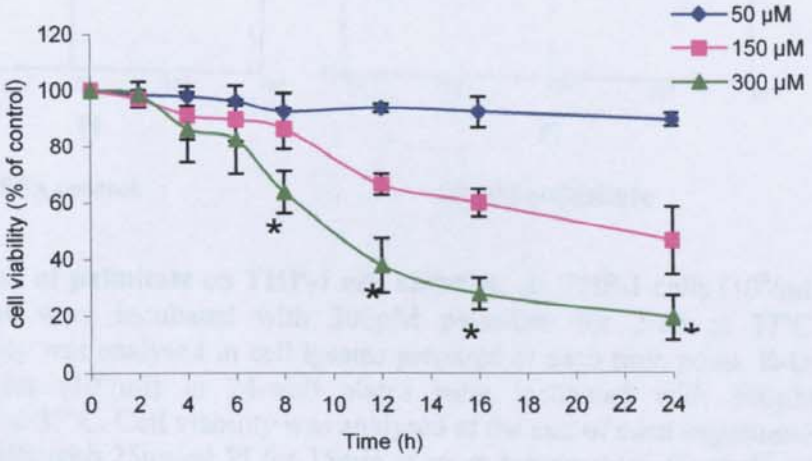

Figure 3.8 Effect of time and concentration of palmitate on THP-1 cell viability. THP-1 cells (10^5/ml) were incubated with palmitate (50,150,300μM) for different time point (0-24h). Cell viability was determined by the MTT assay. Controls are cells incubated with BSA. Data are from 4 independent experiments performed in triplicate. * $P<0.01$ represents 300μM palmitate compared to 50 and 150μM palmitate or controls.

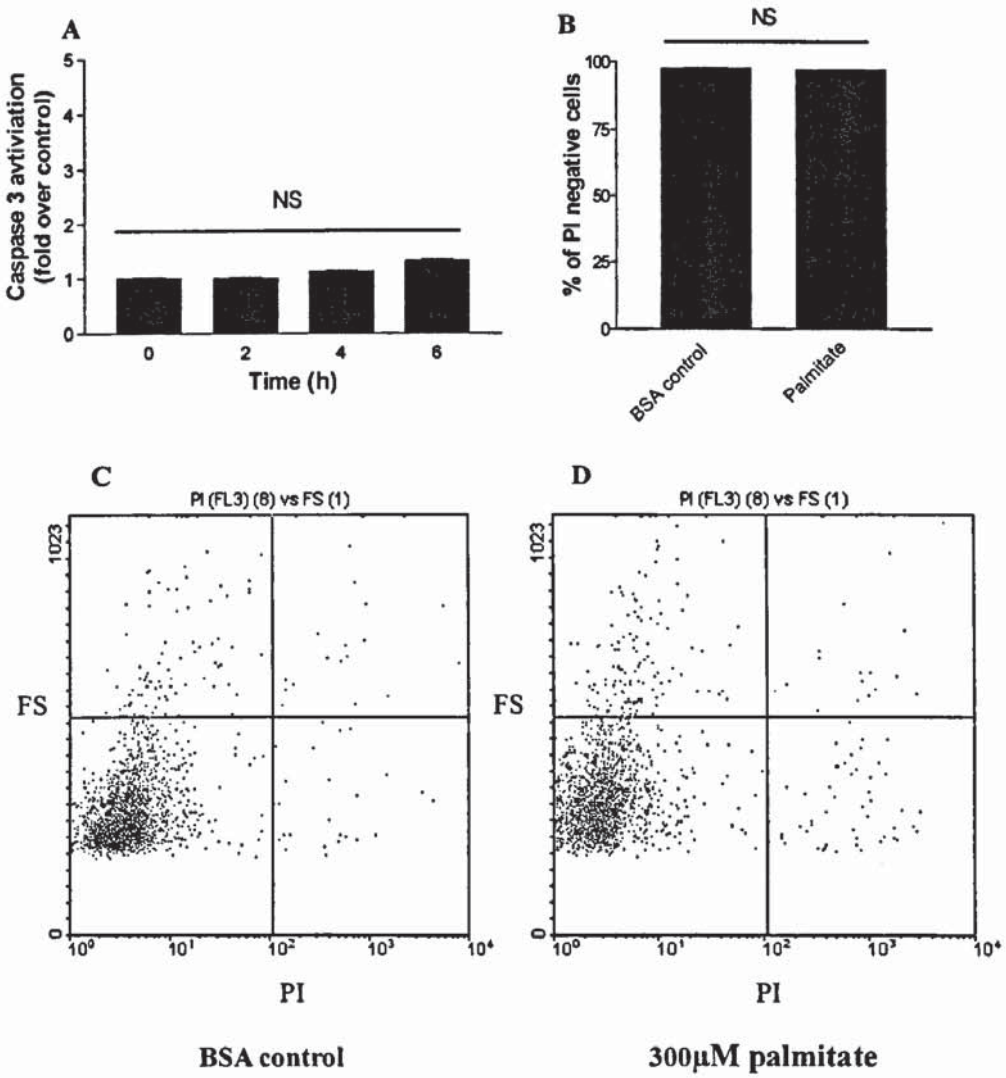

Figure 3.9 Effect of palmitate on THP-1 cell viability. A: THP-1 cells (10^6/ml) in 6-well plates were incubated with 300μM palmitate for 2-6h at 37°C. Caspase-3 activity was analysed in cell lysates prepared at each time point. **B-D:** THP-1 monocytes (10^6/ml) in 24-well plates were incubated with 300μM palmitate for 6h at 37°C. Cell viability was analysed at the end of each experiment by incubating cells with 25μg/ml PI for 15min at room temperature. Controls are cells incubated with BSA. Data are mean±SEM of 3 independent experiments performed in duplicate. NS: non significant.

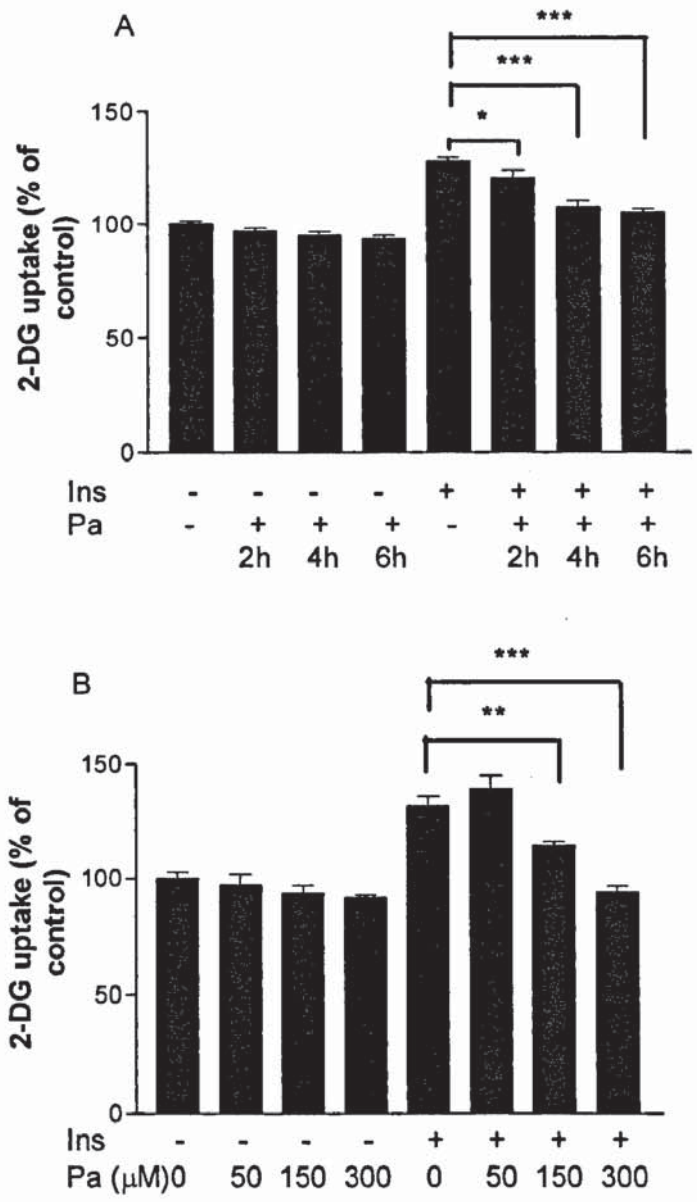

Figure 3.10 Effect of palmitate (Pa) incubation time (A) and (B) concentration on glucose uptake by THP-1 monocytes. THP-1 cells (10^6/ml) in 24-well plates were incubated with 10^{-6} M insulin for 12h at 37°C during which 300μM palmitate was added for the last 2h, 4h, and 6h incubation (A) or various concentrations of palmitate (50-300μM) was added for the last 6h (B). Controls are THP-1 monocytes incubated with BSA. 2-deoxy-D-glucose (2-DG) uptake was carried out after completion of incubation. Data are mean±SEM of 3 independent experiments performed in triplicate. *p<0.05, ** p<0.01, *** p<0.001.

3.4.3 Palmitate-induced insulin resistance in THP-1 monocytes is not reversible.

To investigate whether the palmitate-induced insulin resistance in monocytes can be reversed, THP-1 monocytes were first incubated with and without 10^{-6}M insulin for 12h during which 300μM palmitate was added at the last 6h. Then the medium was replaced with fresh RPMI 1640 and the cells were incubated in this fresh medium for another 24h and 48h before being stimulated with and without 10^{-6}M insulin for a further 12h (Fig. 3.11). The basal and insulin-stimulated glucose uptake was determined after the completion of incubation.

As shown in Figure 3.12 A and B, 12h treatment with insulin caused approximately a 30% increase in glucose uptake in BSA-treated cells while 300μM palmitate almost completely abolished this effect. Replacing cell incubation medium after 12h of insulin stimulation with fresh medium for a further 24h and 48h (washout 24h and washout 48h), the insulin-stimulated glucose uptake in BSA-treated cells still remained significantly increased compared to BSA-treated cells without insulin stimulation. However, cells incubated with 300μM palmitate did not show any significant increase in insulin-stimulated glucose uptake.

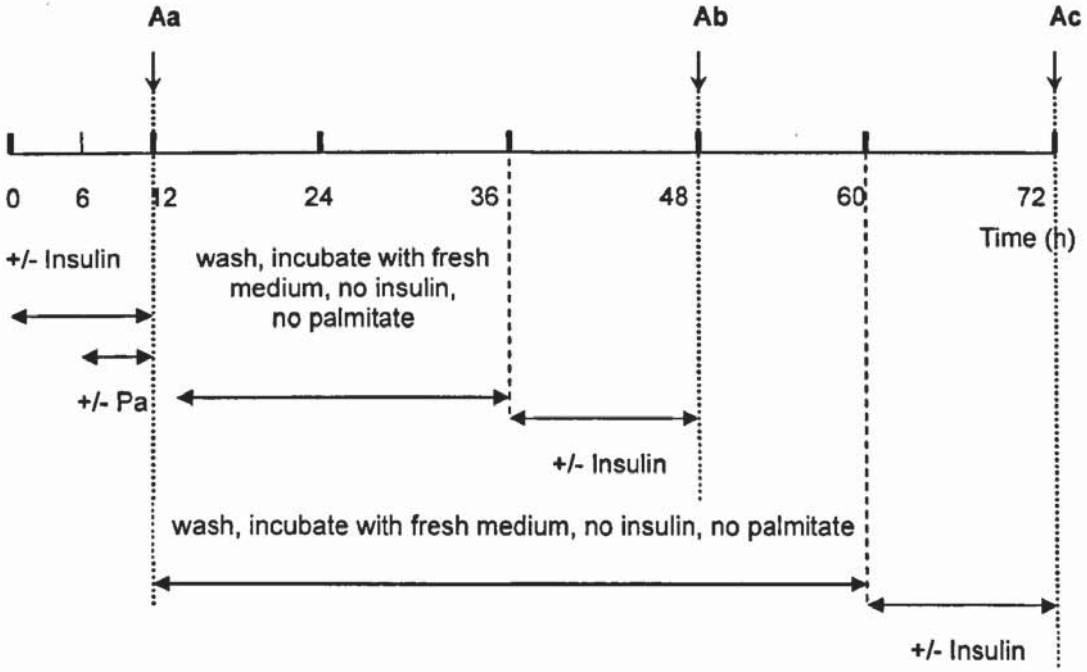

Fig 3.11 Schematic graph of insulin resistance reversibility experimental design. Aa; THP-1 monocytes (10^6/ml) were incubated for 12h with or without insulin (10^{-6} M), and with or without palmitate (300μM) for the last 6h. Controls are cells incubated with BSA. **Ab:** Identically treated monocytes to Aa were washed and re-incubated in fresh medium without insulin or palmitate until 36h, then incubated with or without insulin (10^{-6} M) until 48h, when 2-DG uptake was measured. **Ac:** Monocytes treated identically to Aa were washed and re-incubated in fresh medium without insulin or palmitate until 60h, then incubated with or without insulin (10^{-6} M) until 72h, when 2-DG uptake was measured.

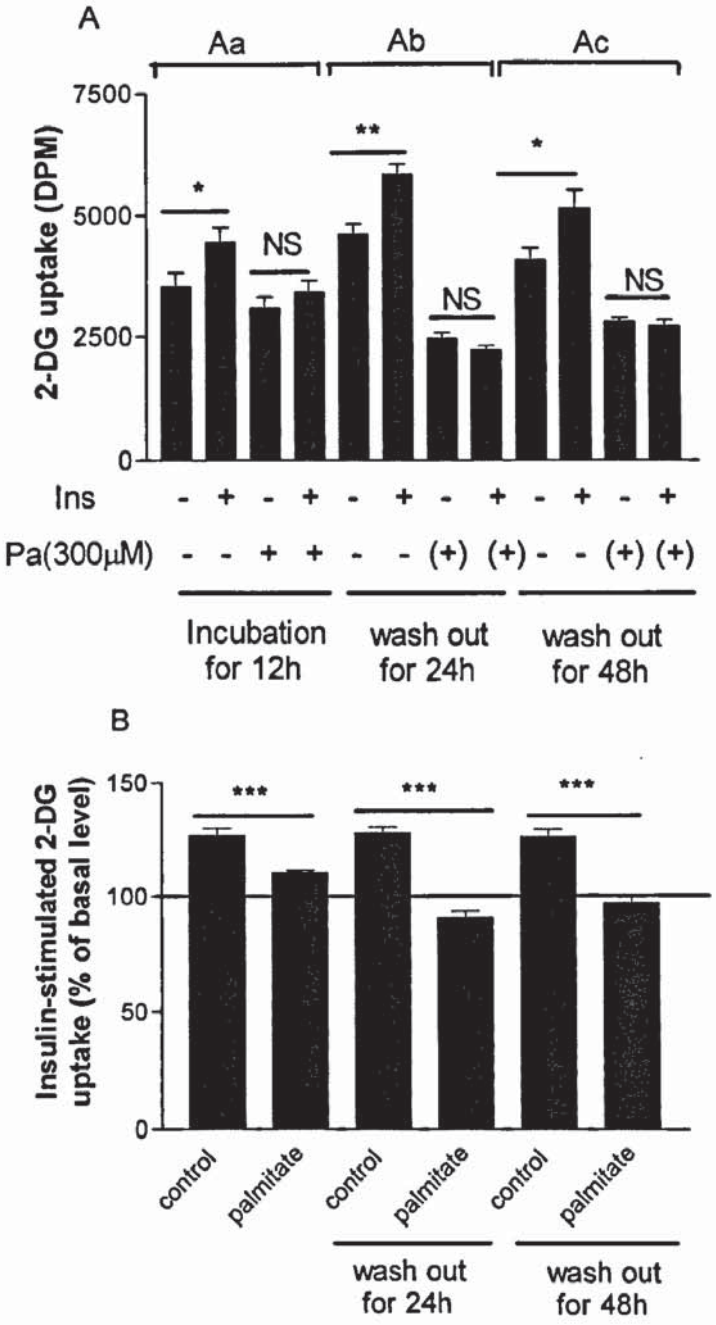

Fig. 3.12 Reversibility of palmitate-induced insulin resistance in THP-1 monocytes. Aa: THP-1 monocytes (10^6/ml) were incubated for 12h with or without insulin (10^{-6} M), and with or without palmitate (300μM) for the last 6h. Controls are cells incubated with BSA. **Ab:** Identically treated monocytes to Aa were washed and re-incubated in fresh medium without insulin or palmitate until 36h, then incubated with or without insulin (10^{-6} M) until 48h. **Ac:** Monocytes treated identically to Aa were washed and re-incubated in fresh medium without insulin or palmitate until 60h, then incubated with or without insulin (10^{-6} M) until 72h. 2-DG uptake was measured at 12h (Aa), 48h (Ab), and 72h (Ac). All 2DG uptake data in panel **A** are expressed as DPM. (+): Palmitate (300μM) was only

added for period 6-12h. **B.** Insulin-stimulated increment in 2-DG uptake data from panel **A** are re-expressed as % change compared with identically treated cells without insulin. Data are mean±SEM of 3 independent experiments performed in triplicate. *p<0.05; **p<0.01; ***p<0.001; NS: not significant.

3.4.4 Effect of palmitate on intracellular reactive oxygen species (ROS) generation in THP-1 cells

To investigate whether palmitate-induced insulin resistance in monocytes is associated with oxidative stress, the intracellular ROS generation was determined in THP-1 monocytes. Figure 3.13 shows that the mean fluorescence intensity was significantly reduced by 20% ($p<0.01$) and 36% ($p<0.001$) in cells incubated with 300μM palmitate for 4h and 6h.

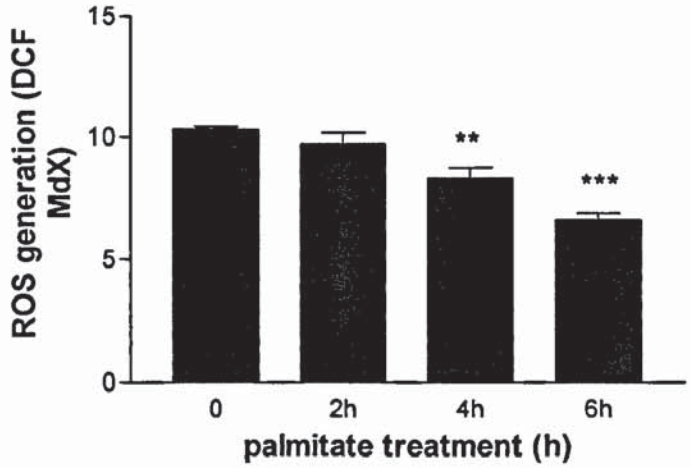

Figure 3.13 Effect of palmitate on ROS generation. THP-1 cells (10^6/ml) were incubated with 300μM palmitate for 0-6h at 37°C. Intracellular ROS generation was measured by flow cytometry. Data are mean±SEM from 3 independent experiments performed in triplicate. ***$p<0.001$.

3.4.5 Fumonisin B1 prevents palmitate-induced insulin resistance in THP-1 monocytes.

Lipid oversupply to peripheral tissues such as skeletal muscles and adipose tissues has been widely acknowledged as an important contributor to the development of

insulin resistance. Several studies using skeletal muscle cells indicated that ceramide, one of the intermediate of lipid metabolites, plays a critical role in palmitate-induced insulin resistance (Chavez, 2003; Straczkowski et al., 2004). Therefore, in order to test this hypothesis and attribute a causal role of ceramide in palmitate-induced insulin resistance in monocytes, fumonisin B1 (FB1), an inhibitor of *de novo* ceramide synthesis was used.

THP-1 monocytes were pre-incubated with 50μM FB1 for 1h and then co-incubated with and without 10^{-6}M insulin for 12h during which 300μM palmitate was added for the last 6h. As shown in Figure 3.14 A, under these conditions, cells incubated with FB1 showed a significant decrease in basal glucose uptake compared to cells incubated without FB1 (70% versus 100%). However, the increase in insulin-stimulated glucose uptake was not affected in FB1 treated cells. To exclude the possibility of cell viability loss caused by FB1, the MTT assay was performed in parallel experiments. As shown in Figure 3.14 C, there was no significant difference in cell viability between cells treated with and without 50μM FB1 for 13h.

Therefore, to optimise the conditions of FB1 treatment without reducing basal glucose transport in monocytes, THP-1 cells were incubated with 25μM FB1 for 5h and 7h, 50μM FB1 for 5h and 7h.

As shown in Figure 3.14 B, incubating THP-1 monocytes with 25μM and 50μM FB1 for 5h and 7h caused a time and concentration dependent decrease in basal

glucose uptake compared to cells without FB1(controls) ($p<0.001$). The decrease in basal glucose uptake was observed at 5h incubation with 50μM FB1 ($p<0.001$) and with a further decrease after 13h incubation ($p<0.001$) compared to controls. However, cells incubated with 25μM FB1 for 5h did not show a significant reduction in basal glucose uptake compared to controls ($p>0.05$). Therefore, 25μM FB1 up to 5h incubation was chosen to investigate whether ceramide generation was involved in palmitate-induced insulin resistance in THP-1 monocytes.

As shown in Figure 3.15, when adding 25μM FB1 to 300μM palmitate for up to 3h, the presence of FB1 preserved the increase in insulin-stimulated glucose uptake up to 2h incubation compared to cells treated with palmitate alone ($p<0.05$). However, this effect disappeared after 3h incubation with FB1.

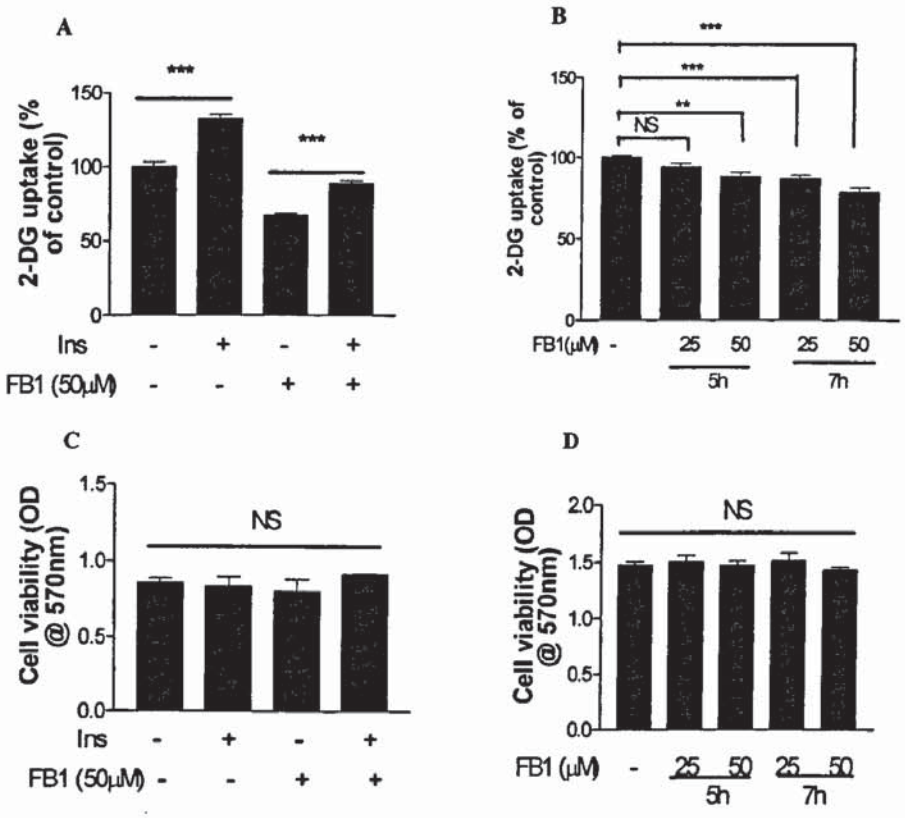

Figure 3.14 Effect of fumonisin B1 (FB1) on basal and insulin stimulated glucose uptake. THP-1 cells (10^6/ml) in 24-well plates were incubated with 1h pre-incubation of 50μM FB1 and then with/without insulin for 12h at 37°C (A and C). THP-1 cells (10^6/ml) in 24-well plates were incubated with FB1 (25μM and 50μM) for various time periods (5h and 7h) at 37°C (B and D). 2-deoxy-D-glucose uptake (2-DG) and cell viability measured by MTT assay were carried out after completion of incubation. Data are mean±SEM of 3 independent experiments performed in triplicate. ** $p<0.01$, *** $p<0.001$. NS: non significant.

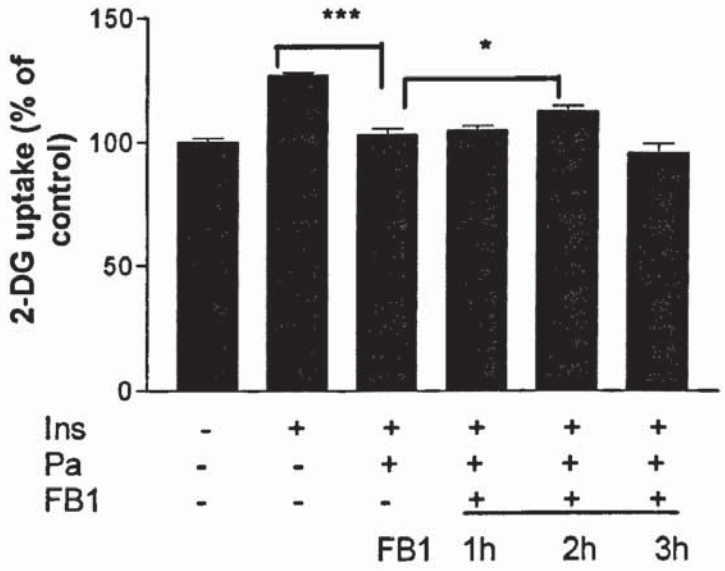

Figure 3.15 Effect of fumonisin B1 (FB1) on palmitate-induced insulin resistance. THP-1 cells (10^6/ml) in 24-well plates were incubated with 10^{-6} M insulin for 12h during which 300μM palmitate was added for the last 6h at 37°C. 25μM of FB1 was also added for the last 1h, 2h and 3h of incubation. Controls are cells treated with BSA. 2-deoxy-D-glucose (2-DG) uptake was measured at 12h. Data are mean±SEM of 3 independent experiments performed in triplicate. * $p<0.05$, *** $p< 0.001$.

3.4.6 Oleate does not induce insulin resistance but protects against palmitate-induced insulin resistance in THP-1 monocytes.

Oleate is one of the most abundant monounsaturated free fatty acids in human plasma, and has been shown *in vitro* not to affect glycogen synthesis in C2C12 muscle cells whereas palmitate has been shown to reduce glycogen synthesis in the same type of cells. Therefore, to compare the effect of oleate on basal and insulin-stimulated glucose transport in monocytes with palmitate, THP-1 cells were incubated 10^{-6}M insulin for 12h during which 300μM oleate with or without 300μM palmitate was added for the last 6h.

As shown in Figure 3.16 A, neither palmitate alone, nor oleate alone, nor palmitate plus oleate showed any significant effect of basal glucose uptake. Palmitate at 300μM almost completely inhibited the insulin-stimulated increase in glucose uptake from a BSA control level of 130%±2.0 to 105%±1.4 (p<0.001). However, cells incubated with 300μM oleate for 6h showed an approximate 20% increase in glucose uptake after insulin stimulation (p<0.001). Furthermore, co-incubating palmitate-treated cells with 150μM oleate significantly increased insulin-stimulated glucose uptake from 105%±1.4 to 126%±2.1 (p<0.001).

To exclude the possibility that any cell loss in those treatments could contribute to the changes in insulin-stimulated glucose uptake. Cell viability was determined by MTT assay after various free fatty acids treatments. As shown in Figure 3.16 B, there was no significant difference in the cell viability after each fatty acids treatment (p>0.05).

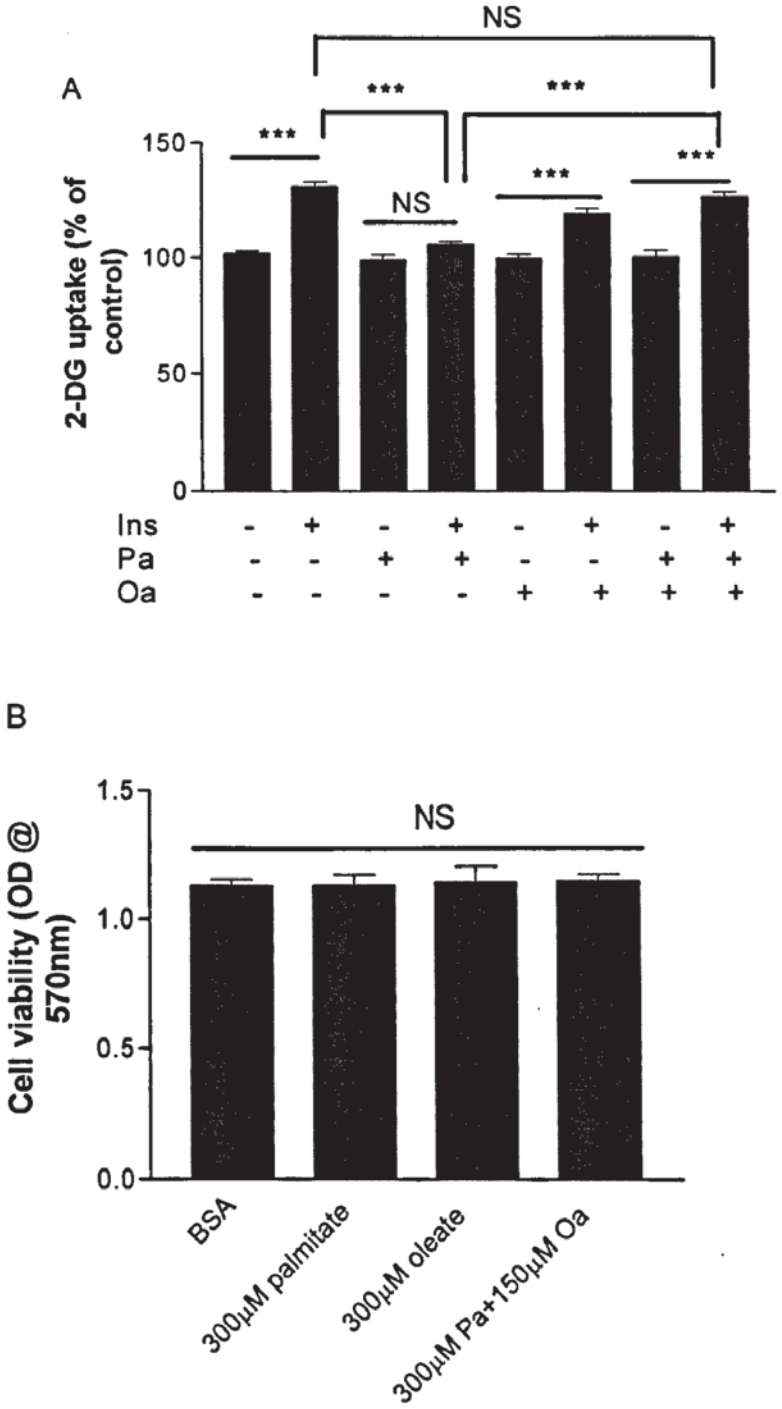

Figure 3.16 Effect of oleate on glucose uptake by THP-1 monocytes. A. THP-1 cells (10^6/ml) in 24-well plates were incubated with insulin (Ins) (10^{-6}M) during which 300μM palmitate (Pa) or 300μM Oleate (Oa) or combination of 150μM oleate and 300μM palmitate were added for the last 6h at 37°C. Controls are cells incubated with BSA. 2-deoxy-D-glucose (2-DG) uptake was measured after completion of incubation. **B.**MTT assay was used as a measurement of cell viability after incubation with palmitate or oleate. Data are mean±SEM of 3 independent experiments performed in triplicate. ***p<0.001. NS: non significant.

3.5 Discussion

The objectives of the present study were to investigate whether palmitate can induce insulin resistance in monocytes and to test the hypothesis that palmitate-induced insulin resistance in monocytes is through altered ceramide metabolism. The results presented in this chapter show that THP-1 monocytes, a matured human monocyte cell line, required at least 12h insulin (10^{-6}M) stimulation to increase glucose uptake up to 30% whereas U937 monocytes, which have an immature phenotype, did not respond to insulin in the conditions tested. Using THP-1 monocytes, the results demonstrate that 300μM palmitate for 6h almost completely abolished the increase in insulin-stimulated glucose uptake by THP-1 cells and this was partly due to ceramide but not reactive oxygen species.

In the classical insulin targeting tissues such skeletal muscle and adipose, GLUT1 and GLUT4 are the major glucose transporters whereas in primary monocytes the expression GLUT1, GLUT3, and GLUT4 has been reported (Dimitriadis et al., 2004). However, the present study found that THP-1 monocytes express only GLUT1 and GLUT3. After insulin stimulation, there is a significant increase in glucose uptake in THP-1 monocytes but not in U937 monocytes, indicating that THP-1 monocytes are a potential candidate for establishing the insulin resistance model. Increasing insulin concentration to 10^{-5}M significantly reduced glucose uptake into monocytes. This effect of 10^{-5}M insulin on glucose uptake in THP-1 monocytes could be explained by the negative feedback mechanism that high levels of insulin reduce surface insulin receptors (Bertacca et al., 2007). The

magnitude of insulin-stimulated glucose uptake by THP-1 monocytes was only 30% compared to the increment in L6 skeletal muscle cells which has been reported to increase glucose uptake by 50%-100% after short term insulin stimulation (Sarabia et al., 1990). There are two possible reasons for this observation. First, it may reflect that monocytes are not a major insulin target tissue and therefore the contribution of monocytes to glucose disposal in response to insulin is much smaller than skeletal muscles which contribute to 70% glucose disposal after a meal in human (DeFronzo et al., 1981). Glucose uptake is mediated by glucose transporters (GLUTs) which are variably expressed in different types of cells and each GLUT has a different response to insulin. It could be argued that the small increase in insulin-stimulated glucose uptake by THP-1 monocytes could be due to the different distributions of GLUT isoforms in THP-1 monocytes compared to skeletal muscles. In muscle and adipose tissues, GLUT4 is the major glucose transporter isoform sensitive to insulin signalling (Douen et al, 1990; James et al, 1989). In human circulating monocytes, measurable amounts of GLUT1 and GLUT3 are detected by western blot analysis but evidence for GLUT4 is controversial. By applying cytochalasin B, a widely used cytoskeletal inhibitor which prevents translocation of glucose transporters to the membrane (Devés and Krupka, 1978), both the basal and insulin-stimulated glucose uptake was reduced by more than 80% and the net increase of glucose uptake is also completely abolished. These data have confirmed that in THP-1 cells the glucose uptake during resting and insulin stimulated conditions were facilitated by glucose transporters. In addition, the western blot analysis in the present study of THP-1 monocytes showed that GLUT1 and GLUT3 were

expressed in these cells but not GLUT4 when compared to L6 skeletal muscle cell lysates that GLUT4 was detected. It has been reported previously that insulin can stimulate GLUT1 expression at the mRNA level (Hajduch et al., 1995). Therefore, the increase in insulin-stimulated glucose uptake by THP-1 cells, which required 12h stimulation compared to muscle cells and adipocytes, could be attributed to the increase in GLUT1 expression. Indeed, by inhibiting protein synthesis using cycloheximide, the net increase in glucose uptake was completely abolished between insulin-stimulated THP-1 cells and non-stimulated cells, indicating that protein synthesis was required and could account for the increase in insulin-stimulated glucose uptake in THP-1 monocytes.

Elevated circulating free fatty acids (FFA) are a major feature in insulin resistant and obese states. Physiological concentrations of total plasma FFA in lean healthy subjects are in the range of ~200-400μM (Bonnadona et al., 1989; Boden and Jadali, 1991; Belfort et al., 2005) and are increased in obesity and type 2 diabetes, with concentrations between 600-1000μM (Kashyap et al., 2004). The fatty acid profiles are not changed by increases in the total FFA concentration. FFA-induced insulin resistance has been extensively studied in skeletal muscles, measured as reduced insulin-stimulated glucose uptake into cells. However, most previous studies used FFA mixtures at supra-physiological levels (>1000μM) which are rarely seen in obesity and insulin resistance. In the present study, the effects of palmitate, the most abundant saturated FFA in human plasma, were evaluated using a pathophysiological concentration. In the present study, palmitate induced a time- and concentration-dependent reduction in insulin-stimulated glucose uptake

in THP-1 monocytes. This effect occurred within 6h after incubation of THP-1 monocytes with 300μM palmitate. These data confirm that palmitate induces insulin resistance in monocytes, as noted in skeletal muscles (Sinha et al., 2004), adipocytes (Van Epps-Fung, 1997) and liver (Cho et al., 2007).

Palmitate-induced insulin resistance and the metabolic memory effect of palmitate in THP-1 monocytes are unlikely to be due to the loss of cell viability. This is indicated by measures of cell viability, notably a mitochondrial reducing capacity assay (MTT), an apoptosis assay (caspase 3 activity), and a membrane integrity assay (PI exclusion) in THP-1 monocytes treated with 300μM palmitate for 6h, which did not show any significant difference between palmitate-treated and BSA-treated monocytes. Also, monocyte viability was not significantly affected by palmitate-pretreatment after re-incubation in the fresh medium for up to 60h (data not shown). However, none of these cell viability assays measured the early markers of apoptosis. To exclude the possibility that palmitate-induced apoptosis mediates the palmitate effect on insulin-stimulated glucose uptake, early cell death markers are required to be examined. For example, activation of caspase 9, an upstream effctor protein of caspase 3 in the initiation of apoptosis cascade (Budihardjo et al., 1999).

The underlying mechanism of palmitate-induced insulin resistance has been investigated previously and most research has focused on palmitate metabolites. Ceramide, one of the *de novo* synthesized metabolites from palmitate, has been suggested to play an important role in FFA-induced insulin resistance in skeletal

muscles. Chavez et al (2003) reported that ceramide rather than DAG played an important role in antagonism of insulin signalling transduction by palmitate. Moreover, a recent study demonstrated that skeletal muscle ceramide content, especially palmitate-derived ceramide content, is associated with insulin resistance in humans (Straczkowski et al., 2004). In the present study, by applying FB1, an inhibitor for *de novo* ceramide generation from palmitate a time dependent increase in insulin-stimulated glucose uptake in THP-1 monocytes pre-exposed to 300μM palmitate was observed, indicating that ceramide is at least involved in the palmitate-induced insulin resistance in this cell model. It has been reported in skeletal muscles, that exposure to synthetic ceramide (C2 ceramide) for less than 6h reduces membrane insulin receptors and its substrate tyrosine phosphorylation, increases serine/threonine phosphorylation (Storz et al., 1999), and inhibits PI-3 kinase activity (Dresner et al., 1999), but these effects seem to be dependent on cell type. However, inactivation of PKB/Akt is the common effect in all cell/tissue models tested so far. There are two possible mechanisms for ceramide-induced inactivation of PKB/Akt. First of all, ceramide has been shown to specifically block the insulin-stimulated translocation of PKB/Akt to the plasma membrane (Hajduch et al., 2001; Stratford et al., 2004). Secondly, several studies supported a role of ceramide in activating protein phosphatase 2A (PPA2) and therefore dephosphorylating PKB/Akt (Schmitz-Pfeiffer et al., 1999; Salinas et al., 2000). PP2A has been shown to be variably regulated by ROS in different cells (Maalouf and Rho, 2008). Ceramide (Listenberger et al., 2001; Cacicedo et al., 2005) and free fatty acids (Zhang et al., 2006) have been reported to cause an increased ROS generation. However, in the present study, treating THP-1

monocyte with various concentrations of palmitate did not cause any significant change in ROS generation measured as an intracellular ROS by DCF. Indeed, a previous study using treating U937 monocyte with C6 and C2 ceramide only found a transient elevation in mitochondrial ROS generation (Philips et al., 2002). A further study is required to determine effect of palmitate on the mitochondrial ROS generation using dihydrorhodamine123 (DHR) dye. Finally, it has reported that exposure to C2-ceramide for 12h decreased both GLUT4 gene transcription and translocation in 3T3-L1 adipocytes (Summers et al, 1998).

In the present study, fumonisin B1 (FB1) alone was found to reduce basal glucose uptake in a concentration and time dependent manner. FB1 is a potent inhibitor of ceramide synthase which mediates the *de novo* pathway of ceramide generation from palmitate and also the biosynthetic pathway from sphingosine. Therefore, inhibition of ceramide synthase may cause both sphinganine and sphingosine to accumulate (Fig.3.17). *In vitro* sphinganine and sphingosine have been shown to decrease insulin-stimulated glucose uptake in skeletal muscles (Turinsky and Nagel, 1992). Also, a recent study in muscle cells overexpressing the acid ceramidase, an enzyme catalyses the conversion of ceramide to sphingosine, has shown to protect from palmitate-induced insulin resistance in C2C12 cells, indirectly indicating that sphingosine was not contributing to insulin resistance (Chavez et al., 2005). *In vivo*, one study has shown that both muscle sphingosine and sphinganine have a significant negative association with whole body insulin sensitivity while there is no association between sphingomyelin and insulin sensitivity (Straczkoski et al., 2004). Furthermore, a recent study reported a role

of ceramide glycosphingolipid metabolites rather than ceramide itself in insulin resistance induced by dietary or genetic factors (Aerts et al., 2007).

Therefore, the decrease in basal glucose uptake by treating THP-1 cells with FB1 alone might be due to the accumulation of sphingosine or ceramide glycosphingolipid metabolites in THP-1 monocytes or due to the decrease in sphingosine-1-phosphate (S-1-P) which has been shown to have beneficial effects on glucose uptake in skeletal muscle cells (Nicholl et al., 2007). Therefore, loss of this molecule could exert a negative effect on the glucose transport or insulin signal transduction pathway, indicating another possible mechanism for palmitate-induced insulin resistance.

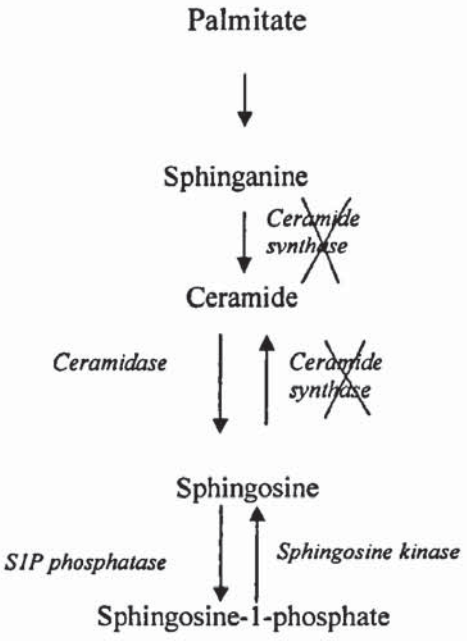

Figure 3.17 Fumonisin B1 inhibits *de novo* ceramide synthesis.

In the present study, co-incubation of 25μM FB1 with 300μM palmitate for up to 2h partially prevents the loss of insulin-stimulated glucose uptake due to palmitate in THP-1 monocytes, indicating that ceramide is partly involved in palmitate-induced decrease in insulin-stimulated glucose uptake but may not be central for the palmitate effect. However, this effect no longer existed after longer time incubation (3h) with FB1 to palmitate-treated cells, indicating that in addition to inhibiting ceramide *de novo* formation, FB1 also might cause accumulation of sphingosine or sphinganine which has been shown to interfere with the insulin signal transduction pathway.

In addition to the above observations, the present study also demonstrated that palmitate-induced inhibition of insulin-mediated glucose uptake by THP-1 monocytes has a lasting effect after prior exposure to and removal of palmitate. The inhibitory effect continued to prevent insulin-stimulated glucose uptake by monocytes up to 60h after palmitate was removed from the culture medium. These data confirm that palmitate induces insulin resistance in monocytes and additionally show that this effect is 'memorised' by monocytes for at least 60h. This suggests that palmitate has a long term detrimental effect on insulin action in monocytes.

Finally, the effects of oleate, one of the most abundant monounsaturated fatty acids in plasma, on basal and insulin-stimulated glucose uptake THP-1 monocytes were investigated. In contrast to palmitate, 300μM oleate treatment of THP-1 cells for 6h did not have any effect on either basal or insulin-stimulated glucose uptake.

Since palmitate and oleate are the most abundant saturated and monounsaturated free fatty acids in plasma, these data suggest that the increased free fatty acid-induced insulin resistance is primarily due to saturated fatty acids such as palmitate. It is not known whether short chain saturated fatty acids have the same effects. In addition, co-incubation THP-1 cells with 150μM oleate significantly prevented the decrease in insulin-stimulated glucose uptake induced by 300μM palmitate. This observation is consistent with a recent study in which 100μM oleate was shown to prevent 500μM palmitate-induced insulin resistance in C2C12 myotubes (Coll et al., 2008). One possible mechanism for oleate preventing palmitate-induced insulin resistance is through the ability of oleate to channel the formation of diacylglycerol (DAG) from palmitate into triacylglycerol (TAG) which is a neutral lipid that has not been shown to induce insulin resistance in muscle cells (Conp et al., 2001; Listenberger et al., 2003; Coll et al., 2008). Also, since ceramide is implicated in inducing insulin resistance in the present study, it remains to be determined whether the protection by oleate against palmate is due to altered ceramide generation.

In summary, the present study demonstrated that the saturated free fatty acid palmitate, induced insulin resistance in THP-1 monocytes whereas monounsaturated free fatty acid oleate did not. Co-incubation with oleate protected THP-1 monocytes from palmitate-induced insulin resistance. Ceramide synthesis pathway was partially involved in palmitate-induced insulin resistance in THP-1 monocytes.

Chapter 4

Oleate protects against palmitate-induced insulin resistance in L6 myotubes

4.1 Preface

This chapter examines the effect of oleate on palmitate-induced insulin resistance using L6 myotubes as a cell model and the involvement of PI3-kinase in the protective effect of oleate.

4.2 Introduction

Insulin resistance is a common component of obesity and type 2 diabetes, and is an independent risk factor for the development of macrovascular diseases (Wyne, 2003; Carlsson et al., 2000). Skeletal muscle is a major site of insulin resistance contributing to the disturbances in glucose and lipid metabolism that accompany obesity and Type 2 diabetes (Baron et al., 1988).

A large body of evidence from both *in vivo* and *in vitro* studies supports the concept that increased plasma free fatty acid is a principal contributor to the development of insulin resistance (McGarry, 2002). Insulin resistance caused by cellular lipid accumulation is mainly associated with saturated fatty acids (Lee et al., 2006). For example, palmitate, one of the most abundant saturated fatty acids, representing around 30% of the total free fatty acids in plasma, has been shown to induce insulin resistance in skeletal muscles and adipose tissues (Dobrzyn and Summers, 2003; Epps-Fung et al., 1997). Early insulin signalling through phosphatidylinositol 3-kinase (PI3-kinase) is one of the essential events for maintaining insulin signalling transduction and regulating glucose uptake into these tissues. However, it is uncertain how palmitate induces insulin resistance and whether this involves a direct effect on PI3-kinase or through disturbing other

insulin signal transduction steps such as activation and translocation of protein kinase B (PKB/Akt) (Boden et al., 1994; Roden et al., 1996; Kruszynska et al., 2002; Dresner et al., 1999).

Oleate represents about 90% of the monounsaturated free fatty acids and 30% of the total free fatty acids in plasma. Several beneficial metabolic effects have been attributed to oleate (Ryan et al., 2000). For example, the Mediterranean-style diet, in which olive oil is the primary source of fat, has been reported to be associated with reduced mortality from CVD (Keys et al., 1986; Willet, 1990). Also, oleate protects endothelial cells from cytokine-induced activation of nuclear factor-κB (NF-κB) (Massaro et al., 2002). Additionally, oleate has been reported to attenuate palmitate-induced apoptosis in cancer MDA-MB-231 cells due to an ability to activate PI3-kinase (Hardy et al., 2000).

Therefore, the present study describes an investigation into whether oleate is capable of protecting L6 skeletal muscle cells from palmitate-induced insulin resistance. The effect of PI3-kinase inhibition and ceramide synthesis inhibition on the effect of oleate on palmitate-induced insulin resistance is also examined to provide insight into the molecular mechanisms of fatty acid-mediated insulin resistance.

4.3 Methods

4.3.1 Cell Culture

L6 cell culture was carried out according to Section 2.2.3.

4.3.2 Incubation with fatty acids and metabolic inhibitors

L6 myotubes were incubated with various concentrations of palmitate (50-300μM) or oleate (50-750μM) alone or a combination of 300μM palmitate with oleate (50-300μM) with or without the PI3-kinase inhibitors (10^{-7}M wortmannin for 6h or 25μM LY-294,002 for 1h) or the ceramide de novo synthesis inhibitor (25-50μM fumonisin B1 for 6h) at 37°C. Control cells received BSA and/or other vehicles as appropriate. The justifications of insulin and palmitate and oleate concentrations are presented in Section 3.3.2.

4.3.3 2-Deoxy-D-glucose uptake

Uptake analysis was undertaken immediately after completion of the 6h incubation with fatty acids in which insulin (10^{-6}M) had been added for the last 1h according to Section 2.5.2.

4.3.4 Phase contrast microscopy

L6 myotubes were photographed under a phase-contrast microscope (Olympus, UK) at magnification 20× for morphological analysis.

4.3.5 Cell viability and apoptosis assay

To test whether fatty acids have toxic effects on L6 cells, membrane integrity was assessed by trypan blue exclusion, mitochondrial reducing capacity was estimated by MTT assay, and apoptosis was quantified by caspase-3 activity assay. These methods were carried out according to Section 2.14.1, 2.14.2.2, and 2.13.

4.3.6 Statistical analysis

Data are expressed as mean ± SEM, and 2-deoxy-D-glucose uptake is expressed as percentage compared with control (100%). Statistical analyses were performed by one-way ANOVA with Tukey-Kramer post hoc tests. A p value less than 0.05 was considered significant.

4.4 Results

4.4.1 Effect of palmitate and oleate alone on glucose uptake

To investigate the effect of free fatty acids on glucose up by L6 skeletal muscle cells, the initial experiments were conducted to characterise the effect of palmitate or oleate alone on basal and insulin-stimulated glucose uptake by L6 myotubes using 50-300μM palmitate for 0-6h incubation as have used in THP-1 monocytes in Chapter 3. Since palmitate was conjugated to BSA, the control and the oleate incubations were conducted with the same concentration of BSA. L6 myotubes were incubated with palmitate (50-300μM) and oleate (50-750μM) alone for 6h. Both palmitate and oleate at the concentrations tested showed no significant effect on basal glucose uptake compared to controls (Fig.4.1 A and B). When BSA-treated control cells were stimulated with 10^{-6}M insulin for 1h, this produced a significant increase in glucose uptake by ~40-50%. However, when L6 myotubes were incubated with palmitate for 6h, there was a concentration-dependent decrease in insulin-stimulated glucose uptake. Insulin-stimulated glucose uptake was almost completely prevented by exposure to palmitate at a concentration of 300μM (Fig.4.1A). Therefore, this concentration of palmitate was chosen to induce insulin resistance in subsequent studies.

Compared to palmitate, oleate was a less potent inducer of insulin resistance. Oleate also caused a concentration-dependent decrease in insulin-stimulated glucose uptake. However, even the highest oleate concentration tested (750μM) did not completely prevent insulin-stimulated glucose uptake (Fig. 4.1B).

A

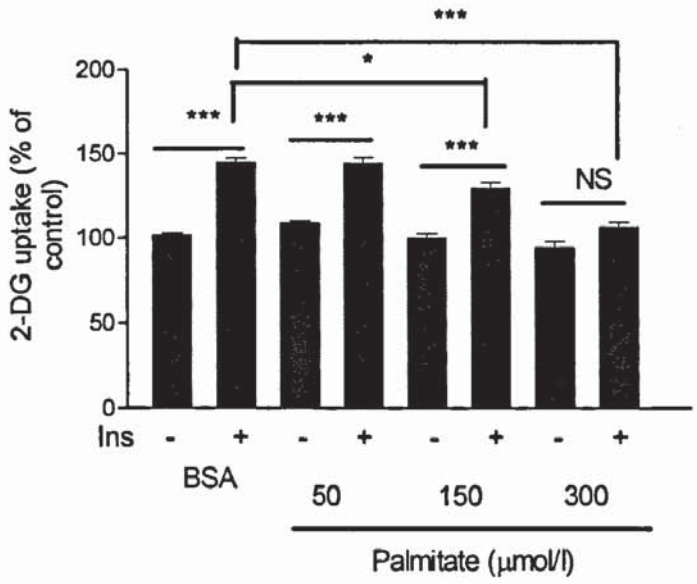

B.

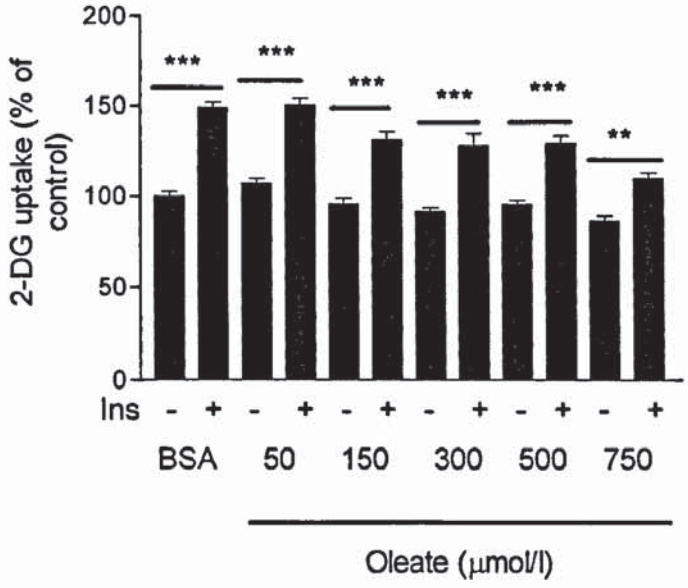

Figure 4.1 Effect of palmitate (A) and oleate (B) alone on basal and insulin-stimulated 2-deoxy-D-glucose (2-DG) uptake by L6 myotubes. L6 myotubes were incubated with palmitate (50-300μM) and oleate (50-750μM) alone for 6h at 37°C. Controls are cells treated with BSA. Insulin (Ins) (10^{-6}M) was added for the last 1h of incubation. 2-deoxy-D-glucose (2-DG) uptake was measured after completion of incubation. Data are mean±SEM of 3 independent experiments performed in triplicate. *p<0.05, **p<0.01, *** p<0.001. NS: non significant.

4.4.2 Oleate protects L6 cells from palmitate-induced insulin resistance.

The effect of oleate on palmitate-induced insulin resistance was examined by co-incubating increasing concentrations of oleate (50, 150, and 300μM) with 300μM palmitate for 6h with and without 10^{-6}M insulin stimulation for the last 1h. Whereas 300μM palmitate alone abolished insulin-stimulated glucose uptake, co-incubation with oleate (50μM) partially restored (to 75%) insulin-stimulated glucose uptake in the presence of 300μM palmitate, but co-incubation with 50μM BSA (control) did not exert any protective effect against the inhibition of insulin-stimulated glucose uptake by palmitate. The protective effect of oleate against palmitate-induced insulin resistance was not further affected by increasing the oleate concentration to 300μM (Fig. 4.2).

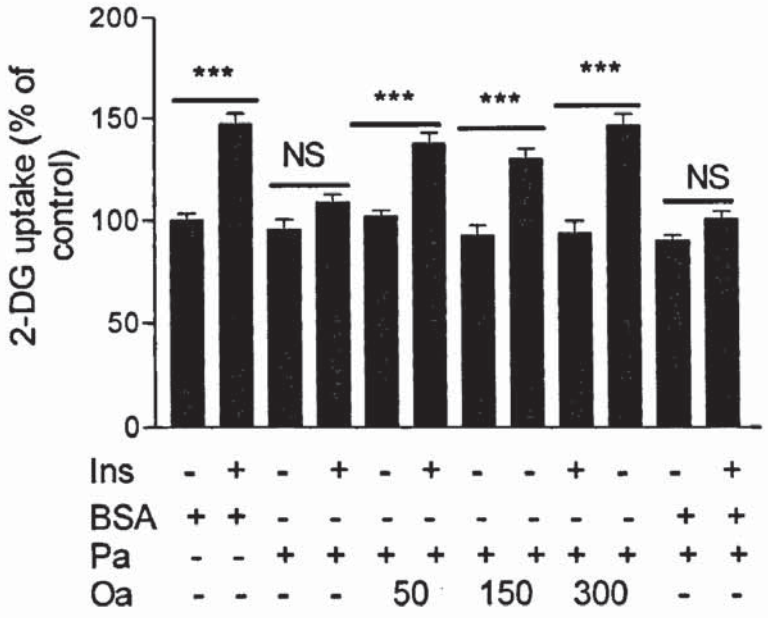

Figure 4.2 Effect of combinations of 300μM palmitate (Pa) with various concentrations of oleate (Oa) on basal and insulin-stimulated 2-deoxy-D-glucose uptake by L6 myotubes. L6 myotubes were incubated with 300μM palmitate and oleate (50, 150, 300μM) or equivalent BSA (as a control for oleate treatment) present in 50μM oleate for 6h at 37°C. Insulin (Ins) (10^{-6}M) was added for the last 1h of incubation. Controls are cells treated with BSA. 2-deoxy-D-glucose (2-DG) uptake was measured after completion of incubation.

Data are mean±SEM of 3 independent experiments performed in triplicate.
*** $p<0.001$. NS: non significant.

4.4.3 Oleate prevents the palmitate-induced alteration in L6 cell morphology.

There was a distinct difference between the effects of palmitate and oleate alone on L6 myotube morphology. When L6 myotubes were incubated with 300μM palmitate, the muscle cells lost their muscle spindle shape (Fig.4.3b), whereas cells incubated with the same concentration of oleate maintained a similar shape to BSA controls (Fig.4.3c). When 50μM oleate was co-incubated with 300μM palmitate, the muscle spindle shape was retained (Fig.4.3d). This protective effect of oleate was not further enhanced when the oleate concentration was raised to 150μM and 300μM (Fig.4.3 e,f). To exclude the possibility that the fatty acid carrier protein BSA could contribute to the protection by oleate, Fig.4.3 g-i show that the loss of muscle spindle shape caused by palmitate was not prevented by increasing concentrations of BSA which equals to the BSA presented in oleate.

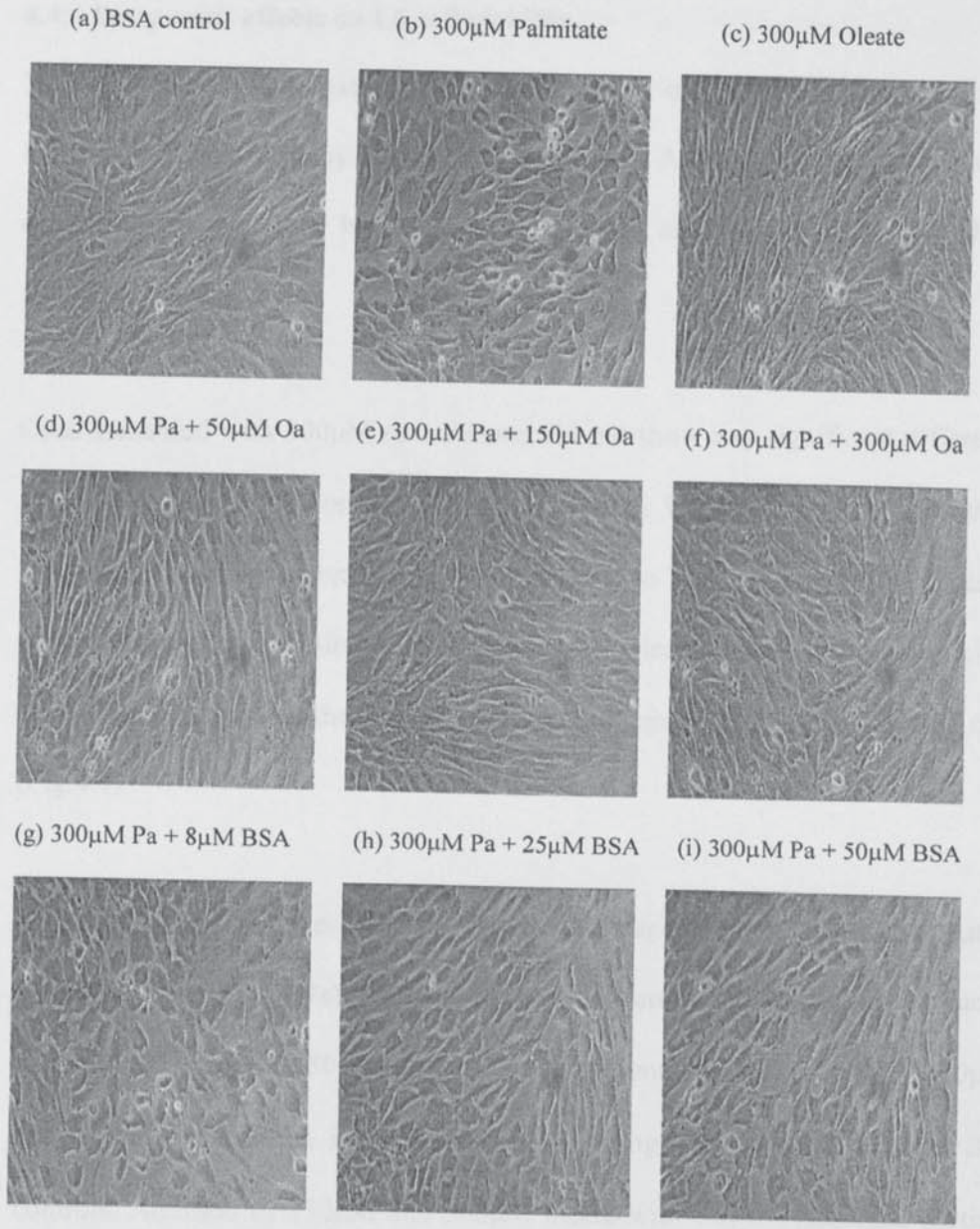

Figure 4.3 Effect of palmitate (Pa), oleate (Oa), combinations of palmitate with various concentrations of oleate or BSA on L6 myotube morphology. L6 myotubes were incubated with 300μM palmitate and 300μM oleate alone and combinations of 300μM palmitate with various concentrations of oleate (50, 150, 300μM) or equivalent BSA present in each oleate concentrations as indicated in the graph for 6h at 37°C. Controls are cells treated with BSA. The cell cultures were photographed using an inverted phase contrast light microscope at magnification ×20.

4.4.4 Fatty acids effects on L6 cell viability

To test whether fatty acids have adverse effects on L6 myotubes, membrane integrity was assessed by trypan blue exclusion. Also, mitochondrial reducing capacity was measured by an MTT assay and apoptosis was quantified by caspase-3 activity.

Cells incubated with 300μM oleate alone did not show any significant difference in membrane integrity compared to BSA controls. With 300μM palmitate, there was a reduction in membrane integrity compared to BSA controls (74%±4 versus 88%±3, $p<0.001$). Co-incubating 50-300μM oleate with 300μM palmitate significantly prevented the loss of membrane integrity in palmitate-treated cells (Fig.4.4).

The overall pattern in mitochondrial reducing capacity was similar to that of membrane integrity. Palmitate (300μM) decreased mitochondrial reducing capacity by more than 50%, whereas the same concentration of oleate (300μM) caused a 25% decrease in mitochondrial reducing capacity compared to BSA controls. Addition of 150μM and 300μM oleate with 300μM palmitate partially prevented the decrease in mitochondrial reducing capacity associated with palmitate. A lower concentration of oleate (50μM) did not show a significant protective effect against the palmitate-induced decrease in mitochondrial reducing capacity (Fig.4.5).

To investigate whether fatty acid treatment can induce apoptosis in L6 myotubes,

caspase-3 activity was measured. Neither palmitate (300μM) nor oleate (300μM) had any significant effect on caspase-3 activity in L6 myotubes compared to BSA controls over the 6h incubation period (Fig.4.6).

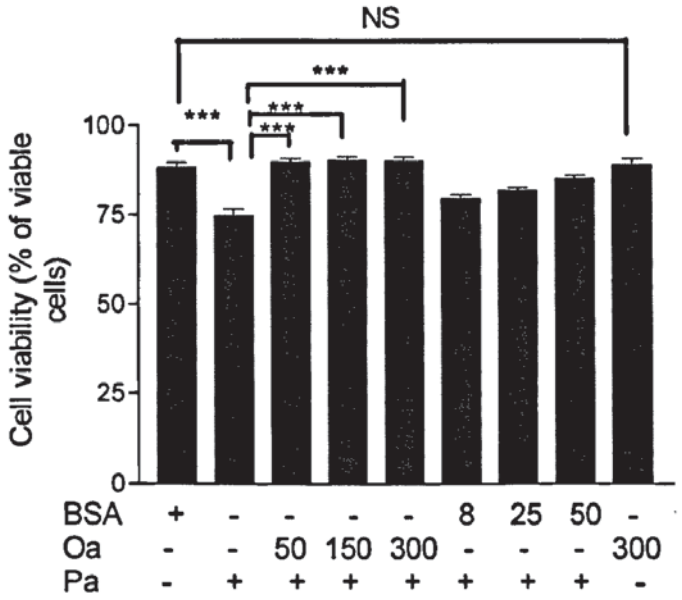

Figure 4.4 Effect of palmitate (Pa) and oleate (Oa) on membrane integrity measured by trypan blue exclusion. L6 myotubes were incubated with 300μM palmitate and 300μM oleate alone and combinations of 300μM palmitate with various concentrations of oleate (50, 150, 300μM) or equivalent concentration of BSA present in each oleate concentration as indicated in the figure for 6h at 37°C. Controls are cells treated with BSA. Cells were trypsinised and the number of viable cells and dead cells were determined by trypan blue exclusion. The cell viability is expressed as % viable cells of total cell. Data are mean±SEM of 3 independent experiments performed in triplicate. *** $p<0.001$. NS: non significant.

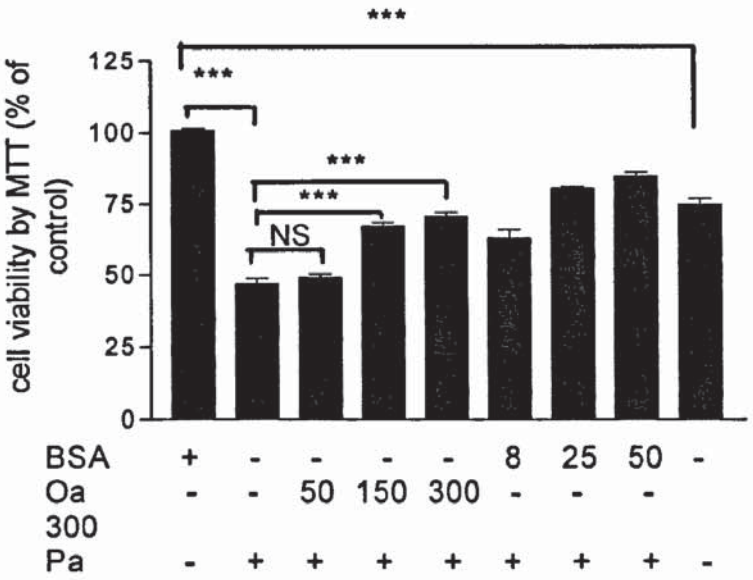

Figure 4.5 Effect of palmitate (Pa) and oleate (Oa) on mitochondrial reducing activity measured by MTT assay. L6 myotubes were incubated with 300μM palmitate and 300μM oleate alone and combinations of 300μM palmitate with various concentrations of oleate (50, 150, 300μM) or equivalent concentration of BSA present in each oleate concentration as indicated in the figure for 6h at 37°C. Controls are cells treated with BSA. Data are mean±SEM of 3 independent experiments performed in triplicate. *** $p<0.001$. NS: non significant.

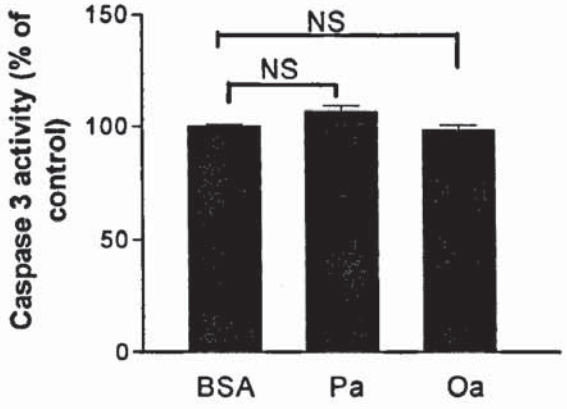

Figure 4.6 Effect of palmitate (Pa) and oleate (Oa) on caspase-3 activity. L6 myotubes were incubated with 300μM palmitate and 300μM oleate alone for 6h at 37°C. Controls are cells treated with BSA. Caspase 3 activity was measured according to Section 2.13. Data are mean±SEM of 3 independent experiments performed in triplicate. NS: non significant.

4.4.5 PI3-kinase activity is involved in oleate protection against palmitate-induced insulin resistance.

To investigate the underlying mechanism responsible for the protective effect of oleate against palmitate-induced insulin resistance in L6 myotubes, the involvement of PI3-kinase activation was examined by using two different types of PI-3 kinase inhibitors: wortmannin and LY-294,002.

When L6 myotubes were incubated with wortmannin for 6h, there was a concentration dependent reduction in both basal and insulin stimulated-glucose uptake. Wortmannin (10^{-7}M) slightly reduced basal glucose uptake by 10% ($p<0.05$) and almost completely prevented insulin-stimulated glucose uptake by L6 myotubes (Fig.4.7A). Compared to wortmannin, the effect of LY-294,002 on basal and insulin stimulated-glucose uptake was in a similar manner. As shown in Figure 4.7 B and Figure 4.7 C, L6 myotubes were incubated with (0-25μM) LY-294,002 for 6h and 1h, respectively. The basal glucose uptake was reduced by 50% by 25μM LY-294,002 for 6h and 12% for 1h. The insulin-stimulated glucose uptake was significantly reduced by incubating L6 myotubes with 25μM LY-294,002 for 1h. Therefore, wortmannin at concentration of 10^{-7}M and LY-294,002 at concentration of 25μM were used for investigating the involvement of PI3-kinase in the protection by oleate against palmitate-induced insulin resistance.

As shown in Figure 4.8 A and Figure 4.8 B, the reduction in insulin-stimulated glucose uptake by palmitate (300μM) was partially prevented by co-incubating with 50μM oleate. With addition of wortmannin or LY-294,002, the improvement in insulin-stimulated glucose uptake by 50μM oleate in the presence of 300μM palmitate was significantly reduced.

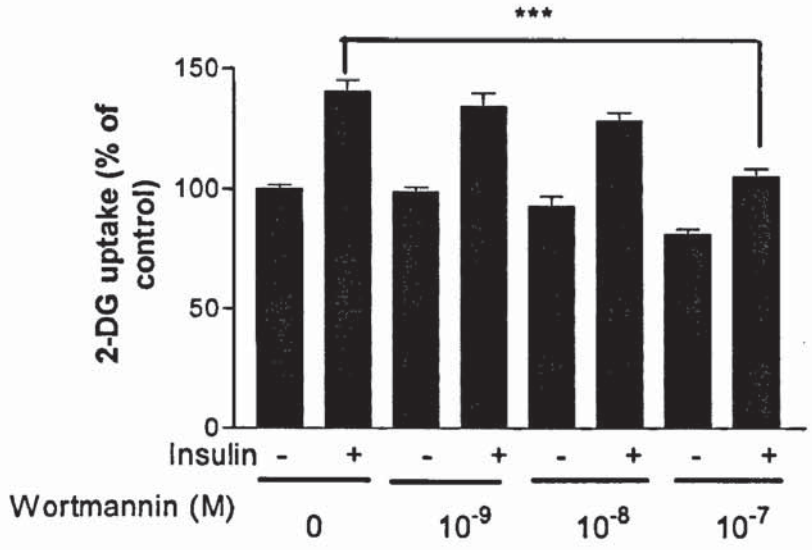

Figure 4.7A Effect of wortmannin on basal and insulin-stimulated 2-deoxy-D-glucose uptake by L6 myotubes. L6 myotubes were incubated with and without wortmannin (10^{-9}-10^{-7}M) for 6h at 37°C. Insulin (10^{-6}M) was added for the last 1h of incubation. 2-deoxy-D-glucose (2-DG) uptake was measured after completion of incubation. Data are mean±SEM of 3 independent experiments performed in triplicate. ***p<0.001.

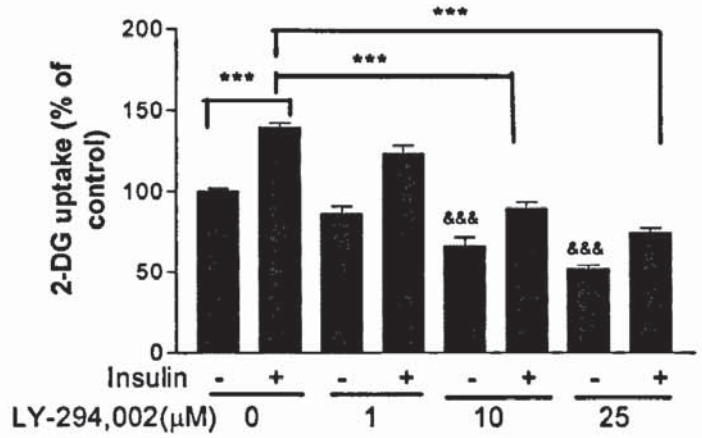

Figure 4.7B Effect of LY-294,002 (6h) on basal and insulin-stimulated 2-deoxy-D-glucose uptake by L6 myotubes. L6 myotubes were incubated with LY-294,002 (1μM-25μM) for 6h at 37°C. Insulin (10^{-6}M) was added for the last 1h. 2-deoxy-D-glucose (2-DG) uptake was measured after completion of incubation. Data are mean±SEM of 3 independent experiments performed in triplicate. ***p<0.001. &&&P<0.001 compared to control.

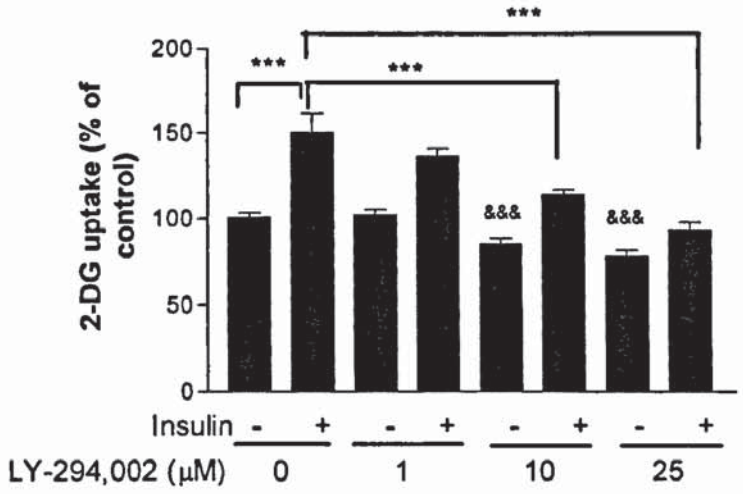

Figure 4.7C Effect of LY-294,002 (1h) on basal and insulin-stimulated 2-deoxy-D-glucose uptake by L6 myotubes. L6 myotubes were pre-incubated with LY-294,002 (1μM-25μM) for 10min and further incubated with insulin (10^{-6}M) for 1h at 37°C. 2-deoxy-D-glucose (2-DG) uptake was measured after completion of incubation. Data are mean±SEM of 3 independent experiments performed in triplicate. ***p<0.001. &&&P<0.001 compared to control.

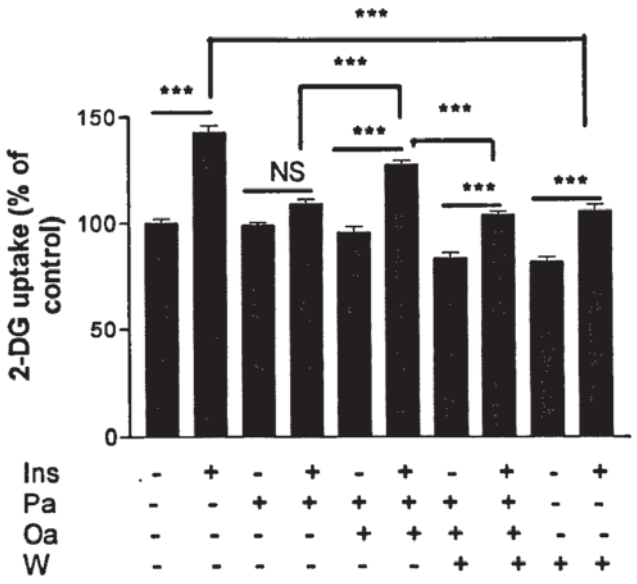

Figure 4.8A Effect of wortmannin on basal and insulin-stimulated 2-deoxy-D-glucose uptake by L6 myotubes in the presence of palmitate (Pa) plus oleate (Oa). L6 myotubes were incubated with 300μM palmitate and 50μM oleate with and without wortmannin (W) (10^{-7}M) for 6h at 37°C. Insulin (Ins) (10^{-6}M) was added for the last 1h of incubation. 2-deoxy-D-glucose (2-DG) uptake was measured after completion of incubation. Data are mean±SEM of 3 independent experiments performed in triplicate. ***p<0.001. NS: non significant.

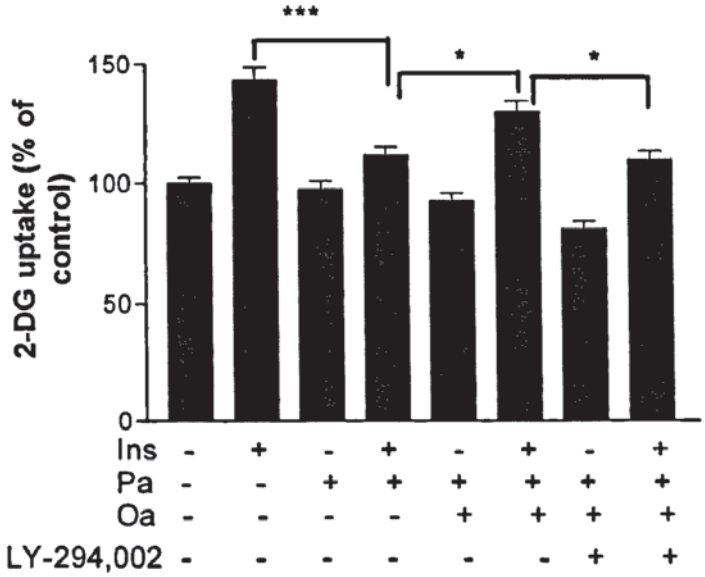

Figure 4.8B Effect of LY-294,002 on basal and insulin-stimulated 2-deoxy-D-glucose uptake by L6 myotubes in the presence of palmitate (Pa) plus oleate (Oa). L6 myotubes were incubated with 300μM palmitate and 50μM oleate for 6h at 37°C. LY-294,002 (25μM) was added for 10min before insulin

stimulation. Insulin (Ins) (10^{-6}M) was added for the last 1h of incubation. 2-deoxy-D-glucose (2-DG) uptake was measured after completion of incubation. Data are mean±SEM of 3 independent experiments performed in triplicate. *p<0.05. ***p<0.001.

4.4.6 Fumonisin B1 (FB1) does not prevent palmitate-induced insulin resistance in L6 myotubes.

It has been implicated that ceramide is involved in palmitate-induced insulin resistance in L6 muscle cells (Chavez et al., 2003). To test this hypothesis, Fumonisin B1 (FB1), an inhibitor of ceramide *de novo* synthesis from palmitate, was used. L6 myotubes were pre-incubated with 50μM Fumonisin B1 for 10min and then co-incubated 300μM palmitate for 6h with and without insulin stimulation for the last 1h. As shown in Figure 4.9, FB1 did not affect either basal or insulin-stimulated glucose uptake in L6 myotubes. However, co-incubation with FB1 in the presence of palmitate did not prevent the reduction in insulin-stimulated glucose uptake caused by palmitate.

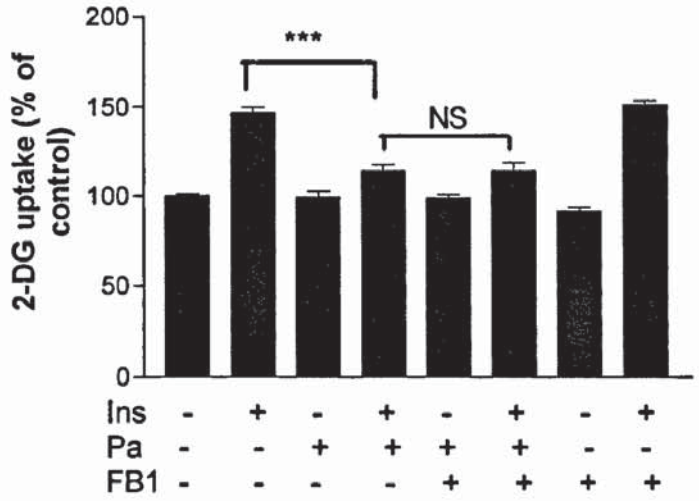

Figure 4.9 Effect of Fumonisin B1 (FB1) on basal and insulin-stimulated 2-deoxy-D-glucose uptake by L6 myotubes. L6 myotubes were incubated 50μM FB1 and 300μM palmitate for 6h at 37°C. Insulin (Ins) (10^{-6}M) was added for the last 1h of incubation. 2-deoxy-D-glucose (2-DG) uptake was measured after completion of incubation. Data are mean±SEM of 3 independent experiments performed in triplicate. ***p<0.001.

4.4.7 FB1 does not prevent palmitate-induced alterations in L6 cell morphology.

As shown in Figure 4.3b, palmitate-induced insulin resistance was associated with a loss of muscle spindle shapes in L6 myotubes. To test whether FB1 treatment can prevent this alteration in cell morphology, L6 myotubes were treated with 300μM palmitate with and without 50μM FB1 for 6h and cell cultures were photographed by an inverted phase contrast microscope. Again, compared to BSA-treated myotubes, palmitate caused a loss in muscle spindle shape loss whereas the addition of FB1 did not prevent this loss (Fig.4.10).

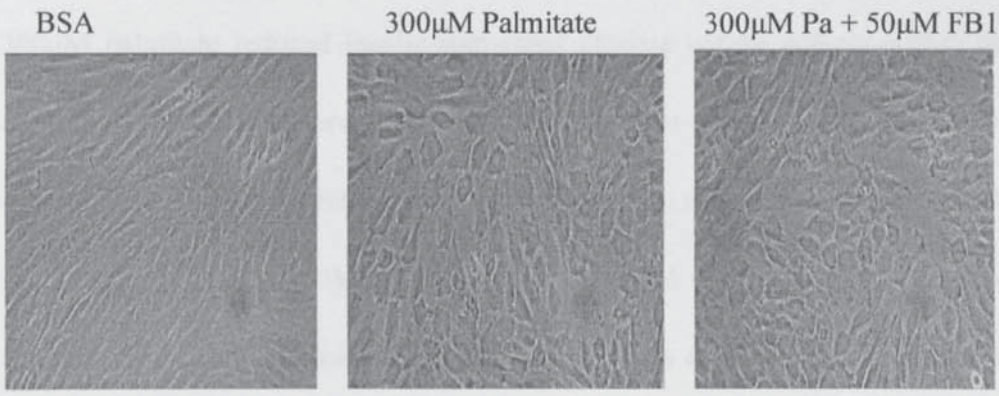

Figure 4.10 Effect of Fumonisin B1 (FB1) on L6 cell morphology. L6 myotubes were incubated 50μM FB1 and 300μM palmitate (Pa) for 6h at 37°C. Controls are cells treated with BSA. The cell cultures were photographed using an inverted phase contrast light microscope at magnification 20×.

4.5 Discussion

In this study, the effect of oleate on palmitate-induced insulin resistance in a well established skeletal muscle cell model - L6 myotubes has been investigated. The data presented here show that treating L6 cells with 300μM palmitate for 6h almost completely abolished insulin-stimulated glucose uptake. Cells treated with oleate up to a concentration of 750μM showed only a slight reduction in insulin-stimulated glucose uptake. However, addition of 50μM oleate reduced the inhibitory effect of 300μM palmitate on insulin-stimulated glucose uptake. This protective effect was not further increased with increasing concentrations of oleate up to 300μM, but the protective effect required the activity of PI3-kinase.

Fatty acid-induced insulin resistance has been extensively studied *in vitro u*sing skeletal muscle cells (McGarry, 2002; Lee et al., 2006). In the present study,

300μM palmitate reduced insulin-stimulated glucose uptake acutely within 6h, confirming previous observations using L6 myotubes (Sinha et al., 2004). Two distinct fatty acid metabolites formed from oversupply of lipids to skeletal muscle have been implicated in the development of skeletal muscle insulin resistance: ceramide and DAG (Boden et al., 1994). Palmitate is an important precursor for *de novo* synthesis of ceramide (Kolesnick and Krönke, 1998), and ceramide is a strong inhibitor of insulin action (Hajduch et al., 2001), affecting both membrane-associated and cytosolic components of the post-receptor insulin signalling pathways (Summers et al., 1998). Ceramide-mediated palmitate-induced insulin resistance is mainly mediated through direct disruption of the proximal insulin signal pathway via activation and translocation of PKB/Akt to the cell membrane (Schmitz-Peiffer et al., 1999; Chavez et al., 2003; Powell et al., 2004). Studies involving skeletal muscles from lipid infusion-induced insulin resistance in both animals and humans support a role of palmitate-derived DAG in the activation the PKCθ-NF-κB pathway (Itani et al., 2002). This involves serine phosphorylation of insulin receptor substrate-1 (IRS-1) and an associated reduction of PI3-kinase activity (Griffin et al., 1999).

The co-incubation with FB1 in the presence of palmitate did not show any protective effect against palmitate-induced insulin resistance in L6 myotubes. This is in contrast to the observation that Chavez et al (2003) reported previously in

which C2C12 muscle cells co-incubated with 50μM FB1 in the presence of 750μM palmitate for 8h prevented the reduction in the insulin-stimulated Akt (Ser^{473}) phosphorylation. However, the effect of FB1 on insulin-stimulated glucose uptake in C2C12 cells after palmitate treatment was not determined in their study. Although Akt (Ser^{473}) phosphorylation is a key signalling event for insulin-stimulated glucose uptake, Kitamura et al. (1998) reported that adipocytes stably transfected with dominant negative Akt at Ser^{473} and Thr^{308} showed an 80% reduction in endogenous Akt activity but no impairment in insulin-stimulated glucose transport, suggesting that there was no correlation between Akt and glucose transport. Therefore it is possible that the prevention of palmitate-induced decrease in insulin-stimulated Akt (Ser^{473}) phosphorylation by FB1 may not be associated with an increase in insulin-stimulated glucose uptake after palmitate treatment. Also, the effect of ceramide is highly cell-type specific, therefore, the discrepancies between the present study and the previous finding could be due to this reason. In addition, the cell morphology alterations caused by palmitate are not prevented by FB1, indicating that ceramide generation is not responsible for the morphology change caused by palmitate in L6 myotubes.

Although oleate alone exerted little effect on insulin-stimulated glucose uptake by L6 myotubes, only a modest concentration (50μM) of oleate was required to prevent palmitate-induced insulin resistance. This observation is consistent with a

very recent study in which 100μM oleate was shown to prevent 500μM palmitate-induced insulin resistance measured by phosphorylation of PKB (Akt) in C2C12 myotubes (Coll et al., 2008). Work presented in this chapter has shown, by applying PI3-kinase inhibitors, wortmannin and LY294,002 that the effect of oleate to partially reverse palmitate-induced insulin resistance involves PI3-kinase, an insulin signalling intermediate between IRS-1 and 3-phosphoinositide-dependent kinase (PDK). This enzyme regulates PKB/Akt, which in turn promotes glucose transporter-4 translocation and glucose transport (Karlsson and Zierath, 2007). It has been reported previously that long term exposure to oleate can stimulate the activation of PI3-kinase in MDA-MB-231 cancer cells (Hardy et al., 2000). However, since the present study involves only 6 h exposure to oleate, the effect of oleate on PI3-kinase is unlikely to be a direct effect on gene expression. Also, oleate alone did not increase insulin-stimulated glucose uptake.

Therefore, the possible mechanism by which oleate prevents palmitate-induced insulin resistance is likely to be an indirect protection of PI3-kinase activation after insulin stimulation. It has been widely accepted that the increased serine phosphorylation of IRS-1 accounts for reduced PI3-kinase activity. There are several serine kinases reported to contribute to this mechanism, amongst which PKCθ seems to be the major factor (Griffin et al., 1999; Kim et al., 2004).

Activation of PKCθ could be caused by DAG generated from palmitate or by inhibitor κB kinase β (IKKβ), a serine kinase related to activation of NF-κB. Oleate has been reported to inhibit the activation of NF-κB caused by cytokines in endothelial cells (Massaro et al., 2002), whereas palmitate-induced insulin resistance has been reported to associate with activation of NF-κB in L6 myotubes (Sinha et al., 2004). Therefore, it is possible that the protective effect of oleate against palmitate is achieved by preventing the activation of NF-kB in palmitate-treated cells. It is also possible for oleate to rescue cells from palmitate-induced insulin resistance by channelling the generation of DAG into neutral triacylglyceride which does not induce insulin resistance (Voshol et al., 2001; Conp et al., 2001; Listenberger et al., 2003; Coll et al., 2008). It remains to be investigated whether ceramide generation is involved in the protection by oleate against palmitate-induced insulin resistance.

Another detrimental effect of palmitate observed in this study was the loss of muscle spindle shape. Normal cell morphology was restored by co-incubation with 50μM oleate, and this was associated with a small increase in the number of cells showing membrane integrity as measured by trypan blue exclusion. However, the proportion of cells showing inadequate membrane integrity was trivial compared with the large reduction in insulin-stimulated glucose uptake caused by palmitate. This suggests that a small loss in cell membrane integrity is probably

not the primary contributor to palmitate-induced insulin resistance in L6 myotubes. Although Hardy et al. (2000) reported that 100μM palmitate for 24h induced morphological signs of apoptosis in serum-starved MDA-MB-231 breast cancer cells such as cell rounding and nuclear fragmentation, there were less morphological changes observed in the present study in L6 muscle cells after treated with 300μM palmitate for 6h. Also, the caspase 3 activity in palmitate-treated L6 cells was not significantly different from BSA-treated controls, suggesting that apoptosis may not play a primary role in palmitate-induced insulin resistance in L6 muscle cells. However, other assays for apoptosis such as caspase 9 activity, inhibitor of caspase-activated deoxyribonuclease (ICAD) degradation, and DNA fragmentation are required to further exclude the possibility that palmitate-induced cytotoxicity mediates palmitate-induced insulin resistance in L6 myotubes. Furthermore, inhibition of caspase activation by caspase inhibitor Z-VAD-FMK in palmitate-treated L6 cells could also offer another approach to examine whether palmitate-induced insulin resistance in L6 muscle cells was associated with apoptosis.

Although mitochondrial dysfunction has been implicated in the development of insulin resistance (Kelly et al., 2002), the inability of 50μM oleate to prevent the 300μM palmitate-induced reduction in mitochondrial reducing capacity suggests that impaired mitochondrial reducing capacity is not crucial for the development

of muscle insulin resistance in response to palmitate. Addition of 150μM and 300μM oleate partially prevented the palmitate-induced decrease in mitochondrial reducing capacity, and this protective effect was similar to the addition of increasing concentrations of BSA. This suggests that protection by higher concentrations of oleate against the detrimental effects of palmitate on mitochondrial function may partly reflect increased amounts of BSA in the incubation media, which might possibly bind palmitate and reduce its access to the cells.

In summary, the present study demonstrated that saturated free fatty acid palmitate induced insulin resistance in L6 myotubes whereas monounsaturated free fatty acid oleate did not. Furthermore, co-incubation with oleate protected against palmitate-induced insulin resistance in L6 myotubes. This protective effect is associated with the ability of oleate to preserve insulin stimulated PI3-kinase activity in palmitate-treated cells. The protective effect of oleate against the detrimental effect of palmitate has potentially important implications for the balance of dietary monounsaturated and saturated fats in the development of insulin resistance.

Chapter 5

Effect of insulin resistance risk factors on monocyte phenotype and adhesion

5.1 Preface

This chapter describes an investigation into the effects of glucose and free fatty acids (palmitate and oleate) on the monocyte phenotype (measured by cell surface CD11b and CD36 expression), monocyte adhesion to ICAM-1 and EAhy 926 endothelial cells, and monocyte viability. The role of ceramide and ROS in mediating the effect of palmitate on the monocyte phenotype was also examined.

5.2 Introduction

CVD is the leading cause of global morbidity and mortality. It is responsible for >30% of deaths in the general population (World Health Orgnisation (WHO) report, 2003) and up to 80% of deaths in diabetic patients (Haffner et al., 1998). The underlying cause of CVD is atherosclerosis which is a progressive pathological condition characterised by the thickening of the arterial wall mainly due to the accumulation of lipids, leading to the reduction of the artery lumen and reduced supply of oxygen to the heart (Falk, 2006).

The development of atherosclerosis is a multifactorial process. The recruitment of circulating monocytes to, and the extravasation of monocytes through, the endothelium are the earliest and the most critical events contributing to atherosclerosis. This includes the following steps: monocyte tethering, rolling, firm adhesion, and migration. Each step is mediated by the interactions between specific ligands and receptors on monocytes and adhesion molecules expressed on

endothelium. Tethering and rolling are mediated by the selectin family of adhesion proteins in which L-selectin is expressed constitutively on monocytes, but P-selectin and E-selectin are expressed on the surface of activated endothelium (Krieglstein and Granger, 2001). These initial attachments are reversible in both healthy and pathological conditions. However, only the firm adhesion of monocytes to the endothelium can cause the subsequent monocyte extravasation. This is mediated by integrins expressed on monocytes, a class of transmembrane proteins comprising of unrelated α and β subunits. Monocytes express both the β1 integrin (CD49d/CD29) and the β2 integrins which are characterized as a common β chain (CD18) and one of many noncovalently associated α chains, i.e., CD11a (LFA-1), CD11b (Mac-1), and CD11c (P150,95) and CD11d (Larson and Springer, 1990). CD11b is the most abundant integrin in neutrophils and monocytes (Springer et al., 1979). This β2 integrin is mainly responsible for the early stage of adhesion while the β1 integrins for the late stage. The receptors for those integrins are a class of proteins belonging to the immunoglobulin superfamily, such as ICAM-1 and VCAM-1 which are expressed on the surface of the endothelial cells (Carlos and Harlan, 1994). *In vitro* studies have shown that this firm interaction requires the activation of monocytes, endothelial cells, or both (Charo, 1992) and a chemokine signal. Factors inducing this activation include ox-LDL (Liao et al., 1997), inflammatory cytokines (e.g. TNF-α, IL-1β) (Charo, 1992), LPS (Gupta et al., 2005), and free fatty acids (Zhang et al., 2006).

Following the firm adhesion of monocytes to the endothelium, monocytes in the subendothelium differentiate to macrophages and perform a phagocytic role in the clearance of debris and pathogens and in conditions of excess cholesterol they may be transformed into lipid-laden foam cells. This is mainly achieved by the uptake of ox-LDL through scavenger receptors (SR) such as SR-A and CD36. CD36 is an 88-kDa plasma membrane glycoprotein that is expressed on a wide range of cell types such as monocytes/macrophages, endothelial cells, platelets, and myotubes (Greenwalt et al., 1992). In the formation of atherosclerotic lesions, CD36 has been proven to be the major receptor mediating the uptake of ox-LDL uptake by macrophages (Huh et al., 1996; Rahaman et al., 2006). Since CD36 is mainly expressed on macrophages and fairly low levels are found on circulating monocytes. Its expression can be used as a marker for monocyte phenotypic change during atherogenesis and can be related to the extent of differentiation using the accepted monocyte differentiation marker, CD206 (Liang et al., 2006).

According to some epidemiological data, only 5-10% people with impaired glucose tolerance (IGT) ultimately develop to type 2 diabetes (Saltiel, 2000). In patients with type 2 diabetes, cardiovascular disease is the major cause of mortality and morbidity. The estimated risk for development of atherosclerosis is increased by 4 or 5 times in type 2 diabetic patients compared with insulin sensitive subjects (Reaven and Laws, 1999). Furthermore, the Insulin Resistance

and Atherosclerosis Study (Taegtmeyer, 1996) reported an inverse relation between insulin sensitivity and atherosclerosis in Hispanic and non-Hispanic Americans and also showed that insulin resistance *per se* is an independent risk factor for atherosclerosis.

Plasma FFA levels have been shown to be significantly increased in insulin resistant and type 2 diabetic patients compared to healthy controls (Fraze et al., 1985). *In vitro* and *ex vivo* data have shown that fatty acids can activate monocytes and increase their adhesion to endothelium. For example, Hennig et al. (1985) reported that exposure to fatty acids increased human LDL transfer across a cultured endothelial monolayer. More recently, a study using THP-1 monocytes which were chronically (48h) exposed to elevated concentrations of mixed free fatty acids demonstrated a dose and time dependent increase in adhesion of monocyte to endothelial cells (Zhang et al, 2006). CD36 has also been implicated in the development of atherosclerosis in type 2 diabetes. It has been reported that CD36 expression in monocytes from obese type 2 diabetic patients is significantly increased when compared to lean healthy controls (Sampson et al, 2003; Zhang et al., 2005). Furthermore, one *in vitro* study demonstrated that the CD36 expression in macrophages derived from peripheral blood mononuclear cells is regulated by glucose at the translational level (Griffin et al, 2001).

Taken together, these observations suggest that type 2 diabetes and insulin

resistance play an important role in accelerating development of atherosclerosis. However, the molecular mechanism underlying this process is unclear. Therefore, the present study aimed to investigate the effect of excess glucose and free fatty acids, two major features in diabetic conditions, on monocyte phenotype. The effect of pathophysiological free fatty acid the concentrations in the presence of 11mM glucose on monocyte adhesion activity was also examined.

5.3 Materials and Methods

5.3.1 Cell culture

U937 monocyte and EAhy926 endothelial cell cultures were carried out according to the method described in Section 2.2.1 and 2.2.2.

5.3.2 Cell treatment

Palmitate bound to BSA in solution and oleate bound to BSA in solution were prepared and stored according to Section 2.3.

To investigate the effect of glucose on monocyte CD11b expression U937 monocytes (10^5/ml) were incubated in RPMI 1640 medium (containing 11mM glucose) with addition of various glucose concentrations (0, 10, 20, and 40mM) and supplemented with 10% FBS and 100U/ml penicillin and 100μg/ml

streptomycin for 24h, 48h, 72h at 37°C. The glucose concentrations used (0-20mM) are physiologically relevant (Tirosh et al., 2005) and 40mM is relevant to *in vitro* experimental investigations reported previously (Wang et al., 2009).

For 7 day incubations, U937 monocytes (10^5/ml) were incubated in glucose-free RPMI 1640 medium with addition of glucose at concentrations of 0, 11, 22 and 33mM for 3 days. The medium was then changed and further incubated in the glucose-supplemented medium for another 4 days. Cells incubated with 33mM mannitol were used as controls to allow for the osmolarity effects of glucose.

To investigate the effect of free fatty acids on CD11b and CD36 expression, U937 monocytes (10^5/ml) or mononuclear cells (10^6/ml) were incubated with palmitate alone (0, 50, 150 and 300μM), oleate alone (0, 50, 150 and 300μM), 300μM palmitate plus oleate (50, 150, and 300μM), and palmitate plus oleate (25μM+25μM, 75μM+75μM, 150μM+150μM) in RPMI 1640 supplemented with 10% FBS and 1% penicillin and streptomycin for 24h at 37°C. Control cells received BSA without fatty acids. The justification of fatty acids treatment are presented in Section 3.3.2.

5.3.3 Flow cytometric analysis of surface protein expression

Expression of CD11b, CD36, and CD206 was determined by flow cytometric

analysis in viable cells (PI negative) according to Section 2.4.

5.3.4 Cell viability assay

To test whether incubation conditions have adverse effect on cell viability, cell viability was measured by MTT assay and propidium iodide (PI) exclusion analysis using flow cytometry according to Section 2.14.2.1 and 2.14.3.

5.3.5 Intracellular peroxide determination

U937 monocytes were incubated with palmitate (0-300μM) for 24h at 37°C and then analysed by flow cytometry for intracellular peroxide levels using the peroxide sensitive permeable dye dihydrodichlorofluorescein diacetate (DCF-DA) as described in Section 2.10.

5.3.6 Monocyte adhesion assay

Mononuclear cells were isolated from whole blood according to the Section 2.2.4.1. The monocyte population was recognised as $CD14^+$ population by flow cytometry according to the Section 2.4.2.

The adhesion of U937 monocytes and mononuclear cells to immobilised ICAM-1 and un-stimulated EAhy926 endothelial monolayer was investigated according to the methods described in Section 2.11.

5.3.7 Measurement of plasma glucose and FFA level

Blood glucose levels were determined using a glucose analyser (Optimum Plus, UK).

Blood samples were centrifuged at 13,000×g for 5min and the plasma was stored at -80°C. FFA levels in the plasma were determined by a Wako Non-esterified fatty acids (NEFA) kit (Alpha Laboratories Ltd, Hampshire, UK) based on a colorimetric reaction for the quantification of FFA in serum or plasma. The intensity of the formation of a red pigment (quinoneimine dye) is proportional to the concentration of FFA or TAG in the sample and absorbance intensities were read at 550nm.

The principle for FFA assay is as follows:

$$\text{RCOOH (FFA)} + \text{ATP} + \text{CoA-SH} \xrightarrow{\text{Acyl-CoA-Synthetase}} \text{Acyl-CoA} + \text{AMP} + \text{PPi}$$

$$\text{Acyl-CoA} + O_2 \xrightarrow{\text{Acyl-CoA-Oxidase}} \text{2, 3-trans-enoyl-CoA} + H_2O_2$$

$$2H_2O_2 + \text{4-Aminophenazone} + \text{3-Methyl-N-(β-hydroxyethyl) aniline} \xrightarrow{\text{Peroxidase}}$$

$$\text{Quinoneimine dye} + 4H_2O$$

5.3.8 Statistical analysis

Data are expressed as mean ± SEM of at least three independent experiments conducted in triplicate. Statistical analyses were performed by one-way ANOVA

with Tukey-Kramer post hoc tests. To exclude the possibility that confounding factors such fasting glucose, free fatty acids, and BMI that could affect monocyte CD11b expression mononuclear cell adhesion to ICAM-1, a statistical co-variance analysis (Univariate Analysis of Variance) was carried out using SPSS 15.0. A p value less than 0.05 was considered significant.

5.4 Results

5.4.1 Effect of glucose and free fatty acids on monocyte phenotype

Type 2 diabetes is an independent risk factor for accelerating the development of atherosclerosis and elevated blood glucose and plasma free fatty acids levels are major characteristics of type 2 diabetes. To understand the underlying mechanisms for diabetic conditions contributing to atherogenesis, the present study investigated the effect of glucose and free fatty acids on the monocyte phenotype measured as the cell surface expression of CD11b and CD36, and monocyte adhesion to endothelium using U937 cells and primary monocytes.

5.4.1.1 Effect of glucose on CD11b expression in U937 monocytes.

In diabetic conditions, the blood glucose level is higher the normal blood glucose concentration (which is typically about 5.5mM); therefore, the effect of glucose on the monocyte phenotype was examined initially by measuring cell surface CD11b expression in U937 monocytes incubated with various glucose

concentrations from 24h to 7days; for cell incubations longer than 3 days, the cells were split at the third day.

Initial experiments were carried out to determine the level of extracellular glucose uptake by U937 monocytes. As shown in Figure 5.1, over 50% of glucose was taken up by U937 monocytes after 48h compared to 0h.

Figure 5.2 A-D shows the effect of glucose treatment on CD11b expression in U937 monocytes. The MdX of isotype control for CD11b was 0.44 arbitrary fluorescence units. Glucose treatment alone did not elicit any effect on CD11b expression in U937 monocytes at any of the concentrations or over the time periods studied using flow cytometric analysis. Also, glucose treatment under the same condition as shown in Figure 5.2 A-D did not show any significant effect on the expression of CD36 in U937 monocytes (data not shown).

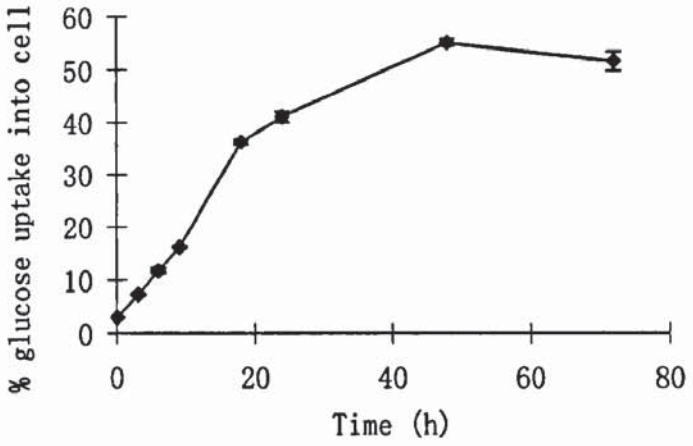

Figure 5.1 Time course of ^{3}H-glucose uptake into U937 monocytes. U937 cells (10^{6}/ml) were incubated in RPM I1640 medium containing 11mM glucose and 10% FBS and 2-deoxy-D-[^{3}H] glucose at 0.1μCi/ml for 0-72h. The levels of glucose uptake into the cells were determined as the % cell-associated radioactivity of total radioactivity. Data are mean±SEM from 3 independent experiments performed in duplicate.

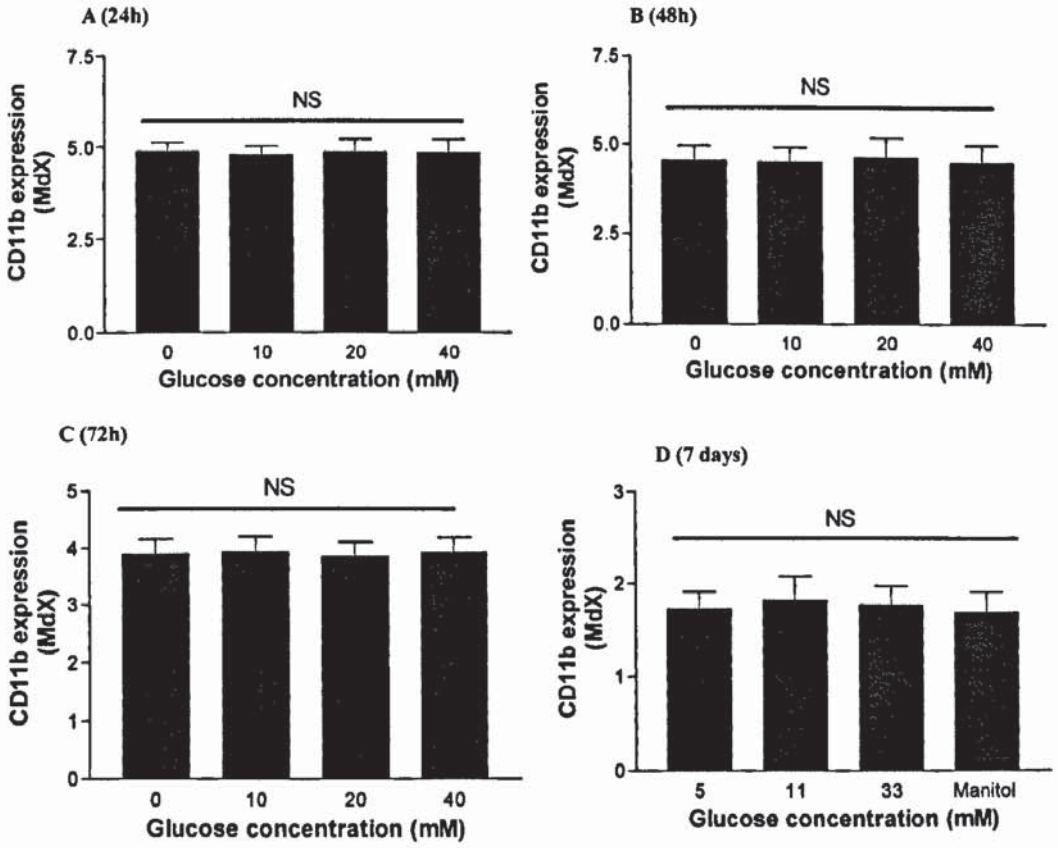

Figure 5.2 Effect of glucose on CD11b expression in U937 monocytes. U937 cells (10^{5}/ml) were incubated with increasing concentrations of glucose as shown

in each figure for 24h(A), 48h(B), 72h(C), and 7days (D) at 37°C. Cell surface CD11b levels were determined by flow cytometry in viable cells (PI negative) and expressed as MdX CD11b fluorescence. Data are mean±SEM from 3 independent experiments performed in triplicate. NS: non significant.

5.4.1.2 Effect of palmitate (30min) on CD11b expression in primary monocytes.

CD11b expression in monocytes has been shown to be acutely up-regulated by inflammatory stimuli such as C-reactive protein and LPS (Woollard et al., 2002). Therefore, initial experiments were carried out to determine whether short term treatment (30min) with palmitate could exert any effect on CD11b expression using primary monocytes as a cell model.

As shown in Figure 5.3, whole blood (50µl) incubated with 10^{-7}M PMA for 30min at 37°C, a potent activator for CD11b expression in human monocytes and neutrophils, showed an up to two-fold increase in MdX CD11b compared to controls ($p<0.001$). However, no difference in MdX CD11b was observed in cells incubated with palmitate under the same conditions (50-300µM) ($p>0.05$). This indicates that palmitate does not alter the CD11b expression in monocytes acutely. Therefore, in the subsequent experiments, the long term (24h) effect of palmitate on CD11b expression was investigated.

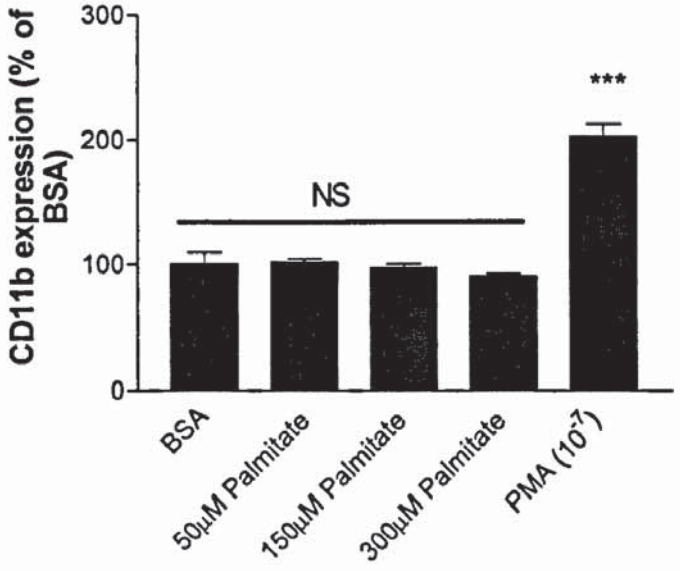

Figure 5.3 Effect of palmitate (30min) on CD11b expression in primary monocytes ($CD14^+$ cells). Whole blood (50μl) was incubated with palmitate (50, 150, and 300μM) for 30min at 37°C. Cells treated with 300μM BSA as a control Phorbol myristate acetate (PMA; 10^{-7}M) treatment was used as a positive control. CD11b levels were determined by flow cytometry and shown as % of BSA control. Data are mean±SEM from 3 independent experiments performed in triplicate. *** $p<0.001$ compared to BSA. NS: non significant.

5.4.1.3 Effect of free fatty acids (24h) on CD11b expression in viable primary monocytes.

The effect of long term exposure (24h) to the two major free fatty acids found in human plasma (palmitate and oleate) on CD11b expression in primary monocytes was investigated.

Ten healthy male volunteers aged between 23 and 60 were recruited and fully gave fully informed oral consent. After overnight fasting, the blood was taken and mononuclear cells were isolated and incubated with specific free fatty acids as

described in Figure 5.4 A-D. The fasting glucose level of the volunteers ranged from 4.5mM to 6.1mM, the free fatty acids level ranged from 384μM to 902μM, and body mass index (BMI) ranged from 19.9-29.4kg/m^2. (Table 5.1)

Table 5.1 Demographic characteristics of the volunteers

Volunteer	FFA (μM)	Glucose (mM)	BMI (kg/m^2)	Condition	Age (y)
1	384	5.5	29.4	Type 1 diabetes	58
2	567	5.5	25.9	Healthy	30
3	521	5.5	25.2	Healthy	61
4	406	4.7	23.0	Healthy	61
5	902	4.5	26.0	Endurance training	24
6	484	6.1	26.6	Healthy	25
7	521	5.8	20.4	Healthy	51
8	437	6.1	21.9	Healthy	59
9	552	5.9	19.9	Healthy	33
10	686	5.9	27.5	Healthy	35

The effect of free fatty acids on CD11b expression in viable monocytes showed a relatively large variation between individuals. Overall, palmitate treatment tended to reduce CD11b expression after 24h whereas oleate tended to increase CD11b expression. There was also a trend for palmitate plus oleate mixture at a ratio of 1:1 to increase CD11b expression. However, none of these trends reached a statistical significance ($p>0.05$).

In order to exclude some confounding factors such as fasting blood glucose level, plasma free fatty acids level, and BMI, co-variance analysis was carried out using

SPSS15.0 software. The results showed that neither fasting glucose level, nor fasting free fatty acids level, nor BMI was significantly associated with CD11b expression.

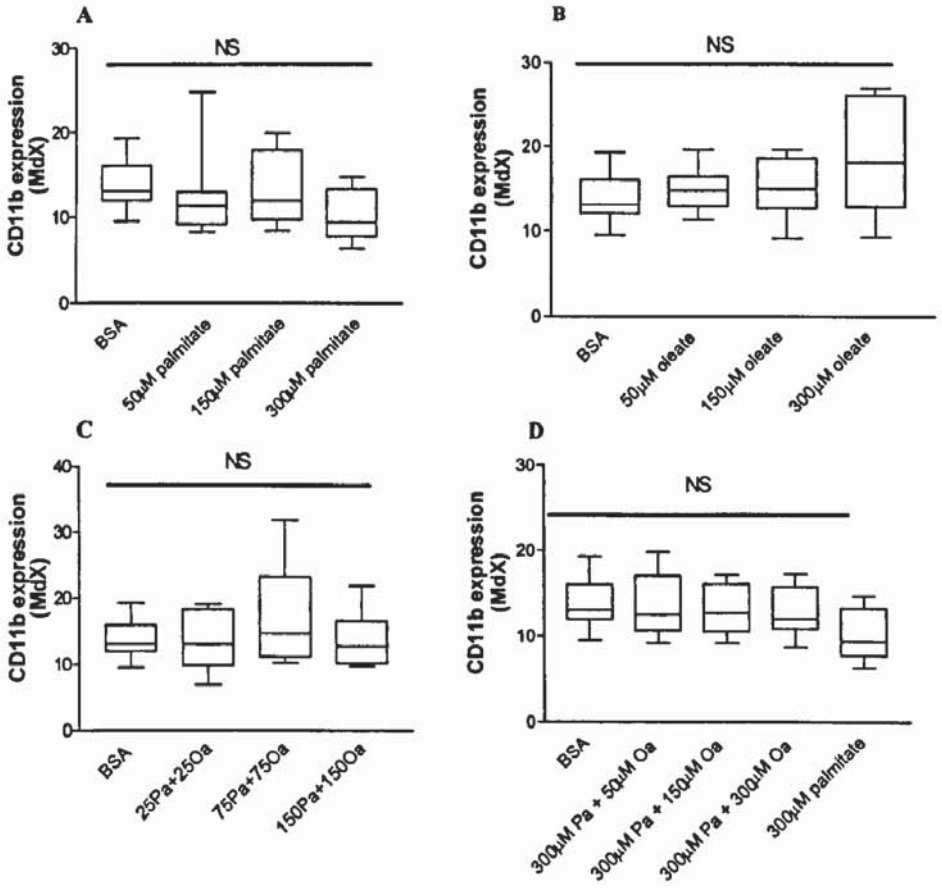

Figure 5.4 Effect of free fatty acids on CD11b expression in viable CD14$^+$ mononuclear cells. Human mononuclear cells (10^6/ml) were isolated from whole blood and incubated with (A) palmitate alone (50-300μM), (B) oleate alone (50-300μM), (C) palmitate plus oleate (25μM+25μM, 75μM+75μM, 150μM+150μM), (D) 300μM palmitate plus various oleate (50-300μM) concentrations for 24h at 37°C. Controls were cells incubated with 300μM BSA without fatty acids. Cell surface CD11b levels were determined by flow cytometry in viable (PI negative) CD14$^+$ cells and expressed as MdX CD11b fluorescence. Data are mean±SEM from 10 independent subjects analysed in duplicate. NS: non significant.

5.4.1.4 Effect of free fatty acids (24h) on CD11b expression in viable U937 monocytes.

In order to minimise the individual variations in response to free fatty acids, U937 monocytes, one of the most widely used human monocytic cell lines, was chosen to investigate further the 24h treatment of free fatty acids on CD11b expression. As shown in Figure 5.5 A, palmitate at 150μM and 300μM significantly increased cell surface MdX CD11b in U937 monocytes from a control value of 1.78 ± 0.14 to 2.3 ± 0.40 and 2.3 ± 0.22 ($p<0.001$). There was also a trend towards an increase in CD11b expression in viable cells incubated with 50μM palmitate, however, it did not reach a statistical significance ($p>0.05$). The palmitate-induced increase in CD11b expression in U937 monocytes is also shown in Figure 5.6 as a peak shift in CD11b fluorescence after incubation with 50-300μM palmitate for 24h. In contrast, oleate at the concentrations tested did not show any significant effect on CD11b expression in U937 monocytes ($p>0.05$) (Fig.5.5 B).

When U937 cells were incubated with increasing concentrations of palmitate and oleate mixture at a ratio of 1:1, the CD11b expression was not significantly changed up to 150μM palmitate and 150μM oleate concentration used ($p>0.05$). (Fig.5.5 C).

The co-incubation of oleate (50μM-300μM) with 300μM palmitate significantly

abrogated the increase in CD11b expression caused by palmitate (Fig.5.5 D). The CD11b expression was reduced by oleate in a concentration dependent manner from 2.33 to 2.04 ± 0.10 (p<0.01), 1.80 ± 0.13. (p<0.001), 1.71 ± 0.10 (p<0.001) for 50μM, 150μM and 300μM oleate, respectively.

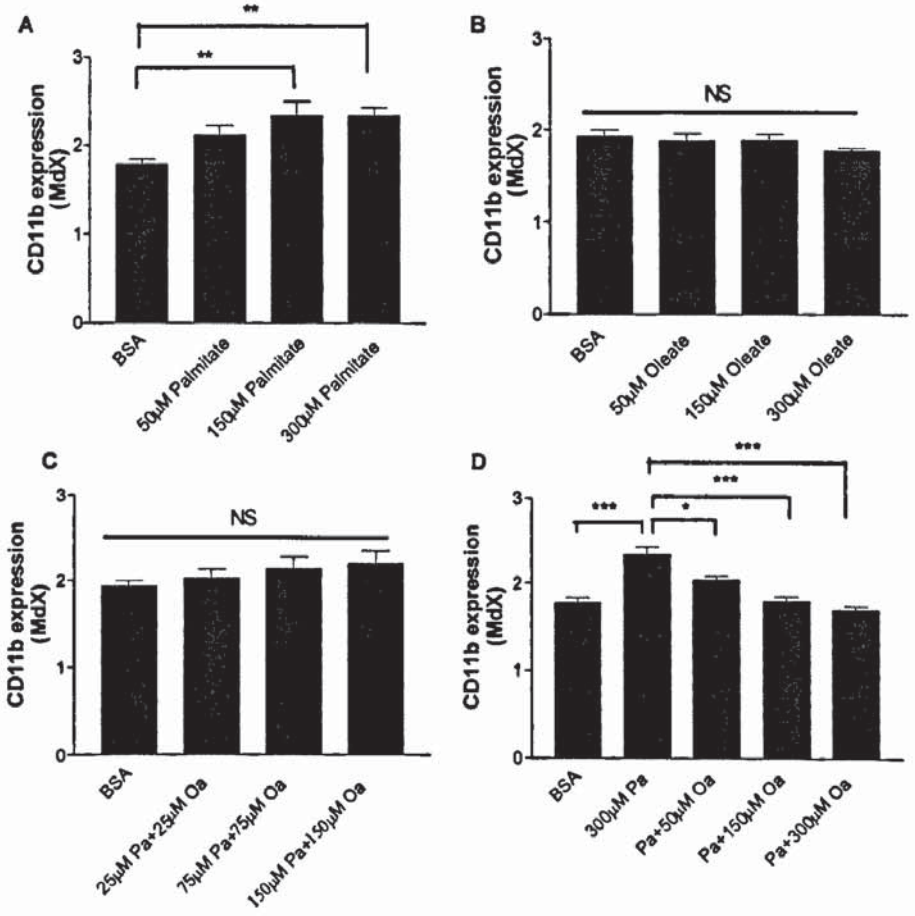

Figure 5.5 Effect of free fatty acids on CD11b expression in viable U937 monocytes. U937 cells (10^5/ml) were incubated with (A) palmitate alone (50-300μM), (B) oleate alone (50-300μM), (C) palmitate plus oleate (25μM+25μM, 75μM+75μM, 150μM+150μM), (D) 300μM palmitate plus oleate (50-300μM) for 24h at 37°C. Controls were cells incubated with BSA without fatty acids. Cell surface CD11b levels were determined by flow cytometry in viable cells (PI negative) and expressed as MdX CD11b fluorescence. Data are mean±SEM from 3 independent experiments performed in triplicate. *p<0.05, **p<0.01, *** p<0.001, NS: non significant.

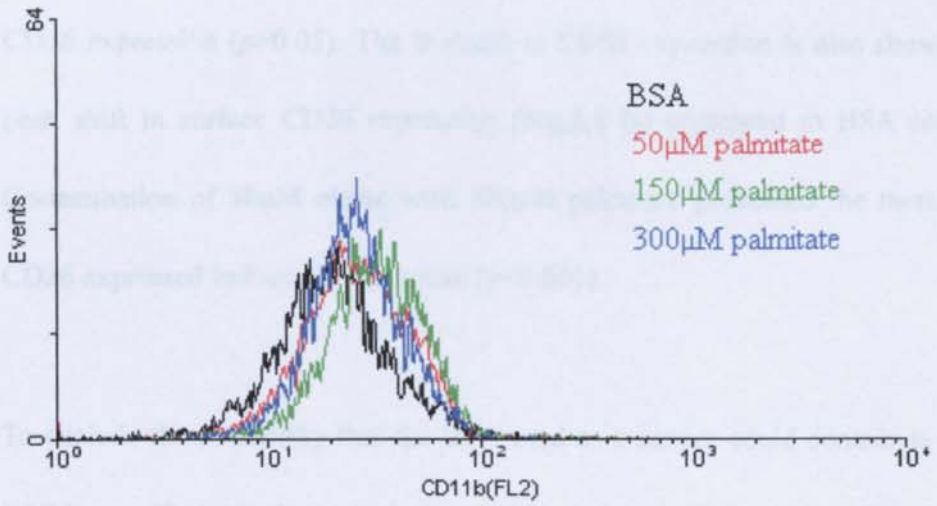

Figure 5.6 Palmitate increases CD11b expression in viable U937 monocytes. U937 cells (10^5/ml) were incubated with palmitate (50-300μM) for 24h at 37°C. Cell surface CD11b levels were determined by flow cytometry in viable cells (PI negative) and the representative CD11b peak fluorescence histogram is shown.

5.4.1.5 Fatty acid modulates CD36 expression in viable U937 monocytes.

The effect of free fatty acids on CD36 expression was investigated by incubating U937 monocytes with 300μM palmitate alone, 300μM oleate alone, 300μM palmitate plus 50μM oleate or BSA for 24h.

The cell surface CD36 expression in viable U937 monocytes incubated with BSA (control) was not significantly different from the isotype negative control; therefore, the level of CD36 in monocytes was expressed as % of CD36 positive cells. As shown in Figure 5.7 B, palmitate at 300μM caused a significant increase in the percentage of CD36 positive cells from a control level of 2% to 15% after

24h incubation ($p<0.001$) whereas oleate at either 50μM or 300μM did not affect CD36 expression ($p>0.05$). The increase in CD36 expression is also shown as a peak shift in surface CD36 expression (Fig.5.8 B) compared to BSA controls. Co-incubation of 50μM oleate with 300μM palmitate prevented the increase in CD36 expressed induced by palmitate ($p<0.001$).

To exclude the possibility that the BSA used as a carrier could contribute to the inhibitory effect of oleate against palmitate-induced CD36 expression, parallel measurements were carried out using U937 monocytes incubated with equivalent BSA presented in 50μM oleate in the presence of 300μM palmitate for 24h. Co-incubation with BSA also reduced the CD36 expression to 8%, however, the magnitude was significantly less than that in cells co-incubated with 50μM oleate ($p<0.01$).

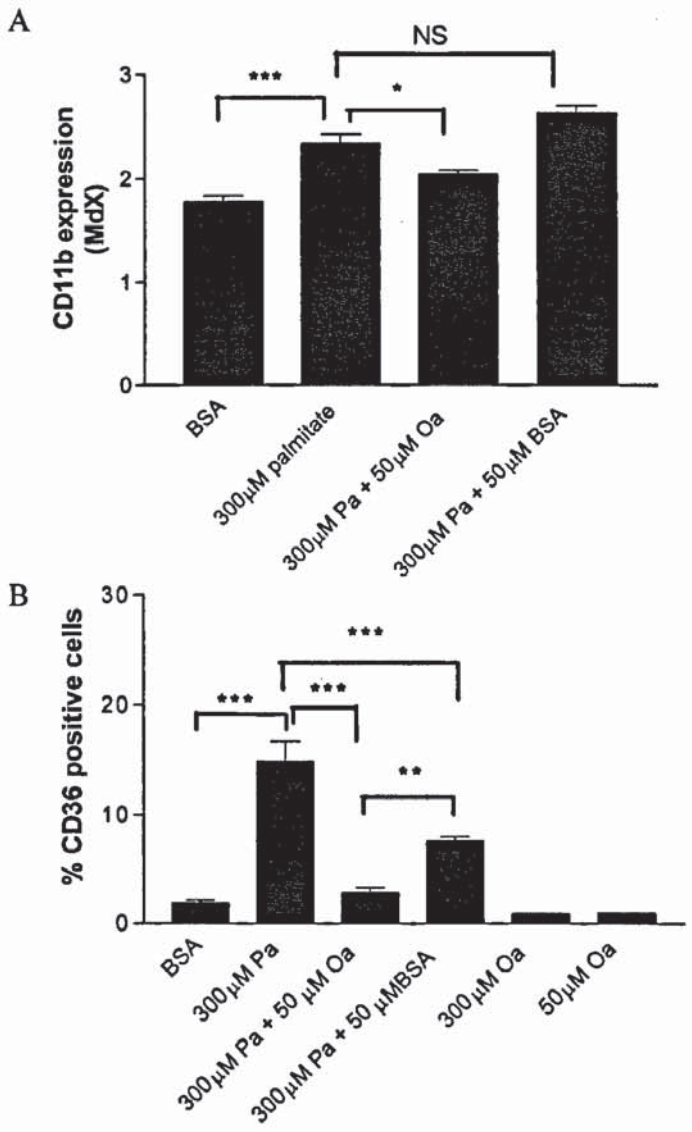

Figure 5.7 Effect of oleate (Oa) on palmitate (Pa)-induced CD11b (A) and CD36 (B) expression in viable U937 monocytes. U937 cells (10^5/ml) were incubated with 300µM palmitate, 300µM palmitate plus 50µM oleate or equivalent BSA presented in 50µM oleate, oleate (50µM and 300µM) for 24h at 37°C. Controls are cells treated with BSA. Cell surface expression of CD11b and CD36 were determined by flow cytometry in viable cells (PI negative). Data are mean±SEM from 3 independent experiments performed in triplicate. *p<0.05, **p<0.01, ***p<0.001, NS: non significant.

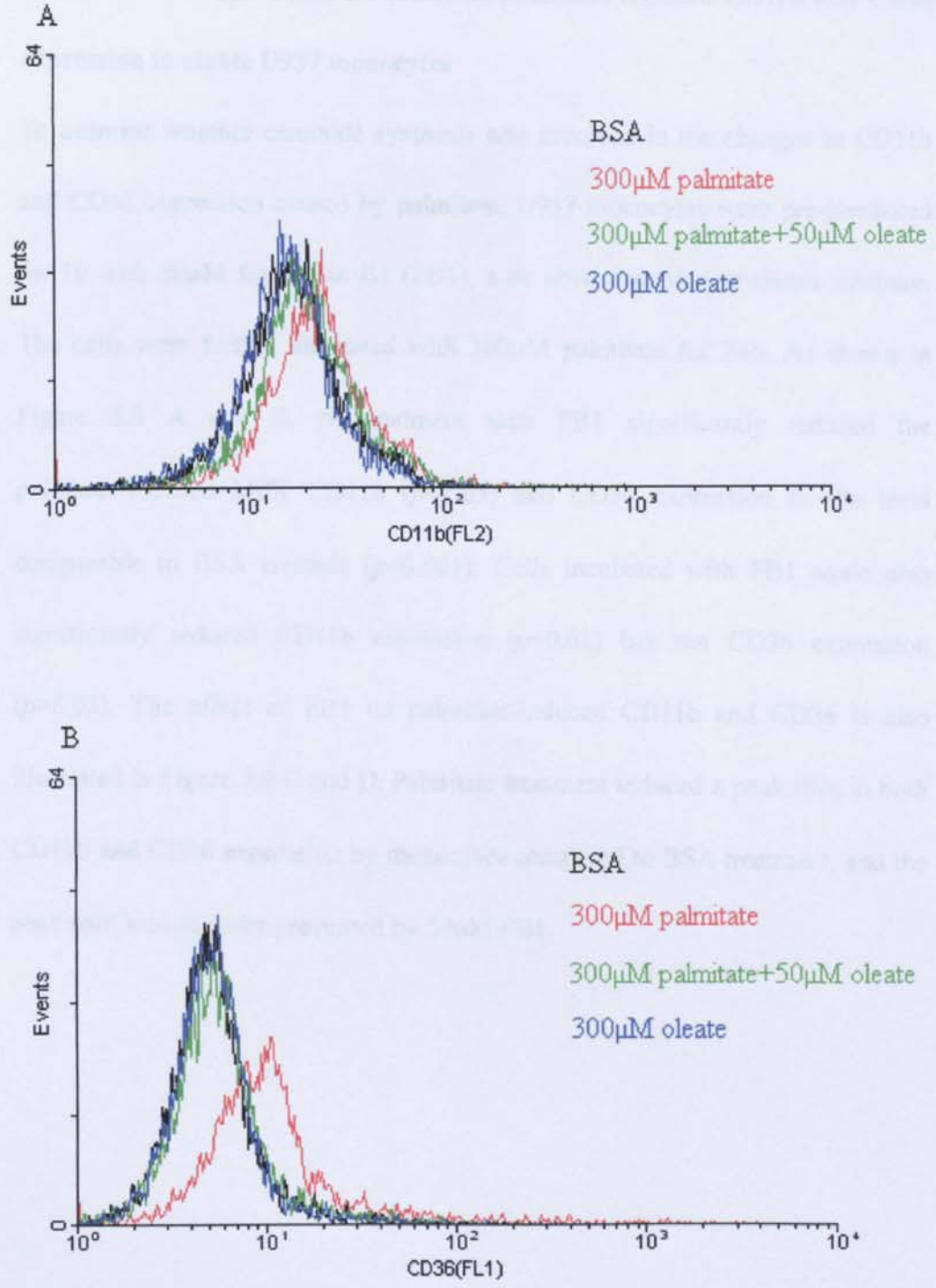

Figure 5.8 Effect of oleate on palmitate-induced CD11b and CD36 expression in viable U937 monocytes. U937 cells (10^5/ml) were incubated with 300μM palmitate, 300μM palmitate plus 50μM oleate, 300μM oleate for 24h at 37°C. Controls are cells treated with BSA. Cell surface CD11b (A) and CD36 (B) levels were determined by flow cytometry in viable cells (PI negative) and representative CD11b and CD36 peak fluorescence histograms are shown.

5.4.1.6 Effect of fumonisin B1 (FB1) on palmitate-induced CD11b and CD36 expression in viable U937 monocytes

To examine whether ceramide synthesis was involved in the changes in CD11b and CD36 expression caused by palmitate, U937 monocytes were pre-incubated for 1h with 50μM fumonisin B1 (FB1), a *de novo* ceramide synthesis inhibitor. The cells were further incubated with 300μM palmitate for 24h. As shown in Figure 5.9 A and B, pre-treatment with FB1 significantly reduced the palmitate-induced MdX CD11b ($p<0.05$) and CD36 expression to the level comparable to BSA controls ($p<0.001$). Cells incubated with FB1 alone also significantly reduced CD11b expression ($p<0.01$) but not CD36 expression ($p>0.05$). The effect of FB1 on palmitate-induced CD11b and CD36 is also illustrated in Figure 5.9 C and D. Palmitate treatment induced a peak shift in both CD11b and CD36 expression by monocytes compared to BSA treatment, and the peak shift was partially prevented by 50μM FB1.

A

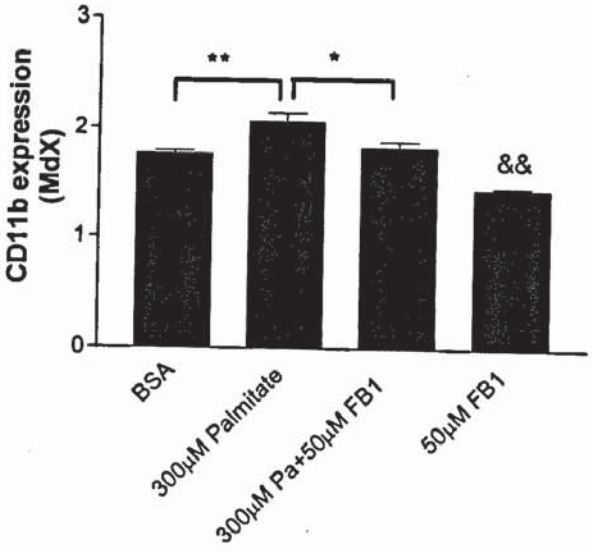
CD11b expression (MdX)
3
2
1
0
**
*
&&
BSA
300μM Palmitate
300μM Pa+50μM FB1
50μM FB1

B

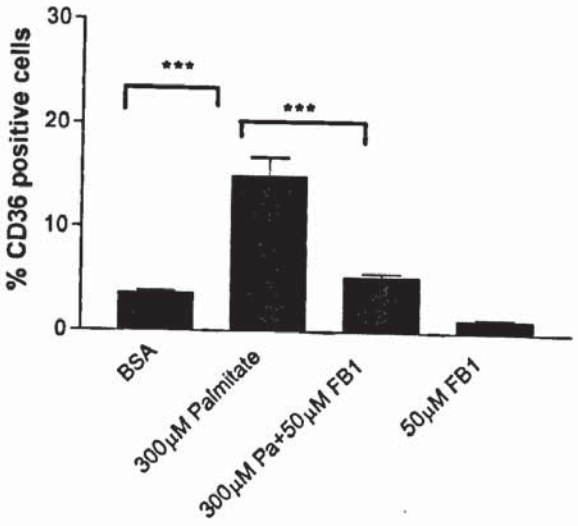
% CD36 positive cells
30
20
10
0
***
***
BSA
300μM Palmitate
300μM Pa+50μM FB1
50μM FB1

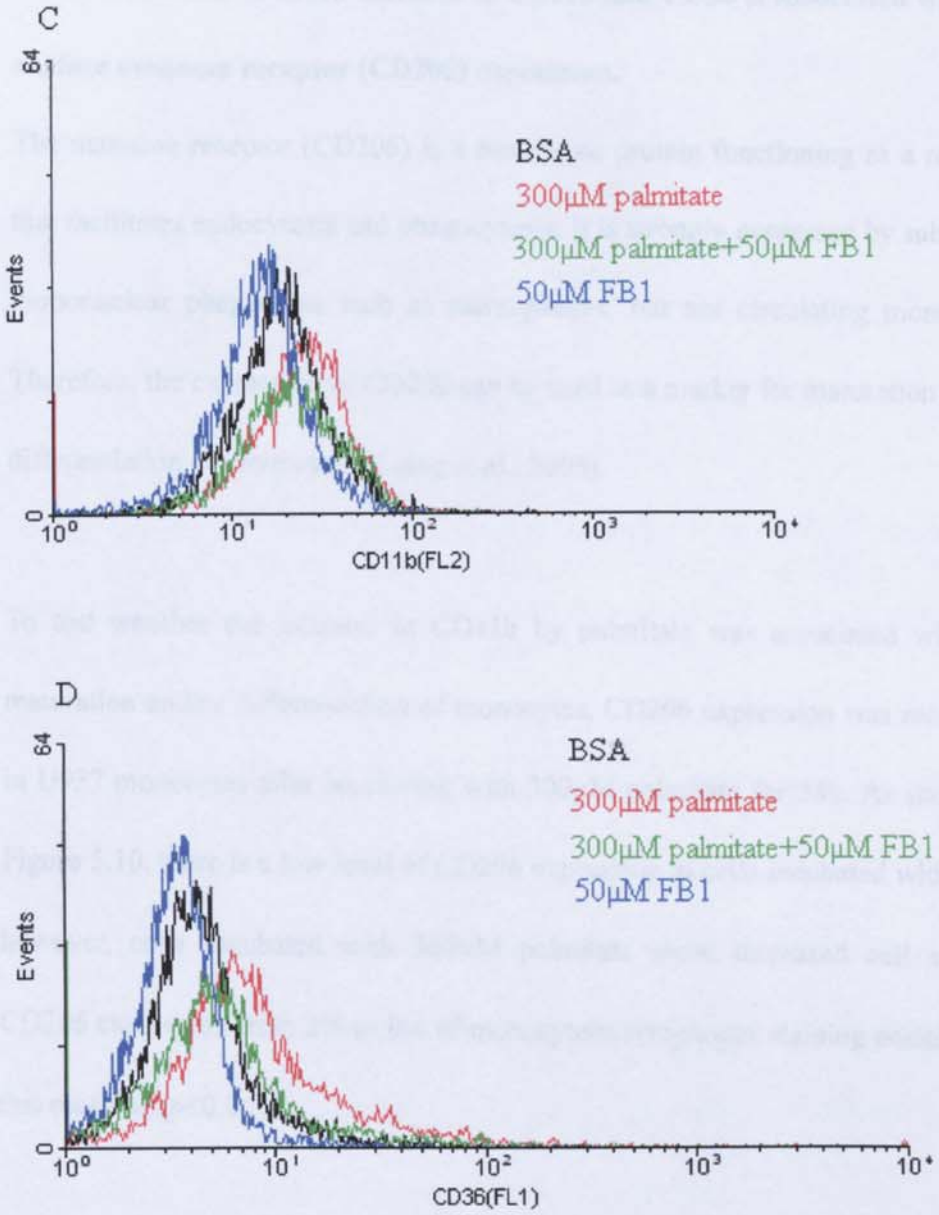

Figure 5.9 Effect of fumonisin B1 (FB1) on palmitate-induced CD11b (A and C) and CD36 (B and D) expression in viable U937 monocytes. U937 cells (10^5/ml) were pre-incubated with 50µM FB1 for 1h and then further incubated with 300µM palmitate for 24h at 37°C. Controls are cells treated with BSA. Cell surface CD11b and CD36 levels were determined by flow cytometry in viable cells (PI negative). Data are mean±SEM from 3 independent experiments performed in triplicate. *p<0.05, **p<0.01, ***p<0.001, NS: non significant. && p<0.01 compared to BSA.

5.4.1.7 Palmitate-induced increase in CD11b and CD36 is associated with cell surface mannose receptor (CD206) expression.

The mannose receptor (CD206) is a membrane protein functioning as a receptor that facilitates endocytosis and phagocytosis. It is strongly expressed by subsets of mononuclear phagocytes such as macrophages, but not circulating monocytes. Therefore, the expression of CD206 can be used as a marker for maturation and/or differentiation of monocytes (Liang et al., 2006).

To test whether the increase in CD11b by palmitate was associated with the maturation and/or differentiation of monocytes, CD206 expression was measured in U937 monocytes after incubating with 300μM palmitate for 24h. As shown in Figure 5.10, there is a low level of CD206 expression in cells incubated with BSA, however, cells incubated with 300μM palmitate show increased cell surface CD206 expression from 2% to 9% of monocyte/macrophages staining positive for this receptor ($p<0.001$).

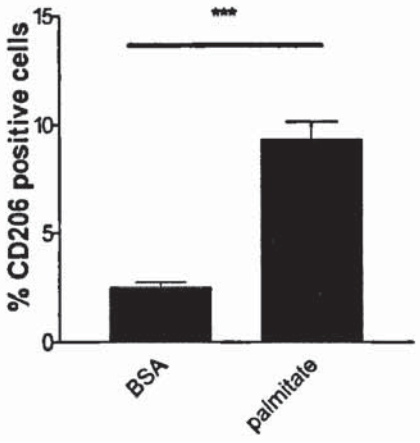

Figure 5.10 Effect of palmitate on CD206 expression in U937 monocytes. U937 cells (10^5/ml) were incubated with 300μM palmitate for 24h at 37°C. Cell surface CD206 expression was measured by flow cytometry. Data are mean±SEM from 3 independent experiments performed in triplicate. ***p<0.001.

5.4.1.8 Effect of palmitate on reactive oxygen species (ROS) generation in U937 monocytes.

CD11b expression has been reported to be redox sensitive. Therefore, to test whether the changes in palmitate-induced CD11b expression were associated with ROS generation, DCF-DA was used as an indicator of intracellular ROS generation in U937 monocytes treated with palmitate for 24h.

As shown in Figure 5.11, the ROS generation measured as the median fluorescence of DCF in cells incubated with 50μM palmitate was significantly higher than BSA controls (17.47±1.37 versus 10.21±0.32, p<0.001). Increasing the palmitate concentration to 150μM and 300μM did not show a significant effect

on intracellular ROS generation although there was a trend towards lower ROS generation at 300μM, however, this did not reach statistical significance (p>0.05).

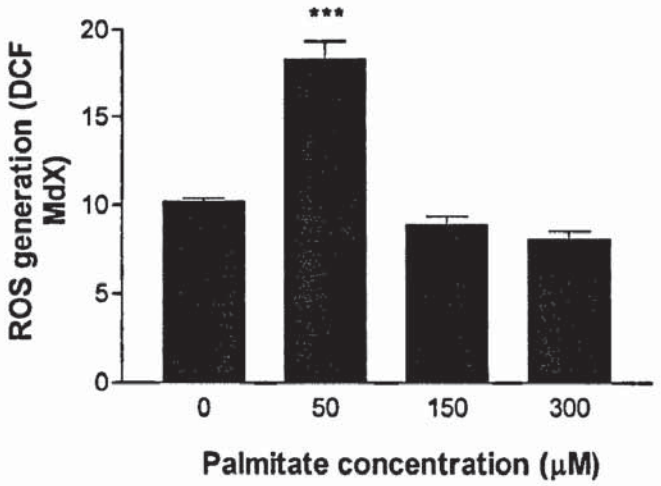

Figure 5.11 Effect of palmitate on reactive oxygen species (ROS) generation. U937 cells (10^5/ml) were incubated with palmitate (0-300μM) for 24h at 37°C. Intracellular ROS generation was measured by flow cytometry of DCF-DA. Data are mean±SEM from 3 independent experiments performed in triplicate. ***p<0.001.

5.4.2 Effect of free fatty acids on monocyte adhesion to endothelium

Monocyte adhesion to the endothelium is one of the earliest events for the development of atherosclerosis, and CD11b is an abundant receptor expressed on monocytes which mediates part of this process. Therefore, the following studies were carried out to investigate whether there was a functional change in monocyte adhesion to endothelium after treatment with free fatty acids using EAhy 926 endothelial cells and immobilised ICAM-1 as in vitro endothelium models.

5.4.2.1 Effect of palmitate on U937 monocyte adhesion to EAhy926 endothelial cells.

The EAhy926 cell is an immortalised micro vascular endothelial cell line produced by fusing human umbilical vein endothelial cells (HUVEC) with A549 epithelial cells (Edgell et al., 1983). To investigate the effect of palmitate treatment on U937 monocyte adhesion to the endothelium, EAhy926 cells were chosen as an in vitro endothelial cell model.

The initial experiments were carried out to characterise the cell surface expression of adhesion molecules such as ICAM-1, VCAM-1, Platelet/endothelial cell adhesion molecule-1 (PECAM-1, CD31), and E-selectin under resting and LPS-stimulated conditions. As shown in Figure 5.12 and Table 5.2, the un-stimulated EAhy926 cells mainly express VCAM-1 and did not show any significant increase in ICAM-1, VCAM-1, E-selectin, PECAM-1 after LPS stimulation (0-5μg/ml) for 24h.

Adhesion of U937 monocytes to unstimulated EAhy926 endothelial cells is shown in Figure 5.13 A. After incubation with 300μM palmitate, there was a significant decrease in U937 monocyte adhesion to EAhy926 endothelium from a basal adhesion level of 26% to 15% after 24h incubation ($p<0.001$). Also in a parallel experiment, there was a significant decrease in PECAM-1 (CD31) expression in

U937 monocytes after 300μM palmitate 24h treatment (p<0.001) (Fig. 5.13 B).

5.4.2.2 Effect of free fatty acids on monocyte adhesion to ICAM-1.

As ICAM-1 rather than VCAM-1 is a ligand for CD11b, therefore, the effect of fatty acids on monocyte CD11b-mediated adhesion was investigated using immobilised with human recombinant ICAM-1 protein as an in vitro model. The effect of palmitate, oleate or palmitate plus oleate on primary mononuclear cells and U937 monocyte adhesion to ICAM-1 was carried out after 24h treatment. Similar to the effect of fatty acids on expression of CD11b in primary monocytes, there was a large variation in mononuclear cells (MNC) adhesion to ICAM-1 between each individual. As shown in Figure 5.14 A, there is a significant reduction in the adhesion of MNC incubated with 300μM palmitate to ICAM-1 (p<0.01). Cells incubated with 300μM oleate or 300μM palmitate plus 150μM oleate did not show any significant difference in the adhesion to ICAM-1 compared to BSA controls (p>0.05). Also, there is a significant decrease in cell surface CD11b expression in viable MNC after 300μM palmitate treatment compared to BSA controls (0.68±0.1 versus 0.43±0.03, p<0.01). Oleate and palmitate plus oleate treatment did not affect the CD11b expression in CD11b expression in MNC compared to BSA controls (p>0.05) (Fig. 5.14 B).

To exclude the possibility that confounding factors such as fasting glucose, free

fatty acids, and BMI that could affect mononuclear cell adhesion after isolation and 24h culture *in vitro*, a statistical co-variance analysis was carried out using SPSS 15.0 and found that there were no significant associations between these factors and mononuclear cell adhesion to ICAM-1.

The effect of free fatty acids on U937 monocyte adhesion to ICAM-1 is shown in Figure 5.15. Incubation of U937 monocytes with PMA (10^{-6}M) for 24h was used as a positive control for verifying the methods used for the adhesion assay. PMA treatment increased U937 cell adhesion to plate immobilised with ICAM-1 from a basal level of 20% to around 70% while non-specific adhesion to 1%BSA-coated plate (negative control for ICAM-1 coating) was around 40% with two washes. The overall adhesion of U937 monocytes treated with various free fatty acids was not significantly different from BSA controls although there was a trend towards increasing cell adhesion at 50μM and 150μM palmitate (p>0.05).

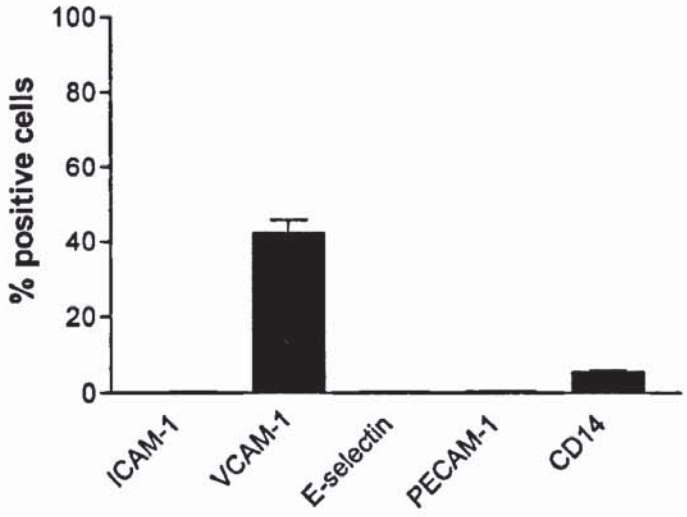

Figure 5.12 Expression of adhesion molecule in unstimulated EAhy926 endothelial cells. EAhy926 cells (10^6/ml) were incubated with 10μg/ml anti-human ICAM-1, anti-human VCAM-1, anti-human E-selectin, anti-human PECAM-1 (CD31), and anti-human CD14 for 30min on ice in the dark. Cell surface adhesion molecule levels were determined by flow cytometry and expressed as % of positive cells. Data are mean±SEM from 3 independent experiments performed in triplicate.

LPS 24h	0μg/ml	0.5μg/ml	1μg/ml	5μg/ml
ICAM-1	0.09%	0.09%	0.09%	0.09%
VCAM-1	0.42%	0.41%	0.41%	0.39%
E-selectin	0.18%	0.18	0.18%	0.18%
PECAM-1	0.43%	0.43%	0.36%	0.34%

Table 5.2 Effect of lipopolysaccharides (LPS) on expression of adhesion molecules in EAhy926 endothelial cells. EAhy 926 cells were incubated with LPS (O26:B6) (0-5μg/ml) for 24h at 37°C. Adhesion molecule expression was determined by flow cytometry. The data are expressed as % of cells staining positive for each adhesion molecule.

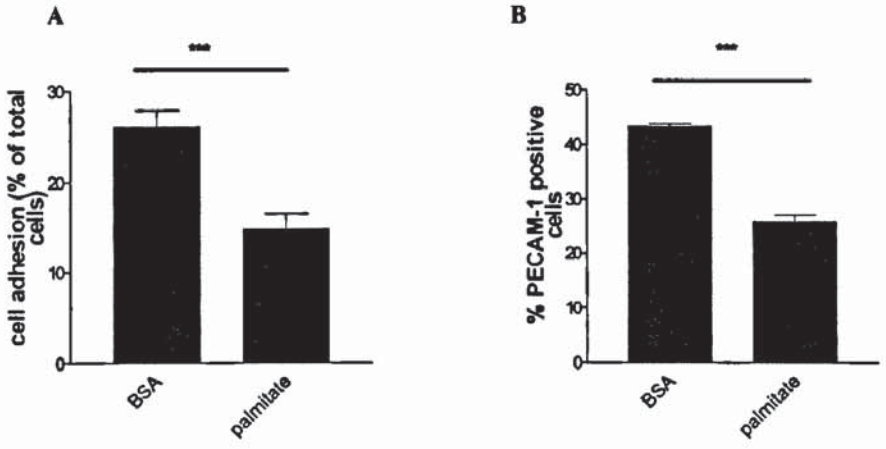

Figure 5.13 Effect of palmitate on U937 monocyte adhesion to unstimulated EAhy 926 endothelium (A) and PECAM-1 (CD31) expression (B). U937 monocytes (2.5×10^5/ml) were incubated with 300μM palmitate for 24h. After that, cells were labelled with 10μg/ml BCECF-AM and re-suspended in serum-free M199 (10mM HEPES) at $2.5*10^5$/ml. Then U937 cells (2.5×10^5/well) were incubated with Eahy926 endothelial monolayer for 30min at 37°C. The unbound monocytes were washed away. The bound cells were quantified by a cell density standard curve. PECAM-1 (CD31) expression in U937 monocytes after palmitate treatment was determined by flow cytometry. Data are mean±SEM from 3 independent experiments performed in triplicates. ***$p<0.001$.

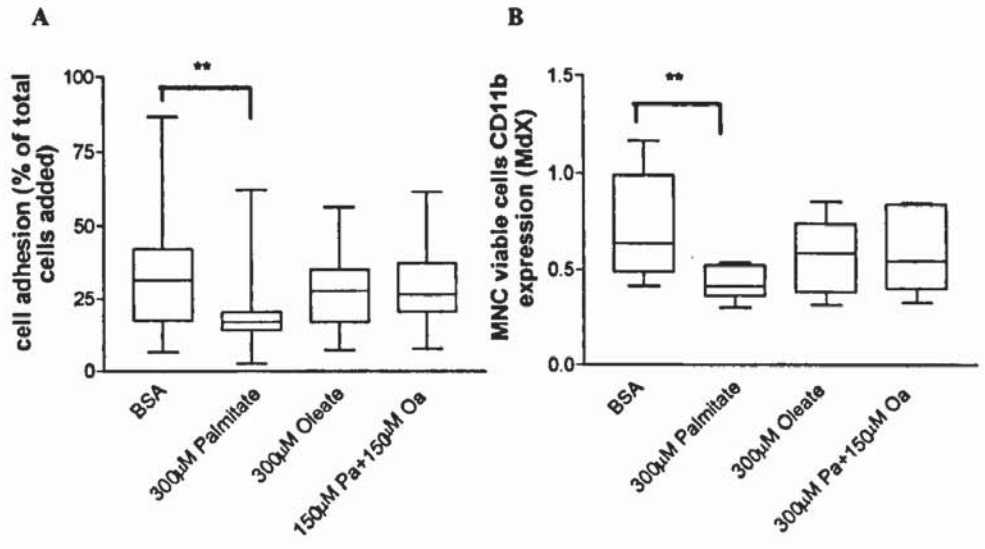

Figure 5.14 Effect of palmitate and oleate on MNC adhesion to ICAM-1. BCECF-AM-labelled mononuclear cells (MNC; 5×10^5/ml) were incubated with immobilised ICAM-1-Fc (captured by mouse anti-human Fc monoclonal antibody) in 96 well plates which had been for 30min at 37°C. The unbound cells were

removed by inverting plates and the bound cells were lysed and BCECF fluorescence determined at excitation 535nm, emission 585nm. Adhesion was calculated from a cell standard curve and expressed as the % bound of total cells added. Data are expressed as mean±SEM (n=10). $^{**}p<0.01$.

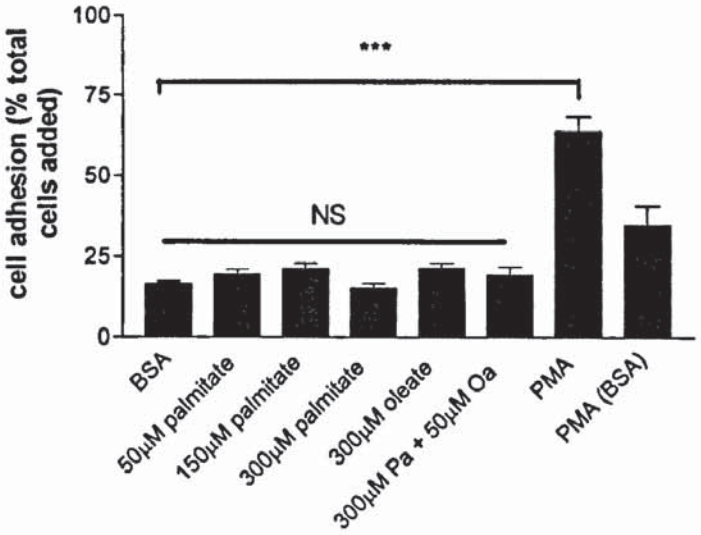

Figure 5.15 Effect of free fatty acids on U937 monocyte adhesion to ICAM-1. U937 monocytes (10^5/ml) were incubated with palmitate (50-300μM) alone, 300μM palmitate+50μM oleate, 300μM oleate, PMA (10^{-6}M) for 24h at 37°C. Monocytes were then labelled with 10μg/ml BCECF-AM and incubated with anti-Fc captured ICAM-1 and 1% BSA as control wells for 30min at 37°C in 96-well plates. The unbound cells were removed by inverting plates and the bound cells were lysed and BCECF fluorescence determined at excitation 535nm, emission 585nm. Adhesion were calculated from a cell density standard curve and expressed as the % bound of total cells added. Data are mean±SEM from 6 independent experiments performed in triplicate. $^{***}p<0.001$. NS, non significant.

5.4.3 Effect of free fatty acids on cell viability

To investigate the effect of various treatments on monocyte viability, a flow cytometric analysis with propidium iodide (PI) staining and an MTT assay were carried out in both mononuclear cells and U937 cells.

5.4.3.1 Effect of free fatty acids on mononuclear cell (MNC) viability.

The isolated MNC was mainly composed by two types of cells: monocytes ($CD14^+$) and lymphocytes ($CD14^-$). After various free fatty acids treatments, the percentage of $CD14^+$ cell population (monocytes) in isolated MNC was increased from 20% before treatment to 30% after the incubation with BSA as a control for 24h. There was a slightly but not significantly decrease in the percentage of $CD14^+$ cell population after treated with 300μM palmitate compared to BSA. Oleate and the various combinations of palmitate and oleate did not exert any significant effect on the percentage of $CD14^+$ cell population.

The viability of monocytes in a primary mononuclear cell population after incubation with fatty acids for 24h was determined in $CD14^+$ cell stained with propidium iodide (PI). As shown in Figure 5.16 B, palmitate (300μM) reduced monocyte cell viability from a control level of 79% to 67% after 24h ($p<0.05$). Oleate alone (300μM) also tended to reduce cell viability (to 71%); however, this did not reach a statistical significance ($p>0.05$). Co-incubation with up to 300μM oleate tended to prevent the decrease in cell viability caused by 300μM palmitate; however, this did not reach statistical significance (67.3% ± 8.0 versus 74.1% ± 5.9, mean ± SD, $p>0.05$).

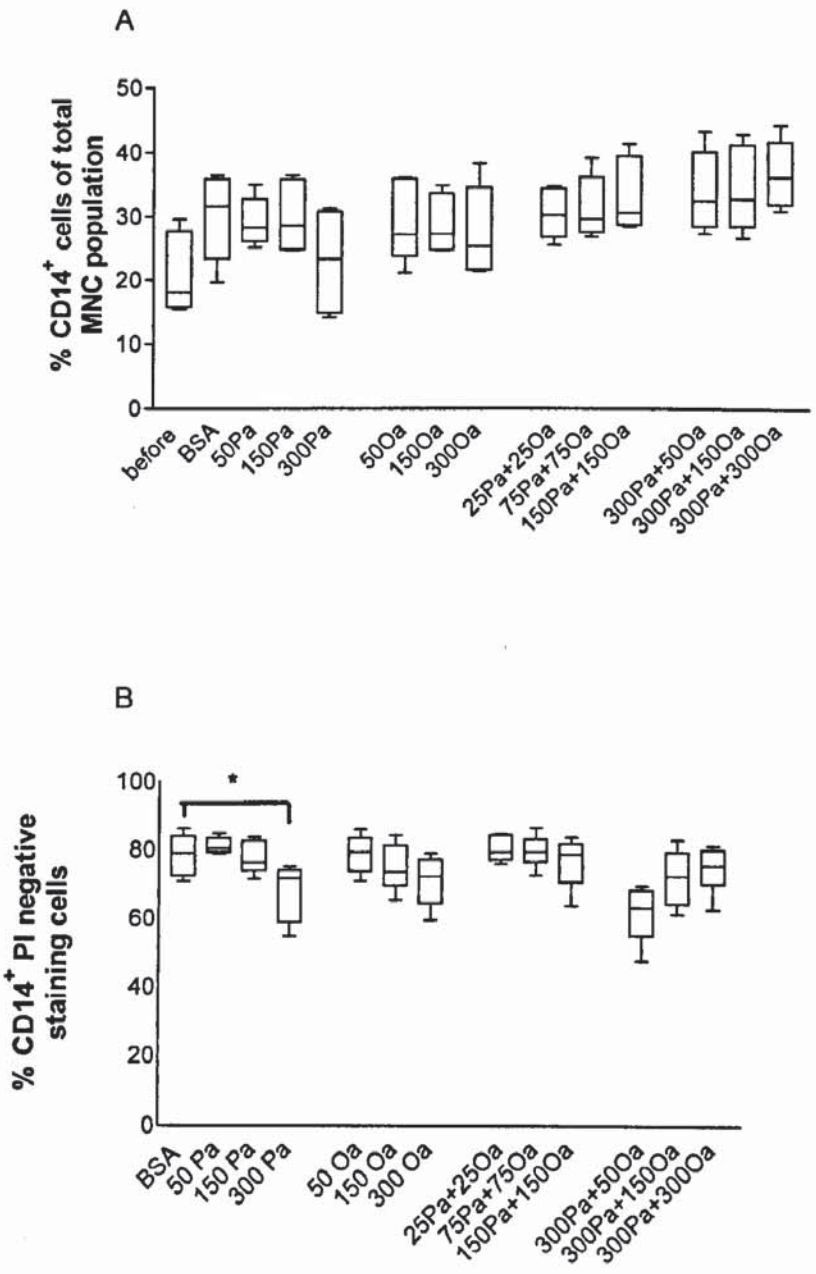

Figure 5.16 Effect of free fatty acids on viability of primary monocyte. Human mononuclear cells (10^6/ml) were incubated with palmitate alone (50-300μM), oleate alone (50-300μM), palmitate plus oleate (25μM+25μM, 75μM+75μM, 150μM+150μM), 300μM palmitate plus various oleate (50-300μM) for 24h at 37°C. Controls were cells incubated with 50μM BSA without fatty acids. (A) % $CD14^+$ cells out of total MNC population before and after various treatments. (B) Monocyte cell viability which was measured by flow cytometric analysis with propidium iodide (PI) staining in $CD14^+$ cells. Data are mean±SD, n=10.
* p <0.05.

5.4.3.2 Effect of glucose and free fatty acids on U937 monocyte viability

The effect of glucose and free fatty acids on U937 monocyte viability was determined by both flow cytometric analysis with PI staining and the MTT assay.

As shown in Figure 5.17, glucose treatment alone did not exert any effect on cell viability at any of the concentrations or over the time periods studied ($p>0.05$).

Figure 5.20 shows the cell profiles (forward scatter versus side scatter and PI fluorescence versus forward scatter) after various free fatty acid treatments. Cell viability was calculated as the percentage of cells in the R1 region over total counts. Palmitate at a concentration of 300μM for 24h reduced the U937 cell viability from a control level of 97% to 42% ($p<0.001$) measured by flow cytometry. Oleate alone at either 50μM or 300μM did not affect the cell viability over 24h ($p>0.05$). The co-incubation of 50μM oleate with 300μM palmitate almost completely prevented the palmitate-induced cell loss and this effect was not due to additional BSA associated with oleate (Fig.5.18A). The protective effect of oleate against palmitate-induced cell loss was further confirmed by the MTT assay (Fig.5.18 B).

It has been shown previously that FB1 pre-treatment partially prevented the palmitate-induced CD11b and CD36 expression in U937 monocytes; therefore, experiments were also carried out to test whether FB1 can protect the

palmitate-induced cell loss. As shown in Figure 5.19 A, cells incubated with 50μM FB1 alone did not significantly affect cell viability (p>0.05). However, the loss in cell viability caused by 300μM palmitate was not prevented by pre-incubation with 50μM FB1 measured by flow cytometric analysis with PI staining (p>0.05). In contrast, the cell viability measured by MTT assay showed a slight but significant increase in cell metabolic activity incubated with 50μM FB1 and 300μM palmitate compared to palmitate treatment alone (Fig 5.19 B).

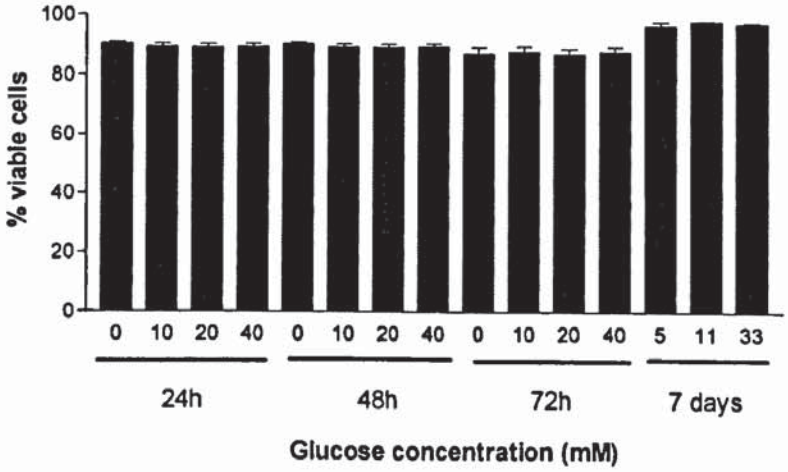

Figure 5.17 Effect of glucose on U937 monocyte viability. U937 cells (10^5/ml) were incubated with increasing concentrations glucose for up to 7 days. Cell viability was measured by flow cytometry based on light scatter properties. Data are mean±SEM from 3 independent experiments performed in triplicate.

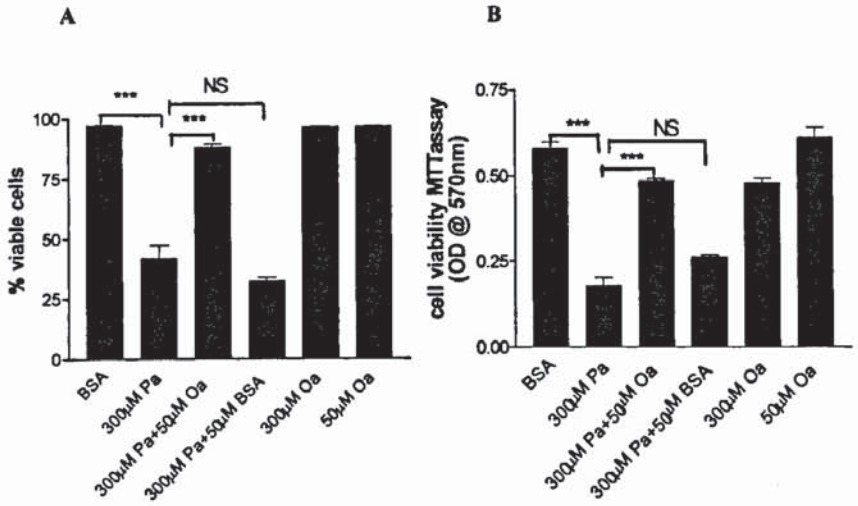

Figure 5.18 Effect of palmitate and oleate on U937 monocyte viability. U937 cells (10^5/ml) were incubated with 300µM palmitate, 300µM palmitate plus 50µM oleate, oleate (50µM and 300µM) for 24h at 37°C. Cell viability was measured by flow cytometric analysis with PI staining (A) and MTT assay (B). Data are mean±SEM from 3 independent experiments performed in triplicate. ***p<0.001, NS: non significant.

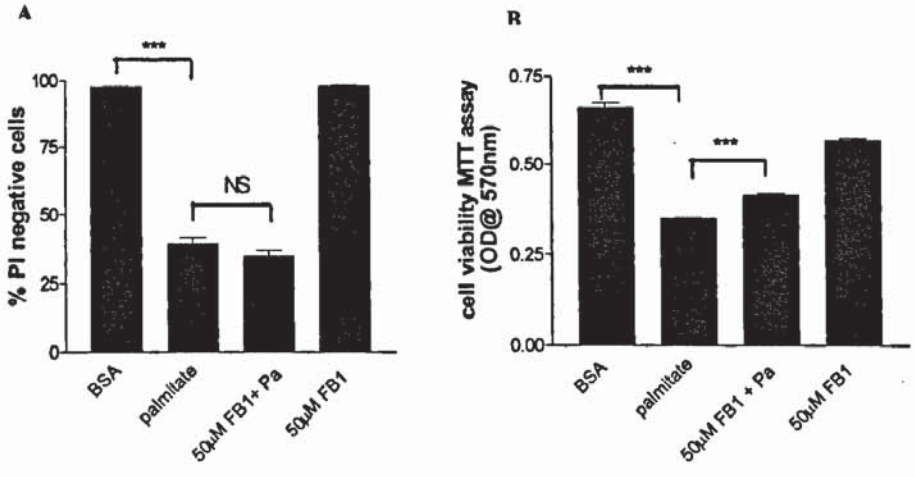

Figure 5.19 Effect of fumonisin B1 (FB1) on palmitate-treated U937 monocyte viability. U937 cells (10^5/ml) were pre-incubated with 50µM FB1 for 1h and then further co-incubated with 300µM palmitate for 24h at 37°C. Cell viability was measured by flow cytometric analysis with PI staining (A) and MTT assay (B). Data are mean±SEM from 3 independent experiments performed in triplicate. ***p<0.001, NS: non significant.

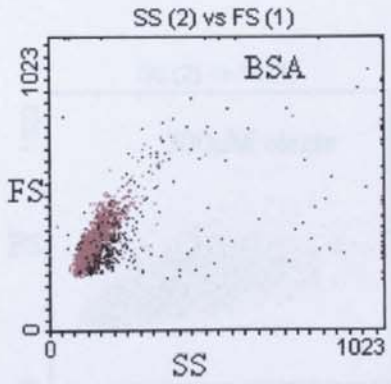
SS (2) vs FS (1)
BSA
FS
SS
0
1023

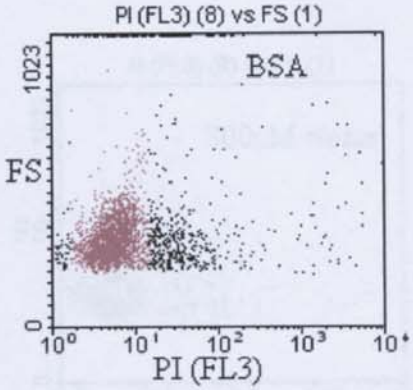
PI (FL3) (8) vs FS (1)
BSA
FS
PI (FL3)
0
1023
10^0
10^1
10^2
10^3
10^4

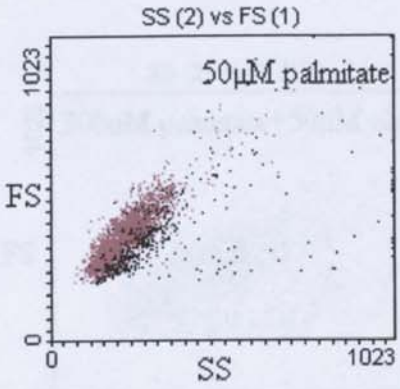
SS (2) vs FS (1)
50µM palmitate
FS
SS
0
1023

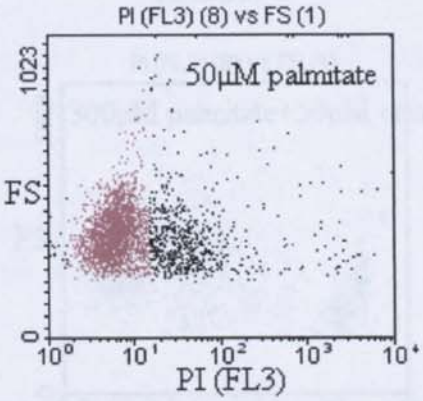
PI (FL3) (8) vs FS (1)
50µM palmitate
FS
PI (FL3)
0
1023
10^0
10^1
10^2
10^3
10^4

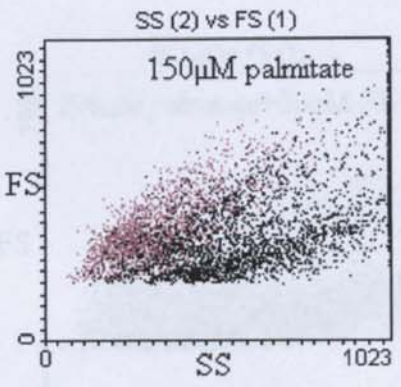
SS (2) vs FS (1)
150µM palmitate
FS
SS
0
1023

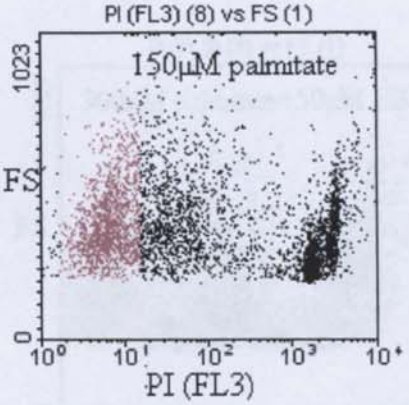
PI (FL3) (8) vs FS (1)
150µM palmitate
FS
PI (FL3)
0
1023
10^0
10^1
10^2
10^3
10^4

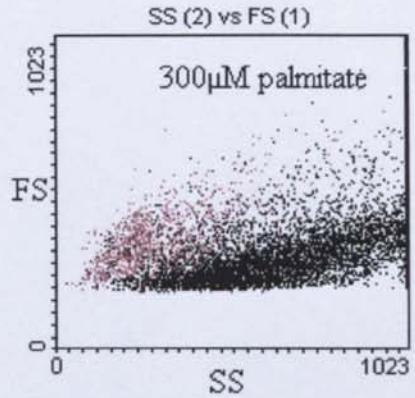
SS (2) vs FS (1)
300µM palmitate
FS
SS
0
1023

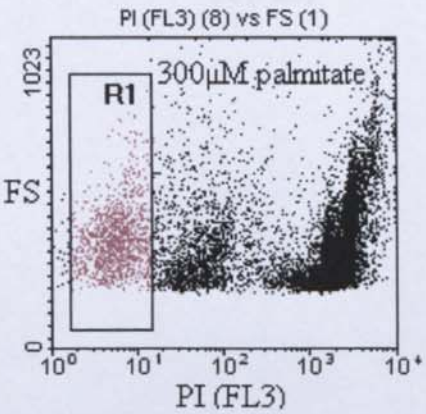
PI (FL3) (8) vs FS (1)
R1
300µM palmitate
FS
PI (FL3)
0
1023
10^0
10^1
10^2
10^3
10^4

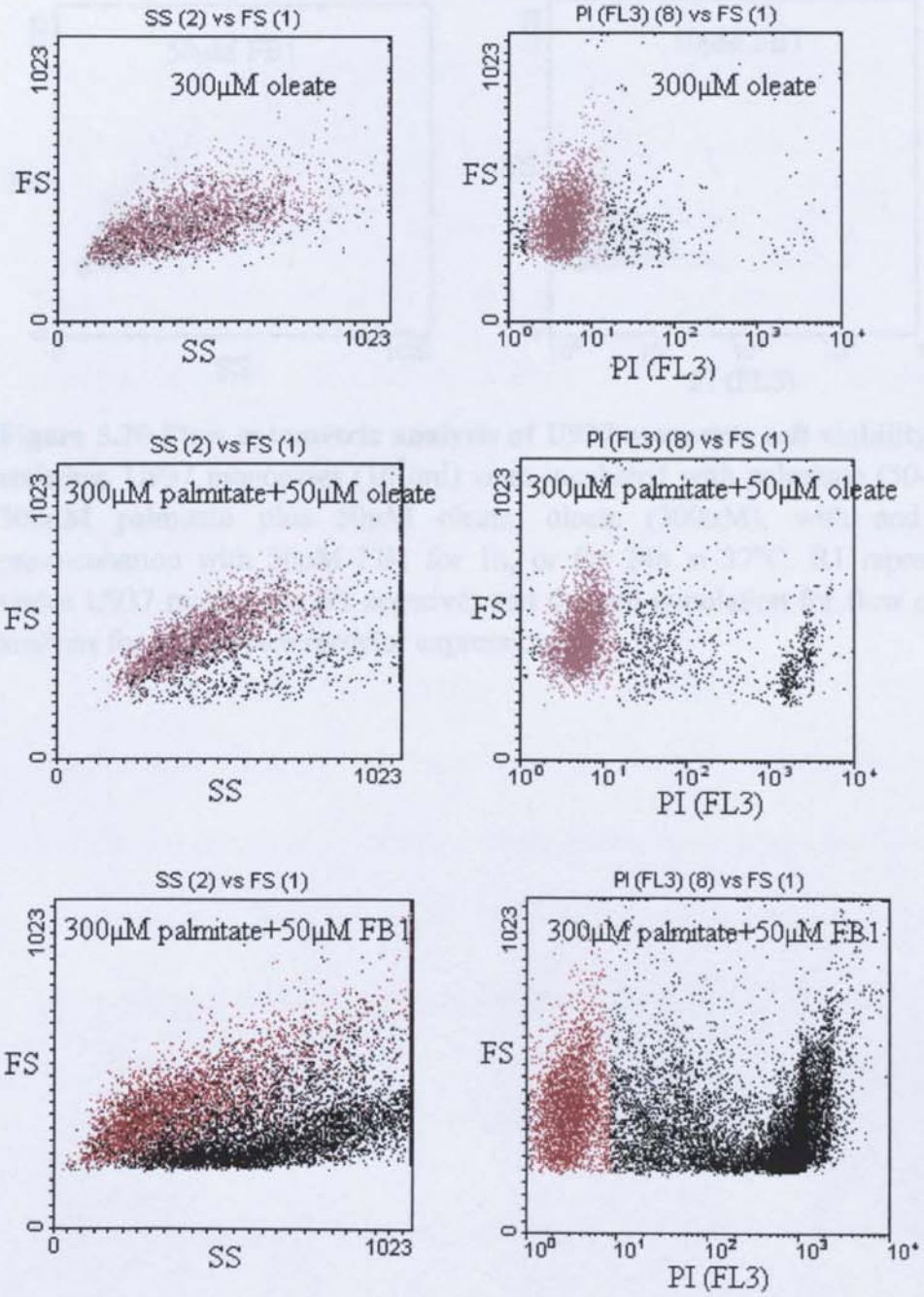
SS (2) vs FS (1)
300μM oleate
FS
SS
0
1023
PI (FL3) (8) vs FS (1)
300μM oleate
PI (FL3)
SS (2) vs FS (1)
300μM palmitate+50μM oleate
PI (FL3) (8) vs FS (1)
300μM palmitate+50μM oleate
SS (2) vs FS (1)
300μM palmitate+50μM FB1
PI (FL3) (8) vs FS (1)
300μM palmitate+50μM FB1

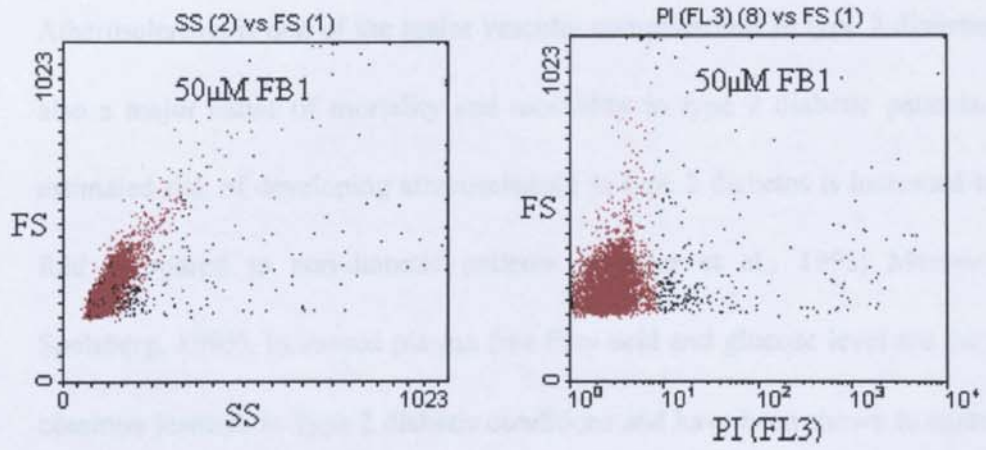

Figure 5.20 Flow cytometric analysis of U937 monocyte cell viability with PI staining. U937 monocytes (10^5/ml) were incubated with palmitate (50-300μM), 300μM palmitate plus 50μM oleate, oleate (300μM), with and without pre-incubation with 50μM FB1 for 1h, or for 24h at 37°C. R1 represents the viable U937 monocytes (PI negative) and the cell population for flow cytometry analysis for cell surface receptor expressions.

5.5 Discussion

Atherosclerosis is one of the major vascular complications in type 2 diabetes and also a major cause of mortality and morbidity in type 2 diabetic patients. The estimated risk of developing atherosclerosis in type 2 diabetes is increased to 2-5 fold compared to non-diabetic patients (Stamler et al., 1993; Manson and Spelsberg, 1996). Increased plasma free fatty acid and glucose level are the most common features in Type 2 diabetic conditions and have been shown to contribute to the development of insulin resistance, a pathological condition contributing to the development of type 2 diabetes, through disrupting post-receptor insulin signal transduction. However, little is known about the molecular mechanisms underlying the association between type 2 diabetic conditions and excess atherogenesis. Therefore, the present study was carried out to examine the effect of increased glucose and free fatty acids on monocyte phenotype and the adhesion of monocytes to endothelial cells. The potential role of ceramide in mediating palmitate-induced effects on monocytes was also investigated.

Monocyte phenotype

Monocyte phenotype was determined in viable cells which are PI negative and the cell surface expressions of CD11b, CD36 and CD206 were measured by flow cytometry. CD11b is the most abundant α-chain of integrins (Springer et al., 1979), highly expressed on activated monocytes and mediates firm adhesion to endothelial cells (Gahmberg et al., 1997). Therefore, the expression of CD11b can

be considered as a monocyte activation marker. CD36 is a multifunctional receptor and responsible for macrophage uptake of different materials such as ox-LDL, free fatty acids, and apoptotic cells (van Berkel et al., 2005). It is also a marker for macrophages since there are very low levels of CD36 expression in monocytes while higher level are observed in macrophages (Greenwalt et al., 1992). CD206 is the most commonly used monocyte/ macrophage differentiation marker and was therefore also included to investigate whether FFAs promote differentiation of monocytes into macrophages, which may ultimately become foam cells.

The data presented in this chapter show that palmitate, one of the most prominent saturated free fatty acids in human plasma, induces a significant increase in CD11b expression in U937 monocytes in a concentration dependent manner whereas glucose does not exert any effect on CD11b expression. The highest palmitate concentration (300μM) also causes a significant increase in CD36 expression. Increased expression of CD11b in monocytes has been mostly reported in short term stimulation, for example with LPS and CRP within 30min by transporting CD11b from the intracellular pools to the cell membrane (Woollard et al., 2002). However, in the present study, there was no effect of palmitate on CD11b expression in the short term stimulation using primary monocytes and the effect of palmitate on monocyte CD11b expression was

observed after 24h incubation. This suggests that palmitate-induced CD11b expression involves protein synthesis rather than protein trafficking. Indeed, a previous study showed that 48h treatment with a mixture of free fatty acids caused an increase in CD11b expression in THP-1 cells, associated with an increase in CD11b mRNA (Zhang et al., 2006). Consistent with the increased CD11b expression in U937 monocytes, a significant increase in expression of the mannose receptor (CD206) was also observed after palmitate treatment in U937 monocytes, indicating that palmitate promotes monocyte differentiation. This could contribute to the up-regulation of CD11b and CD36 expression. It has been reported that increased CD36 protein could also be a response to defective insulin signalling in macrophages (Liang et al., 2004). Uptake of ox-LDL induces CD36 expression through activating the transcription factor, peroxisome proliferator activated receptor-γ (PPAR-γ) (Nagy et al., 1998). Therefore, it is possible that ceramide-mediated palmitate-induced CD36 expression can be achieved through activation of PPAR-γ.

In contrast to U937 monocytes, there was no significant effect of palmitate on CD11b expression in primary monocytes from a mononuclear cell population, but there was a trend to reduce CD11b. There are two possible reasons for lack of statistical significance. Firstly, there were large variations in CD11b expression in monocytes from different individuals in response to palmitate. Secondly, the

expression of CD11b might be affected by the fatty acids levels associated with cell membrane phospholipids and can be affected by individual diets. Further studies are needed to clarify this issue. In addition, the proportion of monocytes in isolated MNC in the present study showed less than 20% of total cells which could not provide sufficient cells for performing adhesion assay. Due to this reason, MNC were used to investigate the effect of FFA on vascular adhesion. Also, it is possible that there may be cross-talk between cell types in MNC after treatment with pathophysiological concentrations of FFA, which could contribute to the different effects of FFA on primary monocytes and the cell lines.

As one of the major mono-unsaturated free fatty acids in human plasma, the effect of oleate on monocyte CD11b and CD36 expression was also investigated. In contrast to palmitate, oleate alone does not affect CD11b and CD36 expression in U937 monocytes. Furthermore, co-incubation of oleate with palmitate almost completely prevents the palmitate-induced increase in CD11b and CD36 expression, indicating that there is an interaction between unsaturated free fatty acids and saturated free fatty acids. Indeed, it has been reported that the cell plasma free fatty acid composition can be influenced by monounsaturated fatty acids such as oleate compared to polyunsaturated fatty acids through channelling the metabolic pathway to the synthesis of TAG inside the cells (Carluccio et al., 1999). More discussion regarding oleate and palmitate interactions is presented

later in the 'palmitate-induced toxicity' section.

Taken together, these data using U937 monocytes suggest that (1) the saturated free fatty acid palmitate is more potent to induce CD11b expression whereas the unsaturated free fatty acid oleate does not; (2) the unsaturated free fatty acid oleate can antagonise the effect of the saturated free fatty acid palmitate on CD11b expression.

Concerning the molecular mechanisms of palmitate-induced CD11b and CD36 expression, the data demonstrates that *de novo* ceramide synthesis is involved in the increased palmitate-induced CD11b and CD36 expression using the ceramide synthesis inhibitor fumonisin B1. Ceramide is one of the intermediate metabolites derived from palmitate and has been implicated in the development of insulin resistance in muscle cells (Hajduch et al., 2001). However, further studies are required to measure ceramide generation to be able to establish a causal role of ceramide in mediating palmitate-induced CD11b and CD36 expression. It has been reported that free fatty acid-induced CD11b expression was associated with ROS generation in human monocytes (Zhang et al., 2006). However, in the present study, the intracellular ROS formation measured by DCF-DA was not affected by 150μM and 300μM palmitate, although there was a significant increase in ROS generation in cells treated with 50μM palmitate. These data

suggest that the alterations in palmitate-induced CD11b and CD36 expression in U937 monocytes are associated with generation of ceramide rather than intracellular ROS.

The postulated role of sphingolipid metabolism in atherosclerosis is well supported by *in vivo* animal models. Park et al. (2004) reported that inhibition of sphingolipid synthesis caused a decrease in β-VLDL and LDL cholesterol, an increase in HDL cholesterol, and a reduction in atherosclerotic lesions in apolipoprotein E-knockout mice treated with the serine palmitoyltransferase (SPT) inhibitor myriocin. Similarly, Hojjati et al. (2005) also reported a significant decrease in atherosclerotic lesion areas in apoE-deficient mice after myriocin treatment. Further analysis of palmitate metabolites is required to determine whether the effect of palmitate on CD11b and CD36 expression is due to changes in sphingolipid synthesis.

Monocyte adhesion to endothelium

Under normal physiological conditions, the interaction of monocytes with endothelial cells is a dynamic and reversible process. However, under pathophysiological conditions such as diabetes, there is increased monocyte adhesion to endothelium (Hoogerbrugge et al., 1996) and to the aorta in animal models (Otsuka et al., 2005). Therefore, the functional consequence of

palmitate-induced changes in CD11b expression was further investigated as monocyte adhesion to the endothelium. The data shows that 300μM palmitate reduces viable mononuclear cell adhesion to ICAM-1 coated plates, but it does not exert a significant effect on viable U937 monocyte adhesion to ICAM-1 coated plates. Blocking PMA-activated U937 monocytes by IgG

Initial experiments were carried out using EAhy926 endothelial cells as a cell model to investigate the effect of palmitate on monocyte-endothelial interactions. The adhesion of 300μM palmitate-treated U937 monocytes to resting EAhy926 endothelial cells shows a significant reduction compared to BSA controls. This is also associated with a 50% reduction in PECAM-1 (CD31) expression on monocytes treated with palmitate. CD31 has been reported to mediate the homotypic cell adhesion such as neutrophil aggregation in response to inflammatory stimuli such as LPS. However, CD31 expression in EAhy926 cells is absent under unstimulated conditions, therefore, it is unlikely that the reduction in palmitate-induced U937 monocyte adhesion to EAhy 926 endothelium is due to the reduction in CD31 expression on monocytes. Furthermore, characterisation of adhesion molecules shows that around 40% of EAhy926 cells express VCAM-1, however, ICAM-1 and E-selectin receptors are almost absent. Therefore, the adhesion between U937 monocytes and EAhy926 endothelial cells is likely to be mediated mainly by VCAM-1. Further study is needed to determine if the

expression of VLA-4, a ligand expressed on monocyte which binds to endothelial VCAM-1, is altered by fatty acid exposure.

Also, in contrast to the literature which reports that expression of those adhesion molecules can be up-regulated in endothelial cells by LPS or TNF-α stimulation for 6h or 24h, EAhy926 cells do not respond to LPS after stimulation for 24h. CD14 is important for mediating LPS stimulation. On EAhy926 endothelial cells, only approximately 6% of cells express CD14. Therefore, the unresponsiveness of the EAhy926 cells to LPS stimulation might be due to the low level of CD14 expression in these cells.

To investigate the CD11b-mediated monocyte adhesion to ICAM-1, a method of using anti-Fc monoclonal antibody to immobilise human recombinant ICAM-1-Fc to 96-well plate to mimic the endothelial cell surface ICAM-1 expression for evaluating the CD11b-mediated monocyte adhesion was developed. The orientation of ICAM-1 was verified by a modified ELISA as shown in Figure 2.8 by competition for immobilisation with 300μg/ml human IgG which causes an almost complete loss in ICAM-1-Fc binding to 1μg/well anti-Fc antibody. In addition, the data demonstrates that the adhesion of PMA-activated U937 monocyte to ICAM-1 was nearly three-fold higher than resting cells, whereas there is no significant difference in PMA-activated U937 monocytes binding to

BSA and human IgG coated plates. PMA is a potent inducer for CD11b and has been shown to increase surface CD11b expression after long term stimulation in U937 monocytes (Deszo et al., 2000). These data, using PMA as a positive control have demonstrated the suitability of this method to detect the integrin CD11b-mediated adhesion to ICAM-1 and therefore this approach was used to investigate the effect of palmitate on U937 monocyte adhesion. However, the adhesion of either palmitate- or oleate-treated U937 monocytes adhesion to ICAM-1 is not significantly different from BSA-treated control cells. There is a previous study which showed that the plate-coated with ICAM-1 was able to detect the increased CD11b avidity but not conformational change (affinity) (Konstandin et al., 2006). Therefore, the dissociations between the observed effects of palmitate-induced increase in CD11b expression and absence of increasing monocyte adhesion to ICAM-1 could be due to an increase in the low affinity cell surface CD11b on U937 monocytes after palmitate treatment. Further study is required to confirm this using a specific antibody that can detect an active form of CD11b or to examine the adhesion of U937 monocytes after palmitate treatment to ICAM-1 coated plate in the presence of a chemoattractant stimuli such as monocyte chemoattractant protein -1 (MCP-1) to activate the CD11b. The adhesion of MNC to ICAM-1 is also shown to be reduced from 38% in BSA controls and 22% in 300μM palmitate-treated cells after 24h treatment. This corresponds to a significant reduction in total MNC CD11b MdX from 0.67a.u in

BSA controls and 0.42a.u in palmitate-treated cells.

Palmitate-induced toxicity

Lipotoxicity is referred to as cell dysfunction and/or cell death due to accumulation of excessive fatty acids in non-adipose tissues such as β-pancreatic cells, skeletal muscles, and cardiomyocytes. Previous studies in various cell types suggest cell apoptosis as a major feature of cytotoxicity induced by saturated fatty acids (e.g. palmitate) (Okuyama et al., 2003; Miller et al., 2005; Cacicedo et al., 2005). The palmitate concentration used here is 50-300μM, which corresponds to ~30% of palmitate in total plasma free fatty acids concentrations in human plasma. A significant toxic effect was observed in U937 monocytes when incubated with palmitate concentrations over 150μM after 24h measured by the MTT assay and PI staining. A similar but less toxic effect was observed in mononuclear cells after incubating with the same concentrations of palmitate for 24h. .

One possible mechanism for palmitate-induced toxicity is the generation of ROS (Listenberger et al, 2001). In the present study, the measurements of intracellular ROS generation using DCF-DA in U937 monocytes showed a trend in decreasing ROS generation with increasing concentration of palmitate. These results are in accordance with the studies carried out by Hickson-Bick et al (2002) who reported a palmitate-mediated decrease in ROS generation measured by both DCFH-DA

and DHE. However, an increase in intracellular ROS induced by palmitate was reported in Chinese hamster ovary (CHO) cells (Listenberger et al., 2001), cultured retinal pericytes (Cacicedo et al., 2005) and measured by DCFH-DA. ROS production by mitochondria in cells requires high membrane potentials; therefore, the opposite observations between the present study and others could be explained by the differences in cells maintaining their membrane potential in response to palmitate.

Another line of evidence suggests that altered fatty acid metabolism is associated with the toxicity induced by palmitate. An increase in palmitate mitochondrial β-oxidation caused a significant decrease in apoptosis, while inhibition of this pathway caused the opposite effect in rat myocytes (Miller et al., 2005). Therefore, the toxicity caused by palmitate could be due to the incomplete β-oxidation and accumulation of alternative intermediate metabolites in cells. One potential candidate is ceramide which has been reported to mediate palmitate-induced apoptosis in pericytes (Cacicedo et al., 2005) and rat cardiac myocytes (Hickson-Bick et al., 2002). However, pre-treating U937 monocytes with FB1, a potent ceramide *de novo* generation inhibitor, does not significantly prevent the palmitate-induced cell loss in U937 monocytes, indicating that ceramide may not be the major cause of palmitate-induced toxicity in this cell type. In contrast, co-incubating 50μM oleate with 300μM palmitate almost

completely protected the cell viability loss caused by palmitate. This beneficial effect of oleate against palmitate-induced toxicity was also reported in CHO cells and cardiac myocytes (Listenberger et al., 2001; Miller et al., 2005).

There are several potential mechanisms proposed for the protective effect of oleate against palmitate-induced toxicity. One of these is that unsaturated fatty acids can prevent the loss of cell membrane fluidity caused by saturated fatty acids and therefore protect the cell from dysfunction or death (Vries et al., 1997). On the other hand, it has been also proposed by Listenberger et al. (2003) that oleate can channel palmitate metabolism to the formation of triglycerides and therefore away from pathways leading to apoptosis such as via diacylglycerol (DAG) formation. They observed an accumulation of triglyceride (TAG) in cells treated with oleate alone or after co-incubation with oleate and palmitate, but not palmitate. This accumulation of TAG is associated with an increased fatty acid desaturase activity, and the presence of oleate in cells promoted conversion of exogenous palmitate to triglyceride stores. They also demonstrated that impaired triglyceride synthesis in cells can lead to lipotoxicity from both oleate and palmitate. However, this has not been investigated in monocytes.

Several epidemiological studies have shown an increase in CD11b or/and CD36 expression on circulating monocytes in obesity, insulin resistance or type 2

diabetic patients (Boschmann et al., 2005; Sampson et al, 2003; Zhang et al., 2005) compared to lean healthy subjects. In the present study, two major diabetic-related cardiovascular risk factors glucose and free fatty acids were investigated for their effect on monocyte phenotype change and adhesion to endothelium. The data demonstrate that glucose does not affect CD11b expression in U937 monocytes whereas the saturated free fatty acid palmitate increases expression of CD11b and CD36. Inhibition of ceramide *de novo* synthesis prevents the increase in CD11b and CD36 induced by palmitate. These data provide evidence of an association between type 2 diabetes and/or insulin resistance with vascular dysfunction.

Chapter 6

In vivo study of palmitate effects on insulin sensitivity and vascular adhesion in Wistar rats

6.1 Preface

This chapter describes an investigation of the effect of orally-dosed palmitate on insulin sensitivity using Wistar rats as an *in vivo* model. Meanwhile, the effect of palmitate on vascular function was investigated by measuring *ex vivo* adhesion of U937 monocytes to rat thoracic aorta excised from rats treated with and without palmitate.

6.2 Introduction

Type 2 diabetes is an independent risk factor for cardiovascular disease. More than 3 out of 4 diabetic patients die of causes related to atherosclerosis, in most cases (75%) because of coronary artery disease (Haffner et al., 1998). The estimated risk for development of atherosclerosis in patients with type 2 diabetes is increased by 4 or 5 times compared with insulin sensitive subjects (Reaven and Laws, 1999). As an underlying mechanism for development of type 2 diabetes, insulin resistance has been strongly implicated in the pathogenesis of atherosclerosis.

The role of increased plasma free fatty acid level in inducing insulin resistance has been established in both *in vivo* and *in vitro* studies. For example, studies investigating intravenous infusion of triglyceride emulsions/heparin to healthy human subjects have demonstrated that the increased plasma free fatty acids within 6h can induce whole body and skeletal muscle insulin resistance (Dresner

et al., 1999; Roden et al., 1996), indicating a causal relationship between increased plasma free fatty acid level and insulin resistance. Additionally, *in vitro* studies identified that palmitate, one of the most abundant saturated free fatty acids in plasma, was the principal free fatty acid contributing to the development of insulin resistance in cultured skeletal muscle cells and adipocytes (Dobrzyn et al., 2003; Epps-Fung et al., 1997). However, very little information is available about the specific effect of palmitate on insulin sensitivity *in vivo*.

Monocyte adhesion to the endothelium is one of the earliest and critical events contributing to the development of atherosclerosis. Monocyte adhesion is mediated through several adhesion molecules on endothelial cells and receptors on monocytes. CD11b is the most abundant α subunit of β_2 integrin expressed in monocytes and mainly responsible for firm adhesion of monocytes to the endothelium through interactions with intercellular adhesion molecule-1 (ICAM-1). The association of increased free fatty acids with monocyte activation and monocyte-endothelial interactions has been implicated in several studies; for example, the surface CD11b expression on monocytes from obese people has been reported to be higher than on monocytes from healthy people and is associated with an increase in adipose tissue lipolysis (Boschmann et al., 2005). One *in vitro* study where monocytes were co-incubated with increasing concentrations of free fatty acid mixture showed a CD11b-mediated increase in human monocyte

adhesion to endothelium, further supporting a role of free fatty acids in the development of atherosclerosis (Zhang et al., 2006).

Taken together, data from existing research suggests that increased plasma free fatty acid concentration is a major contributor to insulin resistance and also a hallmark of insulin resistant conditions. Although there is some evidence showing that the elevated free fatty acid level increases the adhesion of monocytes to endothelial cells, there is very little information on specific plasma fatty acids such as palmitate and/or oleate on *in vivo* insulin sensitivity and monocyte-endothelial interactions. Data from the previous work in this thesis supports a mechanistic role for palmitate in the induction of insulin resistance and acceleration of atherosclerosis, as illustrated by 300μM palmitate causing impaired insulin sensitivity in THP-1 monocytes and L6 skeletal muscles, and an increase in CD11b expression in U937 monocytes. Therefore, to extend these in vitro observations to *in vivo* conditions, the present studies were carried out to test the effect of palmitate on insulin sensitivity and monocyte adhesion to the rat aorta.

6.3 Materials and Methods

6.3.1 Animals

Male Wistar (Han) rats aged 21 days, weighed 150~280g were used in the study.

Animals were housed in polyethylene cages (2 or 3 animals per cage) and had access to a standard maintenance rat diet (Special Diets Service; Essex, UK) and tap water *ad libitum*. The environment was controlled in terms of light (12:12-h light-dark cycle starting at 8:00am) and room temperature (20-23°C). All experiments were performed in compliance with recommendations of the guidelines of the care and use of laboratory animals issued by Aston University and the study was approved by the British Home Office.

6.3.2 Experimental design

The overall experimental design is shown in Figure 6.1. In brief, Wistar male rats were fasted overnight for 12h and initially ascribed to different treatments in a random order. Each treatment group comprised two weighed matched rats. Rats were orally gavaged with water as controls, 0.5ml 120mM palmitate alone, or 0.5ml 120mM palmitate plus 20mM oleate, and 0.5ml 20mM oleate alone. Rats were kept in separate cages with water freely available during the 6h experimentation period. After that, an insulin sensitivity test or glucose tolerance test was carried out. Tail blood samples (50µl) were collected at the beginning and the end of the 6h treatment. All the experimental tests were repeated on three independent occasions with at least three days rest period between tests.

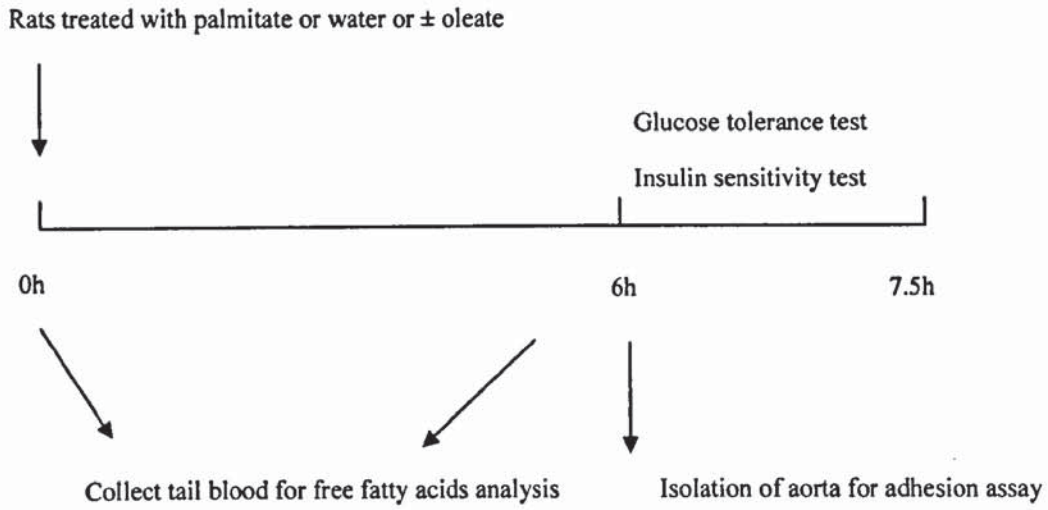

Figure 6.1 Overview of the experimental design.

6.3.3 Plasma free fatty acids (FFA) and triacylglyceride (TAG) assay

To test whether palmitate treatment can increase plasma free fatty acid levels, tail blood samples (50µl) were collected into eppendorf tubes pre-coated with 0.4% citric acid at 0h and 6h. Blood samples were centrifuged at 13,000×g for 5min and the plasma was stored at -80°C. FFA levels in the plasma were determined by a Wako NEFA kit (Alpha Laboratories Ltd, Hampshire, UK) described in Section 5.3.7 and TAG levels were measured by a TAG assay kit from Randox (Co. Antrim, UK).

Both assays apply an *in vitro* colorimetric method for the quantification of FFA and TAG in serum or plasma. The intensity of the formation of a red pigment (quinoneimine dye) is proportional to the concentration of FFA or TAG in the sample and absorbance intensities were read at 550nm.

The principle for TAG assay is as follows:

$$\text{Triglyceride} + H_2O \xrightarrow{\text{Lipase}} \text{Glycerol} + 3\ \text{Fatty Acids}$$

$$\text{Glycerol} + \text{ATP} \xrightarrow{\text{Glycerokinase}} \text{Glycerol-3-P} + \text{ADP}$$

$$\text{Glycerol-3-P} + O_2 \xrightarrow{\text{Glycerol-3-P oxidase}} \text{Dihydroxyacetone-P} + H_2O_2$$

$$2H_2O_2 + \text{4-Aminophenazone} + \text{N, N-Diethyl-m-Toluidine} \xrightarrow{\text{Peroxidase}} \text{Quinoneimine dye} + 4H_2O$$

6.3.4 Oral glucose tolerance test (OGTT)

The OGTT was carried out in Wistar rats after administration of 0.5ml palmitate (120mm) or oleate (10mM) or palmitate (120mM) plus oleate (10mM) for 6h. Rats were orally gavaged with a glucose solution (40% w/v) at a dose of 2g/kg body weight. Tail blood glucose levels were determined at 0, 15, 30, 60, and 90min using a glucose analyzer (Optimum Plus, UK) and areas under the plasma glucose concentration curves were calculated.

6.3.5 Insulin sensitivity test

The insulin sensitivity test was conducted in Wistar rats after administration of 0.5ml palmitate (120mm) or water (control) for 6h. The Wistar rats were initially given a 2g/kg glucose solution (40% w/v) orally. After 10min, a bolus of

short-acting recombinant human insulin (Actrapid, Novo Nordisk Limited, UK) was injected intraperitoneal at 0.1U/kg body weight. Tail blood glucose concentrations were determined at 0, 15, 30, 60, and 90min after the glucose administration.

6.3.6 Preparation of rat aorta

The thoracic aorta (30mm) was removed from Wistar Han rats (230-280g) after administration of 0.5ml palmitate (120mm) or water (control) for 6h and placed in cold, oxygenated PBS (pH 7.4). Each piece of aorta was carefully opened longitudinally and cut into two segments (15mm) and placed in a 35-mm culture dish containing 2ml Hank's Buffered Salt Solution (HBSS) supplemented with 2mM Ca^{2+}, 2mM Mg^{2+}, and 20mM HEPES. The aortic segments were fixed to 35mm culture dishes using 25-gauge needles with the endothelial side up. Culture dishes containing aortic segments were placed on a rocking platform at room temperature for subsequent *ex vivo* monocyte adhesion assay.

6.3.7 *Ex vivo* monocyte adhesion to rat aorta

U937 monocytes (10^6/ml) were incubated with BSA as control and 300μM palmitate for 24h at 37°C. The monocytes were labelled with 10μg/ml BCECF-AM and re-suspended in HBSS at a density of 5×10^5/ml. The monocytes (3ml) were incubated with rat aortic segments for 30min at room temperature in a

moving chamber at 50rpm/min in the dark. After that, the unbound cells were removed by aspiration of the medium, and washed twice with 2ml HBSS for 2min. The bound cells from 6 different sites of the aorta were photographed under a Zeiss fluorescent microscope (Axioskop, excitation from a Mercury-arc lamp between 450-490nm with a filter that allows emission at 515nm) at a magnification of 4×. Figure 6.2 shows the adhesion of resting U937 and PMA-activated U937 monocytes to non-treated Wistar rat aorta to verify the method.

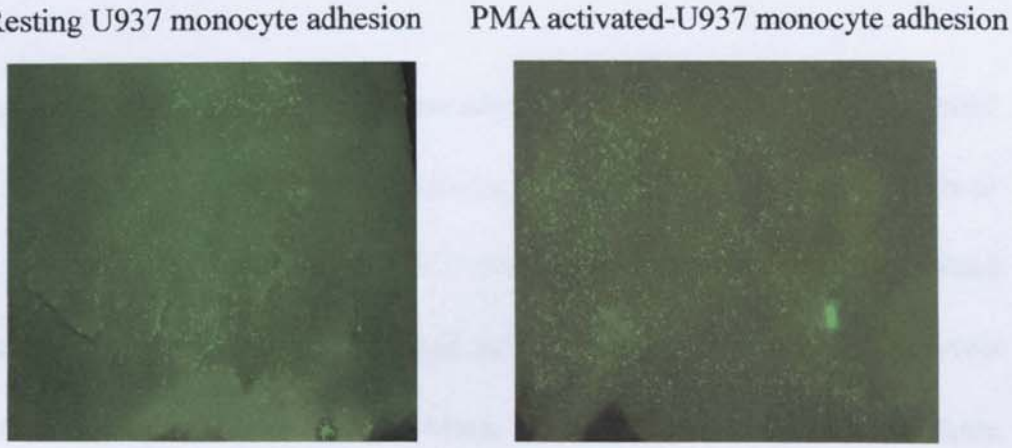

Figure 6.2 Resting and PMA-activated U937 monocyte adhesion to rat aorta. U937 cells (5×10^5/ml) were incubated with PBS or PMA (10^{-7}M) for 72h. U937 monocytes (5×10^5/ml) labelled with 10μg/ml BCECF-AM were incubated with aorta segments (15mm) at room temperature with gentle rotation for 30min. Unbound cells were washed away and bound cells were photographed under a fluorescence microscope at magnification 4×.

6.3.9 Statistical analysis

Data are expressed as mean ± SEM. The Student's unpaired t-test was used to test the differences between two groups and paired t-test was used for test the

differences between FFA and TAG levels before and after oral gavage. One-way ANOVA with Tukey-Kramer post hoc tests used to test the differences for more than 2 groups. A p value less than 0.05 was considered significant.

6.4 Results

6.4.1 Oral glucose tolerance test in untreated rats

To characterise the response to a glucose challenge in Wistar rats, the glucose tolerance test was carried out in two randomly selected Wistar rats after overnight starvation up to 18h.

As shown in Figure 6.3, after glucose administration, the glucose levels exhibited a typical biphasic profile. Plasma glucose rose rapidly from the fasting levels of 3.7mM and 4.7mM to peak levels of 11.5mM and 10.7mM at 15min and remained at this level until 30min (12.8mM and 10.8mM). Subsequently, the glucose levels declined to 9.5mM and 6.2mM at 60min and returned to the baseline by 90min (3.2mM and 5.6mM).

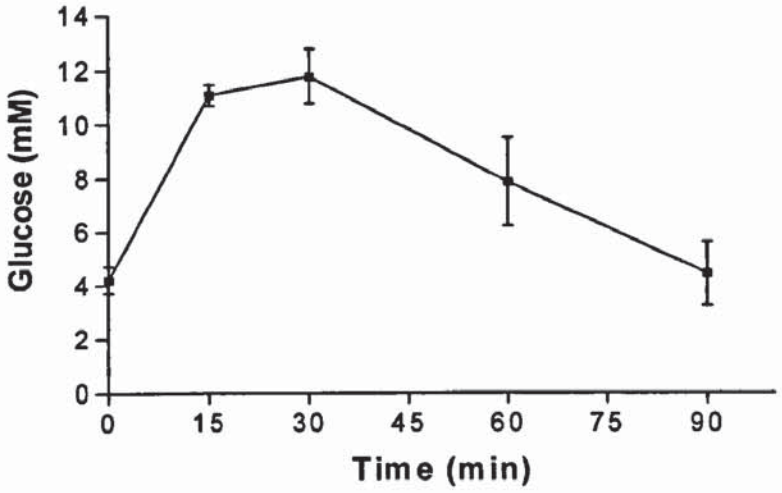

Figure 6.3 Glucose tolerance test on untreated rats. Wistar Han rats (~200g) were starved overnight up to 18h. A glucose tolerance test was carried out by orally giving each rat a glucose solution (40%, w/v) at 2g/kg body weight. The blood glucose levels were then measured at 0, 15, 30, 60 and 90min. Dada are mean±SEM. n=2.

6.4.2 Effect of palmitate on insulin sensitivity

In Chapter 3 and Chapter 4, both THP-1 monocytes and L6 skeletal muscle cells treated with 300μM palmitate for 6h showed a reduced response to insulin-stimulated glucose uptake compared to BSA controls. Therefore, the present studies were carried out to investigate the effect of palmitate on *in vivo* insulin sensitivity using Wistar rats.

Figure 6.4 A shows insulin sensitivity in rats treated with 0.5ml 120mM palmitate or 0.5ml water for 6h. The glucose levels were significantly higher in palmitate-treated rats than the controls after the glucose load for 15min (9.2mM ± 2.0 versus 6.6mM ± 1.2, n=6, $p<0.05$) and 30min (8.9mM ± 1.0 versus 7.5mM ±

0.9, n=6, $p<0.05$). The areas under curve were also calculated and shown in Figure 6.4 B. The areas under curve were arbitory unit of 243.1 ± 29.06 in palmitate-treated rats and 196.6 ± 19.78 in control rats. However, the different mean values in areas under the curves did not reach statistical significance ($p>0.05$).

A

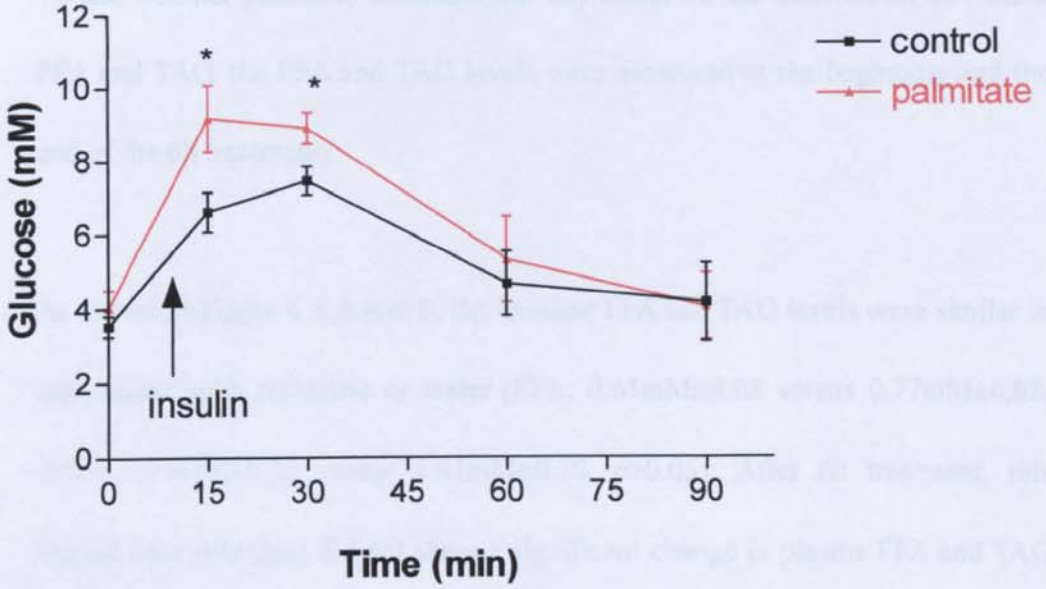

B

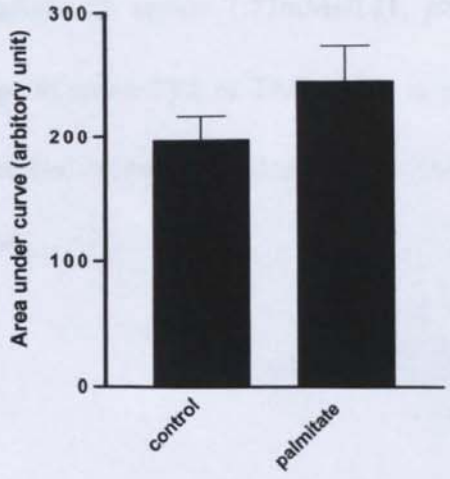

Figure 6.4 Insulin sensitivity test on rats treated with palmitate and water as controls. Wistar Han rats (~200g) were starved overnight for 12h and orally gavaged with 0.5ml 120mM palmitate or 0.5ml water as controls for 6h. An insulin sensitivity test was carried out at the end of 6h. Glucose was given orally to each rat at 2g/kg body weight as a 40% (w/v) glucose solution and insulin at 0.1U/kg was given by an intra-peritoneal injection 10min after glucose administration. Tail blood glucose levels were measured at 0, 15, 30, 60 and 90min after the glucose administration. A. Glucose levels. B. Area under the plasma glucose concentration time curve. Control group n=5, palmitate group n=5. *p<0.05 compared with control at 15min or 30min. Data are mean±SEM.

6.4.3 Effect of palmitate on plasma FFA and TAG concentrations.

To test whether palmitate treatment has any effect on the metabolism of plasma FFA and TAG, the FFA and TAG levels were measured at the beginning and the end of the 6h treatment.

As shown in Figure 6.5 A and B, the baseline FFA and TAG levels were similar in rats treated with palmitate or water (FFA: 0.65mM±0.08 versus 0.77mM±0.08; TAG: 1.77mM±0.21 versus 1.81mM±0.30, $p>0.05$). After 6h treatment, rats treated with palmitate did not show a significant change in plasma FFA and TAG levels compared to basal levels (FFA: 0.76mM±0.04 versus 0.65mM±0.08; TAG: 1.78mM±0.13 versus 1.77mM±0.21, $p>0.05$). Also, there was no significant change in either FFA or TAG levels in palmitate-treated rats and controls (FFA: 0.76mM±0.04 versus 0.81mM±0.10; TAG: 1.78mM±0.13 versus 1.99mM±0.29, $p>0.05$).

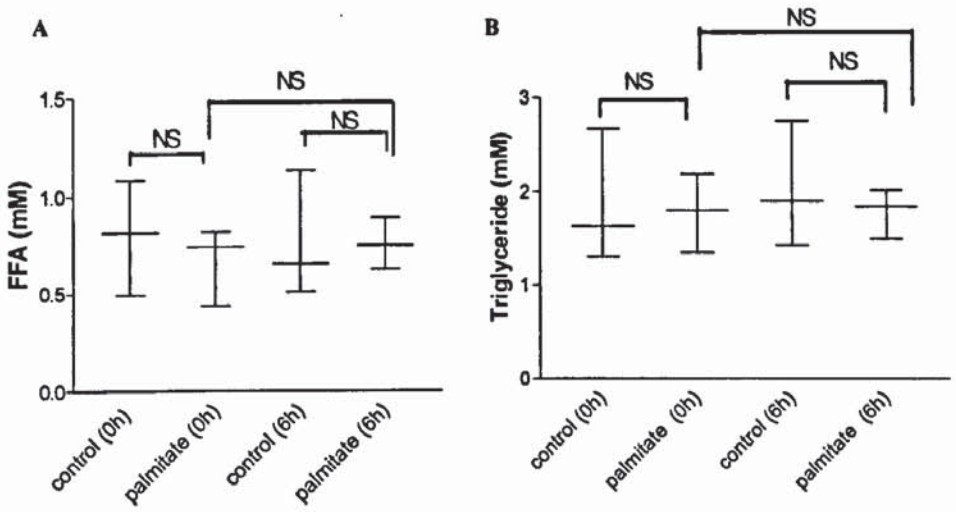

Figure 6.5 Effect of palmitate on plasma free fatty acids (FFA) (A) and Triacylglyceride (TAG) levels (B) in Wistar rats. Wistar Han rats (~200g) were starved overnight for 12h and then orally gavaged with 0.5ml 120mM palmitate or 0.5ml water as a control for 6h. Tail blood samples were collected at 0h and 6h and the plasma FFA and TAG levels were measured using a Wako kit and a Randox kit, respectively. For FFA measurement, control group n=5, palmitate group n=5. For TAG measurement, control group n=4, palmitate group n=3. NS: non significant. Data are mean±SEM.

6.4.4 Effect of oleate on palmitate-induced insulin resistance

It has been shown using *in vitro* cell culture models that 50μM oleate protects against 300μM palmitate-induced insulin resistance in THP-1 monocytes and L6 myotubes. Since *in vivo* it has been demonstrated that the palmitate treatment caused a temporary delay in glucose disposal at 15min and 30min in the insulin sensitivity test compared to controls, the effect of oleate on palmitate-induced insulin resistance was further investigated using the *in vivo* model to test the hypothesis that a small amount of oleate can be beneficial over palmitate-induced insulin resistance *in vivo*.

Wistar rats were treated with 0.5ml 120mM palmitate alone, 0.5 ml 20mM oleate alone as control, and 0.5ml 120mM palmitate plus 20mM oleate for 6h. The effect of fatty acids on glucose metabolism was measured by an oral glucose tolerance test. Consistent with the previous observations in insulin sensitivity tests (Figure 6.4 A), palmitate treatment again caused a temporary delay in glucose disposal at 60min. As shown in Figure 6.6 A, after 6h treatment, the glucose level at 60min was significantly higher in palmitate alone treated rats compared to oleate alone treated rats (8.1mM ± 0.5 versus 6.5mM ± 0.6, $p<0.01$). However, the overall glucose levels in rats treated with palmitate plus oleate did not show any significant difference from those treated with palmitate alone at each time point ($p>0.05$).

Figure 6.6 B shows the areas under the glucose curve calculated as an index of whole body glucose metabolism. There was a significant increase in the area under the curve values in palmitate-treated rats compared to oleate-treated rats (396.4 ± 30.2 versus 281.3 ± 38.6, $p<0.05$). The combination of oleate and palmitate did not affect the values of areas under the curve compared to palmitate alone (382.3 ±46.3 versus 396.4 ± 30.2, $p>0.05$).

A

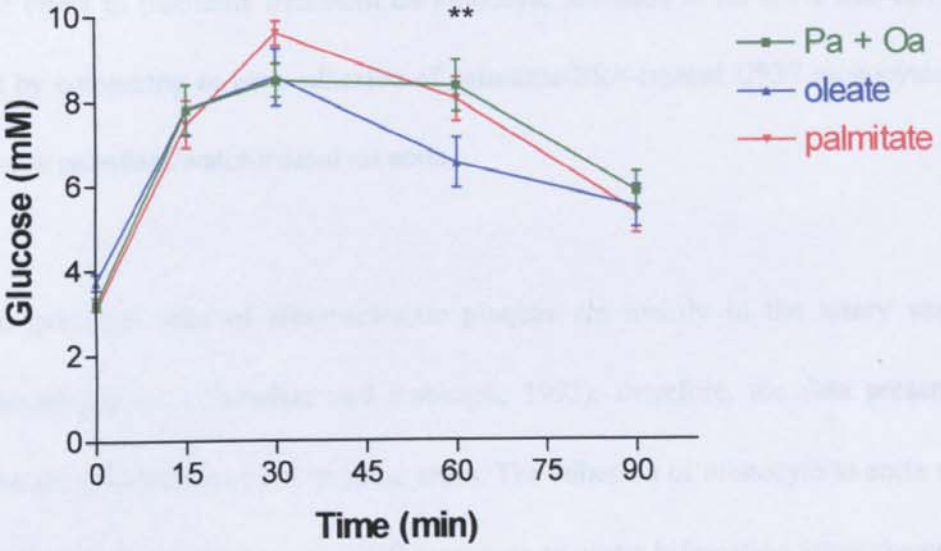

B

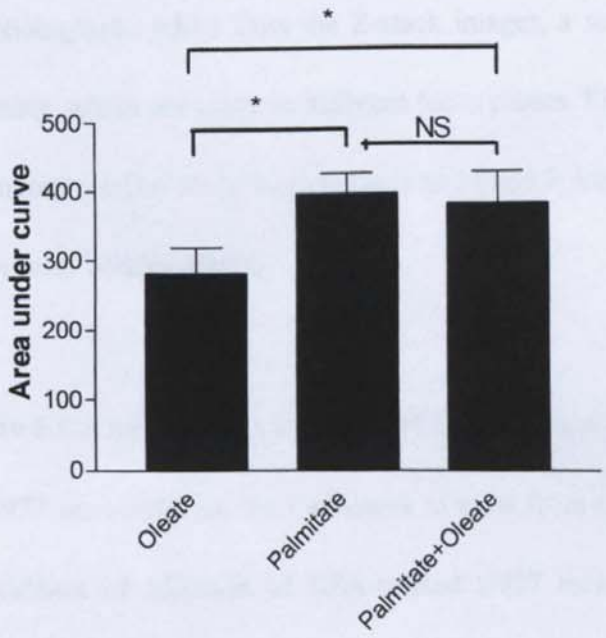

Figure 6.6 Glucose tolerance test on rats treated with palmitate alone, oleate alone, and palmitate plus oleate. Wistar Han rats (150~230g) were starved overnight for 12h and orally gavaged with 0.5ml 120mM palmitate, 0.5ml 20mM oleate, or 0.5ml 120mM palmitate plus 20mM/kg oleate for 6h. A glucose tolerance test was carried out after 6h. Glucose was given orally to each rat at 2g/kg body weight as a 40% (w/v) glucose solution. Tail blood glucose levels were measured at 0, 15, 30, 60 and 90min after the glucose administration. A. Glucose levels. B. Area under plasma glucose concentration time curve. Oleate group n=6, palmitate group n=6, palmitate+oleate group n=6. $^{**}p<0.01$ palmitate compared with oleate, $^{*}p<0.05$, NS: non significant. Data are mean±SEM.

6.4.5 Effect of palmitate on monocyte adhesion to aorta

The effect of palmitate treatment on monocyte adhesion to rat aorta was carried out by comparing *in vitro* adhesion of palmitate/BSA-treated U937 monocytes to *in vivo* palmitate/water-treated rat aorta.

The principal sites of atherosclerotic plaques are mainly in the artery vessel branching areas (Thubrikar and Robicsek, 1995); therefore, the data presented here are primarily focused on these areas. The adhesion of monocyte to aorta was verified as the attachment of U937 monocyte to aortic bifurcation areas shown in the photographs taken from the Z-stack images, a series of images of specimen scanning, which are taken in different focus planes. Figure 6.7 B and D shows the photographs taken from the top planes and Fig.6.7 A and C shows the photograhes taken from bottom planes.

Figure 6.8 A and B shows the effect of *in vitro* palmitate or BSA control treatment of U937 monocytes on their adhesion to aorta from rats treated with water. There is evidence of adhesion of BSA-treated U937 monocytes to aorta (Fig.6.8 A) whereas by comparison the adhesion of palmitate-treated U937 monocytes to aorta was increased (Fig.6.8 B). *In vivo* palmitate treatment of Wistar rats for 6h prior to sacrifice also caused a dramatic increase of U937 monocyte adhesion to aorta especially at the bifurcation edge areas as shown in Figure 6.8 C. However,

the combined *in vitro* treatment of monocytes and *in vivo* treatment of endothelium with palmitate seemed not to further enhance the cell adhesion (Fig.6.8 D).

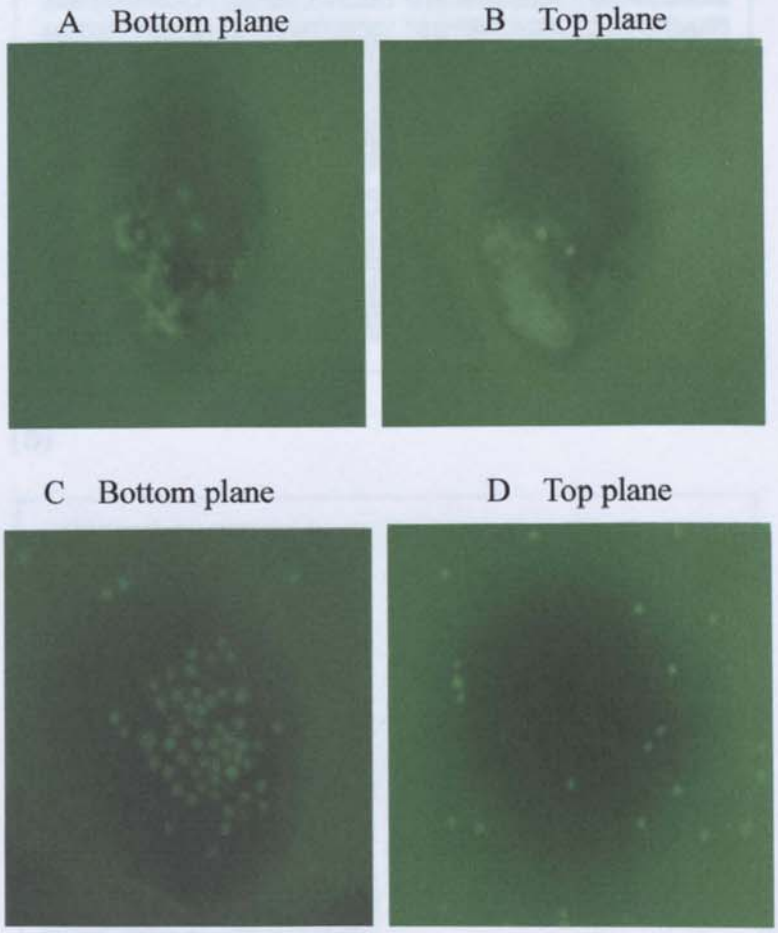

Figure 6.7 U937 monocytes adhesion to rat aorta. U937 monocytes (10^6/ml) were labelled with 10μg/ml BCECF-AM for 30min at room temperature in the dark. The thoracic aorta was carefully isolated and fixed by fine needles in 35mm Petri dishes. The labelled monocytes ($5x10^5$/ml) were added to aorta strips for 30min in the dark at a rotation speed of 50rpm/min.Unbound monocytes were washed away and cell adhesion to aorta was visualised under a fluorescent microscope at magnification of 10x. Photographs were taken by Z-stack scanning which shows the photographs taken from the bottom and the tope planes of the aortic bifurcations.

(A)

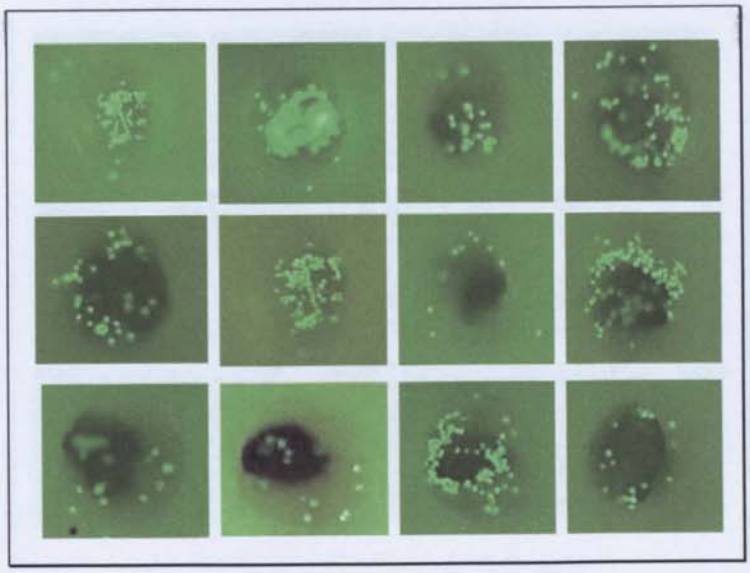

(B)

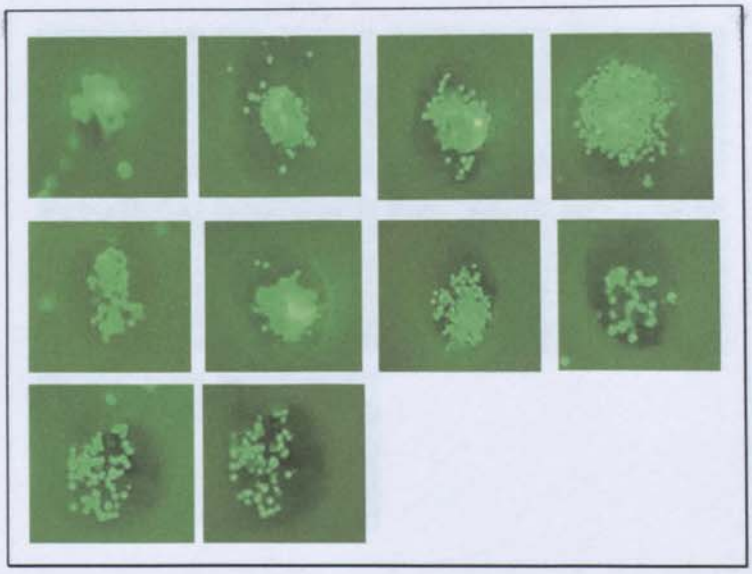

(C)

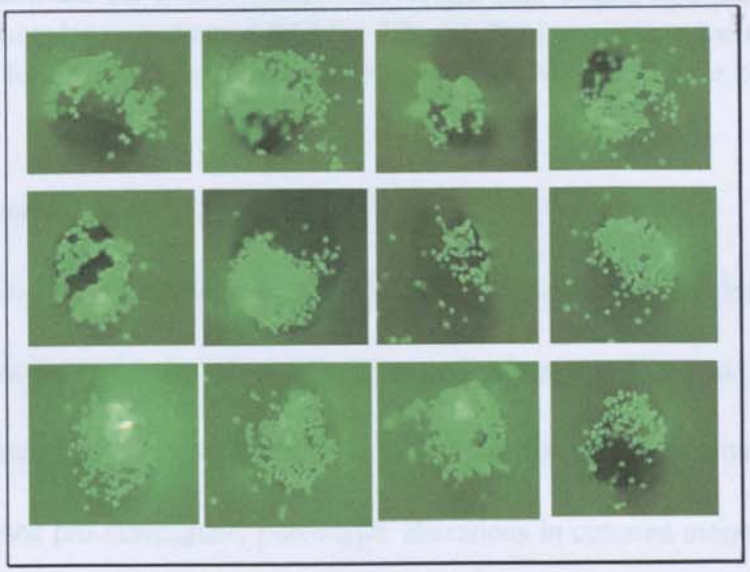

(D)

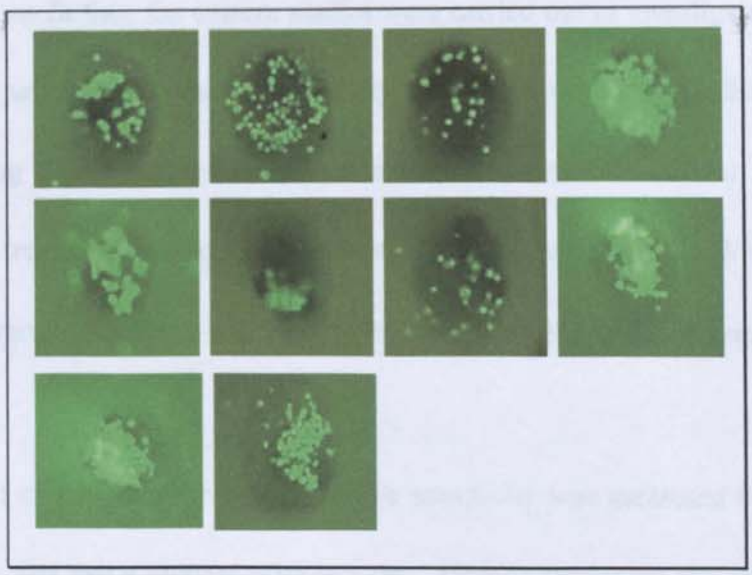

Figure 6.8 Effect of palmitate on U937 monocytes adhesion to rat aorta. Wistar Han rats (250-280g) were starved overnight for 12h and administered with 0.5ml 120mM palmitate or 0.5ml water as controls for 6h. U937 monocytes (10^6/ml) were incubated with BSA as controls or 300μM palmitate for 24h and then labelled with 10μg/ml BCECF-AM for 30min at room temperature in the dark. The thoracic aorta was carefully isolated and fixed by fine needles in 35mm Petri dishes. The labelled monocytes ($5x10^5$/ml) were added to aortic strips for 30min in the dark at a rotation speed of 50rpm/min.Unbound monocytes were washed away and cell adhesion to aorta was visualised under a fluorescent microscope at magnification of 4x. For each aortic segment, 6 different sites were photographed at random and any bifurcation images stored for analysis. (A) Rats

were treated with water for 6h, U937 monocytes were treated with BSA for 24h. (B) Rats were treated with water for 6h, U937 monocytes were treated with 300μM palmitate for 24h. (C) Rats were treated with 60mM/kg palmitate for 6h, U937 monocytes were treated BSA for 24h. (D) Rats were treated with 60mM/kg palmitate for 6h, U937 monocytes were treated 300μM palmitate for 24h.

6.5 Discussion

In previous chapters, an acute effect of palmitate treatment (6h) has been shown to induce insulin resistance in two *in vitro* cell culture models - monocytes and skeletal muscle cells. Also, it has also shown that long term palmitate treatment (24h) caused pro-atherogenic phenotypic alterations in cultured monocytes which may contribute to the development of atherosclerosis. To extend these observations further, the current studies were carried out to investigate the *in vivo* effect of palmitate on insulin sensitivity and *ex vivo* monocyte adhesion to the aorta using Wistar rats as an animal model. The data showed that that *in vivo* palmitate treatment caused a transient delay in glucose disposal in Wistar rats and also an overall increase in monocyte adhesion to aortic bifurcation areas.

The effect of palmitate on *in vivo* insulin sensitivity was measured by an insulin sensitivity test and a glucose tolerance test. After 6h treatment, the glucose levels during insulin sensitivity tests were significantly higher at 15min and 30min in rats treated with 0.5ml 120mM (equivalent to 0.09g/kg body weight) palmitate. However, the difference in plasma glucose levels between palmitate treatment and controls was not maintained at 60min and 90min. There are two methods which

are most commonly used in clinical practice for evaluating insulin sensitivity *in vivo*: the oral glucose tolerance test in which a glucose bolus is given orally and venous blood glucose and insulin levels are determined at frequent intervals within 120min; and the insulin sensitivity test in which a short-acting recombinant human insulin is injected and followed by frequent venous blood samplings to determine the blood glucose levels. In the present study, the effect of palmitate on insulin sensitivity was initially determined by the insulin sensitivity test which comprises an initial oral glucose administration then followed by an immediate injection of insulin. The major advantage of this method is that it provides a direct comparison of insulin-mediated glucose disposal between different treatment groups and minimises the effect of free fatty acid treatment on endogenous insulin secretion. The effect of palmitate on insulin sensitivity evaluated by the glucose tolerance test also showed a transient delay in blood glucose disposal at 60min in 60mM/kg palmitate-treated rats compared to rats treated with 10mM/kg oleate alone as controls. This result further confirmed the effect of palmitate-induced insulin resistance *in vivo*. The non-persistence of the palmitate-induced delay in glucose disposal could be due to the strong insulin signal at the end of the test in response to glucose challenge. After a glucose challenge, insulin is rapidly released into the circulation in order to maintain glucose homeostasis within 2h (Kevin et al., 2004); it is possible that insulin levels are in the highest after 60min in both the test and control In addition, the short (10min) free fatty acids

stimulation time is a potent inducer of insulin secretion by the pancreas (Crespin et al., 1973). Therefore, it is also possible that rats treated with palmitate had higher level of endogenous insulin production than those treated with water which may contribute to the reduction in glucose level after 60min.

The palmitate-induced transient delay of glucose disposal in the present study is similar to a previous study which showed that the insulin-stimulated glucose disposal was delayed in rats after intraperitoneal injection with 0.09g/kg palmitic acid for 1h. Also, in the previously reported study, it was shown that a significant increase in plasma free fatty acids levels in rats occurred after palmitic acid injection (Reynoso et al., 2003). However, in the present study, using the same dose of palmitate, the rise of plasma free fatty acid levels could not be achieved as there was no change in both plasma free fatty acid and triacylglyceride levels after the oral palmitate administration for 6h. The differences observed between plasma free fatty acid elevation in the present study and the previous study could be explained by the differences in the metabolic route between oral intake and peritoneal injection of palmitate; most of the dietary fatty acids are digested and absorbed in the small intestine and repackaged into chylomicrons, transported to the liver through the lymphatic system, and then released into the circulation in the form of a lipoprotein particle - very low density lipoprotein (VLDL). The free fatty acids are then liberated in blood vessels under the action of lipase on VLDL.

Therefore, it is possible that the palmitate administered to rats was in a form of VLDL. However, the data on plasma triglyceride levels seem not to support this possibility since there was no significant difference in plasma TAG levels in rats treated with palmitate and water. Under fasting conditions, free fatty acids are the major energy source to the body especially skeletal muscles, therefore, it is also possible that the exogenous palmitate could be utilised by muscles because during the present studies the rats had undergone starvation for 12h before and during the 6h of experimentation.

Although the present study failed to establish an association of increased plasma free fatty acid levels and the temporary impairment of glucose tolerance, it still does not rule out the possibility that localised accumulation of palmitate such as in skeletal muscles can account for this effect since skeletal muscles are the major site (~70%) for glucose disposal after glucose loading (DeFronzo et al., 1981; Shulman et al., 1990). Indeed, Barma et al. (2006) reported that continuously feeding palmitate (0.0015g/kg) to Indian perch for 100 days induced hyperinsulinaemia and hyperglycemia and this was associated with a significant reduction in glucose uptake in skeletal muscles compared to controls. Therefore, the temporary delay in glucose disposal in rats treated with palmitate could be due to a reduction in glucose uptake by skeletal muscles. The palmitate induced-insulin resistance in cell culture models was likely to be due to the

defects in post-receptor insulin signal transduction at the glucose transport level such as tyrosine phosphorylation of IRS-1 (Storz et al., 1999), IRS-1 associated PI3-kinase activity (Sinha et al., 2004) PKB/Akt activation (Storz et al., 1999; Schmitz-Peiffer et al., 1999; Dimopoulos et al., 2006) and translocation of GLUT4 to cell membranes (Alkhateeb et al., 2007). Furthermore, *in vivo* palmitate administration also induced a reduction of insulin receptor and insulin receptor substrate-1 tyrosine phosphorylation (Reynoso et al., 2003; Barma et al., 2006). Palmitate metabolites such as ceramide and diacylglycerol have been implicated in skeletal muscle insulin resistance (Boden et al., 1994). Future studies are required to investigate the role of these signalling intermediates and the post-receptor insulin signal transduction pathway in palmitate-induced insulin resistance in the present study.

In Chapter 4, it was shown that 50μM oleate protected against 300μM palmitate-induced insulin resistance in L6 skeletal muscle cells, indicating that oleate, in as little as a 1:6 ratio to palmitate, can exert its protective effect *in vitro*. This beneficial effect of oleate was also investigated in our *in vivo* model. In contrast to the *in vitro* observations, there was not a significant difference in blood glucose levels in rats treated with a combination of palmitate and oleate at 6:1 ratio and palmitate alone, this could be explained by the different experimental conditions between *in vivo* and *in vitro* since during in vitro conditions the oleate

was directly delivered to cultured cells at a fix ratio. However, it will be variably complexed with albumin during *in vivo* conditions in which both oleate and palmitate undergo distinct anabolic and metabolic pathways.

The second objective of the present study was to determine the *in vitro* and *in vivo* effect of palmitate treatment on monocyte adhesion to aorta. The effect of palmitate treatment on monocyte adhesion to non-bifurcation areas is not consistent and showed large variations between each site (data not shown). However, there was a relatively uniform pattern of monocyte adhesion to brachial artery areas. We observed an overall increase in adhesion of BSA-treated U937 monocyte to artery bifurcation edges in rats treated with palmitate compared to those treated with water. *In vitro* palmitate treatment was associated with a consistent increase in monocyte adhesion at the aperture of junctions of aorta. However, the distribution of monocytes adhesion to aorta is different between *in vivo* and *in vitro* palmitate treatment. There is an increase in monocyte adhesion to aorta at the edges of the bifurcations after *in vivo* palmitate treatment whereas the increase in monocyte adhesion to aorta after *in vitro* palmitate treatment seems to due to monocytes aggregating in the bifurcations. The combined *in vivo* and *in vitro* palmitate treatments of endothelium and monocytes did not further enhance the adhesion. This indicates that the *in vivo* palmitate treatment seemed to exert a greater impact on monocyte adhesion to artery bifurcation areas. This is the first

study to show that *in vivo* palmitate treatment enhances monocyte adhesion to the aortic endothelium.

Increased monocyte adhesion to the vascular endothelium is mediated by adhesion molecules such as ICAM-1, VCAM-1, and E-selectin expressed on endothelium. The expression of these adhesion molecules is mainly regulated by NF-κB activation. Indeed, palmitate has been shown to induce NF-κB activation in endothelial cells (Cacicedo et al., 2004). Therefore, it is possible that the increased adhesion of BSA-treated U937 monocytes to palmitate-treated rat aortic bifurcations is due to the increased expression of these adhesion molecules. To test this hypothesis, further studies can be carried out to examine the plasma inflammatory cytokines such as IL-6 and TNF-α (expressed by endothelial cells in response to activation of NF-κB) and also to measure the shedding of endothelial cell adhesion molecules in response to increased expression.

In summary, data from the present study suggest a role of palmitate in inducing insulin resistance *in vivo* and increasing monocyte adhesion to aorta. This provides a possible molecular mechanism for insulin resistance and the acceleration of atherosclerosis. This model provides a potential opportunity for the future research for investigating the casual association between insulin resistance and the early development of atherosclerosis by treating palmitate-treated rats

with insulin sensitising drugs such as thiazolidinediones and metformin. Also, the *in vivo* effects of unsaturated fatty acid oleate on insulin sensitivity and monocytes adhesion to aorta requires further studies.

Chapter 7

Discussion and Future Work

7.1 Discussion

Cardiovascular disease (CVD) is one of the most common complications in type 2 diabetes and also the major cause of mortality and morbidity in these patients. A large body of evidence suggests that insulin resistance, the underlying mechanism for the development of type 2 diabetes, is an independent risk factor for accelerating the development of atherosclerosis, the leading cause of CVD. Insulin resistance is characterised by a group of metabolic disorders primarily due to altered metabolism of glucose and fatty acids. More and more evidence supports the view that the oversupply of lipids to peripheral tissues through increased plasma free fatty acid is one of the major contributors to insulin resistance. However, little is known about whether free fatty acids exert any effect on monocytes, one of the vascular cells playing a critical role in the development of atherosclerosis. Therefore, to provide a better understanding of the molecular mechanisms linking insulin resistance and atherosclerotic disease, the present studies were carried out to investigate the role and the mechanisms through which palmitate, the most abundant saturated fatty acids in human plasma, may alter insulin sensitivity and monocyte vascular function using both *in vitro* cell culture and *in vivo* models.

The first objective of the present study was to establish a palmitate-induced insulin resistance model in monocytes and to evaluate the role of ceramide in

mediating of this effect. The data showed that *in vitro*, 6h palmitate (300μM) treatment caused almost a complete impairment in insulin-stimulated glucose uptake in human THP-1 monocytes. Also, a similar effect was observed using rat L6 skeletal muscle cells, one of the best characterised muscle cell models for studying insulin resistance. These results are similar to previous studies using C2C12 skeletal muscle cells and adipocytes (Dobrzyn et al., 2003; Epps-Fung et al., 1997) and further confirm an important role of palmitate as a potent inducer of insulin resistance. Although in THP-1 monocytes and L6 muscle cells, palmitate seemed not to induce apoptosis since there is lack evidence of caspase 3 activation following palmitate treatment, the possibility that palmitate-induced cytotoxicity mediates palmitate-induced insulin resistance in these cells can not be ruled out unless further analysis of early apoptotic marker was measured such as caspase 9 activation. To extend these observations from *in vitro* studies to *in vivo* intake of the saturated fatty acid palmitate, healthy adult Wistar rats after overnight fasting were orally gavaged with 0.5ml palmitate (120mM) for 6h for an insulin sensitivity test/oral glucose tolerance test. The results showed that there was a transient delay in plasma glucose disposal presented in rats treated with palmitate compared to those treated with water shown by both an insulin sensitivity test and oral glucose tolerance test. This is the first study showing that short term dietary intake of palmitate can affect insulin sensitivity *in vivo*. So far, there are two studies which have reported that palmitate induces insulin resistance in vivo. One

study (Barma et al., 2006) chronically fed Indian perch with 0.0015g/kg palmitate for 100 days and reported an induction of obesity and type 2 diabetes at the end of the study. However, in that study, feeding perch with palmitate caused obesity, which could directly contribute the induction of insulin resistance and Type 2 diabetes. A more specific study comes from Reynoso et al (2003) in which 0.9g/kg palmitate was injected intraperitoneally to Wistar rats for 1h reported a significant delay in plasma glucose disposal compared to controls and reduced insulin receptor activity in skeletal muscles. To provide a more practical model which can better represent dietary intake of palmitate without causing obesity, the present study used a similar dose of palmitate (0.5ml 120mM=1.0g/kg) orally gavaging to Wistar rats for 6h, and the results from this study further provided another line of evidence for the potential role of palmitate in inducing insulin resistance *in vivo*.

Regarding to the mechanisms of palmitate-induced insulin resistance, the present studies examined the role of ceramide, a *de novo* synthesised metabolite from palmitate, in mediating palmitate-induced insulin resistance. The data supported a partial role of ceramide in mediating palmitate-induced insulin resistance in THP-1 monocytes whereas no significant effect in L6 skeletal muscles. The effect of ceramide on insulin sensitivity has been well established in several cell culture models such as C2C12 and L6 skeletal muscle cells, and 3T3-L1 adipocytes.

However, data on ceramide in mediating free fatty acid-induced insulin resistance are controversial (Chavez et al., 2003; Yu et al., 2002). Also, it is reported that the biological effects of ceramide are highly dependent on cell type. Therefore, the discrepancies between this study and others might be due to the different cell types. *In vivo* infusion of a triglyceride emulsion combined with heparin acutely increased plasma free fatty acids and also caused impaired insulin-mediated glucose disposal (insulin resistance) (Dresner et al., 1999; Roden et al., 1996). However, none of these studies supported a role of ceramide in mediating FFA-induced insulin resistance. Because a majority of the *in vivo* studies used mixture of lipids compared to single fatty acids which were used *in vitro* cell culture models, caution is needed when extrapolating the information from these *in vivo* studies to *in vitro* experimentation.

The second objective of the present study is to investigate the effect of palmitate on vascular function evaluated by monocyte phenotype and adhesion. The monocyte is one of the most important cells in the vasculature that plays a critical role in the development atherosclerosis. The data showed that 24h incubation with 300μM palmitate caused a significant increase in cell surface CD11b and CD36 expression and an increase in mannose receptor (CD206) expression, indicating a pro-atherogenic monocyte phenotype change and a differentiation of monocytes after palmitate treatment. However, increases in cell surface CD11b expression

after palmitate treatment did not cause an associated increase in monocyte adhesion to EAhy 926 endothelial cells or plates coated with immobilised human recombinant ICAM-1. The adhesion of monocytes to endothelium is the earliest and critical event contributing to the development of atherosclerotic lesions. The integrin-mediated firm adhesion requires an activation of integrin molecules. Therefore, the lack of increase in monocyte adhesion might be due to the increase in low affinity CD11b and is likely to require a co-stimulatory model for activation which is not available in a single cell culture study. Similar to the investigation in palmitate-induced insulin resistance in monocytes, the role of ceramide in palmitate-induced monocytes phenotype was examined. Blocking ceramide generation by FB1 significantly antagonised the palmitate-induced increase in both CD11b and CD36 was significantly antagonised. However, FB1 alone was found to reduce both CD11b and CD36 expression on control cells. Further approaches are required to examine the role of ceramide in mediating palmitate-induced changes in monocytes.

Given the role of CD11b as a ligand in Mac-1 mediated adhesion to ICAM-1 expressed on the surface of activated endothelial cells, the effect of palmitate on monocyte adhesive properties was examined. Palmitate administration to rats increased adhesion of U937 monocytes to the aorta, especially at bifurcations whereas there were large variations in monocyte adhesion to non-bifurcation areas

of the aorta (data not shown). *In vitro* palmitate treatment was associated with a consistent increase in monocyte adhesion at the aperture of junctions. However, the distribution of increase in monocyte adhesion to aorta is different between *in vivo* and *in vitro* palmitate treatment since there is an increase in monocyte adhesion to aorta in the edges of the bifurcations after *in vivo* palmitate treatment whereas the increase in monocyte adhesion to aorta after *in vitro* palmitate treatment seems to due to monocyte aggregate into the bifurcations. Combined *in vivo* and *in vitro* palmitate treatments did not further enhance monocyte adhesion, suggesting that palmitate exposure to either monocytes or endothelium can increase monocyte adhesion, either approach possibly generating a maximal effect in the present model system. Such a phenomenon has been noted during exposure of rats to raised glucose concentrations (Azuma et al., 2006), but the palmitate effect has not been reported. Palmitate has been shown to induce NF-κB activation in endothelial cells (Cacicedo et al., 2004), which increases expression of adhesion molecules such as ICAM-1, VCAM-1, and E-selectin (Shaw et al., 2007). In our study, we have not evaluated the expression of each ligand that is involved in the different stages of tethering, firm adhesion and diapedesis; given the differentiated phenotype of monocytes after treatment with palmitate, it is likely that ligands for E-selectin and VCAM-1 are also upregulated. This offers a potential mechanism to account for increased adhesion of monocytes to palmitate-treated rat aortic endothelium.

In conclusion, the present studies demonstrated that the saturated free fatty acid palmitate induces insulin resistance and a pro-atherogenic monocyte phenotype change. *In vivo* studies also confirmed that palmitate induces insulin resistance and an increase in monocyte adhesion to aorta. Ceramide may play more important roles in palmitate-induced monocyte vascular change than in the development of insulin resistance. The main findings in this thesis are summarised in Table 7.1.

Table 7.1 Results summary of the thesis

	Insulin resistance			Monocyte phenotype and adhesion			
Treatment	THP-1	L6	Rat	CD11b/CD36	EAhy926	ICAM-1	Aorta
Palmitate	+++	+++	+	↑	↓	---	↑
Oleate	---	---	N/A	---	N/A	---	N/A
Oa+Pa	---	---	+	---	N/A	---	N/A
FB1+Pa	+	+++	N/A	---	N/A	N/A	N/A

Pa: palmitate, Oa: oleate, N/A: not available
+++: strongly induce insulin resistance, +: partially induce insulin resistance,
---: no effect, ↑: increase, ↓ : decrease.

7.2 Future work

It would be especially interesting to investigate the role of ceramide metabolism in mediating palmitate-induced changes in CD11b and CD36 by measuring the generation of ceramide and its metabolites (sphingosine, sphingomyelin, and sphinganine) in monocytes. In addition, the application of a ceramide degradation inhibitor e.g.1S,2R-D-erythro-2-(N-myristoylamino)-1-phenyl-1-propanol (MAPP) and increasing serine palmitoyltransferase (SPT) activity would provide important mechanistic information.

To better understand whether the lack of correlation exists between CD11b expression and adhesion, other monocyte integrins can be analysed. Also, the impact of co-stimulatory molecules, possibly induced by palmitate from treated endothelial cells, on CD11b activation could be examined using antibodies that bind to epitopes only present in the active integrin.

Another line of investigation is to determine the adhesion molecule expression (e.g. ICAM-1 and VCAM-1) in rat aorta after *in vivo* palmitate treatment.

Another line of investigation is to determine the adhesion molecule expression (e.g. ICAM-1 and VCAM-1) in rat aorta after *in vivo* palmitate treatment and the effects on NF-κB activation. Plasmas could be further analysed for

pro-inflammatory cytokines and chemokines.

To investigate the molecular mechanism of *in vivo* palmitate-induced transient delay in glucose disposal, further studies are needed to examine the effect of in vivo palmitate treatment on skeletal muscle glucose uptake and glucose production from liver and key proteins such as PKB/Akt in the associated insulin signal transduction pathway.

Chapter 8

References

Adams JM 2nd, Pratipanawatr T, Berria R, Wang E, DeFronzo RA, Sullards MC, Mandarino LJ (2004) Ceramide content is increased in skeletal muscle from obese insulin-resistant humans. Diabetes 53:25-31

Aerts JM, Ottenhoff R, Powlson AS, Grefhorst A, van Eijk M, Dubbelhuis PF, Aten J, Kuipers F, Serlie MJ, Wennekes T, Sethi JK, O'Rahilly S, Overkleeft HS (2007) Pharmacological Inhibition of Glucosylceramide Synthase Enhances Insulin Sensitivity. Diabetes 56:1341-1349

Alkhateeb H, Chabowski A, Glatz JF, Luiken JF, Bonen A (2007) Two phases of palmitate-induced insulin resistance in skeletal muscle: impaired GLUT4 translocation is followed by a reduced GLUT4 intrinsic activity. Am J Physiol Endocrinol Metab 293(3):783-793

Alon R, Kassner PD, Carr MW, Finger EB, Hemler ME, Springer TA (1995) The integrin VLA-4 supports tethering and rolling in flow on VCAM-1. J Cell Biol 128:1243-1253

Anand SS, Yusuf S, Vuksan V, Devanesen Sudarshan, Teo KK, Montague PA, Kelemen L, Yi CL, Lonn E, Gerstein H, Hegele RA, McQueen M (2000) The Lancet 356:279-284

Andrews B, Burnand K, Paganga G, Browse N, Rice-Evans C, Sommerville K, Leake D, Taub N (1995) Oxidisability of low density lipoproteins in patients with carotid or femoral artery atherosclerosis. Atherosclerosis. 112:77-84

Arnal JF, Dinh-Xuan AT, Pueyo M (1999) Endothelium-derived nitric oxide and vascular physiology and pathology. Cell Mol Life Sci 55:1078-1087

Arner P, Pollare T, Lithell H, Livingston JN (1987) Defective insulin receptor tyrosine kinase in human skeletal muscle in obesity and type 2 (non-insulin-dependent) diabetes mellitus. Diabetologia 30:437-440

Arnoult MH (2006) Food Consumption Changes in the UK under Compliance with Dietary Guidelines Workpackage No.1 Draft Report v2

Augé N, Nègre-Salvayre A, Salvayre R, Levade T (2000) Sphingomyelin metabolites in vascular cell signaling and atherogenesis. Prog Lipid Res 39:207-229

Auwerx J (1991) The human leukemia cell line, THP-1: a multifacetted model for

the study of monocyte-macrophage differentiation. Experientia 15:22-31

Azuma K, Kawamori R, Toyofuku Y, Kitahara Y, Sato F, Shimizu T, Miura K, Mine T, Tanaka Y, Mitsumata M, Watada H (2006) Repetitive Fluctuations in Blood Glucose Enhance Monocyte Adhesion to the Endothelium of Rat Thoracic Aorta. Arterioscler Thromb Vasc Biol 26:2275-2280

Babaev VR, Gleaves LA, Carter KJ, Suzuki H, Kodama T, Fazio S, Linton MF (2000) Reduced atherosclerotic lesions in mice deficient for total or macrophage-specific expression of scavenger receptor-A. Arterioscler Thromb Vasc Biol 20:2593-2599

Bailey CJ and Turner SL (2004) Glucosamine-induced insulin resistance in L6 muscle cells. Diabetes, Obesity and Metabolism 6:293-298

Barma P, Dey D, Basu D, Sankar Roy SS, Bhattacharya S (2006) Nutritionally induced insulin resistance in an Indian perch: a possible model for type 2 diabetes. Curr Scie 90:188-194

Baron AD, Bretchel G, Wallace P, Edelman SV (1988) Rates and tissue sites of non-insulin and insulin-mediated glucose uptake in humans. Am J Physiol 255:769-774

Baron AD, Laakso M, Brechtel G, Edelman SV (1991) Reduced capacity and affinity of skelertal muscle for insulin-mediated glucose uptake in noninsulin-dependent diabetic subjects. Effects of insulin therapy. J Clin Invest 87(4):1186-1194

Bastard JP, Jardel C, Bruckert E, Blondy P, Capeau J, Laville M, Vidal Hainque B (2000) Elevated levels of interleukin 6 are reduced in serum and subcutaneous adipose tissue of obese women after weight loss. J Clin Endocrinol Metab 85:3338-3342

Baynes KC, Beeton CA, Panayotou G, Stein R, Soos M, Hansen T, Simpson H, O'Rahilly S, Shepherd PR, Whitehead JP (2000) Natural variants of human p85 alpha phosphoinositide 3-kinase in severe insulin resistance: a novel variant with impaired insulin-stimulated lipid kinase activity. Diabetologia 43:321-331

Belfort R, Mandarino L, Kashyap S, Wirfel K, Pratipanawatr T, Berria R, Defronzo RA, Cusi K (2005) Dose-response effect of elevated plasma free fatty acid on insulin signaling. Diabetes 54:1640-1648

Bell GI, Kayano T, Buse JB, Burant CF, Takeda J, Lin D, Fukumoto H, Seino S (1990) Molecular biology of mammalian glucose transporters. Diabetes Care 13(3):198-208

Bertacca A, Ciccarone A, Cecchetti P, Vianello B, Laurenza I, Del Prato S, Benzi L (2007) High insulin levels impair intracellular receptor trafficking in human cultured myoblasts. Diabetes Res Clin Pract 78(3):316-323

Bergman RN, Ider YZ, Bowden CR, Cobelli C (1979) Quantitative estimation of insulin sensitivity Am J Physiol Endocrinol Metab 236:667-677

Berlin C, Bargatze RF, Campbell JJ, von Andrian UH, Szabo MC, Hasslen SR, Nelson RD, Berg EL, Erlandsen SL, Butcher EC (1995) α4 Integrins mediate lymphocyte attachment and rolling under physiologic flow. Cell 80:413-422
Bickel PE (2002) Lipid rafts and insulin signaling. Am J Physiol Endocrinol Metab 282: E1-E10

Berlin JA and Colditz GA (1990) A meta-analysis of physical activity in the prevention of coronary heart disease. Am J Epidemiol 132:612-628

Boden G and Jadali F (1991) Effects of lipid on basal carbohydrate metabolism in normal men. Diabetes 40:686-692

Boden G, Chen X, Ruiz J, White J V, Rossettiet L (1994) Mechanisms of free fatty acid-induced inhibition of glucose uptake. J Clin Invest 93:2438-2446

Bonetti PO, Lerman LO, Lerman A (2003) Endothelial dysfunction: a marker of atherosclerotic risk. Arterioscler Thromb Vasc Biol 23:168-175

Bonnadona RC, Zych K, Boni C, Ferranini E, DeFronzo RA (1989) Time dependent of the interaction between lipid and glucose in humans. *Am* J Physiol Endocrinol Metab 257:E49-E56

Borst SE (2001) The role of TNF-α in insulin resistance. Endocrine 23: 177–182

Boschmann M, Engeli S, Adams F, Gorzelniak K, Franke G, Klaua S, Kreuzberg U, Luedtke S, Kettritz R, Sharma AM, Luft FC, Jordan J (2005) Adipose tissue metabolism and CD11b expression on monocytes in obese hypertensive. Hypertension 46:130-136

Bradford MM (1976) A rapid and sensitive method for the quantitation of microgram quantities of protein utilizing the principle of protein-dye binding.Anal Biochem 72:248-254

Brady LJ, Goodman MN, Kalish FN, Runderman NB (1981) Insulin binding and sensitivity in rat skeletal muscle: effect of starvation. Am J Physiol 240: E184-E190.

Bray GA, Paeratakul S, Popkin BM (2004) Dietary fat and obesity: a review of animal, clinical and epidemiological studies. Physiology & Behavior 83:549-555

Brechtel K, Dahl DB, Machann J, Bachmann OP, Wenzel I, Maier T, Claussen CD, Häring HU, Jacob S, Schick F (2001) Fast elevation of the intramyocellular lipid content in the presence of circulating free fatty acids and hyperinsulinemia: a dynamic 1H-MRS study. Magn Reson Med 45: 179-183

Budihardjo I, Oliver H, Lutter M, Luo X, Wang X (1999) Biochemical pathways of caspase activation during apoptosis. Annu Rev Cell Dev Biol 15:269-290

Cacicedo JM, Yaqihashi N, Keaney JF, Ruderman NB, Ido Y (2004) AMPK inhibits fatty acid-induced increases in NF-kappaB transactivation in cultured human umbilical vein endothelial cells. Biochem Biophys Res Commun 324(4): 1204-1209

Cacicedo JM, Benjachareowong S, Chou E, Ruderman NB, Ido Y (2005) Palmitate-Induced Apoptosis in Cultured Bovine Retinal Pericytes Roles of NAD(P)H Oxidase, Oxidant Stress, and Ceramide. Diabetes 54:1838-1845

Calderwood DA, Tuckwell DS , Eble J, Kühn K, Humphries MJ (1997) The Integrin α1 A-domain Is a Ligand Binding Site for Collagens and Laminin. J Biol Chem 272:12311-12317

Canlos TM, Schwartz BR, Kovach NL, Yec E, Rosso M, Osborn L, Chi-Rosso G, Newman B, Lobb R, Harlan JM (1990) Vascular cell adhesion molecule-1 mediates lymphocyte adherence to cytokine-activated cultured human endothelial cells. Blood 76:965-970

Carluccio MA, Massaro M, Bonfrate C, Siculella L, Maffia M, Nicolardi G, Distante A, Storelli C, De Caterina R (1999) Oleic acid inhibits endothelial activation: A direct vascular antiatherogenic mechanism of a nutritional component in the mediterranean diet. Arterioscler Thromb Vasc Biol 19(2):220-228

Caro JF, Sinha MK, Raju SM, Ittoop O, Pories WJ, Flickinger EG, Meelheim D, Dohm GL (1987) Insulin receptor kinase in human skeletal muscle from obese subjects with and without noninsulin dependent diabetes. J Clin Invest 79:1330-1337

Carlos TM and Harlan JM (1994) Leukocyte-endothelial adhesion molecules. Blood 84:2068-2101

Carlos TM, Schwartz BR, Kovach NL, Yee E, Rosa M, Osborn L, Chi-Rosso G, Newman B, Lobb R, Harlan JM (1990) Vascular cell adhesion molecule-1 mediates lymphocyte adherence to cytokine-activated cultured human endothelial cells. Blood 76:965-970

Charo IF (1992) Monocyte-endothelial cell interactions. Current Opinion in Lipidology 3:335-343

Carlsson M, Wessman Y, Almgren P, Groop L (2000) High levels of nonesterified fatty acids are associated with increased familial risk of cardiovascular disease. Arterioscler Thromb Vasc Biol 20:1588-1594

Chavez JA, Knotts TA, Wang LP, Li G, Dobrowsky RT, Florant GL, Summers SA (2003) A role for ceramide, but not diacylglycerol, in the antagonism of insulin signal transduction by saturated fatty acids. J Biol Chem 278:10297-10303

Chavez JA, Holland WL, Bair J, Sandhoff K, Summers S (2005) Acid Creramidase overexpression prevents the inhibitory reffects of saturated fatty acids on insulin signaling. J Biol Chem 280:20148-20153

Chen CM (2000) Fat intake and nutritional status of children in China. American J Clin Nutr, 72: 1368S-1372S

Chen NG, Holmes M, Reaven GM (1999) Relationship between insulin resistance, soluble adhesion molecules, and mononuclear cell binding in healthy volunteers. J Clin Endocrinol Metab. 84:3485-3489

Chen M, Kakutani M, Minami M, Kataoka H, Kume N, Narumiya S, Kita T, Masaki T, Sawamura T (2000) Increased expression of lectin-like oxidized low density lipoprotein receptor-1 in initial atherosclerotic lesions of Watanabe heritable hyperlipidemic rabbits.Arterioscler Thromb Vasc Biol 20:1107-1115

Cho HK, Lee JY, Kwon YH (2007) Induction of endoplasmic reticulum stress by palmitate may contribute to insulin-resistance in HepG2 cell lines. The FASEB

Journal 21:830-838

Chung BH, Hennig B, Cho BH, Darnell BE (1998) Effect of the fat composition of a single meal on the composition and cytotoxic potencies of lipolytically-releasable free fatty acids in postprandial plasma. Atherosclerosis 141: 321–332

Collins, RG., Velji R, Guevara NA, Hicks MJ, Chan L, Beaudet AL (2000) P-Selectin or intercellular adhesion molecule (ICAM)-1 deficiency substantially protects against atherosclerosis in apolipoprotein E-deficient mice. J Exp Med 191:189-194

Coll T, Eyre E, Rodriguez-Calvo R, Palomer X, Sánchez RM, Merlos M, Laguna JC, Vázquez-Carrera M (2008) Oleate reverses palmitate-induced insulin resistance and inflammation in skeletal muscle cells. J Biol Chem 283: 11107-11116

Committee on Medical Aspects of Food Policy, Department of Health (1991) Dietary Reference Values for Food Energy and Nutrients for the United Kingdom. Report on Health and Social Subjects no. 41. London: H. M. Stationery Office

Conp M, Hannaert JC, Hoorrens A et al. (2001) Inverse relationship between cytotoxicity of free fatty acids in pancreatic islet cells and cellular triglyceride accumulation. Diabetes 50:1771-1777

Cozzone D, Frojdo S, Disse E, Debard C, Laville M (2008) Isoform-specific defects of insulin stimulation of Akt/protein kinase B (PKB) in skeletal muscle cells from type 2 diabetic patients. Diabetologia 51:512–521

Crespin SR, Greenough WB 3rd, Steinberg D (1973) Stimulation of insulin secretion by long-chain free fatty acids. A direct pancreatic effect. J Clin Invest. 52(8):1979-1984

Crowther MA (2005) Patheogenesis of Atherosclerosis. Hematology 1:436-441

Cushing SD, Berliner JA, Valente AJ, Territo MC, Navab M, Parhami F, Gerrity R, Schwartz CJ, Fogelman AM (1990) Minimally modified low density lipoprotein induces monocyte chemotactic protein 1 in human endothelial cells and smooth muscle cells. Proc Natl Acad Sci USA 87:5134-5138

Cutfield, W, Luk, W, Skinner, S, Robinson, E (2000) Impaired insulin-mediated glucose uptake in monocytes of short children with intrauterine growth retardation.

Pediatric Diabetes 1:186-192

Cybulsky MI and Gimbrone MA (1991) Endothelial expression of a mononuclear leukocyte adhesion molecule during atherogenesis. Science 251:788-791

Cybulsky MI, Iiyama K, Li H, Zhu S, Chen M, Iiyama M, Davis V, Gutierrez-Ramos JC, Connelly PW, Milstone DS (2001) A major role for VCAM-1, but not ICAM-1, in early atherosclerosis. J Clin Invest 107:1255-1262

Daneman D, Zinman B, Elliott ME, Bilan PJ and Klip A (1992) Insulin-stimulated glucose transport in circulating monocuclear cells from nondiabetic and IDDM subjects. (insulin-dependent diabetes mellitus). Diabetes 41:227-234

Daugherty A, Cornicelli JA, Welch K, Sendobry SM, Rateri DL (1997) Scavenger receptors are present on rabbit aortic endothelial cells in vivo.Arterioscler Thromb Vasc Biol 17:2369-2375

De Fea K and Roth RA (1997) Protein kinase C modulation of insulin receptor substrate-1 tyrosine phosphorylation requires serine 612. Biochemistry 36:12939-12947

DeFronzo RA, Jacot E, Jequier E, Wahren J, Felber JP (1981) The effect of insulin on the disposal of intravenous glucose: results from indirect calorimetry and hepatic and femoral venous catheterization. Diabetes 30:1000-1007

Degerman E, Landstrgm TR, Wijkander J, Holst LS, Ahmad F, Belfrage P, and Manganiello V (1998) Phosphorylation and activation of hormone-sensitive adipocyte phosphodiesterase type 3B. Methods 14:43-53

Deszo EL, Brake DK, Cengel KA, Kelley KW, Freund GG (2000) CD45 Negatively Regulates Monocytic Cell Differentiation by Inhibiting PMA-Dependent Activation and Tyrosine Phosphorylation of PKCδ. J Biol Chem 276:10212-10217

Deves R and Krupka RM (1978) Cytochalasin B and the kinetics of inhibition of biological transport: a case of asymmetric binding to the glucose carrier. Biochim Biophys Acta 510:339-348

Dimitriadis G, Maratou E, Boutati E, Psarra K, Papasteriades C, Raptis SA (2005) Evaluation of glucose transport and its regulation by insulin in human monocytes using flow cytometry. Cytometry part A 64A:27-33

Dimopoulos N, Watson M, Sakamoto K, Hundal HS (2006) Differential effects of palmitate and palmitoleate on insulin action and glucose utilization in rat L6 skeletal muscle cells. Biochem J 399:473-481

Dobrzyn A and Summers SA (2003) Characterizing the effects of saturated fatty acids on insulin signalling and ceramide and diacylglycerol accumulation in 3T3-L1 adipocytes and C2C12 myotubes. Arch Biochem Biophys 419:101-109

Dong ZM, Chapman SM, Brown AA, Frenette PS, Hynes RO, and Wagner DD (1998) The combined role of P- and E-selectins in atherosclerosis. J Clin Invest 102:145-152

Dong ZM, Brown AA, and Wagner DD (2000) Prominent role of P-selectin in the development of advanced atherosclerosis in ApoE-deficient mice. Circulation 101: 2290-2295

Douen AG, Ramlal T, Rastogi S, Bilan PJ, Cartee GD, Vranic M, Holloszy JO, Klip A (1990) Exercise induces recruitment of the 'insulin-responsive glucose transporter.' J Biol Chem. 265:13427-13430

Dresner A, Laurent D, Marcucci M, Griffin ME, Dufour S, Cline GW, Slezak LA, Andersen DK, Hundal RS, Rothman DL, Petersen KF, Shulman GI (1999) Effects of free fatty acids on glucose transport and IRS1-associated phophatidylinositol 3-kinase activity. J Clin Invest 103:253-259

Edgell CJS, McDonald CC, Graham JB (1983) Permanent cell line expressing human factor VIII-related antigen established by hybridization. Proc Natl Acad Sci USA 80:3734–3737

Elices MJ, Osborn L, Takada Y, Crouse C, Luhowskyj S, Hemler ME, and Lobb RR (1990) VCAM-1 on activated endothelium interacts with the leukocyte integrin VLA-4 at a site distinct from the VLA-4/fibronectin binding site. Cell 60:577-584

Endemann G, Stanton LW, Madden KS, Bryant CM, White RT, Protter AA (1993) CD36 is a receptor for oxidised low density lipoprotein. J Biol Chem. 268:11811-11816

Epps-Fung MV, Williford J, Wells A, Hardy RW (1997) Fatty acid-induced insulin resistance in adipocytes. Endocrinology 138:4338-4345

Eriksson J, Koranyi L, Bourey R, Schalin-Jäntti C, Widén E, Mueckler M, Permutt AM, Groop LC (1992) Insulin resistance in type 2 (non-insulin-dependent) diabetic patients and their relatives is not associated with a defect in the expression of the insulin-responsive glucose transporter (GLUT-4) gene in human skeletal muscle. Diabetologia 35:143-147

Farese RV Jr, Yost TJ, Eckel RH (1991) Tissue-specific regulation of lipoprotein lipase activity by insulin/glucose in normalweight humans. Metabolism 40:214–216

Falk E (2006) Pathogenesis of Atherosclerosis. J Am Coll Cardiol 47:7-12

Febbraio M, Podrez EA, Smith JD (2000) Targeted disruption of the class B scavenger receptor CD36 protects against atherosclerotic lesion development in mice. J Clin Invest 105:1049-1056

Febbraio M, Guy E, Silverstein RL (2004) Stem cell transplantation reveals that absence of macrophage CD36 is protective against atherosclerosis. Arterioscler Thromb Vasc Biol 24:2333-2338

Feng J, Han J, Pearce SF, Silverstein RL, Gotto AM Jr, Hajjar DP, Nicholson AC (2000) Induction of CD36 expression by oxidized LDL and IL-4 by a common signaling pathway dependent on protein kinase C and PPAR-gamma. J Lipid Res 41:688-696

Freeman MW (1997) Scavenger receptors in atherosclerosis. Curr Opin in Heamatology 4:41-47

Fraze E, Donner CC, Swislocki AL, Chiou YA, Chen YD, Reaven GM (1985) Ambient plasma free fatty acid concentrations in noninsulin-dependent diabetes mellitus: evidence for insulin resistance. J Clin Endocrinol & Metab 61:807-811

Frostegård J, Nilsson J, Haegerstrand A, Hamsten A, Wigzell H, Gidlund M (1990) Oxidized low density lipoprotein induces differentiation and adhesion of human monocytes and the monocytic cell line U937. Proc Natl Acad Sci USA 87:904-908

Galkina E and Ley K (2007) Vascular Adhesion Molecules in Atherosclerosis. Arterioscler Thromb Vasc Biol 27:2292-2301

Gahmberg CG, Tolvanen M, Kotovuori P (1997) Leukocyte adhesion—structure and function of human leukocyte beta2-integrins and their cellular ligands. Eur J

Biochem 245:215–232

Garvey WT, Olefsky JM, Matthaei S, Marshall S (1987) Glucose and insulin co-regulate the glucose transport system in primary cultured adipocytes. A new mechanism of insulin resistance J Biol Chem 262:189-197

Gerszten RE, Luscinskas FW, Ding HT, Dichek DA, Stoolman LM, Gimbrone MA Jr, Rosenzweig A (1996) Adhesion of memory lymphocytes to vascular cell adhesion molecule-1-transduced human vascular endothelial cells under simulated physiological flow conditions in vitro. Circ Res 79:1205-1215

Goodyear LJ, Giorgino F, Sherman LA, Carey J, Smith RJ, and Dohm GL (1995) Insulin receptor phosphorylation, insulin receptor substrate-1 phosphorylation, and phosphatidylinositol 3-kinase activity are decreased in intact skeletal muscle strips from obese subjects. J Clin Invest 95:2195–2204

Gould GW and Holman GD (1993) The glucose transporter family: structure, function and tissue specific expression. Biochem J 295:329-341

Gupta H, Dai L, Datta G, Garber DW, Grenett H, Li Y, Mishra V, Palgunachari MN, Handattu S, Gianturco SH, Bradley WA, Anantharamaiah GM, White CR (2005) Inhibition of lipopolysaccharide-induced inflammatory reponse by an apolipoprotein AI mimetic peptide. Circ Res 97:236-243

Grasso G, Frittitta L, Anello M, Russo P, Sesti G, Trischitta V (1995) Insulin receptor tyrosine-kinase activity is altered in both muscle and adipose tissue from non-obese normoglycaemic insulin-resistant subjects. Diabetologia. 38:55-61

Greenwalt DE, Lipsky RH, Ockenhouse CF, Ikeda H, Tandon NN, Jamieson GA (1992) Membrane glycoprotein CD36: a review of its roles in adherence, signal transduction, and transfusion medicine. Blood 80:1105-1115

Griffin ME, Marcucci MJ, Cline GW, Bell K, Barucci N, Lee D, Goodyear LJ, Kraegen EW, White MF, Shulman GI (1999) Free fatty acid-induced insulin resistance is associated with activation of protein kinase C theta and alterations in the insulin signalling cascade. Diabetes 48:1270–1274

Griffin E, Re A, Hamel N, Fu C, Bush H, McCaffrey T, Asch AS (2001) A link between diabetes and atherosclerosis: glucose regulates expression of CD36 at the level of translation. Nat Med 7:840-846

Guo ZK, Hensrud DD, Johnson CM, Jensen MD (1999) Regional postprandial fatty acid metabolism in different obesity phenotypes. Diabetes 48:1586-1592

Haffner SM, Lehto S, Ronnemaa T, Pyorala K, Laakso M (1998) Mortality from coronary heart disease in subjects with type 2 diabetes and in nondiabetic subjects with and without prior myocardial infarction. N Engl J Med 339:229-234

Hajduch E, Hainault I, Meunier C, Jardel C, Hainque B, Guerre-Millo M, Lavau M (1995) Regulation of glucose transporters in cultured rat adipocytes: synergistic effect of insulin and dexamethasone on GLUT4 gene expression through promoter activation. Endocrinol 136:4782-4789

Hajduch E, Balendran A, Batty IH, Litherland GJ, Blair AS, Downes CP, Hundal HS (2001) Ceramide impairs the insulin-dependent membrane recruitment of protein kinase B leading to a loss of downstream signalling in L6 skeletal muscle cells. Diabetologia 44:173-183

Hainque B, Guerre-Millo M, Hainault I, Moustaid N, Wardzala LJ, Lavau M (1990) Long term regulation of glucose transporters by insulin in mature 3T3-F442A adipose cells. Differential effects on two glucose transporter subtypes. J Biol Chem. 265(14):7982-7986

Handberg A, Vaag A, Damsbo P, Beck-Nielsen H (1990) Vinten J.Expression of insulin regulatable glucose transporters in skeletal muscle from type 2 (non-insulin-dependent) diabetic patients. Diabetologia 33:625-627

Hardy S, Langelier Y, Prentki M (2000) Oleate activates phosphatidylinositol 3-kinase and promotes proliferation and reduces apoptosis of MDA-MB-231 breast cancer cells, whereas palmitate has opposite effects. Cancer Res 60:6353-6358

Hennig B, Shasby DM, Spector AA (1985) Exposure to fatty acid increases human low density lipoprotein transfer across cultured endothelial monolayers. Circ Res 57:776-780

Herijgers N, de Winther MP, Van Eck M, Havekes LM, Hofker MH, Hoogerbrugge PM, Van Berkel TJ (2000) Effect of human scavenger receptor class A overexpression in bone marrow-derived cells on lipoprotein metabolism and atherosclerosis in low density lipoprotein receptor knockout mice. J Lipid Res 41:1402-1409

Hickson-Bick DLM, Sparagna GC, Buja LM, McMillin JB (2002) Palmitate-induced apoptosis in neonatal cardimyocytes is not dependent on the generation of ROS. AJP-Heart 282:656-664

Hogg N, Henderson R, Leitinger B, McDowall A, Porter J, Staneley P (2002) Mechanisms contributing to the activity of integrins on leukocytes. Immunol Rev 186:164-171

Hojjati MR, Li Z, Zhou H, Tang S, Huan C, Ooi E, Lu S, Jiang XC (2005). Effect of myriocin on plasma sphingolipid metabolism and atherosclerosis in apoE-deficient mice. J Bio Chem 280:10284-10289

Holm C (2003) Molecular mechanisms regulating hormone-sensitive lipase and lipolysis. Biochem Soc Trans 31:1120-1124

Holman GD and Kasuga M (1997) From receptor to transporter: insulin signaling to glucose transport. Diabetologia 40: 991-1003

Holman GD and Sandoval IV (2001) Moving the insulin-regulated glucose transporter GLUT4 into and out of storage. Trends Cell Biol 11:173-179

Holmäng A, Jennische E, Björntorp P (1995) The effects of long-term hyperinsulinaemia on insulin sensitivity in rats. Acta Physiol Scand 153(1):67-73

Hoogerbrugge N, Verkerk A, Jacobs ML, Postema PT, Jongkind JF (1996) Hypertriglyceridemia enhances monocyte binding to endothelial cells in NIDDM. Diabetes Care 19(10):1122-1125

Hostmark AT (2003) Serum albumin and prevalence of coronary heart disease: a population-based, cross sectional study. Norsk Epidemiologi 13:107-113

Hotamisligil GS, Shargill NS, Spiegelman BM (1993) Adipose expression of tumor necrosis factor-alpha: direct role in obesity-linked insulin resistance. Science 259:87-91

Hotamisligil GS, Murray DL, Choy LN, Spiegelman BM (1994a) Tumor necrosis factor alpha inhibits signaling from the insulin receptor. Proc Natl Acad Sci USA 91:4854-4658

Hotamisligil GS, Budavari A, Murray D, Spiegelman BM (1994b) Reduced tyrosine kinase activity of the insulin receptor in obesity-diabetes. Central role of tumor necrosis factor-alpha. J Clin Invest 94:1543-1549

Hotamisligil GS, Arner P, Caro JF, Atkinson RL, Spiegelman BM (1995) Increased adipose tissue expression of tumor necrosis factor-alpha in human obesity and insulin resistance. J Clin Invest 95:2409-2415

Hotamisligil GS, Peraldi P, Budavari A, Ellis R, White MF, Spiegelman BM (1996) IRS-1-mediated inhibition of insulin receptor tyrosine kinase activity in TNF-alpha- and obesity-induced insulin resistance. Science 271:665-668

Hou JC and Pessin JE. (2007) Ins (endocytosis) and outs (exocytosis) of GLUT4 trafficking. Curr Opin Cell Biol 19:466-473

Hunnicutt JW, Hardy RW, Williford J, McDonald JM (1994) Saturated fatty acid-induced insulin resistance in rat adipocytes. Diabetes 43:540-545

Huh HY, Pearce SF, Yesner LM, Schindler JL, Silverstein RL (1996) Regulated expression of CD36 during monocyte-to-macrophage differentiation: potential role of CD36 in foam cell formation. Blood 87:2020-2028

Hubert HB, Feinleib M, McNamara PM (1983) Obesity as an independent risk factor for cardiovascular disease: a 26-year follow-up of participants in the Framingham Heart Study. Circulation 67:968-977

Hurtado I, Fiol C, Gracia V, Caldú P (1996) *In vitro* oxidised HDL exerts a cytotoxic effect on macrophages. Atherosclerosis 125:39-46

Itani SI, Ruderman NB, Schmieder, Boden G (2002) Lipid-induced insulin resistance in human muscle is associated with changes in diacylglycerol, protein kinase C, and IκB-α. Diabetes 51:2005-2011

Jackson S, Bagstaff SM, Lynn S, Yeaman SJ, Turnbull DM, Walker M (2000) Decreased insulin responsiveness of glucose uptake in cultured human skeletal muscle cells from insulin-resistant nondiabetic relatives of type 2 diabetic families. Diabetes 49:1169-1171

James DE, Strube M, Mueckler M (1989) Molecular cloning and characterization of an insulin-regulatable glucose transporter. Nature 338:83-87

Jensen MD, Caruso M, Heiling V, Miles JM (1989) Insulin regulation of lipolysis in nondiabetic and IDDM subjects. Diabetes 38:1595–1601

Jonasson L, Holm J, Skalli O, Bondjers G, Hansson GK (1986) Regional accumulations of T cells, macrophages, and smooth muscle cells in the human atherosclerotic plaque. Arteriosclerosis 6:131-138

Jong SL, Pinnamaneni SK, Su JE, In HC, Jae HP, Chang KK, Sinclair AJ, Febbraio MA, WATT MJ (2006) Saturated, but not n-6 polyunsaturated, fatty acids induce insulin resistance: role of intramuscular accumulation of lipid metabolites. J Appl Physiol 100:1467-1474

Jucker, BM, Rennings AJ, Cline GW, and Shulman GI (1997) 13C and 31P NMR studies on the effects of increased plasma free fatty acids on intramuscular glucose metabolism in the awake rat. J Biol Chem 272:10464-10473

Kahn BB (1998) Type 2 diabetes: when insulin secretion fails to compensate for insulin resistance. Cell 92:593-596

Kaitosaari T, Ronnemaa T, Viikari J, Raitakari O, Arffman M, Marniemi J, Kallio K, Pahkala K, Jokinen E, Simell O (2006) Low–Saturated Fat Dietary Counseling Starting in Infancy Improves Insulin Sensitivity in 9-Year-Old Healthy Children. The Special Turku Coronary Risk Factor Intervention Project for Children (STRIP) study. Diabetes Care 29:781–785

Karlsson HK, Zierath JR (2007) Insulin signalling and glucose transport in insulin resistant human skeletal muscle. Cell Biochem Biophys 48:103-113

Kashyap SR, Belfort R, Berria R, Suraamornkul S, Pratipranawatr T, Finlayson J, Barrentine A, Bajaj M, Mandarino L, DeFronzo R, Cusi K (2004) Discordant effects of a chronic physiological increase in plasma FFA on insulin signalling in healthy subjects with or without a family history of type 2 diabetes. Am J Physiol Endocrinol Metab 287:E537-E546

Kasuga M, Karlsson FA, Kahn CR (1982) Insulin stimulates the phosphorylation of the 95,000-dalton subunit of its own receptor. Science 215:185-187

Kataoka H, Kume N, Miyamoto S, Minami M, Moriwaki H, Murase T, Sawamura T, Masaki T, Hashimoto N, Kita T (1999) Expression of lectinlike oxidized low-density lipoprotein receptor-1 in human atherosclerotic lesions. Circulation 99:3110-3117

Kelly DE, He J, Menshikova EV, Ritov VB (2002) Dysfunction of mitochondria in human skeletal muscle in type 2 diabetes. Diabetes 51:2944-2950

Kemp HF, Hundal HS, Taylor PM (1997) Glucose transport correlates with GLUT2 abundance in rat liver during altered thyroid status. Mol Cell Endocrinol 128:97-102

Kern PA, Saghizadeh M, Ong JM, Bosch RJ, Deem R, Simsolo RB (1995) The expression of tumor necrosis factor in human adipose tissue. Regulation by obesity, weight loss, and relationship to lipoprotein lipase. J Clin Invest 95:2111-2119

Kern PA, Ranganathan S, Li C, Wood L, Ranganathan G (2001) Adipose tissue tumor necrosis factor and interleukin-6 expression in human obesity and insulin resistance. Am J Physiol Endocrinol Metab 280:E745-51

Kevil CG, Patel RP, Bullard DC (2001) Essential role of ICAM-1 in mediating monocyte adhesion to aortic endothelial cells. Am J Physiol Cell Physiol 281:1442-1447

Kevin M. Krudys, Michael G. Dodds, Stephanie M. Nissen, and Paolo Vicini (2004) Integrated model of hepatic and peripheral glucose regulation for estimation of endogenous glucose production during the hot IVGTT. Am J Physiol Endocrinol Metab 288:1038-1046

Keys A, Menotti A, Karvonen M et al. (1986) The diet and 15-year death rate in the seven Countries Study. Am J Epidemiol 124:903-915

Kim JK, Fillmore JJ, Sunshine MJ, Albrecht B, Higashimori T, Kim DW, Liu ZX, Soos TJ, Cline GW, O'Brien WR, Littman DR, Shulman GI (2004) PKC-θ knockout mice are protected from fat-induced insulin resistance. J Clin Invest 114: 823–827

Kinlay S, Libby P, Ganz P (2001) Endothelial function and coronary artery disease. Curr Opin Lipidol 12:383-389

Kitamura T, Ogawa W, Sakaue H, Hino Y, Kuroda S, Takata M, Matsumoto M, Maeda T, Konishi H, Kikkawa U, Kasuga M (1998) Requirement for Activation of the Serine-Threonine Kinase Akt (Protein Kinase B) in Insulin Stimulation of Protein Synthesis but Not of Glucose Transport. Mol Cell Biol 18:3708-3717

Kleinfeld AM, Prothro D, Brown D, Davis R, Richieri GV, DeMaria A (1996) Increase in serum unbound free fatty acid level following coronary angioplasty. Excerpta Medica Inc 78:1350-1354

Kolesnick, RN, Krönke M (1998) Regulation of ceramide production and apoptosis. Annu Rev Physiol 60:643-665

Kodama T, Freeman M, Rohrer L, Matsudaira ZP, Krieger M (1990) Type□macrophage scavenger receptor contains alphahelical and collagen-like coiled coils. Nature 343:531-535

Konstandin MH, Sester U, Klemke M, Weschenfelder T, Wabnitz GH, Samstag Y (2006) A novel flow-cytometry-based assay for quantification of affinity and avidity changes of integrins. J Immunol Methods 310:67-77

Krieglstein CF and Granger DN (2001) Adhesion molecules and their role in vascular disease. Am J Hypertens 14:44-54

Krook A, Roth RA, Jiang XJ, Zierath JR, Wallberg-Henriksson H (1998) Insulin-stimulated Akt kinase activity is reduced in skeletal muscle from NIDDM subjects. Diabetes 47:1281–1286

Kruszynska YT, Worrall DS, Ofrecio J, Frias JP, Macaraeg G, Olefsky JM (2002) Fatty acid-induced insulin resistance: decreased muscle PI3K activation but unchanged Akt phosphorylation. J Clin Endocrinol & Metab 87:226-234

Kunjathoor VV, Febbraio M, Podrez EA, Moore KJ, Andersson L, Koehn S, Rhee JS, Silverstein R, Hoff HF, Freeman MW (2002) Scavenger receptors class A-I/II and CD36 are the principal receptors responsible for the uptake of modified low density lipoprotein leading to lipid loading in macrophages. J Biol Chem 277:49982-49988

Larson RS, and Springer TA (1990) Structure and function of leukocyte integrins. Immunol Rev114:181-217

Le Marchand-Brustel Y, Gual P, Gremeaux T, Gonzalez T, Barres R and J.-F. Tanti (2003) Fatty acid-induced insulin resistance: role of insulin receptor substrate 1 serine phophorylation in the retroregulation of insulin signalling. Biochem Soc Trans 31:1152-1156

Lee JS, Pinnamaneni SK, Eo SJ, Cho IH, Pyo JH, Kim CK, Sinclair AJ, Febbraio MA, Watt MJ (2006) Saturated, but not n-6 polyunsaturated fatty acids, induce insulin resistance: role of intramuscular accumulation of lipid metabolites. J Appl Physiol 100:1467–1474

Leon AS and Connett J (1991) Physical activity and 10.5 year mortality in the Multiple Risk Factor Intervention Trial (MRFIT). Int J Epidemiol 20:690-697

Liang CP, Han S, Okamoto H, Carnemolla R, Tabas I, Accili D, Tall AR (2004) Increase CD36 protein as a response to defective insulin signalling in macrophages. J Clin Invest 113:764-773

Liao L, Starzyk RM, Granger DN (1997) Molecular determinants of oxidized low-density lipoprotein-induced leukocyte adhesion and microvascular dysfunction. Arterioscler Thromb Vasc Biol 17:437-444

Ley K and Kansas GS (2004) Selectins in T-cell recruitment to non-lymphoid tissues and sites of inflammation. Nat Rev Immunol 4:325-335

Liang F, Seyrantepe, Landry K, Ahmad R, Ahmad A, Stamatos NM, Pshezhetsky AV (2006) Monocyte Differentiation Up-regulates the Expression of the Lysosomal Sialidase, Neu1, and Triggers Its Targeting to the Plasma Membrane via Major Histocompatibility Complex Class II-positive Compartments. J Biol Chem 281:27526-27538

Listenberger LL, Ory DS, Schaffer JE (2001) Palmitate-induced apoptosis can occur through a ceramide-independent pathway. J Biol Chem 276:14890-14895

Listenberger LL, Han XL, Lewis SE, Cases S, Farese RV Jr, Ory DS, Schaffer JE (2003) Triglyceride accumulation protects against fatty acid-induced lipotoxicity. PANS 100: 3077-3082

Locksley RM, Killeen N, Lenardo MJ (2001) "The TNF and TNF receptor superfamilies: integrating mammalian biology". Cell 104: 487–501

Long SD and Pekala PH (1996) Lipid mediators of insulin resistance: ceramide signalling down-regulates GLUT4 gene transcription in 3T3-L1 adipocytes. Biochem J. 319:179-184

Lougheed M and Steinbrecher UP (1996) Mechanism of uptake of copper-oxidized low density lipoprotein in macrophages is dependent on its extent of oxidation. J Biol Chem 271:11798-11805

Luft FC (2002) Proinflammatory effects of angiotensin II and endothelin: targets for progression of cardiovascular and renal disease. Curr Opin Nephrol Hypertens 11:59-66

Maalouf M and Rho JM (2008) Oxidative impairment of hippocampal long-term potentiation involves activation of protein phosphatase 2A and is prevented by ketone bodies. J Neurosci Res 86:3322-3330

Mangan DF and Wahl SM (1991)Differential regulation of human monocyte programmed cell death (apoptosis) by chemotactic factors and pro-inflammatory cytokines. J Immunol 147:3408-3412

Mano T, Masuyama T, Yamamoto K, Naito J, Kondo H, Nagano R, Tanouchi J, Hori M, Inoue M, Kamada T (1996) Endothelial dysfunction in the early stage of atherosclerosis precedes appearance of intimal lesions assessable with intravascular ultrasound. Am Heart J 131:231-238

Manson JE, Willett WC, Stampfer MJ (1995) Body weight and mortality among women. N Engl J Med 333:677-685

Manson JE, Spelsberg A (1996) Risk modification in the diabetic patient. In: Manson JE, Ridker PM, Gaziano JM, Henekens CH, eds. Prevention of myocardial infarction. Oxford: Oxford University Press 241-273

Marleau S, Harb D, Bujold K, Avallone R, Iken K, Wang Y, Demers A, Sirois MG, Febbraio M, Silverstein RL, Tremblay A, Ong H (2005). EP 80317, a ligand of the CD36 scavenger receptor, protects apolipoprotein E-deficient mice from developing atherosclerotic lesions. FASEB J 19:1869-1871

Maron DJ, Fair JM, Haskell WL (1991) Saturated fat intake and insulin resistance in men with coronary artery disease. The Stanford Coronary Risk Intervention Project Investigators and Staff. Circulation 84:2020–2027

Marshall JA, Bessesen DH, Hamman RF (1997) High saturated fat and low starch and fibre are associated with hyperinsulinaemia in a non-diabetic population:
the San Luis Valley Diabetes Study. Diabetologia 40:430–438

Marquez VE, Blumberg PM (2003) Synthetic diacylglycerols (DAG) and DAG-lactones as activators of protein kinase C (PK-C). Acc Chem Res 36:434-443

Massaro M, Carluccio MA, Paolicchi A, Bosetti F, Solaini G, Caterina RD (2002) Mechanisms for reduction of endothelial activity by oleate: inhibition of nuclear factor-κB through antioxidant effects. Prostaglandins Leukot Essent Fatty Acids 67:175-181

Matsumoto A, Naito M, Itakura H, Ikemoto S, Asaoka H (1990) Human macrophage scavenger receptors: primary structure, expression, and localisation in atherosclerotic lesions. Proc Natl Acad Sci USA 87:9133-9137

Mayer-Davis EJ, Monaco JH, Hoen HM, Carmichael S, Vitolins MZ, Rewers MJ, Haffner SM, Ayad MF, Bergman RN, Karter AJ (1997) Dietary fat and insulin sensitivity in a triethnic population: the role of obesity. The Insulin Resistance Atherosclerosis Study (IRAS). Am J Clin Nutr 65:79–87

Medina RA and Owen GI (2002) Glucose transporters, expression, regulation, and cancer. Biol Res 35:9-26

Merrill AH Jr and Jones DD (1990) An update of the enzymology and regulation of sphingomyelin metabolism. Biochim Biophys Acta 1044:1-12

McGarry JD (2002) Banting lecture: 2001: dysregulation of fatty acid metabolism in the aetiology of type 2 diabetes. Diabetes 51:7-18

Michel C, van Echten-Deckert G, Rother J, Sandhoff K, Wang E, Merrill AH Jr (1997) Characterization of Ceramide Synthesis. A dihydroceramide desaturase introduces the 4, 5-trans-double bond of sphingosine at the level of dihydroceramide. J Biol Chem 272:22432-22437

Miller TA, LeBrasseur NK, Cote GM, Trucillo MP, Pimentel DR, Ido Y, Ruderman NB, Sawyer DB (2005) Oleate prevents palmitate-induced cytotoxic stress in cardiac myocytes. Biochem Biophys Res Commun 336:309-315

Minami M, Kume N, Shimaok T, Kataoka H, Hayashida K, Akiyama Y, Nagata I, Ando K, Nobuyoshi M, Hanyuu M, Komeda M, Yonehara S, Kita T (2001) Expression of SR-PSOX, a Novel Cell-Surface Scavenger Receptor for Phosphatidylserine and Oxidized LDL in Human Atherosclerotic Lesions. Arterioscler Thromb Vasc Biol 21:1796-1800

Miranda MB, Dyer KF, Grandis JR, Johnson DE (2003) Differential activation of apoptosis regulatory pathways during monocytic Vs granulocytic differentiation: a requirement for Bcl-X_L and XIAP in the prolonged survival of monocytic cell (2003) Leukemia 17:390-400

Montague W (1983) Diabetes and the endocrine pancreas. A biochemical approach. P62.

Montell E, Turini M, Marotta M, Roberts M, Noé V, Ciudad CJ, Macé K, Gómez-Foix AM (2001) DAG accumulation from saturated fatty acids desensitizes insulin stimulation of glucose uptake in muscle cells. Am J Physiol Endocrinol Metab 280:E229-237.

Mossman, T (1983) Rapid colorimetric assay for cellular growth and survival: application to proliferation and cytotoxicity assays. J Immunol Methods 65:55-63

Mould AP and Humphries MJ (2004) Regulation of integrin function through conformational complexity: not simply a knee-jerk reaction? Curr Opin Cell Biol 15:544-551

Nageh, MF, Sandberg ET, Marotti KR, Lin AH, Melchior EP, Bullard DC, Beaudet AL (1997) Deficiency of inflammatory cell adhesion molecules protects against atherosclerosis in mice. Arterioscler Thromb Vasc Biol 17:1517-1520

Nagy L, Tontonoz P, Alvarez JG, Chen H, Evas RM (1998) Oxidized LDL regulates macrophage gene expression through ligand activation of PPAR gamma. Cell 93:229-240

Naito M, Suzuki H, Mori T, Matsumoto A, Kodama T, Takahashi K(1992) Coexpression of type I and type II human macrophage scavenger receptors in macrophages of various organs and foam cells in atherosclerotic lesions.Am J Pathol 141:591-599

Nakashima Y, Raines EW, Plump AS, Breslow JL, and Ross R (1998) Upregulation of VCAM-1 and ICAM-1 at atherosclerosis-prone sites on the endothelium in the ApoE-deficient mouse. Arterioscler Thromb Vasc Biol 18:842-851

Napoli C, DArmiento FP, Mancini FP, Postiglione A, Witztum JL, Palumbo G (1997) Fatty streak formation occurs in human fetal aortas and is greatly enhanced by maternal hypercholesterolemia-Intimal accumulation of low density lipoprotein and its oxidation precede monocyte recruitment into early atherosclerotic lesions. J Clin Invest 100:2680-2690

Navab M, Imes SS, Hama SY, Hough GP, Ross LA, Bork RW, Valente AJ, Berliner JA, Drinkwater DC, Laks H (1991) Monocyte transmigration induced by modification of low density lipoprotein in cocultures of human aortic wall cells is due to induction of monocyte chemotactic protein 1 synthesis and is abolished by high density lipoprotein. J Clin Invest 88:2039-2046

Nicholl SM, Roztocil E, Davies MG (2007) Role of Sphingosine-1-Phosphate (S1P) In Insulin Signaling. Circulation 116:239

Nicholson DW, Ali A, Thornberry NA, Vaillancourt JP, Ding CK, Gallant M, Gareau Y, Griffin PR, Labelle M, Lazebnik YA, Munday NA, Raju SM, Smulson ME, Yamin TT, Yu VL, Miller DK(1995) Identification and inhibition of the ICE/CED-3 protease necessary for mammalian apoptosis. Nature 376:37–43

Nie Q, Fan J, Haraoka S, Shimokama T, Watanbe T (1997) Inhibition of mononuclear cell recruitment in aortic intima by treatment with anti-ICAM-1 and anti-LFA-1 monoclonal antibodies in hypercholesterolemic rats: Implications of the ICAM-1 and LFA-1 pathway in atherogenesis. Lab Invest 77:469-482

O'Brien KD, Allen MD, McDonald TO, Chait A, Harlan JM, Fishbein D, McCarty J, Hudkins K, Benjamin CD et al (1993) Vascular cell adhesion molecule-1 is expressed in human coronary atherosclerotic plaques. Implications for the mode of progression of advanced coronary atherosclerosis. J Clin Invest 92:945-951

Ofei F, Hurel S, Newkirk J, Sopwith M, Taylor R (1996) Effects of an engineered human anti-TNF-alpha antibody (CDP571) on insulin sensitivity and glycemic control in patients with NIDDM. Diabetes 45:881-885

Ogihara T, Asano T, Katagiri H, Sakoda H, Anai M, Shojima N, Ono H Fujishiro M, Kushiyama A, Fukushima Y, Kikuchi M, Noguchi N, Abruratani H, Gotoh Y, Komuro I, Fujita T (2004) Oxidative stress induces insulin resistance by activating the nuclear factor-kappa B pathway and disrupting normal subcellular distribution of phosphatidylinositol 3-kinase. Diabetologia 47:794-805

Okuyama R, Fujiwara T, Ohsumi J (2003) High glucose potentiates palmitate-induced NO-mediated cytotoxicity through generation of superoxide in clonal beta-cell HIT-T15. FEBS Lett 545:219-223

Olefsky JM (1976) Decreased insulin binding to adipocytes and circulating monocytes from obese subject. J Clin Invest 57:1165-1172

Oquendo P, Hundt E, Lawler J, Seed B (1989) CD36 directly mediates cytoadherence of Plasmodium falciparum parasitized erythrocytes. Cell 58:95-101

Osborn, L., Hession, C., Tizard, R., Vassallo, C., Luhowskyi, S., Chi-Rosso, G., Lobb, R (1989) Direct expression of vascular cell adhesion molecule 1, a cytokine-induced endothelial protein that binds to lymphocytes. Cell

59:1203-1211

Otsuka A, Azuma K, Iesaki T, Sato F, Hirose T, Shimizu T, Tanaka Y, Daida H, Kawamori R, Watada H (2005) Temporary hyperglycaemia provokes monocyte adhesion to endothelial cells in rat thoracic aorta. Diabetologia 48:2667-2674

Papucci L, Formigli L, Schiavone N, Tani A, Donnini M, Lapucci A, Perna F, Tempestini A, Witort E, Morganti M, Nosi D, Orlandini GE, Orlandini SZ, Capaccioli S (2004) Apoptosis shifts to necrosis via intermediate types of cell death by a mechanism depending on c- *myc* and *bcl-2* expression. Cell Tissue Res 316:197-209

Park, JY, Kim CH, Hong SK, Suh KI, and Lee KU (1998) Effects of FFA on insulin-stimulated glucose fluxes and muscle glycogen synthase activity in rats. Am J Physiol Endocrinol Metab 275:E338-E344

Park TS, Panek RL, Mueller SB, Hanselman JC, Rosebury WS, Robertson AW, Kindt EK, Homan R, Karathanasis SK, Rekhter MD (2004) Inhibition of sphingomyelin synthesis reduces atherogenesis in apolipoprotein E-knokout mice. Circulation 110:3465-3471

Parker DR, Weiss ST, Troisi R, Cassano PA, Vokonas PS, Landsberg L (1993) Relationship of dietary saturated fatty acids and body habitus to serum insulin concentrations: the Normative Aging Study. Am J Clin Nutr 58:129-136

Patel SS, Thiagarajan R, Willerson JT, and Yeh ET (1998) Inhibition of alpha4 integrin and ICAM-1 markedly attenuate macrophage homing to atherosclerotic plaques in ApoE-deficient mice. Circulation 97:75-81

Paz K, Hemi R, LeRoith D, Karasik A, Elhanany E, Kanety H, Zick YA (1997) molecular basis for insulin resistance. Elevated serine/threonine phosphorylation of IRS-1 and IRS-2 inhibits their binding to the juxtamembrane region of the insulin receptor and impairs their ability to undergo insulin-induced tyrosine phosphorylation. J Biol Chem 272:29911-29918

Pedersen O, Bak JF, Andersen PH, Lund S, Moller DE, Flier JS, Kahn BB (1990) Evidence against altered expression of GLUT1 or GLUT4 in skeletal muscle of patients with obesity or NIDDM. Diabetes 39:865-870

Podrez EA, Febbraio M, Sheibani N, Schmitt D, Silverstein RL, Hajjar DP, Cohen PA, Frazier WA, Hoff HF, Hazen SL (2000) Macrophage scavenger receptor

CD36 is the major receptor for LDL modified by monocyte-generated reactive nitrogen species. J Clin Invest 105:1095-1108

Podrez EA, Poliakov E, Shen Z, Zhang R, Deng Y, Sun M, Finton PJ, Shan L, Gugiu B, Fox PL, Hoff HF, Salomon RG, Hazen SL (2002) Identification of a novel family of oxidized phospholipids that serve as ligands for the macrophage scavenger receptor CD36. J Biol Chem 77:38503-38516

Powell D, Turban S, Gray A, Hajduch E, Hundal HS (2004) Intracellular ceramide synthesis and protein kinase Cζ activation play an essential role in palmitate-induced insulin resistance in rat L6 skeletal muscle cells. Biochem J 382:619-629

Pyorala K, Laakso M, Uusitupa M (1987) Diabetes and atherosclerosis: an epidemiologic view. Diabetes Metab Rev 3:463-524

Quehenberger O (2005) Molecular mechanisms regulating monocyte recruitment in atherosclerosis. J Lipid Res 46:1582-1590

Rahaman SO, Lennon DJ, Febbraio M, Podrez EA, Hazen SL, Silverstein RL (2006) A CD36-dependent signaling cascade is necessary for macrophage foam cell formation. Cell Metab 4:211-221

Ramlo-Halsted BA, Edelman SV (2000) The Natural History of Type 2 Diabetes: Practical Points to Consider in Developing Prevention and Treatment Strategies. Clin Diabetes 18:80-84

Ramos CL, Huo Y, Jung U, Ghosh S, Manka DR, Sarembock IJ, and Ley K (1999) Direct demonstration of P-selectin- and VCAM-1-dependent mononuclear cell rolling in early atherosclerotic lesions of apolipoprotein E-deficient mice. Circ Res 84:1237-1244

Randle PJ, Garland PB, Newsholme EA, Hales CN (1965) The glucose fatty acid cycle in obesity and maturity onset diabetes mellitus.Ann N Y Acad Sci 131:324-333

Rajavashisth TB, Andalibi A, Territo MC, Berliner JA, Navab M, Fogelman AM, Lusis AJ (1990) Induction of endothelial cell expression of granulocyte and macrophage colony-stimulating factors by modified low-density lipoproteins. Nature 344:254-257

Reaven GM, and Laws A (1999) Insulin resistance: the metabolic syndrome X.

Reynoso R, Salgado LM, Calderón V (2003) High levels of palmitic acid lead to insulin resistance due to changes in the level of phosphorylation of the insulin receptor and insulin receptor substrate-1.Mol Cell Biochem 246(1-2):155-162

Roden M, Price TB, Perseghin G et al. (1996) Mechanism of free fatty acid–induced insulin resistance in humans. J Clin Invest 97:2859-2865

Rhodes CJ (2005) Type 2 diabetes-a matter of beta-cell life and death? Science307: 380-384

Rohrer L, Freeman M, Kodama T, Penman M, Krieger M (1990) Coiled-coil fibrous domains mediate ligand binding by macrophage scavenger receptor type □.Nature 343:570-572

Ross R, Glomset J, Harker L (1977) Response to injury and atherogenesis. Am J Pathol 86:675-684

Ross R and Glomset J (1976) The pathogenesis of atherosclerosis. N Engl J Med 295:369-377

Ross R (1993) Atherosclerosis: current understanding of mechanisms and future strategies in therapy.Transplant Proc 25:2041-2043

Ryan M, McInerney D, Owens D, Collins P, Johnson A, Tomkin GH (2000) Diabetes and the Mediterranean diet: a beneficial effect of oleic acid on insulin sensitivity, adipocyte glucose transport and endothelium-dependent vasoreactivity. QJM 93:85-91

Saghizadeh M, Ong JM, Garvey WT, Henry RR, Kern PA (1996) The expression of TNF alpha by human muscle. Relationship to insulin resistance. J Clin Invest 97:1111-1116

Sakaguchi H, Takeya M, Suzuki H, Hakamata H, Kodama T, Horiuchi S, Gordon S, van der Laan LJ, Kraal G, Ishibashi S, Kitamura N, Takahashi K (1998) Role of macrophage scavenger receptors in diet-induced atherosclerosis in mice. Lab Invest 78:423-434

Salinas M, López-Valdaliso R, Martín D, Alvarez A, Cuadrado A (2004) Regulation of insulin action by ceramide: dual mechanisms linking ceramide accumulation to the inhibition of Akt/protein kinase. B J Biol Chem 279:36608-36615

Saltiel AR. (2000) Series introduction: the molecular and physiological basis of insulin resistance: emerging implications for metabolic and cardiovascular diseases. J Clin Invest 106:163-164

Samaras K, McElduff A, Twigg SM, Proietto J, Prins JB, Welborn TA, Zimmet P, Chisholm DJ, Campbell LV (2006) Insulin levels in insulin resistance: phantom of the metabolic opera? Med J Aust 185:159-161

Sampson M, Davies IR, Braschi S, Ivory K, Hughes DA (2003) Increased expression of a scavenger receptor (CD36) in monocytes from subjects with type 2 diabetes. Atherosclerosis 167:129-134

Sarabia V, Ramlal T, Klip A (1990) Glucose uptake in human and animal muscle cells in culture. Biochem Cell Biol 68:536-542

Sargeant RJ, Pâquet MR (1993) Effect of insulin on the rates of synthesis and degradation of GLUT1 and GLUT4 glucose transporters in 3T3-L1 adipocytes. Biochem J 290:913-919

Sawada M, Kiyono T, Nakashima S, Shinoda J, Naganawa T, Hara S, Iwama T, Sakai N (2004) Molecular mechanisms of TNF-alpha-induced ceramide formation in human glioma cells: P53-mediated oxidant stress-dependent and -independent pathways. Cell Death Differ 11: 997–1008

Sawamura T, Kume N, Aoyama T, Moriwaki H, Hoshikawa H, Aiba Y, Tanaka T, Miwa S, Katsura Y, Kita T, Masaki T (1997). An endothelial receptor for oxidized low-density lipoprotein. Nature 386:73-77

Senior PA, Marshall SM, Thomas TH (1999) Dysregulation of PMN antigen expression in Type 2 diabetes may reflect a generalized defect of exocytosis: influence of hypertension and microalbuminuria. J Leukoc Biol 65:800-807

Scalia R, Appel JZ, and Lefer AM (1998) Leukocyte-endothelium interaction during the early stages of hypercholesterolemia in the rabbit: role of P-selectin, ICAM-1, and VCAM-1. Arterioscler Thromb Vasc Biol 18:1093-1100

Scharrer E and Amann B (1980) Evidence for carrier-mediated uptake of sugars at

the serosal side of lamb colon mucosa. Pflfigers Arch 384:279-282

Schmitz-Peiffer C, Craig DL, Biden TJ (1999) Ceramide generation is sufficient to account for the inhibition of the insulin-stimulated PKB pathway in C2C12 skeletal muscle cells pretreated with palmitate. J Biol Chem 274:24202-24210

Schwartz RH, Biancot AR, Handwerger BS, Kahnt CR (1975) Demonstration that monocytes rather than lymphocytes are the insulin binding cells in preparation of Human peripheral blood mononuclear leukocytes: implications for studies of insulin-Resistant states in man. Proc Nat Acad Sci USA 72:474-478

Senn JJ, Klover PJ, Nowak IA, Mooney RA (2002) Interleukin-6 Induces Cellular Insulin Resistance in Hepatocytes. Diabetes 51:3391-3399

Shaw DI, Hall WL, Jeffs NR, Williams CM (2007) Comparative effects of fatty acids on endothelial inflammatory gene expression. Eur J Nutr 45:521-528

Shih PT, Brennan ML, Vora DK, Territo MC, Strahl D, Elices MJ, Lusis AJ, and Berliner JA (1999) Blocking very late antigen-4 integrin decreases leukocyte entry and fatty streak formation in mice fed an atherogenic diet. Circ Res 84:345-351

Shoelson SE, Lee J, Goldfine AB (2006) Inflammation and insulin resistance. J Clin Invest 116:1793-1801

Shulman GI, Rothman DL, Jue T, Stein P, DeFronzo RA, Shulman RG (1990) Quantitation of muscle glycogen synthesis in normal subjects and subjects with non-insulin-dependent diabetes by 13C nuclear magnetic resonance spectroscopy. N Engl J Med 322:223-228

Siddiqi M, Stein DS, Denny TN, Spolarics Z (2001) Relationship between oxidative burst and CD11b expression in neutrophils and monocytes from healthy individuals: Effects of race and gender. Cytometry Part B: Clinial Cytometry 46: 243-246

Sinha MK, Pories WJ, Flickinger EG, Meelheim D, Caro JF (1987) Insulin receptor kinase activity of adipose tissue from morbidity obese humans with and without noninsulin-dependent diabetes. Diabetes 36:620-625

Sinha MK, Raineri-Maldonado C, Buchanan C, Pories WJ, Carter-Su C, Pilch PF, Caro JF (1991) Adipose tissue glucose transporters in NIDDM. Decreased levels of muscle/fat isoform. Diabetes 40:472-477

Sinha S, Perdomo G, Brown NF, O'Doherty RM (2004) Fatty acid-induced insulin resistance in L6 myotubes is prevented by inhibition of activation and nuclear localization of nuclear factor κB. J Biol Chem 279:41294-41301

Silverstein RL, Asch AS, Nachman RL (1989) Glycoprotein IV mediates thrombospondin-dependent platelet-monocyte and platelet-U937 cell adhesion. J Clin Invest 84:546-552

Skidmore PM, Yarnell JW (2004) The obesity epidemic: prospects for prevention. QJM 97: 817-825

Skovbro M, Baranowski M, Skov-Jensen C, Flint A, Dela F, Gorski J, Helge JW (2008) Human skeletal muscle ceramide content is not a major factor in muscle insulin sensitivity. Diabetologia 51:1253-1260
Smith, PK et al. (1985) Measurement of protein using bicinchoninic acid. Anal Biochem 150:76-85

Solberg LA and Strong JP (1983) Risk factors and atherosclerotic lesions. A review of autopsy studies. Arteriosclerosis. 3:187-198

Spector AA and Fletcher JE (1978) Transport of fatty acid in the circulation. . Am Physiol SOC 14:229-249

Springer TA, Galfre G, Secher DS, Milstein C (1979). Mac-1: a macrophage differentiation antigen identified by monoclonal antibody. Eur J Immunol 9:301-306

Stamler J, Vaccaro O, Neaton JD, Wentworth D (1993) Diabetes, other risk factors, and 12 year cardiac mortality for men screened in the multiple risk factor intervention trial. Diabetes Care 16:434-444

Steensberg A, Fischer CP, Sacchetti M, Keller C, Osada T, Schjerling P, van Hall G, Febbraio MA, Pedersen BK (2003) Acute interleukin-6 administration does not impair muscle glucose uptake or whole-body glucose disposal in healthy humans. J Physiol 48:631-638

Steinbrecher UP, Parthasarathy S, Leake DS, Witztum JL, Steinberg D (1984) Modification of low density lipoprotein by endothelial cells involves lipid peroxidation and degradation of low density lipoprotein phospholipids. Proc Natl Acad Sci USA 81:3883-3887

Steinbrecher UP (1987) Oxidation of human low density lipoprotein results in derivatization of lysine residues of apolipoprotein B by lipid peroxide decomposition products. J Biol Chem 262:3603-3608

Steinberg D and Witztum JL (2002) Is the oxidative modification hypothesis relevant to human atherosclerosis? Do the antioxidant trials conducted to date refute the hypothesis? Circulation 105:2107–211

Storlien LH, Jenkins AB, Chisholm DJ, Pascoe WS, Khouri S, Kraegen EW (1991) Influence of dietary fat composition on development of insulin resistance in rats. Relationship to muscle triglyceride and omega-3 fatty acids in muscle phospholipid. Diabetes 40:280-289

Storz P, Döppler H, Wernig A, Pfizenmaier K, Müller G (1999) Cross-talk mechanisms in the development of insulin resistance of skeletal muscle cells palmitate rather than tumour necrosis factor inhibits insulin-dependent protein kinase B (PKB)/Akt stimulation and glucose uptake. Eur J Biochem 266:17-25

Straczkowski M, Komalska I, Nikolajuk A, Straczkowski SD, Kinalska I, Baranowski M, Piotrowska MZ, Brzezinska Z, Gorski J. (2004) Relationship between insulin sensitivity and sphingomyelin signalling pathway in human skeletal muscle. Diabetes 53:1215-1221

Straczkowski M, Kowalska I, Baranowski M, Nikolajuk A, Otziomek E, Zabielski P, Adamska A, Blachnio A, Gorski J, Gorska M (2007) Increased skeletal muscle ceramide level in men at risk of developing type 2 diabetes. Diabetologia 50:2366-2373

Stratford S, Hoehn KL, Liu F, Summers SA (2004) Regulation of insulin action by ceramide: dual mechanisms linking ceramide accumulation to the inhibition of Akt/protein kinase B. J Biol Chem 279:36608-36615

Summers SA, Garza LA, Zhou H, Birnbaum MJ (1998) Regulation of insulin-stimulated glucose transporter GLUT4 translocation and Akt kinase activity by ceramide. Mol Cell Biol 18:5457-5464

Surmi BK; Hasty AH (2008) Macrophage infiltration into adipose tissue: initiation, propagation and remodeling. Future Lipidol 3:545-556

Szmitko PE, Wang CH, Weisel RD, de Almeida JR, Anderson TJ, Verma S (2003) New markers of inflammation and endothelial cell activation: Part I. Circulation 108:1917-1923

Taegtmeyer H (1996) Insulin Resistance and Atherosclerosis. Common roots for two common diseases? Circulation 93:1777-1779

Takada Y, Ye X, Simon S (2007) The integrins. Genome Biology 8:215-223

Taylor KE, Glagov S, Zarins CK (1989) Preservation and structural adaptation of endothelium over experimental foam cell lesions: quantitative ultrastructural study. Arteriosclerosis 9:881-894

Thubrikar and Robicsek F (1995) Pressure-Induced Arterial Wall Stress and Atherosclerosis. Ann Thorac Surg 59:1594-1603

Tirosh A, Shai I, Tekes-Manova D, Israeli E,, Pereg D, Shochat T, Kochba I, Rudich A (2005) Normal Fasting Plasma Glucose Levels and Type 2 Diabetes in Young Men. N Engl J Med 353:1454-1462

Tognon CE, Kirk HE, Passmore LA, Whitehead LP, Der CJ, Kay RJ (1998) Regulation of RasGRP via a phorbol ester-responsive C1 domain. Mol Cell Biol 18:6995-7008

Tsakiridis T, Marette A, Klip A (1994) Glucose transporters in skeletal muscle of animal models of diabetes In: Shafrir E, ed. Lessons from Animal Models of Diabetes V 141-159

Turinsky J, O'Sullivan DM, Bayly BP (1990) 1,2-Diacylglycerol and ceramide levels in insulin-resistant tissues of the rat *in vivo*. J Biol Chem 265:16880-16885

Turinsky J and Nagel GW (1992) Effect of sphingoid bases on basal and insulin-stimulated 2-dexoglucose transport in skeletal muscle. Biochem Biophys Res Commum 188:358-264

Uysal KT, Wiesbrock SM, Marino MW, Hotamisligil GS (1997) Protection from obesity-induced insulin resistance in mice lacking TNF-alpha function. Nature 389:610-614

van Berkel TJ, Out R, Hoekstra M, Kuiper J, Biessen E, van Eck M (2005) Scavenger receptors: friend or foe in atherosclerosis? Curr Opin Lipidol 16:525-535

Van Eck M, De Winther MP, Herijgers N, Havekes LM, Hofker MH, Groot PH, Van Berkel TJ (2000) Effect of human scavenger receptor class A overexpression in bone marrow-derived cells on cholesterol levels and atherosclerosis in ApoE-deficient mice. Arterioscler Thromb Vasc Biol 20:2600-2606

Van Kooyk Y, Figdor CG (2000) Avidity regulation of integrins: the driving force in leukocyte adhesion. Curr Opin Cell Biol 12:542-547

Van Oostrom AJ, van Wijk JP, Sijmonsma TP, Rabelink TJ, Castro Cabezas M (2004) Increased expression of activation markers on monocytes and neutrophils in type 2 diabetes. Neth J Med 62:320-325

Varki A (1994) Selectin ligands. Proc Natl Acad Sci USA 91:7390-7397

Vries JE, Vork MM, Roemen THM, Jong YF, Cleutjens JPM, Vusse GJ, Bilsen M (1997) Saturated but not mono-unsaturated fatty acids induce apoptotic cell death in neonatal rat ventricular myocytes. J Lipid Res 38:1384-1394

Voshol PJ, Jong MC, Dahlmans VE et al. (2001) In muscle-specific lipoprotein lipase-overexpressing mice, muscle triglyceride content is increased without inhibition of insulin-stimulated whole-body and muscle-specific glucose uptake. Diabetes 50:2585-2590

Vozarova B, Weyer C, Hanson K, Tataranni PA, Bogardus C, Pratley RE (2001) Circulating interleukin-6 in relation to adiposity, insulin action, and insulin secretion. Obes Res 9:414-417

Walker PS, Ramlal T, Donovan JA, Doering TP, Sandra A, Klip A, Pessin JE (1989) Insulin and glucose-dependent regulation of the glucose transport system in the rat L6 skeletal muscle cell line. J Biol Chem 264:6587-6595

Wallenius V, Wallenius K, Ahrén B, Rudling M, Carlsten H, Dickson SL, Ohlsson C, Jansson JO (2002) Interleukin-6-deficient mice develop mature-onset obesity. Nat Med 8:75-79

Wang Q, Muffley LA, Hall K, Chase M, Gibran NS (2009) Elevated glucose and fatty acid levels impair substance P induced dermal microvascular endothelial cell migration and proliferation in an agarose gel model system. Shock [Epub ahead of print]

WHO report. 2003 http://www.who.int/cardiovascular_diseases/resources/atlas/en/

WHO (2003) Diet, Nutrition, and the Prevention of Chronic Diseases: Report of a Joint WHO/FAO Expert Consultation, Geneva, 28 January – 1 February 2oo2. WHO Technical Report Series: 916. World Health Organisation, Geneva.

Willet W (1990) Diet and coronary heart disease. Monogr Epidemiol Biostat 15:341-379

Wilson JD (1998) Williams Textbook of Endocrinology. 9th ed. Philadelphia: WB Saunders 1155

Woollard KJ, Phillips DC, Griffiths HR (2002) Direct modulatory effect of C-reactive protein on primary human monocyte adhesion to human endothelial cells. Clin Exp Immunol 130:256-262

Wyne KL (2003) Free fatty acids and type2 diabetes mellitus. Am J Med 115:29-36

Xu X, Bittman R, Duportail G, Heissler D, Vilcheze C, London E (2001) Effect of the structure of natural sterols and sphingolipids on the formation of ordered sphingolipid/sterol domains (rafts). Comparison of cholesterol to plant, fungal, and disease-associated sterols and comparison of sphingomyelin, cerebrosides, and ceramide. J Biol Chem 276:33540-33546

Yu C, Chen Y, Cline GW, Zhang D, Zong H, Wang Y, Bergeron R, Kim JK, Cushman SW, Cooney GJ, Atcheson B, White MF, Kraegen EW, Shulman GI (2002) Mechanism by which fatty acids inhibit insulin activation of insulin receptor substrate-1 (IRS-1)-associated phosphatidylinositol 3-kinase activity in muscle.J Biol Chem 277:50230-50236

Zhang H, Yang Y (1993) Steinbrecher UP.Structural requirements for the binding of modified proteins to the scavenger receptor of macrophages. J Biol Chem 268:5535-5542

Zhang HM, Zhang XL, Zhou X, Li D, Gu JG, Wu JJ (2005) Mechanism linking atherosclerosis and type 2 diabetes: increased expression of scavenger receptor CD36 in monocytes. Chinese Med J 18:1717-1722

Zhang WY, Schwartz E, Wang YJ, Attrep J, Li Z, Peter Reaven (2006) Elevated concentrations of nonesterified fatty acids increase monocyte expression of CD11b and adhesion to endothelial cells. Arterioscler Thromb Vasc Biol 26:514-519

Zheng Y, Liu H, Coughlin J, Zheng J, Li L, Stone JC (2005) Phosphorylation of RasGRP3 on threonine 133 provide a mechanistic link between PKC and RAS signaling systems in B cells. Blood 105:3648-3654

Zorzano A., Wilkinson W, Kotliar N, Thoidis G, Wadzinkski BE, Ruoho AE, Pilch PF (1989) Insulin-regulate d glucose uptake in rat adipocytes is mediated by two transporter isoforms present in at least two vesicle populations. J Biol Chem 264:12358-12363

Appendix II Publications

Gao D, Griffiths HR, Bailey CJ (2007) Palmitate induces insulin resistance in monocytes and increases expression of the integrin CD11b (Abstract) Proceedings of the Nutrition Society 66: 44A